A

Ph.D. Thesis

on

STUDIES ON ETHANOL FUELLED C.I. ENGINE OPERATED END UTILITY SYSTEM

Submitted in Fulfillment of the requirements for the degree of

DOCTOR OF PHILOSOPHY

Supervisors:
Prof. DILIP SHARMA
Prof. S.L. SONI

Submitted by:
DORAJ KAMAL JAMUWA
Scholar ID: 2009RME104

DEPARTMENT OF MECHANICAL ENGINEERING

MALAVIYA NATIONAL INSTITUTE OF TECHNOLOGY, JAIPUR

INDIA

November, 2016

Dedicated to

the loving memories

of my parents

Late. Shri K.N. Sharma

&

Late. Smt. Parvati Sharma

DEPARTMENT OF MECHANICAL ENGINEERING
MALAVIYA NATIONAL INSTITUTE OF TECHNOLOGY, JAIPUR

CERTIFICATE

This is to certify that the thesis entitled "**Studies On Ethanol Fuelled C.I. Engine Operated End Utility System**" submitted by Mr. **Doraj Kamal Jamuwa** (2009RME104), to the Malaviya National Institute of Technology, Jaipur for the award for the degree of **Doctor of Philosophy** is a bonafide record of original research work carried out by him. He has worked under our guidance and supervision and has fulfilled the requirement for the submission of this thesis.

The results contained in thesis have not been submitted in part or full, to any other University or Institute for the award of any degree or diploma.

(Prof. Dilip Sharma)
Professor
Department of Mechanical Engineering
Malaviya National Institute of Technology
Jaipur

(Prof. S.L. Soni)
Professor
Department of Mechanical Engineering
Malaviya National Institute of Technology
Jaipur

Date:

ACKNOWLEDGEMENT

I wish to express my deep sense of regard and gratitude to my reverend and learned supervisors **Prof. Dilip Sharma** and **Prof. S. L. Soni**, Department of Mechanical Engineering, Malaviya National Institute of Technology Jaipur, whose unfailing support, co-operation and supervision helped me throughout dissertation work. Their painstaking efforts in going through the manuscript and giving valuable suggestion for the experimentation work cannot be described into words and only I can recall with profound gratitude, the long indefatigable hours spent in discussions and thrashing out the minutest details of the work through numerous revisions. Their patience and support helped me overcome many critical situations and finish this dissertation. They have been always there to listen me patiently and give invaluable advice, wherever required.

I extend my sincere thanks to my doctoral guidance committee members, **Prof. Jyotirmay Mathur, Dr. G.D. Agrawal and Dr. N. Rohatagi**, for their valuable suggestions and cooperation throughout the course of study. It gives me immense pleasure to express my deep sense of gratitude to **Prof. A. Bhardwaj and Shri N.S.Yadav** for their perennial encouragement and valuable suggestions extended to me during entire period of the work.

I extended my heartiest thanks and gratitude to parents **Late Shri K.N. Sharma** and **Late Smt Parvati Sharma** residing at heavenly abode, without the eternal blessings of whom this work would not have been possible and to whom this dissertation is dedicated to.

Most importantly, none of this would have been possible without the love and patience of my wife, **Smt. Bharti Sharma** and son **Aditya Sharma.** By all the means I am indebted to my beloved brothers, **Shri P. K. Sharma** and **Shri Doraj Vimal Jamuwa** for their invaluable consolation provided to me from time to time. Here, my sister-in-laws **Smt. Meena Sharma** and **Smt. Purva Sharma** cannot be forgotten for encouraging me to work tirelessly. I am also thankful to my father-in-law and mother-in-law, **Shri M. K. Sharma** and **Smt Krishna Sharma** for their ever ending encouragement and moral support extended to me on every walk of my work.
My sisters, **Smt. Premlata Sharma**, **Smt. Pushplata Sharma**, **Smt. Anita Sharma** and niece-in-law **Smt. Kritika Doraj** have been a constant source of concern, support and strength throughout

the duration of work. I would also thank my nephews and niece, **Mr. Doraj Vikram, Mr. Sumit Doraj, Snigdha Doraj , Ananya Doraj** and little angel **Akshaj Doraj**.

I also would like to thank **Mr. Tarun Kumar Aseri**, Assistant Prof. GEC Ajmer for his continuous help during preparation of manuscript. I would like to acknowledge **Dr. Rohit Misra** and **Dr. Chandan Sharma** Associate Prof., GEC Ajmer for the many valuable discussions that helped me understand my research area better.

I am also grateful to the All India Council of Technical Education, New Delhi, India (Ref. No. 8023/RID/RPS/040/11/12,1604) and Department of Science and Technology, Rajasthan, India (Ref. No. F 7(3) DST/R&D/2013/4378) for providing financial assistance.

Place: Jaipur Doraj Kamal Jamuwa

Date:

ABSTRACT

The indiscriminate utilization of fossil fuels for decades have alarmed the researchers around the globe for the quest of the alternate fuel that not only possesses the advantage of ample availability but also curb the menace of environmental degradation and climate change to a considerable extent. In the broader spectrum of India's energy future, the encouragement of the usage of renewable fuels is not only a vital tool for augmenting the climate change mitigation projects and fulfilling their commitments to reduce emissions but also improve the livelihood of communities through the creation of employment or increased economic activity by means of Clean Development Mechanism (CDM). Renewables can play a greater role in our sustainable energy future thus strengthening India's energy security and reducing reliance on oil imports from politically unstable regions. Among the renewable fuels that includes alcohols (such as ethanol and methanol), ethers, vegetable oils, animal fats, gaseous fuels (hydrogen, bio-gas and bio-methane) and bio-diesel, two lower alcohols, viz., methanol and ethanol have attracted increasing attention.

In the present research, the engine performance, emission and combustion characteristics have been investigated for the following cases (i) different ethanol/total fuel ratio (by volume) (ii) different ethanol flow rates (iii) different ethanol energy fractions (iv) different diesel injection timings for different constant ethanol flow rate (v) different pre-heating temperatures with different constant ethanol flow rates.

For the first three modes, BTE and NOx decreased at low loads but increased at high loads for different ethanol fumigation modes. The rise in HC and CO emissions along with decrease of CO_2 and smoke for the entire load range was observed with ethanol fumigation. The values of peak pressure, heat release rate and ignition delay increases whereas combustion duration decreases for all levels of fumigation.

At fixed ethanol flow rate and given load, the efficiency increased by advancing diesel injection timing. As compared to original injection timing, NOx and smoke opacity increases with simultaneous decrease of HC and CO emissions by advancing diesel injection timing. Advanced diesel injection extends the limit of utilisation of higher ethanol flow rate. With increase in injection advance, considerably higher peak pressure and high rate of pressure rise along with extended ignition delay and shorter combustion duration is observed. The extent of injection advance is limited by occurrence of knock.

Fuel preheating increases efficiency. NOx emissions due to rapid burning and increased fuel inlet temperatures. Increase in NOx emissions with decrease in smoke opacity, HC and CO with fuel preheating. The increase in peak pressure and maximum rate of pressure rise results along with simultaneous improvement in heat release rate due to improved atomisation and vaporisation of the ethanol. The preheated ethanol exhibits reduced ignition delay.

Further, a diesel engine CFD model has also been developed to simulate the combustion phenomenon of the engine operated on diesel as well as with ethanol the results of the same have been validated with the experimental investigations.

CONTENTS

Certificate i

Acknowledgements ii

Abstract iv

List of figures xi

List of tables xv

Nomenclature xvi

CHAPTER 1

INTRODUCTION 1

1.1 Energy demand and crisis 1

1.2 Various alternate fuels 6

1.3 Challenges of biofuels 9

1.4 Alcohol as alternative fuel 9

1.4.1 Advantages of alcohol 10

1.4.2 Disadvantages of alcohol 11

1.4.3 Use of alcohol in CI engine. 12

1.5 Stationary diesel engines 14

1.5.1 Continuous and prime generators 14

1.5.2 Standby Power generators 15

CHAPTER 2

LITERATURE REVIEW 17

2.1 Research gap 28

2.2 Objective 28

2.3 Research Methodology 28

CHAPTER 3 30

EXPERIMENTAL SET UP AND METHODOLOGY 30

3.1 Experimental set-up 30

3.2 Experimental methodology 32

CHAPTER 4 35

EXPERIMENTAL RESULTS AND DISCUSSIONS 35

4.1 Effect of ethanol on engine-performance, exhaust emission and combustion 35

parameters for constant ratio (v/v) of ethanol and diesel
4.1.1 Effective equivalence ratio and brake specific energy consumption 35
4.1.2 Brake thermal efficiency 37
4.1.3 Exergy efficiency 38
4.1.4 Exhaust gas temperature 40
4.1.5 Volumetric efficiency 41
4.1.6 NOx emissions 41
4.1.7 HC and CO emissions 43
4.1.8 CO_2 emissions 45
4.1.9 Smoke opacity 46
4.1.10 Cylinder pressure and rate of pressure rise 47
4.1.11 IMEP 50
4.1.12 Heat release rate 50
4.1.13 Ignition delay, combustion duration and mass fraction burned 52
4.2 Effect of ethanol on engine-performance, exhaust emission and combustion parameters for constant flow-rate of ethanol 55
4.2.1 Relative air-fuel ratio and ethanol energy ratio 55
4.2.2 Brake thermal efficiency 56
4.2.3 Exergy efficiency 57
4.2.4 Exhaust gas temperature 58
4.2.5 NOx emissions 58
4.2.6 HC and CO emissions 59
4.2.7 CO_2 emissions 61
4.2.8 Smoke opacity 63
4.2.9 Cylinder pressure and rate of pressure rise 63
4.2.10 Cylinder gas temperature 66
4.2.11 Heat release rate 66
4.2.12 Ignition delay, combustion duration and mass fraction burned 67
4.3 Effect of ethanol on engine-performance, exhaust emission and combustion parameters with varying ethanol energy fractions at constant ethanol flow rate 69
4.3.1 Fuel consumption and Effective equivalence ratio 69
4.3.2 Brake thermal efficiency 70
4.3.3 Exergy efficiency 71

4.3.4 Exhaust gas temperature 71
4.3.5 NOx emissions 73
4.3.6 HC and CO emissions 73
4.3.7 CO_2 emissions 75
4.3.8 Smoke opacity 76
4.3.9 Cylinder pressure and rate of pressure rise 76
4.3.10 Heat release rate 77
4.3.11 Ignition delay, combustion duration and mass fraction burned 78
4.4 Effect of ethanol on engine-performance, exhaust emission and combustion parameters with various diesel-injection advance angles at constant ethanol flow rate 79
4.4.1 Brake thermal efficiency 79
4.4.2 NOx emissions 79
4.4.3 HC emissions 80
4.4.4 CO emissions 82
4.4.5 CO_2 emissions 82
4.4.6 Smoke opacity 83
4.4.7 In-Cylinder pressure 84
4.4.8 Heat release rate 86
4.4.9 Burn duration 87
4.5 Effect of ethanol on engine-performance, exhaust emission and combustion parameters with pre-heating of ethanol at constant ethanol flow rate 89
4.5.1 Brake thermal efficiency 89
4.5.2 NOx emissions 90
4.5.3 HC emissions 90
4.5.4 CO emissions 91
4.5.5 Smoke opacity 92
4.5.6 In-Cylinder pressure 93
4.5.7 Heat release rate 95
4.5.8 Ignition delay and combustion duration 95

CHAPTER 5 97
CFD MODELLING OF CI ENGINE 97
5.1 CFD methodology 97

5.2 Advantages of CFD 98
5.3 Overview of CFD simulation 98
5.3.1 Pre-processor 99
5.3.2 Solver 99
5.3.3 Post-processor 100
5.4 CFD analysis procedure 100
5.5 Governing Equations 101
5.5.1 Species Mass Balance 102
5.5.2 Momentum Equation 103
5.5.3 Energy Equation 103
5.6 Averaging of Equations 103
5.7 Modelling and Meshing 104
5.8 Computational Models 105
5.8.1 Turbulence Models 105
5.8.1.1 The Spalart-Allmaras model 105
5.8.1.2 Standard k-ε model 106
5.8.1.3 RNG k-ε model 106
5.8.1.4 Realizable k- ε model 107
5.9 Combustion Models 107
5.9.1 Species Transport 108
5.9.1.1 The Laminar Finite-Rate Model 108
5.9.1.2 The Eddy-Dissipation Model 108
5.9.1.3 The Eddy-Dissipation-Concept (EDC) Model 108
5.9.2 Non-Premixed Combustion 109
5.9.3 Premixed Combustion 109
5.10 Auto ignition 110
5.11 Injections 110
5.12 Solver Settings 111
5.13 Procedure for Solver Setting 116
5.14 Boundary Conditions & Initial Conditions 116
5.15 Validation of computational model 117
5.15.1 Validation of geometry and boundary conditions 118
5.15.2 Validation of results 118

CHAPTER 6 137
CONCLUSIONS 137
REFERENCES 139
APPENDIX A A1

LIST OF FIGURES

F.No.	Title	Page No.
1.1	Major region-wise production of crude-oil (estimated)	4
1.2	Major region-wise consumption of crude-oil (estimated)	4
1.3	Shares of sectors in total final consumption for the world (1973 and 2011)	5
1.4	Share of the various sources in the world transport energy consumption	5
1.5	Energy consumption by energy source for passenger transport and freight transport (for a total of 23 OECD countries, 2010)	6
3.1	Schematic diagram of experimental set-up	31
3.2	Single Cylinder Constant Speed Stationary C.I Engine	32
4.1	Variation of effective equivalence ratio at various loads for different percentage of ethanol fumigation	36
4.2	Comparison of brake specific energy consumption at various loads for different percentage of ethanol fumigation	36
4.3	Variation of brake thermal efficiency with load for different percentage of ethanol fumigation	38
4.4	Variation of Exergy efficiency with load for different percentage of ethanol fumigation	39
4.5	Variation of Exhaust gas temperature at various loads for different percentage of ethanol fumigation	40
4.6	Variation of Volumetric efficiency at various loads for different percentage of ethanol fumigation	41
4.7	Variation of NOx with load for different percentage of ethanol fumigation	43
4.8	Variation of HC with load for different percentage of ethanol fumigation	45
4.9	Variation of CO with load for different percentage of ethanol fumigation	45
4.10	Variation of CO_2 with load for different percentage of ethanol fumigation	46
4.11	Variation of Smoke opacity with load for different percentage of ethanol fumigation	47
4.12	Variation in cylinder pressure with crank angle at full load	48
4.13	Variation in peak cylinder pressure with load and fumigation	49
4.14	Variation in rate of pressure rise with crank angle at full loading.	50
4.15	Variation in IMEP with different percentage of ethanol fumigation	51
4.16	Variation in heat release rate with crank angle at full load	52
4.17	Variation of burn duration with ethanol content at full load	53
4.18	Variation in mass fraction burned with crank angle at full load	54
4.19	Variation of relative air fuel ratio, λ with load for different ethanol fumigation rates	55
4.20	Variation of ethanol energy fraction for different values of λ for different ethanol fumigation rates	56
4.21	Variation of brake thermal efficiency with load for different ethanol fumigation rates	57
4.22	Variation of Exergy Efficiency with load for different ethanol	57

fumigation rates
4.23 Variation of Exhaust temperature at various loads for different ethanol fumigation rates 58
4.24 Variation of NOx with load for different ethanol fumigation rates 59
4.25 Variation of HC with load for different ethanol fumigation rates 60
4.26 Variation of CO with load for different ethanol fumigation rates 61
4.27 Variation of CO_2 with load for different ethanol fumigation rates 62
4.28 Variation of Smoke Opacity with load for different ethanol fumigation rates 62
4.29 Variation in cylinder pressure with crank angle at full load 64
4.30 Variation in rate of pressure rise with crank angle at full load 64
4.31 Variation in peak cylinder pressure with load and fumigation rates 65
4.32 Variation in CoV of IMEP with ethanol fumigation rates 65
4.33 Variation in cylinder gas temperature with crank angle at full load 66
4.34 Variation in heat release rate with crank angle at full load 67
4.35 Variation of Burn Duration with ethanol content at full load 68
4.36 Variation in mass fraction burned with crank angle at full load 68
4.37 Comparison of mass consumption rate of diesel at various loads for different ethanol energy fraction 69
4.38 Comparison of effective equivalence ratio at various loads for different ethanol energy fraction 70
4.39 Variation of brake thermal efficiency with load for different ethanol energy fraction 71
4.40 Variation of Exergy Efficiency with load for different ethanol energy fraction 72
4.41 Variation of Exhaust temperature at various loads for different ethanol energy fraction 72
4.42 Variation of NOx with load for different ethanol energy fraction 73
4.43 Variation of HC with load for different ethanol energy fraction 74
4.44 Variation of CO with load for different ethanol energy fraction 74
4.45 Variation of CO_2 with load for different ethanol energy fraction 75
4.46 Variation of Smoke Opacity with load for different ethanol energy fraction 75
4.47 Variation in cylinder pressure with crank angle at full load 76
4.48 Variation in rate of pressure rise with crank angle at full load 77
4.49 Variation in heat release rate with crank angle at full load 77
4.50 Variation of Burn Duration with different ethanol energy fraction at full load 78
4.51 Variation in mass fraction burned with crank angle at full load 79
4.52 Variation of Brake Thermal efficiency with ethanol flow rate and diesel injection timing 80
4.53 Variation of NOx emission with ethanol flow rate and diesel injection timing 81
4.54 Variation of HC emission with ethanol flow rate and diesel injection timing 81
4.55. Variation of CO emission with ethanol flow rate and diesel injection timing 82

4.56.	Variation of CO_2 emission with ethanol flow rate and diesel injection timing	83
4.57.	Variation of Smoke Opacity with ethanol flow rate and diesel injection timing	84
4.58.	Variation of in-cylinder pressure with ethanol flow rate and diesel injection timing	85
4.60.	Variation of heat release rate with ethanol flow rate and diesel injection timing	86
4.61	Variation of Burn Duration with ethanol flow rate and diesel injection timing	87
4.62	Variation of Brake Thermal efficiency with ethanol flow rate and its pre-heating temperatures	88
4.63	Variation of NOx emissions with ethanol flow rate and its pre-heating temperatures	89
4.64	Variation of HC emissions with ethanol flow rate and its pre-heating temperatures	90
4.65	Variation of CO emissions with ethanol flow rate and its pre-heating temperatures	91
4.66	Variation of Smoke opacity with ethanol flow rate and its pre-heating temperatures	92
4.67	Variation of in-cylinder pressure with ethanol flow rate and its pre-heating temperatures	94
4.68	Variation of rate of pressure rise with ethanol flow rate and its pre-heating temperatures	94
4.69	Variation of heat release rate with ethanol flow rate and its pre-heating temperatures	95
4.70	Variation of Burn Duration with ethanol flow rate and its pre-heating temperatures	96
5.1	Engine Geometry (Sector of 120°)	114
5.2	Mesh of Sector (Top view)	114
5.3	Mesh of Sector (Front view)	115
5.4	Mesh of Sector at IVC	115
5.5	Comparison of experimental and simulation pressure histories for pure diesel	119
5.6	Comparison of experimental and simulation pressure histories for e1	119
5.7	Comparison of experimental and simulation pressure histories for e2	120
5.8	Comparison of experimental and simulation pressure histories for e3	120
5.9	Comparison of experimental and simulation pressure histories for e4	121
5.10	Comparison of experimental and simulation pressure histories for e5	121
5.11	Comparison of experimental and simulation heat release rate for pure diesel	122
5.12	Comparison of experimental and simulation heat release rate for e1	122
5.13	Comparison of experimental and simulation heat release rate for e2	123
5.14	Comparison of experimental and simulation heat release rate for e3	123
5.15	Comparison of experimental and simulation heat release rate for e4	124
5.16	Comparison of experimental and simulation heat release rate for e5	124
5.17	Pressure contours for pure diesel at different crank angle	125
5.18	Pressure contours for e1 at different crank angle	126

5.19	Pressure contours for e2 at different crank angle	127
5.20	Pressure contours for e3 at different crank angle	128
5.21	Pressure contours for e4 at different crank angle	129
5.22	Temperature contours for e5 at different crank angle	130
5.23	Temperature contours for pure diesel at different crank angle	131
5.24	Temperature contours for e1 at different crank angle	132
5.25	Temperature contours for e2 at different crank angle	133
5,26	Temperature contours for e3 at different crank angle	134
5.27	Temperature contours for e4 at different crank angle	135
5.28	Temperature contours for e5 at different crank angle	136

LIST OF TABLES

T. No.	Title	Page No.
1.1	Crude Oil and Natural Gas Production	2
1.2	Production and Consumption of Petroleum Products	2
1.3	Imports of Crude Oil and average Crude Oil Prices	3
1.4	Imports & Exports of Petroleum products	3
3.1	Comparison of the Physical properties of Various Fuels	33
3.2	Specifications of diesel engine	33
3.3	Specifications of Exhaust Gas Analyser	34
3.4	Specifications of Smoke-meter	34
6.1	Boundary and Initial Condition	117
5.2	Specifications of the fuel Injector	117
5.3	Characteristic parameters for computational modelling	117

NOMENCLATURE

Symbols:

AFR	-	Air fuel ratio
B	m	bore
$\frac{\delta Q_{net}}{\delta \theta}$	J/deg CA	Heat Release Rate
$\frac{\delta p}{\delta \theta}$	bar/deg CA	Rate of pressure rise
$\dot{E}x_w$	kJ/sec	net exergy work rate
$\dot{E}x_{in}$	kJ/sec	input exergy rate.
i	-	integer crank angle location
l	m	length of connecting rod
N		number of crank intervals (or expected combustion duration)
p	bar	in-cylinder pressure
Δp_c^*	bar	pressure rise due to combustion for the combustion duration
$q_{m,}$	kg/hr	mass flow rate
Q_{LHV}	kJ/kg	Lower heating value
r	m	crank throw
V	m^3	in-cylinder volume
V_c	m^3	clearance volume at TDC

Greek symbols

ε	kJ/kg	specific exergy of ethanol
γ	-	ratio of specific heats,
φ	-	chemical energy factor
ψ	-	Exergy Efficiency
θ	degree	crank angle measured from the beginning of induction stroke

Abbreviations

aTDC	after top dead centre
bTDC	before top dead centre

BTE	Brake Thermal Efficiency
BSEC	Brake specific energy consumption (MJ/kW-hr)
CI	Compression ignition
CO	Carbon monoxide
CO_2	Carbon dioxide
°CA	degree crank angle
HC	Hydrocarbons
HRR	Heat Release Rate
Mfb	Mass fraction burned
NO_x	Nitric oxides of Nitrogen
O_2	Oxygen

Subscripts

air	air
d	diesel
e	ethanol
st	stoichiometric

APPENDIX-A

A.1 Error analysis

Error in the experimental value can arise from instrument selection condition calibration environment and observation. Error analysis is performed to prove measurement accuracy of the physical quantities during the experimentation. For example the error of various emissions was estimated based on the accuracy of the gas-analyser and smoke-meter used. Error analysis of the derived quantities such as brake power and brake thermal efficiency have been estimated analytically based on root mean square method as given by following equation:

$$\Delta R = \left[\left(\frac{\partial R}{\partial x_1}\Delta x_1\right)^2 + \left(\frac{\partial R}{\partial x_2}\Delta x_2\right)^2 + \ldots\ldots\ldots\ldots\left(\frac{\partial R}{\partial x_n}\Delta x_n\right)^2\right]^{1/2}$$

where R is the derived quantity ΔR is the error limit and Δx_1 Δx_2 Δx_3 and Δx_n are error limits of the measured values. The details of the error analysis for some measured and derived quantities are shown in Table A.1 It is evident that the error ranges from 0.2% to 5%. Hence it can be concluded that the error in measured and derived quantities does not significantly influence the overall uncertainty of the results.

Table A.1 Instrument and their Uncertainties

Instrument	**Range**	**Resolution**	**Uncertainties (%)**
Load Bank (kW)	0-3.7	0.1	0.2
Temperature Indicator (°C)	0-600	1	0.2
Burette (cc)	1-50	1	2
Speed sensor (rpm)	0-6000	1	0.2
Exhaust Gas Analyser			
NOx (ppm)	0-5000	1	0.3
HC (ppm)	0-20000	1	0.3
CO (%)	0-15	0.01	0.4
CO_2 (%)	0-20	0.1	0.4
O_2 (%)	0-25	0.1	0.5
Smoke meter (HSU in %)	0-100	0.1	0.2

CHAPTER 1

INTRODUCTION

1.1 Energy Demand and Crisis

The incessant exploitation of petroleum reserves leading to its depletion, environmental degradation and the stringent emission legislations all over the world has led to the search for alternative fuels that not only promises a harmonious correlation with energy conservation and efficiency but also serve as a tool for the sustainable development thus catering to the needs of environmental protection.

Therefore, the researchers have focused their attention on the development of the bio-fuels that possess the added advantage of being renewable fuels that can be replenished through the growth of plants or production of livestock thus reducing the emitted carbon dioxide. The fuels of bio-origin may be alcohol, vegetable oils, bio-mass and bio-gas. Some of these fuels can be used directly while others need to be processed upon to achieve the desired properties.

Compression-ignition (CI) or diesel engines are widely used in the fields of commercial transportation, automotive, agricultural applications and industrial sector due to their high energy conversion efficiency, robustness and ease of operation. The improvement in their performance and emission levels is likely to enhance fuel economy along with reduced emissions.

In India, the production of crude oil for the year 2014-15 is at 37.461 Million Metric Tonnes (MMT) as against production of 37.788 MMT in 2013-14, showing a decrease of about 0.87%. For the year 2014-15, production of natural gas is 33.656 Billion Cubic Meters (BCM) which is 4.94 % lower than production of 35.407 BCM in 2013-14.Year-wise production of crude oil and natural gas during 2007-08 to 2014-15 are presented in Table. 1.1.

The production of petroleum products is at 221.136 MMT in year 2014-15 as against 220.756MMT achieved in 2013-14, showing a marginal increase of about 0.17%.During the year 2014-15, the consumption of petroleum products in India was164.987 MMT with a growth of 4.15% as compared to consumption of 158.407 MMT during 2013-14.Year-wise production and consumption of petroleum products during 2007-08 to 2014-15 are presented in Table. 1.2.

Table 1.1: Crude oil and natural gas production

Year	Crude oil production (MMT)	%Growth in Crude oil production	Natural gas production (BCM)	% Growth in Natural gas production
2007-08	34.118	0.38	32.417	2.11
2008-09	33.508	-1.79	32.845	1.32
2009-10	33.690	0.54	47.496	44.61
2010-11	37.684	11.85	52.219	9.94
2011-12	38.090	1.08	47.559	-8.92
2012-13	37.862	-0.60	40.679	-14.47
2013-14	37.788	-0.19	35.407	-12.96
2014-15*	37.461	-0.87	33.656	-4.94

*Provisional

Table1.2: Production and consumption of petroleum products[1]

Year	Production of Petro-products (MMT)	%Growth in production of Petro-products	Consumption of Petro-products (MMT)	%Growth in consumption of Petro-products
2007-08	149.472	7.02	128.946	6.79
2008-09	155.148	3.80	133.599	3.61
2009-10	184.608	18.99	137.808	3.15
2010-11	194.821	5.53	141.040	2.35
2011-12	203.202	4.30	148.132	5.03
2012-13	217.736	7.15	157.057	6.02
2013-14	220.756	1.39	158.407	0.86
2014-15	221.136	0.17	164.987	4.15

Note: Production of petroleum products includes petroleum products from fractionators. Consumption of Petroleum products excludes refinery fuels and includes imports also.

Import of Crude Oil during 2014-15 was 189.432 MMT valued at Rs. 6,87,350 crore which marked a decrease of 0.10% in quantity terms and 20.53% decrease in value terms over the same period of last year. The decline in value terms is related to reduced crude oil prices by around 50% from June 2014 to Dec 2014. During the year 2013-14 the import of crude oil was 189.238 MMT valued at Rs.8,64,875 crore. The average international crude oil price (Indian Basket) was US$ 84.20/bbl. during April-March,2014-15 as compared to US$ 105.52/bbl in the same period of 2013-14, i.e. lower by 20.20% as compared to the same period last year. During the last 6 months, there is continuous declining trend in the price of crude oil in the international market. The price of Indian basket crude oil which was at $111.84/bbl on 19thJune 2014, has continuously decreased thereafter to US$ 53.64/bbl on 31st March,2015. The trend in growth of crude oil imports and crude oil international (Indian Basket) prices is shown in Table-1.3.

Table 1.3: Imports of crude oil and average crude oil prices [1]

Year	Imports of crude-oil (MMT)	% Growth in imports of crude-oil	Average crude-oil (USD/bbl.)	% Growth in average crude-oil prices
2007-08	121.672	9.12	79.250	26.88
2008-09	132.775	9.13	83.570	5.45
2009-10	159.259	19.95	69.760	-16.53
2010-11	163.595	2.72	85.090	21.98
2011-12	171.729	4.97	111.890	31.50
2012-13	184.795	7.61	107.970	-3.50
2013-14	189.238	2.40	105.520	-2.27
2014-15*	189.432	0.10	84.200	-20.20

*Import value is provisional and crude price is on average basis.

The trends in quantity of Petroleum Products and LNG imports & exports are presented below in Table1.4. As conspicuous, imports of crude oil have increased steadily, despite considerable variations in international prices of crude oil, primarily to meet domestic demand of a burgeoning economy. During April-March, 2014-15 imports of petroleum products were 20.423 MMT valued at Rs.72,778 crore which shows an increase of 22.16% in quantity terms and 2.45% decrease in value terms against the same period of previous year. The quantity of petroleum products imported during 2013-14was 16.718 MMT valued at Rs. 74,605 crore. During April-March, 2014-15 the exports of petroleum products were 63.928 MMT valued at Rs.2,88,563 crore which shows a decrease of 5.80% in quantity terms and 21.65% decrease in value terms against the exports of 67.864 MMT valued at Rs. 3,68,279 crore for the same period of last year. During April-March, 2014-15 the import of LNG is

Table 1.4: Imports & Exports of Petroleum products [1]

Year	Imports of petroleum products (MMT)	% Growth in imports of petroleum products	Exports of petroleum products (MMT)	% Growth in exports of petroleum products	Imports of LNG (MMT)	% Growth in imports LNG
2007-08	22.462	25.25	40.779	21.28	8.320	22.17
2008-09	18.586	-17.26	38.944	-4.50	8.060	-3.13
2009-10	14.665	-21.10	51.155	31.35	9.148	13.50
2010-11	17.379	18.51	59.077	15.49	9.931	8.56
2011-12	15.849	-8.80	60.837	2.98	13.214	33.06
2012-13	15.774	-0.48	63.408	4.23	13.136	-0.60
2013-14	16.718	5.99	67.864	7.03	13.032	-0.79
2014-15*	20.423	22.16	63.928	-5.80	15.470	18.71

*Provisional

15.470 MMT valued at Rs. 63,110 crore which marked an increase of 18.71% in quantity terms and 18.39% increase in value terms against imports of13.032 MMT of LNG, valued at Rs. 53,307 crore was imported for the same period of previous year.

Fig. 1.1and 1.2 shows the region-wise production and consumption of petroleum in the world respectively, during year 2014-15. The total estimated production of crude oil in the world has increased from about 3950 MMT in 2007-08 to about 4220 MMT during 2014-15. The geographical distribution of total world production during 2014-15 across major regions reveals that Middle East accounted for the highest share (31.74%), followed by North America (20.54%), Europe & Eurasia (19.77%), Asia Pacific (9.40%), Africa (9.29%) and South & Central America (9.26%).

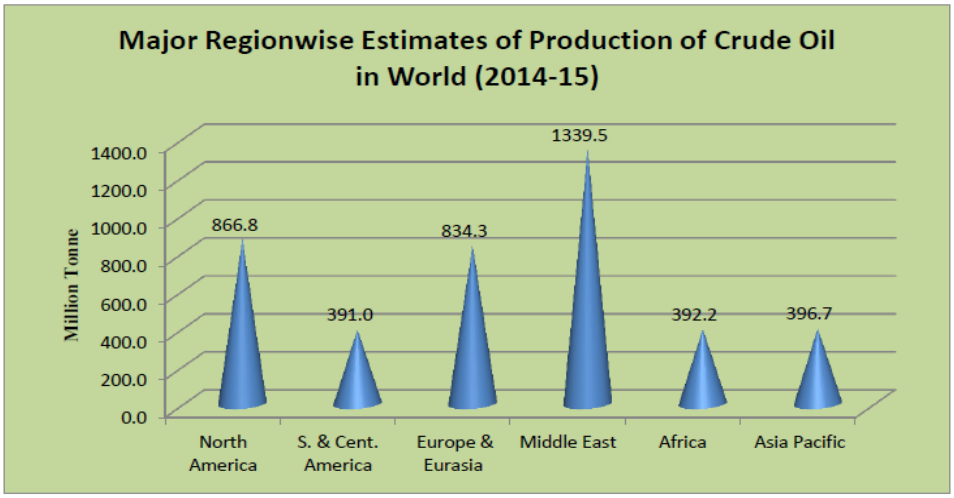

Fig. 1.1: Major region-wise production of crude-oil(estimated)

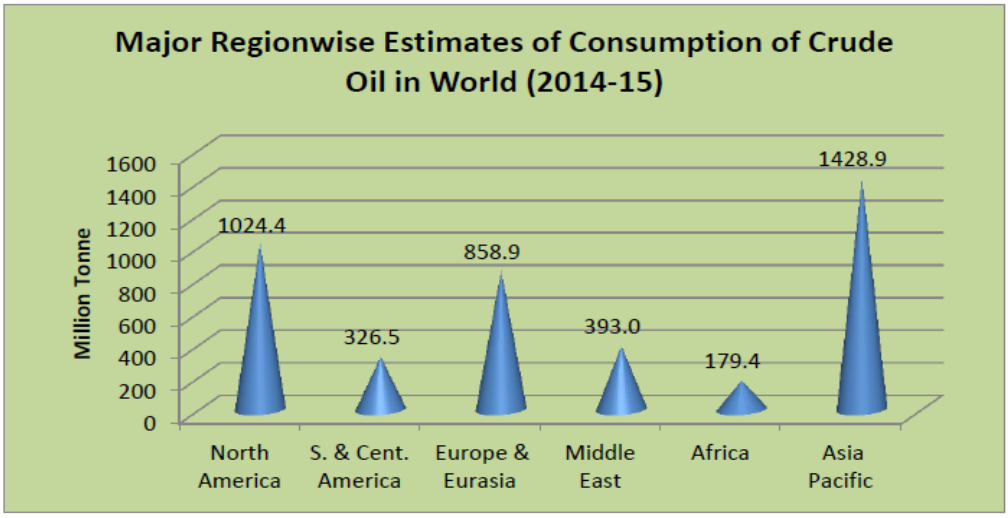

Fig. 1.2 Major region-wise consumption of crude-oil(estimated)

Based on the International Energy Agency (IEA)energy balances for the world, Figure 1.3 shows the shares of the various sectors within the world, total final consumption (TFC), and how they evolved over time. Although these shares vary greatly by country- industry, transport and residential are the largest end-use sectors globally, with the share of transport increasing over time at the expense of industry, and the share of residential remaining stable.

When looking at the share of each energy source in the consumption of the transport sector, as shown in Figure 1.4, oil has historically been the predominant energy source, with global shares higher than 90%. Conversely, transport drives global demand for oil, accounting for almost two-thirds of its final consumption. Examples of other sources, still covering small percentages of transport consumption, include electricity, liquid biofuels and CNG.Figure 1.5 shows that three-quarters of passenger transport relies on motor gasoline, while three-quarters of freight transport relies on diesel.

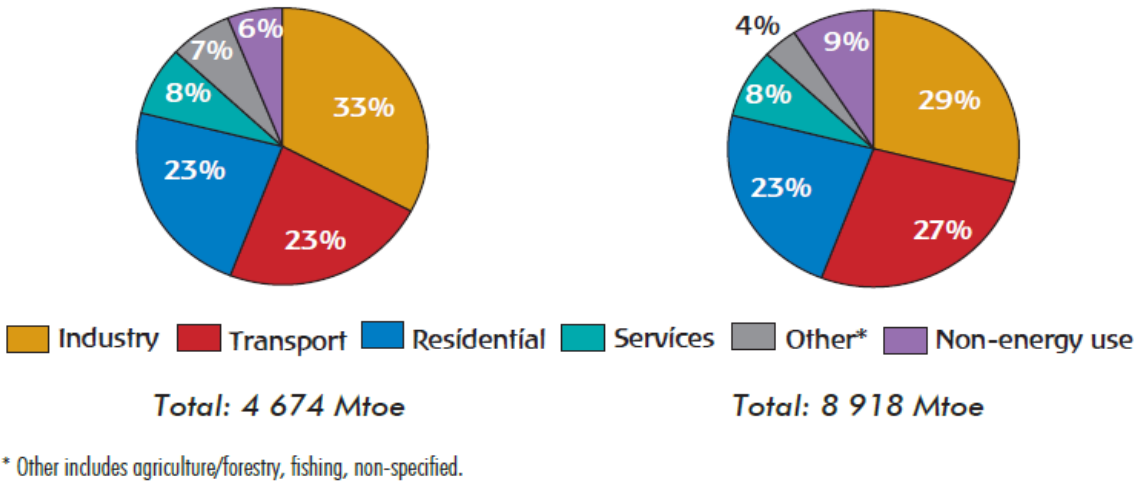

Fig. 1.3 Shares of sectors in total final consumption for the world (1973 and 2011)

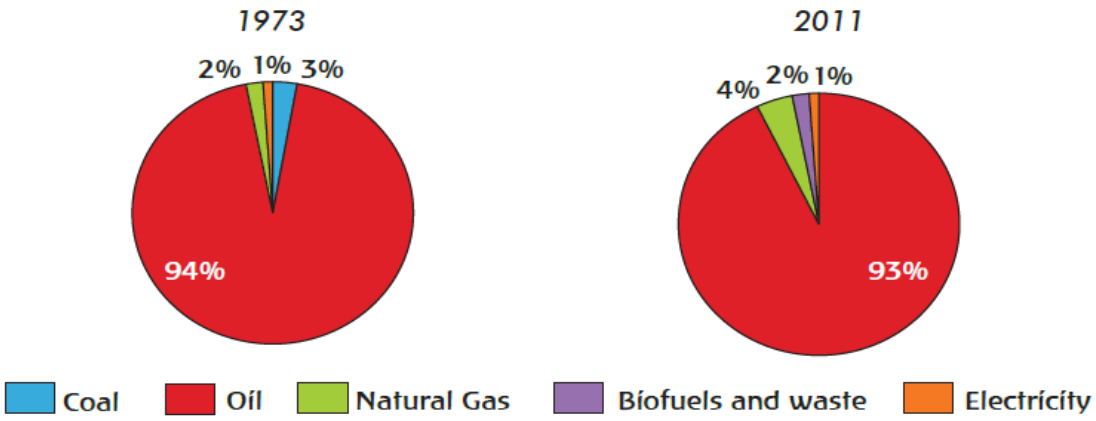

Fig. 1.4Share of the various sources in the world transport energy consumption

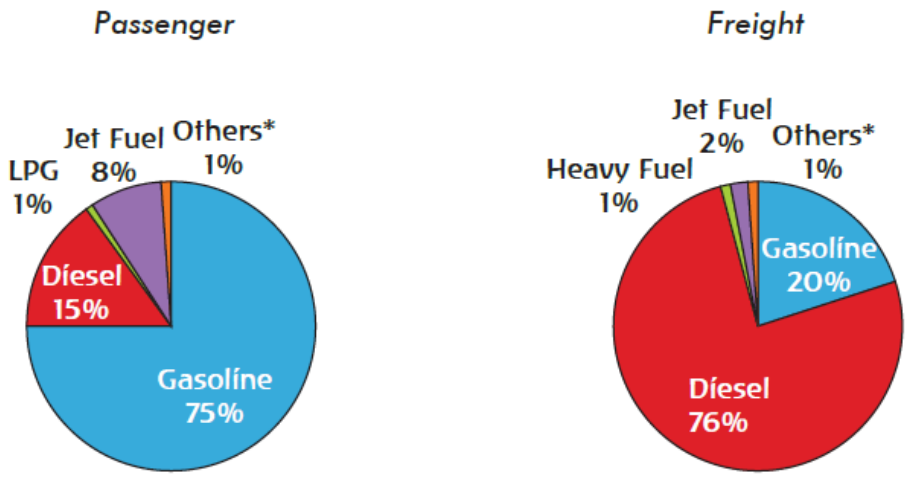

* Others includes heavy fuel, natural gas, electricity and coal (passenger); and liquefied petroleum gas, natural gas, electricity and coal (freight).

Fig. 1.5 Energy consumption by energy source for passenger transport and freight transport (for a total of 23 OECD countries, 2010)

The petroleum fuels play a significant role in the development of industrial growth, transportation, agricultural sector and to meet many other basic human needs. But, ever increasing energy demand, problem of environmental pollution and depletion of fossil fuel resources inevitably necessitate not only the optimum utilization of exhaustible fossil fuel but the development of renewable energy resources. Hence, the scientists are looking for alternative fuels to fulfill the energy demand of the world.

1.2 Various Alternate Fuels

Alternative fuels possess the potential to address many of the current social problems and concerns ranging from energy-scarcity and reliance on depleting fossil fuels to the deteriorating environmental conditions and challenges to tread a path of sustainability as a whole. Researchers have focused their attention on the development of alternative fuel sources in various countries with particular emphasis on the bio-fuels that not only reduce the greenhouse gas emissions but also has an added advantage of being renewable fuels that can be replenished through the growth of plants or production of livestock [2]. Bio-fuels made from agricultural products are oxygenated by nature and offer several benefits such as, opportunity of better energy security, greenhouse gas (GHG) emissions reduction, declining reliance on oil imports and strengthening of indigenous agro-based industries thus, boosting rural economy. Selection of an alternate fuel depends upon various factors such as (a) relative cost of the fuel (b) availability and current use of the fuel (c) operational efficiency and emissions (d) area of use etc. Based on these factors the possible alternate fuels are alcohol

(methanol or ethanol), hydrogen, liquefied petroleum gas (LPG), compressed natural gas (CNG), bio-gas and bio-fuels (mainly biodiesels).

Liquefied petroleum gas (LPG) is a mixture of hydrocarbon gases that are primarily butane, propane and traces of propylene and butylene that possesses the advantage of abatement of obnoxious pollutants, improved engine life[3] due to decrease in lubricating oil deterioration and reduced noise levels as compared to conventional fossil fuels. The high molecular weight of LPG that is more than that of air due to which it settles down when exposed to atmosphere forming an explosive mixture near ground level and hence hazardous. Moreover, the energy density per unit volume of LPG is lower than either petrol or diesel.

Compressed natural gas (CNG) is mainly methane (80 to 95%) with a small percentage of ethane, butane, propane and other paraffins along with carbon dioxide, nitrogen and hydrogen sulphide etc. It is an environmentally clean fuel and can be used in both petrol and diesel engines. It is widely available, has better combustion characteristics than conventional fuels and burns clean, emitting negligible GHGs. CNG being lighter than air, can be stored in overhead spaces. The high pressure of approximately 200 bar that is required for storing and dispensing CNG is the major safety concern. Sudden release of CNG due to damage from collision or equipment failure can prove to be fatal[4]. Further storing of CNG at such a high pressure requires heavy cylinder that makes the vehicle bulky and hence a costly affair.

Producer gas is a mixture of carbon monoxide, hydrogen and methane together with carbon dioxide and nitrogen. It is generated from solid fuels such as wood, charcoal, coal, peat and agricultural residues. Basically, producer gas is made when a thin stream of air passes through a bed of glowing coals. The coals may come from the burning of wood, charcoal, coke, coal, peat or from wastes such as corncobs, peanut shells, sawdust, bagasse and paper. Small size CI engines fuelled with producer gas can be employed for farm applications with considerable saving in cost. However, the main drawback associated with the use of producer gas is increase in exhaust CO and smoke.

Biodiesel refers to vegetable oil and their derivatives, especially methyl esters. Vegetable oils can be converted into their methyl esters via a transesterification process [5-6] in the presence of a catalyst, i.e. potassium and/or sodium alkoxides as catalysts. Transesterification process not only lowers the viscosity of oil but offers a less expensive way of transforming the large, branched molecular structure of bio-oils into smaller, straight-chain molecules of the type

required in CI engines. The renewable characteristics and non-polluting attribute of vegetable oils as opposed to conventional diesel render it a technically competitive over other alternative fuels. Biodiesel is not much popular now-a-days due to filter clogging and cold weather engine starting problems.

Biogas can be obtained from several sources including the decomposition of organic material. It is composed of methane (CH_4), carbon dioxide (CO_2), air, ammonia, carbon monoxide, hydrogen sulfide gases, nitrogen and oxygen. As compared to conventional fossil fuels, the biogas generates less deposits and exhibits clean burning characteristics as compared to conventional fossil fuels. It offers advantages of easy starting, reliable idling and smooth acceleration. Though the characteristic of being lighter than air makes it an inherently safe fuel, but the problem associated with the storage of biogas still persists. The requirement of large area for the installation of biogas plants and increase in GHG emissions restricts its use for stationary engines only.

Biomethane (96% CH_4) is a gas from biogas. It is obtained by withdrawal of water vapor, carbon dioxide, hydrogen sulfide and has high power combustion.

Hydrogen can be manufactured from water with either fossil or non-fossil energy sources or synthesized through thermochemical conversion processes, such as pyrolysis, gasification and steam gasification. Hydrogen-powered fuel cells are an important enabling technology for the hydrogen future and offer more efficient alternatives to the fossil fuels[7-11]. Hydrogen has the potential to solve two major energy problems: reliance on petroleum and greenhouse gas emissions. Though, hydrogen is currently more expensive than conventional energy sources but different technologies are being developed to produce hydrogen economically from biomass technologies.

Alcohols are used as major fuel substitute for IC engines and are produced by fermentation of biomass (enzyme action on biomass in absence of oxygen). Alcohols are attractive alternative fuels because they can be obtained from both natural and manufactured sources. Alcohol can be manufactured from grain and certain waste products and as petroleum supplies become depleted, it will possibly become an increasingly important fuel. Methanol and ethanol are two kinds of alcohols that seem most promising.

1.3 Challenges of Biofuels

Injudicious use of fossil fuels which has decimated the huge reserves of fossil fuels due to ever increasing energy demand have resulted in unprecedented levels of greenhouse gas emissions. Among the alternative fuels, bio-fuels holds the key of sustainability. But, bio-fuels has certain drawbacks. The production of biofuel involves a change in land use that may cause additional emission impacts and need to be taken into account while calculating the GHG balance. The land-use change can be: (a) direct, as when biofuels feed stocks are produced on land that was previously forest (b) indirect, when biofuel production displaces the production of other commodities which are then produced on land converted elsewhere (perhaps in another region or country).In a scenario, in which production costs are strongly coupled with oil prices, they would remain slightly more expensive than fossil fuels. Scale and efficiency improvements will reduce biofuel production costs over time. In a low-cost scenario, most biofuels could be competitive with fossil fuels by 2030. A key non-economic barrier to development of biofuels is uncertainty regarding their sustainability. The controversial issues related to competition with food production and the potential destruction of valuable ecosystems has rendered the development of biofuels that concerns all forms of bioenergy and pertains to agricultural and forestry sector as one of the most difficult conundrums for the researchers.

For all biofuels, there is scope for cost reductions that will help to improve competitiveness with fossil fuels and drive commercial deployment. Co-location with existing biofuel plants, power plants or other industrial facilities not only reduces capital costs but also offer the advantages such as more efficient use of by-products, reduced conversion costs due to evolution of better technologies and improvement of conversion efficiency. Although some low-carbon and energy-efficient technologies are competitive today, many others are considerably more expensive than their fossil-based alternatives that need to be addressed not merely by carbon pricing but by the intervention of the government with targeted technology policies to mitigate the cost-competitiveness gap.

1.4 Alcohol as alternative fuel

Alcohols are examples of the most attractive alternative non-petroleum fuels used in internal-combustion engines. Significant research have been conducted investigating the use of alcohols in spark ignition engines in the past, little attention has been given to the utilization of alcohols in diesel engines. At the early stage, poor fuel economy and low ignitability were

the main barriers to apply alcohol fuel on diesel engines. Since late 1990s, alcohols, mainly ethanol and to a much lesser extent methanol, have been considered as alternative fuels for diesel engines [12-13]to modify their emission characteristics. Methanol is produced by distillation of wood distillation of coal or by natural gas and petroleum gas. Ethanol is produced mainly from biomass transformation or bioconversion. Ethanol can also be produced by synthesis from petroleum or mineral coal. Ethanol is renewable fuel and can be obtained from perennial sources viz., plants and live-stocks and thus help to achieve energy security and sustainability.

1.4.1 Advantages of alcohol

a) *Higher flame speeds and extended flammability limits*: Formation of more number of moles of exhaust gases, enhanced flame speeds and higher heat release rate results in alcohol fuelled engines with improved fuel conversion efficiency. Wider flammability limits of alcohols permit smooth engine operation even at very lean mixtures.

b) *Miscibility with water/hydrocarbons*: The alcohols mix in all proportions with water due to the polar nature of OH group. Methanol is not miscible with hydrocarbons and separation ensues readily in the presence of small quantities of water, particularly with reduction in temperature.

c) *High latent heat of vaporization*: The high latent heat of vaporization of alcohols cools the air entering the combustion chamber of the engine thereby increasing the air density and mass flow. This may lead to increased volumetric efficiency and reduced compression temperatures. However, the high heat of vaporization and constant boiling point make cold starting very difficult with neat alcohols. The problem is not as severe, as in case of alcohols blended with gasoline. Ethanol has a constant boiling point of 80 °C (78.8° C). Gasoline which has a high vapor pressure (therefore highly volatile) can be used for cold start. Low volatility of alcohols is indicated by high boiling point and high flash point.

d) Ethanol has cleaner characteristics as compared to that of fossil fuels. It reduces the GHG emissions and thus mitigate the problem of ozone depletion. Ethanol can reduce unburnt hydrocarbons and nitrogen oxide emissions significantly.

e) Even with the low energy content of the fuel, engine power for a given displacement would be same. This is because of the lower air-fuel ratio required by alcohol. Alcohol

contains oxygen and thus requires less air for stoichiometric combustion. More fuel can be burned with the same amount of air.

f) High oxygen content of ethanol enhances the combustion and thus may increase fuel conversion efficiency up to certain extent.

1.4.2 Disadvantages of alcohol

a) *Storage transportation and other infrastructural requirements*: Automobiles as well as distribution stations would require twice as much storage capacity as required in case of petro-diesel, owing to lower calorific value of ethanol. In the case of diesel/ethanol blends the distribution system needs special attention to avoid problems caused by water as blends are very sensitive to moisture. As a good practice, the ethanol is blended into the diesel at a product terminal just before it is delivered to retail or end-user due to water-solubility of ethanol.

b) *Poor auto ignition*: Due to low cetane number, alcohols have poor auto-ignition characteristics. However, it can be used in gasoline engines with higher compression ratios owing to its high octane number. It has poor cold weather starting characteristics due to low vapor pressure and evaporation.

c) *Vapor lock*: The relatively low boiling points and high vapor pressure of ethanol causes vapor lock particularly at high altitudes on warm summer days thus, leading to a serious problem. High vapour pressure and low viscosity of ethanol as compared to that of pure diesel results in the formation of vapor lock in the fuel delivery system. This vapor lock formation occurs at the locations of lowest static pressure, such as the fuel intake of the injector, resulting in reduced quantity of fuel being delivered to the injector and subsequent cavitation inside the injector. To prevent the vapor lock and subsequent cavitation, the static pressure of the fuel delivery system must be increased either by reducing the size of the restrictive orifice in the diesel fuel return line or by introducing a backpressure regulator to the diesel fuel return line. There is the danger of storage tank flammability due to low vapor pressure. Air can leak into storage tanks and create combustible mixtures.

d) *Charge quenching*: The relatively high latent heats of vaporization of ethanol may cause cooling of the charge at the intake manifold of the engine which necessitates the heating of the intake manifold in cold weathers or for starting conditions. The heating of intake

manifold may decrease the volumetric efficiency of the engine. Further, relatively high latent heats of ethanol can also cause problems in mixing ethanol with air and transporting them through the intake manifold of the engine.

e) *Phase Separation and corrosion*: It absorbs water and may cause phase separation in mixtures even by presence of water in traces. The propensity to absorb water and susceptibility to corrosion are two major issues regarding transport and storage of ethanol. While selecting the equipment for storing and dispensing ethanol, the issue of material compatibility poses challenge. Alcohol is much more corrosive than gasoline on copper, brass, aluminum, rubber and many plastics. This puts some restrictions on the design and manufacturing of engines to be used with this fuel. Fuel lines and tanks gaskets and even metal engine parts gets deteriorated with long-term alcohol use (resulting in cracked fuel lines the need for special fuel tank etc. Methanol is very corrosive on metals.

   Certain single-walled fiber glass reinforced plastic tanks, some gaskets, sealants, adhesives and tank liners may not be compatible. Fuel dispensers must have appropriate elastomers for ethanol and must not use plain aluminum components. Current fuel distribution and storage systems are not watertight and water tends to carry impurities with it. In addition to water-related problems, quantities large enough for transportation through pipelines are difficult to find (ethanol plants are too small). Railroads also face problems with unloading facilities.

f) *Low lubricity*: Ethanol has low lubricity which increases the friction power of the engine. Moreover the lubricity of ethanol is not desired for high-pressure injection pumps in diesel engines.

1.4.3 Use of alcohol in CI engine

There are several techniques involving alcohol-diesel in dual fuel mode. The ignition of alcohol in dual fuel operation is ensured by the high self-ignition diesel fuel. The most common methods for achieving dual fuel operation are:

1. *Alcohol-diesel fuel blend[14-26]:* mixture of the fuels just prior to injection, displacing up to 25% of diesel fuel demand. The addition of ethanol to diesel lowers fuel viscosity and lubricity. Fuel viscosity also affects the atomization and spray characteristics in the combustion chamber. Lower fuel viscosities results greater pump and injector leakage reducing maximum fuel delivery and power output.

2. *Alcohol fumigation[27-33]:* the addition of alcohols to the intake air charge, displacing up to 50% of diesel fuel requirement. Fumigation is a process of introducing alcohol into a diesel engine by means of a carburetor or vaporizer in the inlet manifold. At the same time, the diesel pump operates at a reduced flow. In this process diesel fuel is used for generating a pilot flame, and alcohol is used as a fumigated fuel. At low loads, the quantity of alcohol must be reduced to prevent misfire whereas at high loads the quantity of alcohol must also be regulated to prevent pre-ignition.

3. *Dual injection:* necessitates separate injection systems for each fuel thus, adding to the initial cost. In dual injection systems, a small amount of diesel is injected (prior to injection of alcohol) as a pilot fuel for the ignition source and a large amount of alcohol is injected as the main fuel. This method not only enhances thermal efficiency but lowers NOx emissions with insignificant changes in CO and HC emissions.

4. *Alcohol-diesel fuel emulsion [34]*: using an emulsifier to mix the fuels to prevent separation, displacing up to 25% diesel fuel demand. A hydro-shear emulsification unit can be used to produce emulsions of diesel alcohol. However, the emulsion can only remain stable for 45 s. Moreover, this method suffers the disadvantage of high specific fuel consumption at low speeds and high cost. Therefore, other methods have been developed.

Out of these techniques, fumigation is the simplest one. The problem of miscibility of alcohol with diesel render the use of diesel-alcohol blends unviable. Also, the blends were not stable and separation ensues even in the presence of trace amounts of water. Fumigation is a method by which alcohol is introduced into the engine by carbureting, vaporizing or injecting the alcohol into the intake air stream. This requires the addition of a carburetor, vaporizer or injector along with a separate fuel tank lines and controls.

Fumigation has following advantages:

a) It requires minimum modifications in the engine since alcohol injector is placed at the intake air manifold. Also, flow control of the fuel can be managed by a simplified device and fuel supply system.

b) The alcohol fuel system is separated from the diesel system. This flexibility enables diesel engines equipped with the fumigation system to be operated with diesel fuel only. The engine can be switched from diesel only mode to dual fuel mode and vice-versa by connection and disconnection of the alcohol source to the injector.

c) Fumigated ethanol could increase the power output because alcohol tends to reduce smoke. This is because of good mixing of the injected charge with alcohol.

d) Diesel can be substituted with alcohol up to 50% by fumigation.

1.5 Stationary Diesel Engines

The diesel engine possesses the advantages of robustness, high conversion efficiency and good fuel economy. Diesel-engines are widely used in both stationary and mobile installations. For example, diesel-engines having capacities ranging from 100 to 5000 hp have been employed in industrial and municipal electric generators and in continuous operating pumps (e.g., in oil pipelines). Moreover, these occupy relatively little space compared with steam units since no boiler is needed-a factor of importance aboard ships.

The diesel engine differs from the gasoline engine, as the ignition of fuel is caused by compression of air instead of by a spark and the high compression ratio allows the air in the cylinder to become hot enough to ignite the fuel. Owing to the high temperatures of operation a diesel engine must be water-cooled.

The speed and power of the diesel engine are controlled by varying the amount of fuel injected into the cylinder and not by the amount of air admitted as in the case of gasoline engines. Small and medium-size ships may have several diesel-engines producing as much as 50,000 hp. Heavy-duty land transports such as trains, trucks, buses and tractors are often diesel-powered.

Electric power generators can be classified based on their mode of operation: continuous, prime and standby. Continuous and prime power generators are very similar as they function as the main source of power and are designed to operate continuously or for extended periods of time. The major difference between the two is that continuous generator sets are designed to operate continually with a consistent load while prime generators are designed to operate for long durations at variable load. The other type of generator, standby/emergency is to be run only when there is an outage to the utility grid or the main source of power in a backup situation.

1.5.1 Continuous and Prime generators

Continuous and prime generators are primarily used in remote locations such as mining, oil and gas operations, construction and ships etc. where there is no access to the grid to supply electric power. These are also used when there is a limitation on the amount of electric power that can be drawn from the grid. In rare cases, it may also be cheaper to generate power

through a diesel generator than to buy electric power from the grid. On the other hand, the need for standby power arises when there is a temporary disruption in the primary supply of electrical power, such as, when main grid goes out from a storm.

Like any other machinery running continuously for long hours, continuous or prime generators also need to be rugged to handle the heavy loads supported by them. Additionally, these units have to be able to handle friction between moving parts for longer periods of time and also handle sustained heat generation. This leads to prime generators being more expensive than generators of similar capacities used for standby or backup support.

Continuous/Prime generators typically have a large cooling system. Continuous fuel combustion in the engine generates enormous amounts of heat that is absorbed by cooling water circulated in water jacket which in turn is cooled by a large-sized radiator fitted with a fan. Cooling tower or other elaborate cooling-system is required for very large industrial generators, to make them function efficiently over long periods of time.

The alternator also being subjected to temperature rise due to continuous flow of current through the windings of the alternator. Therefore, the alternator needs to have heavy-duty winding. The cooling system usually restricts the temperature rise of an alternator to 105ºC.Therefore, continuous power generators usually being in continuous operation which makes it difficult to clean its internal parts and components intermittently thus requires heavy-duty air cleaners, air filters and air cleaner assemblies.

Continuous power generators usually operate at lower revolution speeds. This increases the life of the unit significantly and reduces maintenance costs. Continuously operated generators usually provide 25% to 100% of the rated capacity for an unlimited amount of time. Also, these units usually provide only constant output at the rated capacity.

1.5.2 Standby Power generators

Standby power generators typically work for short durations such as a few hours at a time and hence offer two advantages over continuously operated power generators. Standby units have time to cool down naturally when not in operation. Also, maintenance activities can be carried out on standby units without disrupting the power supply. Therefore, these units do not require some of the more elaborate and robust features of continuous power diesel generators. Since standby units work are operational for only a limited period of time, these

units require smaller cooling systems. Some small capacity standby power generators can even be air-cooled, eliminating the need for water circulation.

The alternators of diesel generators can withstand high temperatures for small periods of time but not on a continuous basis. Therefore, alternators of standby power generators are not designed to withstand prolonged exposure to high temperatures. Standby generators usually provide varying outputs for the time period specified. These generators should be connected with an automatic transfer switch so that they can start automatically when there is an outage from the main electrical supply.

CHAPTER-2

LITERATURE REVIEW

This chapter deals with literature review regarding use of alcohol as an alternative fuel for CI engine with or without modification and different techniques which can be adopted for the same. On the basis of data from literature survey and from analysis of properties of alcohol, the research procedure and methodology was decided.

Alcohols such as methanol and ethanol have also received extensive interest for application to diesel engines. Methanol fueled compression ignition engines received active research in the 1980s and the early 1990s. Numerous papers have been published relating the effect of using methanol in CI engines on the exhaust emissions and engine performance. Methanol has a high latent heat of vaporization, it is oxygenated, sulfur free and has high burning speed. When burned at high temperature, it can reduce the smoke and nitrogen oxides emissions of diesel engines. The major problems in the application of methanol in motor vehicles are the difficulty of cold start and the high aldehyde emissions at cold start, warming up and low load operations. The low cetane number of methanol makes auto ignition difficult that renders the application of methanol to diesel engines negligible. Because of limitations on the development of neat methanol compression ignition engines, researchers have focused their attention on the partial replacement of diesel with methanol either premixed with diesel or injected into the air intake. Both methods can be readily applied in diesel engines.

Najafi and Yusaf [35] investigated the application of methanol-diesel fuel blends in diesel engine at mixing ratios of 1:9, 2:8 and 3:7 and observed that the output power and torque of methanol-diesel blends was found to be higher than those of neat diesel fuel. Increase in brake thermal efficiency along with decrease in the exhaust temperature and insignificant change in brake specific fuel consumption blended fuel (BSFC) was noticed for methanol-diesel fuel blends as compared to diesel fuel under almost all operating conditions.

Huang et al.[36] studied the combustion characteristics of a CI engine fuelled with diesel-methanol blends with difference injection advance angles. With the increase in methanol mass fraction in the diesel-methanol blends, the heat release rate in the premixed burning phase increased and the combustion duration of the diffusive burning phase both decreased. For both diesel fuel and diesel-methanol blends, the ignition delay, rapid burn duration and total combustion duration increased with the increase in fuel delivery advance angle. The

peak cylinder pressure, the maximum rate of pressure rise and the heat release rate, all increased as the injection advance angle of the diesel–methanol blends increased.

Yao et al.[37] examined the effects of diesel-methanol compound combustion (DMCC) in two different four cylinder diesel engines, one naturally aspirated and the other turbocharged. Test runs at maximum torque speed were carried out for both engines. The naturally-aspirated engine was operated at 2000 rpm, while the turbocharged engine was tested at 1600 rpm. Diesel alone was used to start the engines at low load operation. The injection method supplied methanol whereas the fixed amount of diesel fuel was regulated with the help of governor. In both cases DMCC was found to decrease BSFC, NOx and smoke emissions while CO and HC emissions were increased.

In another research-work Yao et al.[38]investigated the effects of DMCC and its application to a four cylinder naturally aspirated DI diesel engine operating at various engine loads 10%, 25%, 50%, 75% and 100%) at 2200 rpm and 3200 rpm with and without an oxidation catalytic converter. Methanol was injected into the air intake of each cylinder to form a homogeneous mixture when combined with the intake air and the resultant methanol-air mixture was ignited by diesel. The different combustion characteristics, viz., ignition delay, maximum pressure and peak heat release all enhanced with the application of the DMCC system. The results revealed that the soot and NOx emissions reduced with increase in HC and CO emissions for DMCC system as compared with that of pure diesel case.

Icingur and Altiparmak [39] investigated the influence of different injection pressures (100, 150, 200 and 250 bar) and various fuel CNs (46, 51, 54.5 and 61.5) in a diesel engine and reported that increasing the injection pressure reduced smoke opacity and increased NOx and SO_2 emissions.

Payri et al. [40] observed that retarded fuel injection has little effect on smoke opacity and NOx emissions, but resulted in higher CO and HC emissions with significant adverse effects on BSFC. Retarded fuel injection and exhaust gas recirculation (EGR) together proved very efficient for achieving reduced smoke opacity and NOx levels at low load conditions.

Canakci et al. [41] evaluated the effects of injection timing on the performance, exhaust emissions and combustion characteristics of a single cylinder diesel engine fuelledwith different blend ratio of methanol and diesel fuel. The experiments were conducted at three different injection timings 15°, 20° and 25° CA BTDC and different engine loads (5, 10, 15 and 20 Nm) with a constant engine speed of 2200 rpm. BSFC, BSEC, combustion efficiency,

NOx and CO_2 emissions exhibited increasing trend with the increase in content of methanol in the blend while BTE, smoke number and CO emissions decreased. With the advance of injection timing the smoke number CO and unburned HC emissions decreased whereas, NOx and CO_2emissions increased. The ORG injection timing was found to show the best results for BSFC BSEC and BTE.

Huang et al.[42] evaluated the performance and emissions of oxygenated blends (by adding methanol and a solvent to diesel fuel) in a CI engine under various injection advance angles. As the injection advances, the thermal efficiency of the engine enhanced. NOx concentration in the oxygenated blends increased with the advancement of fuel injection whereas the drop in NOx was evident as the amounts of oxygenates to diesel fuel blends enhanced for given injection advance angles. The influence of the blending of oxygenates with diesel fuel on the NOx concentrations was prominent at high engine loads. The fuel injection advance had insignificant effects on HC emissions with the application of diesel-oxygenate blends. Smoke reduced with the advancement of fuel injection for both diesel fuel and diesel-oxygenate blends. The CO emissions decreased with decrease in injection advance angle at high engine loads, whereas at low and medium loads, the CO emission varied only insignificantly with variation of the injection advance angle but was generally low for diesel-oxygenate blends.

Sayan et al.[43] investigated the influence of injection pressure and timing on the performance and emission characteristics of a single cylinder four stroke DI diesel engine using methanol(5% , 10% and 15%) blended diesel fuel at given engine load (20 Nm) and speed (2200 rpm). With the increase or decrease in injection pressure (180, 200 and 220 bar) or timing (15°, 20°and 25° CA bTDC), BSFC, BSEC and NOx emissions were reported to increase, whereas BTE, smoke opacity, CO and THC emissions decreased. BSFC, brake specific energy consumption (BSEC) and NOx emissions increased while BTE, smoke opacity, CO and HC reduced when the content of methanol in the blend was increased.

Canakci et al. [44] tested the effects of injection pressure on the combustion, performance and emission characteristics of a single cylinder four-stroke naturally aspirated DI engine at different engine loads (5, 10, 15 and 20 Nm) and a constant engine speed of 2200 rpm. The results obtained were similar to their previous study [42]. With the increase in injection pressure (220 bar) increased NOx and CO_2 emissions were observed while the smoke number,CO and HC emissions were found to decrease. The best results for BSFC, BSEC and BTE were obtained at the original injection pressure (200 bar).

Sayin et al.[45]investigated the performance and exhaust emissions of a single cylinder DI diesel engine using methanol blended diesel fuel with varying methanol content (0-15%) for three different injection timings (15°, 20° and 25° CA bTDC) and various engine loads (5 Nm, 10 Nm, 15 Nm and 20 Nm) for constant engine speed of 2200 rpm. The results obtained showed that the injection timing and methanol-content affect the combustion process significantly. The combustion, emissions and engine performance with respect to increasing methanol substitution were similar to those observed in a previous study [42]. Increasing the methanol concentration in the fuel blend led to an increase in the BSFC and decrease in BTE. The best results in terms of BTE and BSFC were obtained for original injection timing. As the injection timing advanced, smoke opacity, CO and HC emissions decreased while the NOx and CO_2 emissions increased.

The effect of a 5% ethanol diesel fuel blend in a three cylinder four-stroke DI tractor engine was studied by Koganti et al. [46]. In the experimental study, NOx emissions were increased but CO and PM emissions were reduced. Further, slight drop in engine power and torque were observed thus deteriorating fuel economy. Different ethanol-diesel blends (5-20%) were reported to increase the BSFC of ethanol blend compared to pure diesel case in a stationary diesel engine operated at a constant speed by Ajav et al. [47]. The application of these blends not only reduced the exhaust gas temperature and lubricating oil temperature (though with insignificant power reduction) but also decreased CO and NOx emissions considerably.

In another investigation, a diesel engine operated at constant speed was fuelled with neat diesel fuel using various ethanol-diesel blends at different compression ratios. The addition of 4% ethanol to diesel fuel increased the power output and efficiency of the engine while BSFC was decreased over a range of compression ratios. The best efficiency was attained at a compression ratio of 21 with an increment ratio over 3.5% [48].

The influence of different ethanol-diesel blends (5-20%) was investigated in a single-cylinder DI diesel engine by Li et al. [49] and it was reported that BTE, BSFC and THC increased while CO, NOx and smoke reduced significantly, in comparison with neat diesel fuel.

Arapatsakos[50] studied the effects of diesel-ethanol blends on exhaust emissions of a tractor engine under full load. The addition of ethanol had positive effects on CO and HC emissions but engine power was observed to decrease.

Rakopoulos et al. [51] investigated the effects of ethanol blends (5 and 10%) on the performance and emissions of a turbocharged DI diesel engine and compared the results with

conventional diesel fuel. HC emissions increased whereas, CO and NOx emissions decreased with the use of ethanol. With the increase in ethanol substitution BSFC increased and BTE decreased.

In another study, Rakopoulos et al. [52] evaluated and compared the performance and exhaust parameters of high speed DI diesel engine at different loads and constant speed (2000 rpm) using ethanol as a supplement to conventional diesel fuel at different blend ratios (5-15%). Significant reduction in smoke density and CO was reported. While NOx emissions decreased slightly with the use of ethanol–diesel fuel blends compared to the neat diesel fuel,considerable reduction in NOx emissions was obtained by increasing the percentage of ethanol in the blend. On the other hand, increasing the content of ethanol in the blend HC emissions increased with slight increase in specific fuel consumption and BTE.

The engine performance and exhaust emissions of a diesel engine fuelled with various ethanol-blended diesel fuels (10%, 20%, 25% and 30%) with and without 5% n-butanol as an additive were studied by Huang et al. [53]. As the amount of ethanol in the diesel-ethanol blends increased, BTE deteriorated. HC emissions exhibited negative effects at all conditions except at full load and high speeds whereas NOx emissions varied at different speeds, loads and blends. Smoke emissions showed positive effects when the engine was fuelled with the blend compared to diesel alone,while CO emissions decreased at and above half loads, but increased at low load and low speed.

Di et al. [54] investigated the emissions of a DI diesel engine fuelled by ultra-low sulphur diesel with ethanol and biodiesel in different fractions, i.e. 2-8%. Slight improvement in BTE was noticed as with the increase in the amount of ethanol and biodiesel in the fuel blends. NOx emissions increased, while HC and CO emissions decreased as compared to those of neat diesel fuel.

Banugopan et al. [55] investigated the performance and emissions characteristics of a DI diesel engine using different ethanol-diesel blend (10-30%) fuels when inlet air was preheated to 40°, 50° and 60 °C. An additive was used for augmenting homogeneity and preventing phase separation in blends. With the increase in ethanol concentration, total fuel consumption and specific fuel consumption reportedly increased. BTE also increased along with rise in CO and HC emissions upon preheating inlet air.

Park et al. [56] evaluated the combustion and emission characteristics of bioethanol-diesel blended fuel by conducting the test-runs in a naturally aspirated single-cylinder DI diesel

engine under various bioethanol blending ratios (10%, 20% and 30%), injection timings and EGR ratios (0%, 20% and 40%). Increasing amounts of bioethanol in the blend prolongs the ignition delay owing to low cetane number and decreased in-cylinder temperature. On the other hand, HC emissions increased as the amount of bioethanol increased and the injection timing was advanced. With the advance of injection timing, differences in ignition delay between pure diesel fuel and diesel-bioethanol blended fuels widens while NOx and soot emissions decreased as amount of bioethanol increased and the use of EGR and bioethanol-diesel blending further increased NOx emissions.

Park et al. [57] analysed the combustion and exhaust emissions characteristics of a four-cylinder diesel engine fuelled with pure diesel and an ethanol-diesel fuel blend. With the advancement of the injection timing, in-cylinder pressure increased. NOx emissions were observed to increase with the engine load and injection timing. CO and HC emissions increased whereas NOx emission decreased with an increase in ethanol blending ratio. On the other hand, low NOx and high CO and HC emissions were observed at low engine loads.

Rakopoulos et al. [58] carried out an experimental investigation to evaluate combustion characteristics using various ethanol-diesel blends (with blending ratio of 5%, 10% and 15%) at different loads in an engine working at a constant speed of 2000 rpm. The application of ethanol blends instead of neat diesel increased ignition delay significantly whereas only slight variation for the rate of maximum pressure and maximum cylinder pressures were noticed.

The effects of ethanol fumigation on engine performance and emissions have been investigated by several researchers. The alcohol fumigation which requires simple modification of engine by addition of carburettor, vaporiser or injector offers ease of switching the engine from pure diesel mode to dual fuel mode and vice versa.Ethanol fumigation resulted increase in HC and CO with considerable reductions in smoke and NOx emissions. Insignificant changes in CO_2 emissions were noticed along with a slight reduction in BTE. The reduction in CO, HC and PM emissions was observed with the use of diesel oxidation catalyst when the exhaust gas temperature was sufficiently high. NOx emissions decreased considerably.

Can et al. [59] assessed the influence of ethanol-diesel fuel blends on diesel engine emissions using different injection pressures (150, 200 and 250 bars)at full load. Increasing the injection pressure of an engine fuelled with an ethanol-diesel blend increased NOx emissions while CO emissions and smoke both decreased.

Lapuerta et al. [60] investigated the stability of diesel-bioethanol blends for use in diesel engines. It was established experimentally that high ethanol content in the presence of water at low temperatures ensues phase separation, which may be prevented by the addition of a fuel additive. Further, it was reported that the blends with bioethanol content up to 10% v/v can be used in diesel engines in areas where winter temperatures rarely fall to -5 °C.

In this context, Lu et al. [61] compared the effects of ethanol-diesel fuel blends and a cetane enhancing additive on BSFC, BTE, exhaust emissions (smoke number, CO, NOx and THC) and combustion characteristics in a single-cylinder diesel engine. The cetane enhancer decreased CO and NOx emissions, whereas BSFC, BTE and THC emissions increased as compared to baseline diesel case. The application of ethanol-diesel blended fuels led to increased ignition delay, decreased total combustion and lower peak combustion temperature.

Kim and Choi [62] investigated the performance and emissions of a common-rail direct injection diesel engine using three different fuels (an ethanol-diesel blend, an ethanol–diesel blend with a CN improver and pure diesel). It was found that the HC and CO emissions of ethanol-diesel blend fuels increased slightly while the smoke emissions decreased, considerably.

Li et al. [63] evaluated the combustion characteristics of a CI engine fuelled with diesel-ethanol blends with and without cetane number(CN) improver. For a given brake mean effective pressure (BMEP) and engine speed the maximum cylinder pressure (P_{max}), ignition delay, premixed combustion duration and fraction of heat release in the premixed combustion phase increased while the diffusive combustion duration fraction of diffusive combustion phase and total combustion duration decreased as the ethanol fractions in the blends increased. The maximum rates of heat release and pressure rise increased with the increase in ethanol fraction in the blends. In addition, the application of cetane enhancer to diesel-ethanol blends diminishes the decrease in ignition delay, cylinder peak pressure, maximum rate of pressure rise and combustion noise.

Sahin et al. [64] investigated experimentally the effects of 2%, 4%, 6%, 8% and 10% (by vol.) gasoline fumigation in a single cylinder direct injection (DI) Diesel engine at the speed of 900 to 1600 rpm and at the selected compression ratios of 18 to 23. The introduction of gasoline into the inlet air was accomplished using an elementary carburetor and thus dispensing any major modification on the engine. The experimental results indicated the maximum increase of 9% and 4% in effective power output and effective efficiency along

with maximum decrease of 4% in specific fuel consumption by the application of gasoline fumigation. The fumigation ratio range of 4-6% was found to be most favorable for gasoline at the selected compression ratios for this engine. The heat balance tests for 18 and 21 compression ratios shows that the heat lost through exhaust decreases until 4-6% gasoline fumigation ratios and decrease afterwards, whereas the heat rejected to the cooling water decreases at low fumigation ratios but at high fumigation ratios, it increases. Other losses generally show an increasing trend at low fumigation ratios.

The study with objective of comparing the effect of applying a biodiesel with either 10% blended methanol or 10% fumigation methanol on a 4-cylinder naturally aspirated direct injection diesel engine operating at a constant speed of 1800 rev/min with five different engine loads was undertaken by Cheng et al [65]. The biodiesel used in this study was converted from waste cooking oil. The reduction of CO_2 and NOx were evident in both cases compared with diesel fuel. Both modes of fuelling with methanol in combination with biodiesel were compared. Only slightly higher brake thermal efficiency at low engine load was evident for the blended mode while at medium and high engine loads, the fumigation mode gives slightly higher brake thermal efficiency. In the fumigation mode, an increase in CO, HC and NOx were found which are disadvantages compared with the blended mode.

Zhang et al.[66] conducted the experiments on a four-cylinder direct-injection diesel engine with methanol or ethanol injected into the air intake of each cylinder to compare their effect on the engine performance, gaseous emissions and particulate emissions at various loads at the maximum torque speed of 1800 rev/min. The experimental results show that the brake thermal efficiency (BTE) deteriorates at low engine load whereas, it improves at high load condition for both fumigation methanol and fumigation ethanol. The influence of fumigation methanol on the BTE was more significant as compared to fumigation ethanol. Compared with baseline diesel fuel, fumigation methanol or ethanol both reduces NOx, and the reduction is more effective with increasing level of fumigation. However, in general fumigation fuels increase the HC and CO emissions. It was observed that in comparison to ethanol fumigation, methanol fumigation has more impact on the in-cylinder gas temperature, the air/fuel ratio, the combustion processes and hence the emissions of the engine.

Zhang et al [67] conducted the experiments on same engine with methanol fumigation to investigate performance parameters and emissions of four-cylinder direct-injection diesel engine at speed of 1920 rpm. For each test-run, the part of the engine load was taken up by

fumigation methanol injected into the air intake of each cylinder to investigate the performance and exhaust emissions characteristics under five engine loads. It was shown that at low engine loads, the brake thermal efficiency (BTE) decreased with increase in fumigation methanol but at high engine loads, insignificant changes were evident in BTE. Significant increase in HC and CO along with decrease in NOx was observed with methanol fumigation. A diesel oxidation catalyst (DOC) reduced significantly most of the pollutant when the exhaust gas temperature is sufficiently high.

Further, Zhang et al. [68] investigated the combined application of fumigation methanol and a diesel oxidation catalyst for reducing emissions of naturally aspirated direct-injection diesel engine operating at a constant speed of 1800 rev/min at five different engine loads. It was shown experimentally that brake thermal efficiency decreased at low engine loads but increased slightly at high loads with increase in fumigation methanol. The fumigation method resulted in a significant increase in hydrocarbon (HC) and carbon monoxide (CO) with decrease in nitrogen oxides (NOx) and smoke opacity.

Chauhan et al. [69] developed a fumigation system for introduction of ethanol in a small capacity diesel engine and to determine its effects on its performance and emission. Fumigation was achieved by using a constant volume carburettor. Different percentages of ethanol fumes with air were then introduced in the diesel engine under various load conditions. In the study undertaken, the author observed that the gaseous emission decreased with ethanol fumigation. The results obtained showed that fumigated diesel engine exhibited better engine performance with lower NOx CO CO_2 and exhaust temperature. Moreover, increase of unburned hydrocarbon (HC) has resulted with ethanol fumigation for the entire load range. Considering the parameters, the optimum percentage was found as 15% for ethanol fumigation.

Hansdah and Murugan [70] investigated the influence of bioethanol fumigation on the performance emission and combustion characteristics of single cylinder four stroke air cooled diesel engine. Bioethanol produced by the fermentation of Madhuca-indica flower was used as an alternative fuel in this investigation. Bioethanol was fumigated at four different flow rates in the suction with the help of a vaporiser and a microprocessor controlled injector. The results of the combustion performance and emissions of the engine running with the bioethanol fumigation were compared with those of the diesel operation. The observed results

suggested an optimum value of 0.48 kg/h of bioethanol fumigation to achieve better performance and lower emissions.

An experimental investigation to explore the effects of using ethanol/water mixtures fumigation into the inlet air on the performance and exhaust emissions of a single cylinder diesel engine was carried out by Morsy et al [71]. Ethanol/water with various mixing ratios (25%, 50%, 75% and 100% by volume) are used as a secondary fuel with diesel as the main fuel. Slight improvements in thermal and exergy efficiencies with ethanol/water mixtures fumigation were observed. The results obtained showed that NO emission decreased with mixtures containing water and exhibited increasing trend with pure ethanol fumigation. Exhaust gas temperatures tend to decrease while CO, HC emissions and fuel consumption tend to increase with all mixtures of ethanol/water fumigation.

Sudheesh and Mallikarjuna [72] carried out experimental investigations of a homogeneous charge compression ignition engine using biogas as a primary fuel and diethyl ether as an ignition improver. The results obtained in this study were compared with those of the available biogas-diesel dual-fuel and biogas spark ignition modes. In another study, Can et al.[73] studied the effects of premixed ratio of diethyl ether on the combustion and exhaust emissions of a single-cylinder homogeneous charge compression ignition direct injection engine. The amount of the premixed diethyl ether was controlled by a programmable electronic control unit. The effect of the variation of energy ratio of premixed DEE fuel on various performance emission and combustion parameters was investigated and the results obtained were compared with neat diesel operation. Hou et al [74] modified two-cylinder direct injection diesel engine for a homogeneous charge compression ignition-direct injection engine fuelled with dimethyl ether and investigated experimentally the effects of premixed ratio on various combustion characteristics.

Jamuwa et al. [75] undertook the experimental investigation to determine the performance, exhaust emission and combustion characteristics of the engine used in the research work, which has been operated with pure diesel and different fumigated ethanol proportions, viz. 10% 20% 30% and 40% (v/v) of total fuel comprising of fumigated ethanol and diesel, that are designated as E0, E10, E20, E30 and E40 respectively. The performance characteristics, exhaust emissions and combustion parameters have been recorded and analysed at different engine loads, i.e., no load to full load. The results indicate 2.5% increase in brake thermal efficiency with ethanol fumigation. It has been found that application of various ethanol

fumigation modes has led to significant reduction in CO_2 (carbon-di-oxide), NOx (oxides of nitrogen) and smoke. However the increase in CO (carbon mono-oxide) and HC (hydrocarbons) have been observed with the use of ethanol fumigation. Moreover, the study reveals that the occurrence of the maximum in-cylinder pressure at full load for different ethanol fumigation levels is delayed by 1-2° CA as compared to that of pure diesel operation. The magnitude of maximum rate of pressure rise and maximum heat release rates respectively, increases by 0.3-0.5 bar/°CA and 3-10 J/° CA as compared to the corresponding values for baseline diesel case.

Further, Jamuwa et al. [76] investigated the thermal performance exhaust emissions and combustion characteristics of small capacity single-cylinder four-stroke water-cooled stationary CI engine using fumigated ethanol. The studies undertaken by few researchers included expensive micro controller operated device for supply of ethanol whereas in the present study simplified low cost ethanol fuelling system was developed. In the present research, the engine has been operated with pure diesel and different ethanol fumigation rates (0.1, 0.2, 0.3, 0.4 and 0.5 kg/hr) that are designated as e0, e1, e2, e3, e4 and e5. The performance characteristics, exhaust emissions and combustion parameters have been recorded and analysed at different engine loads. Further, these parameters have been compared with those of pure diesel case. Fumigated ethanol at different flow rates is supplied to the cylinder during suction with the help of a simplified low cost ethanol fuelling system. With ethanol fumigation, brake thermal efficiency decreased up to 11.2% at low loads due to deteriorated combustion, whereas improved combustion increased efficiency up to 6% at higher loads as compared to pure diesel. Maximum reduction of 22% 41% and 27% respectively in nitrogen oxide, smoke and carbon-di-oxide emissions with simultaneous increase in hydrocarbon and carbon-mono-oxide emissions up to maximum of 144% and 139% respectively for different rates of ethanol fumigation have been observed when compared to pure diesel operation. The rise in peak pressure of cycle, heat release rate and ignition delay along with decrease in combustion duration for different rates of ethanol fumigation have been observed. The increasing fumigation levels of ethanol resulted in increased maximum rate of pressure rise by 0.3–0.5 bar/° CA and the crank angle after top dead centre where peak pressure occurs, shifts by 1-4 ° CA. It is also observed that maximum heat release rate increases by 2-9 J/°crank angle as compared to baseline diesel case.

Coefficient of variance of indicated mean effective pressure increases with ethanol fumigation.

2.1 Research Gap

From the above literature-review, it is clear that several investigations have been carried out to determine performance and exhaust emission parameters of multi-cylinder CI engines using ethanol in fumigation mode, but only a small quantum of work has been undertaken to study the performance, exhaust emissions and combustion characteristics of ethanol fuelled small capacity single-cylinder four-stroke stationary water-cooled CI engine. These diesel fuelled gensets are not only used as a source of backup electricity in urban areas for commercial and industrial purposes, but also as a source of power-generation for agrarian purpose in far-flung areas where grid-electricity is unavailable. Owing to their widespread use in developing countries, the quest to make these diesel engines more efficient and environment friendly has motivated us to develop low cost fumigation system for diesel engines.

2.2 Objectives

(i) To develop a fumigation system to supply metered quantity of ethanol in stationary CI engine operated end utility.

(ii) To carry out performance and emission studies to determine optimum ethanol and diesel ratio that gives lower emission and improved performance.

(iii) To develop a model to predict the performance of ethanol fuelled stationary CI engine in dual fuel mode.

2.3 Research Methodology

Research-work was undertaken to experimentally analyse the performance, emission and combustion parameters for a stationary C.I. engine operated end-utility system in dual fuel mode (alcohol-diesel). The work was divided into the following phases:

(i) Detailed literature review regarding the utilization of alcohol in compression-ignition engines.

(ii) Development of fumigation system consisting of 12 V DC pump.

(iii) Engine test runs to be carried out with the developed and modified system for its accuracy, reliability, durability and leak-proof requirements.

(iv) Engine instrumentation for ethanol-diesel fuelling and experimentation over a wide range of operating parameters such as load, injection timing, % of ethanol etc.

(v) Experimental evaluation of engine performance (Brake Thermal efficiency, Exhaust gas temperature, Effective Equivalence ratio or relative air fuel ratio, Exergy Efficiency etc.), emission (CO, HC, Smoke and NO_x) and combustion characteristics(pressure histories, rate of pressure rise, CoV of IMEP, heat release rate, combustion duration, ignition delay, pre-mixed burn duration) for the following cases:

(a) Different flow rates of ethanol

(b) Different ethanol/total fuel ratio (by vol.)

(c) Different ethanol energy fractions

(d) Different diesel injection timings for constant ethanol flow rate.

(e) Different pre-heating temperatures.

(vi) Evaluation and comparison of engine exhaust emission from ethanol-diesel operated engine at various loads and ethanol flow rates.

(vii) Experimental investigation of various combustion characteristics, viz., for various ethanol fumigation rates.

(viii) Experimental investigation of various performance, emission and combustion parameters for various ethanol fumigation modes, 10%, 20%, 30% and 40% ethanol (by vol.).

(ix) Experimental investigation of various performance, emission and combustion parameters for various ethanol fumigation rates at various loads and injection timing.

(x) To develop a diesel engine CFD model that can simulate the combustion phenomena of the engine and validate the CFD simulation of DI diesel engine with experimental results.

(xi) Determination and comparison of various performance, emission and combustion parameters for different pre-heating temperature of ethanol utilizing heat of exhaust gases.

CHAPTER -3

EXPERIMENTAL SET UP AND METHODOLOGY

In the present research work, the experimental investigation of performance, emission parameters and combustion characteristics for different constant flow rates of ethanol as well as variable flow rates of ethanol have been carried out. The performance parameters viz., brake thermal efficiency, exergy efficiency, volumetric efficiency and exhaust gas temperature have been determined whereas exhaust emission parameters like NOx, HC, CO, CO_2 and smoke opacity have been recorded. The various indicators of combustion behavior of ethanol fuelled CI engine includes in-cylinder pressure histories, rate of pressure rise, heat release rate, ignition delay and combustion duration. The waste heat from the exhaust has been utilized to preheat the ethanol.

3.1 Experimental set-up

The study was undertaken on the experimental engine test rig as shown in Fig 3.1, comprising of a single cylinder water-cooled four-stroke stationary diesel engine (3.7 kW at 1500 rpm) coupled to an AC alternator. The standard properties of the fuel used for the investigation are given in Table 3.1 and the detailed technical specifications of the engine are presented in Table 3.2.

For the measurement of mass flow-rate of air, an air box made of mild steel having suitable dimensions was fitted with the intake manifold of the engine so as to dampen the cyclic fluctuations of pulsating air. A manometer fitted in the air box which showed the readings of the differential pressure across the orifice in terms of water head was used to calculate the rate at which air is sucked-in by the engine. The flow-rate measurement of each fuel was carried out separately with the help of burette. The measured quantity of diesel flows from fuel tank and burette into the engine through fuel pump injector whereas regulated and quantified ethanol was introduced in the intake manifold of the engine with the help of 12 V DC pump normally used in cars to spray pressurised water on the windscreen at high pressure. Speed governor adjusts the quantity of diesel injected to keep the engine speed almost constant at different load conditions. Proximity rpm sensor is used to measure the speed. A series of incandescent bulbs of 100 W each and suitable on or off switches have also been provided to vary the load on the engine alternator. Rota-meters have been provided to measure flow-rate of cooling water. K type thermocouples and multi-channel digital

temperature indicators were used to measure and display the temperature at the salient points of the test rig viz., inlet and outlet of the cooling water, exhaust gas and intake air. All instruments and the methods selected were of standard quality and the error was within the permissible range.

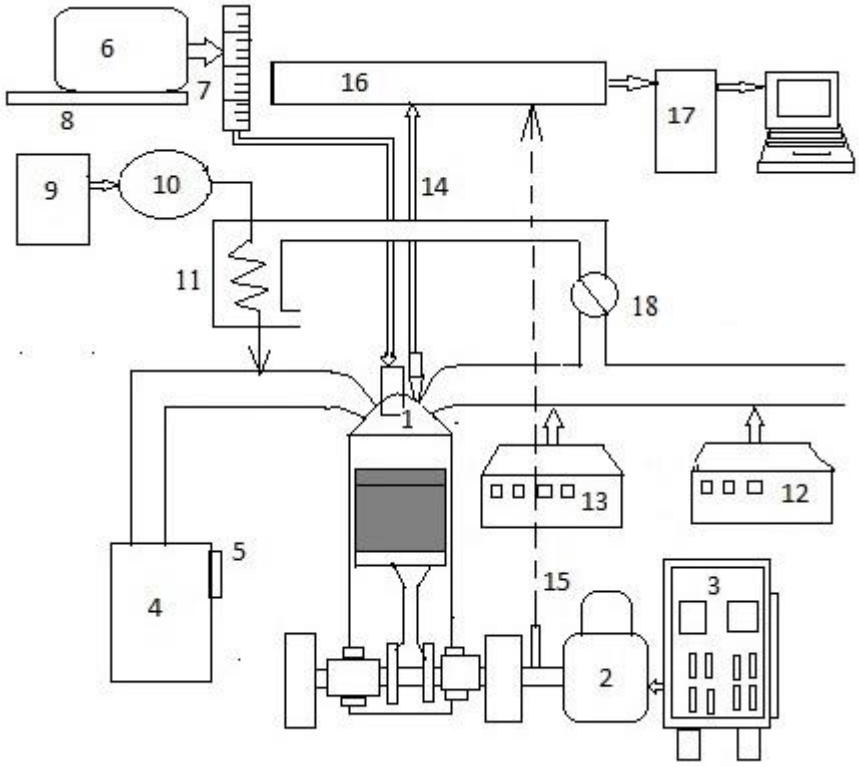

1 .Engine 2 Alternator 3. Resistance load bank 4. Air box 5. Manometer 6. Fuel tank for diesel 7. Burette 8. Strain gauge 9. Fuel tank for ethanol 10. Fuel pump 11. Vaporiser/Heat exchanger 12. Smoke meter 13. Gas analyser 14. Piezoelectric transducer 15. Speed sensor 16. Control Panel board 17. Data acquisition system and computer 18. Exhaust gas regulating valve

Fig 3.1 Schematic diagram of experimental set-up

For acquiring the variation of in-cylinder pressure with crank-angle, pressure pick-up assembly consisting of piezoelectric transducer (Make: PCB Piezotronics Inc. USA) with pressure range of 200 bar, resolution of 0.1 bar and response time of 4 micro seconds is flush mounted to the cylinder head. The charge of the cylinder pressure is converted into an analogue signal using a charge amplifier (Make: Parametric) and it is then converted into a digital signal using the data acquisition system for post-processing of combustion parameters. A crank angle encoder (Make: Delta) with resolution of 1°CA, is mounted on the engine shaft for the measurement of crank angle for every cycle. The interface-unit receives the pressure

signals from the output of charge amplifier that gets stored in its internal memory after being processed and displayed as digital data on computer after completion of 50 combustion cycles.

Fig 3 2. Single Cylinder Constant Speed Stationary C.I Engine

3.2 Experimental methodology

Engine can be started manually using decompression lever. Initially, the engine was started on diesel fuel and run for 20-30 minutes to attain steady state conditions and then measured quantity of ethanol was introduced. The engine loading was changed by varying the load on the engine alternator and different physical quantities viz. temperature at the salient points of the test rig (inlet and outlet of the cooling water; exhaust gas and intake air and other lubricating oil) consumption rates of diesel and ethanol, pressure head at manometer, flow rate of cooling water and engine speed were recorded to calculate the various performance indicators.

Table 3.1: Fuel properties

Parameter	Diesel	Ethanol
Density (kg/m^3) at 15.5 °C	827	789
Molecular weight	190-220	46.07
Boiling point (°C) at 1 atm	180-360	78.4
Auto-ignition temperature (°C)	230	423
Stoichiometric air-fuel ratio	14.5	9
Lower heating value at 25°C (MJ/kg)	42.5	26.8
Latent heat of vaporization at 20°C kJ/kg	250	920
Cetane Number	50	8
Viscosity(cP) at 20°C and1 atm	3.35	1.2
Carbon content (wt%)	87	52.1
Research octane number	-	105
Flash point temp. °C	65-88	13
Hydrogen content (wt%)	13	13.1
Oxygen content (wt%)	-	34.8

Table 3.2. Specifications of diesel engine

Details	Specification
Model	Kirloskar-AV1
Type of engine	Vertical/Single acting 4 stroke totally enclosed high speed compression ignition diesel engine
Rated power and speed	5.0 H.P. (3.75 kW) at 1500 RPM
No. of cylinders	One
Direction of rotation	Counter clockwise (When looking at flywheel)
Bore × stroke (mm)	80 × 110
Compression ratio	16.5:1
Cubic capacity	0.553 litres
Piston (Standard)	Hemispherical
Cooling system	Water cooled
Cooling water flow rate	7 lit/min
Recommended fuel specification	Diesel as per IS: 1460
sfc at rated hp per 1500rpm	245 g/kWh (180 g/bhp/hr)
Lubricating Oil specification	HD- type 3 as per IS: 496–1982
Mode of Starting	Gear end / flywheel end hand-start
Apparatus required for starting	Extension shaft starting handle Decompression arrangement
Lubrication system	Forced feed
Lubricating oil sump capacity (lit)	3.3
Injection timing	23º bTDC
Type of governor	Mechanical centrifugal type
Dynamometer	Eddy current dynamometer at 230 V A.C. 12 amperes at 1500 rpm

(Source: Kirloskar Oil Engines limited)

ARAI certified 5 gas analyser (Make i3sys) was used to analyse NOx, CO, HC, CO_2 and O_2. Out of these emissions, CO, HC and CO_2 were measured by NDIR technique and NOx and

O_2 were measured by electrochemical sensors. The values of HC and NOx emissions are provided in ppm whereas that of other gases in percentage. Smoke in exhaust is measured with the help of ARAI certified smoke meter of i3sys make. Smoke meter works on the principle of attenuation of light beam as it propagates in matter owing to the joint action of the absorption and scattering of light. The specifications of gas analyser and smoke meter respectively are being presented in Table 3.3 and 3.4, respectively.

Table 3.3 Specifications of Exhaust gas analyser

Details	Specifications
Make	i3sys
Gases measured	CO, CO_2, O_2, HC and NOx
Principle	Non-dispersive Infrared for CO, CO_2 and HC electrochemical sensor for $O_2$and NOx
Measuring range	CO: 0 – 15% vol., O_2:0 – 25% vol., CO_2:0 – 20% vol. HC: 0 -30000 ppm, NOx: 0-5000 ppm.
Data Resolution	CO:0.01%, O_2 and CO_2: 0.1%, HC and NOx: 1 ppm.
Accuracy	± 3 % relative± 0.02 % absolute.

The original injection timing of the engine is 23 °CA BTDC. Thickness of advance shim located in connection place between engine and fuel pump is 0.25 mm. The addition/removal of one shim advances/retards the injection timing by 3 °CA. Experiments were carried out for five different injection timing (17°, 20°, 23°, 26° and 29 °CA BTDC) values with decreasing or increasing advance shim. For each test run-from no load to 3.5 kW at load interval of 0.5 kW and then for full load - all the parameters were recorded. Each test was repeated three times and the average of these three results was taken.

Table 3.4. Specifications of Smoke-meter

Details	Specifications
Make	i3sys
Principle	Attenuation of light beam
Geometry	Folded Hartridge geometry
Measurement	Smoke opacity in Hartridge smoke units (HSU) & K (m^{-1})
Range	0 To 100 % opacity in HSU:0 To ∞ K (m^{-1})
Resolution	0.1 % in HSU 0.1 m^{-1} in K
Light Source and Detector	Led & Photocell
Time Constant	1 milliseconds

CHAPTER 4

EXPERIMENTAL RESULTS AND DISCUSSIONS

4.1 Effect of ethanol on engine performance exhaust emission and combustion parameters for constant ratio (v/v) of ethanol and diesel

In the first test-mode, the engine has been operated with pure diesel and different ethanol proportions, viz., 0%, 10%, 20%, 30% and 40% (v/v) of total fuel comprising of fumigated ethanol and diesel, that are designated as E0, E10, E20, E30 and E40, respectively.

4.1.1 Effective equivalence ratio and fuel-energy-consumption

As the composition of combustion products vary significantly with the strength of the mixture and because stoichiometric air fuel ratio depends on fuel composition, effective equivalence ratio is an indicator for defining mixture composition. Effective equivalence ratio (β) is defined by the equation 4.1.

$$\beta = \frac{\left[\left(q_{m,d} \times AFR_{st,d}\right) + \left(q_{m,e} \times AFR_{st,e}\right)\right]}{q_{m,air}} \tag{4.1}$$

The stoichiometric air fuel ratio is 14.5 for diesel and 9 for ethanol. For the different fumigation levels used, the effective equivalence varies from 0.2 to 0.7 at various loads in the present study. In direct injection engines, exhaust smoke limits the equivalence ratio to 0.7 at full load condition.

Fig. 4.1 depicts the variation of effective equivalence ratio at various loads for different percentage of ethanol fumigation. Fig. 4.2 portrays the brake specific energy consumption at varying engine loads for different ethanol fumigation modes. The increased flow rate of diesel with increasing loads results in higher values of effective equivalence ratio is shown in Fig 4.1. It is evident from Fig 4.2 that when percentage of ethanol is increased at particular load, brake specific energy consumption increases for an equivalent power which is significant at lower load. The BSEC of the engine was higher at part loads used as shown in Fig. 4.2. This is due to the poor combustion efficiency of ethanol fuelled dual fuel modes.

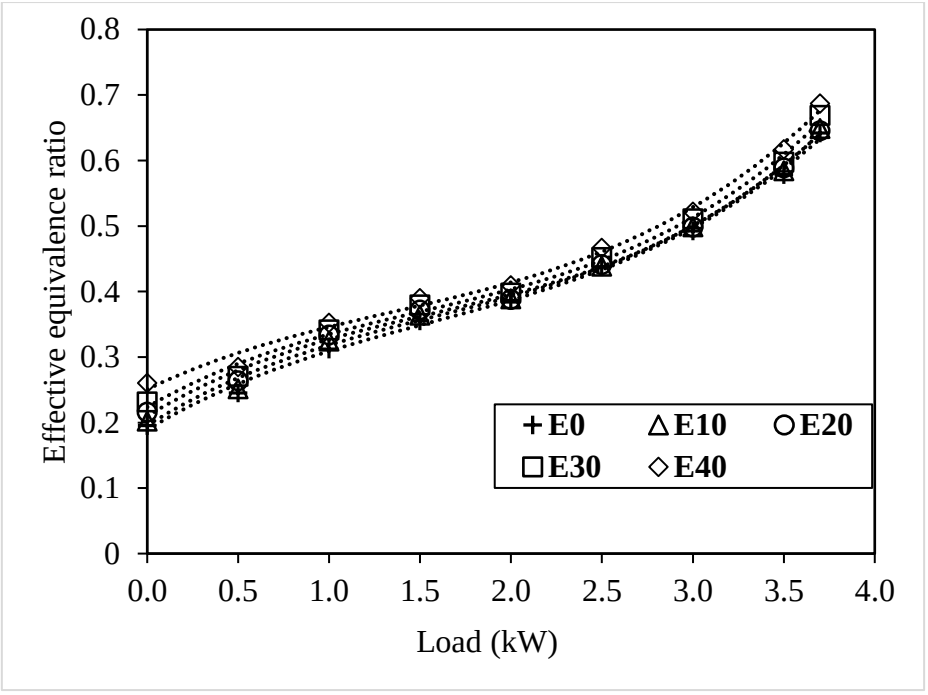

Fig. 4.1 Variation of effective equivalence ratio at various loads for different percentage of ethanol fumigation

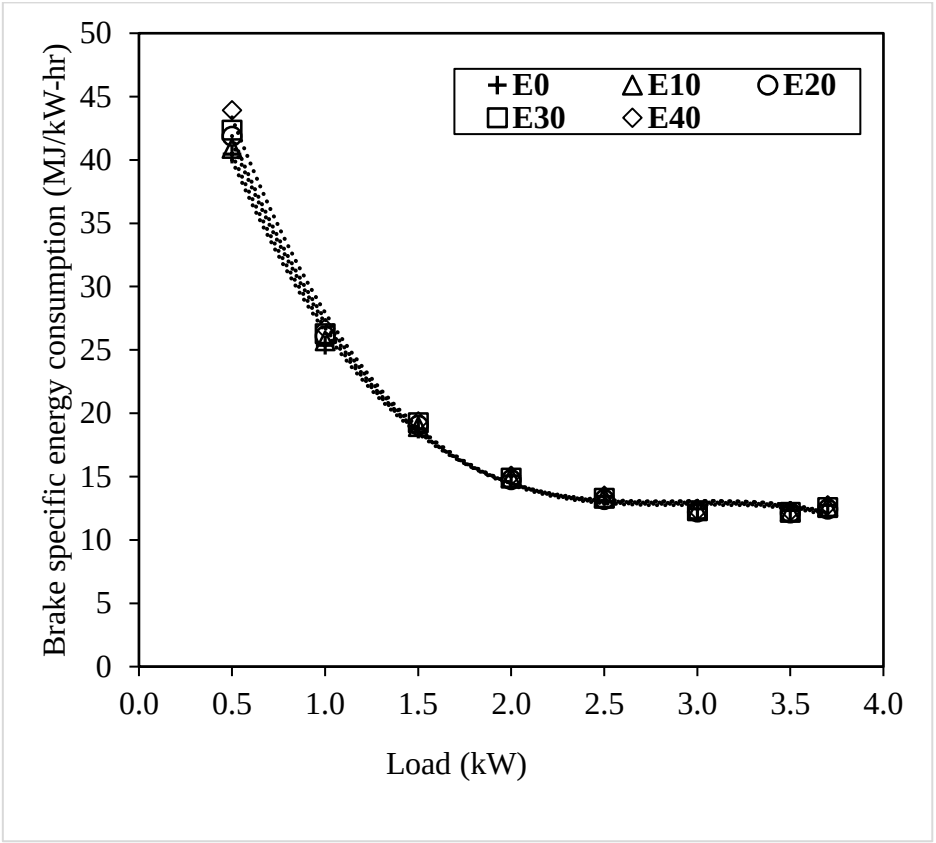

Fig. 4.2 Comparison of brake specific energy consumption at various loads for different percentage of ethanol fumigation

4.1.2 Brake thermal efficiency (BTE)

Brake Thermal efficiency (BTE) is defined as the ratio of useful power (i.e., brake power) to that of chemical energy input rate in the form of fuel(s). Thermal efficiency is expressed by the equation 4.2.

$$BTE = \frac{P_b}{[(q_{m,d} \times LHV_d) + (q_{m,e} \times LHV_e)]} \quad (4.2)$$

Fig.4.3 shows the variation of BTE with different levels of ethanol fumigation for various engine loads. Ethanol fumigation reduces BTE at low engine load and increases it at high engine load compared to diesel fuel. At low loads, decrease in BTE up to 8% was observed, whereas BTE increased up to 2.5% at high loads as compared to E0. In the mid load range, BTE increased marginally.

It is evident that alcohol fumigation decreases the BTE at lower and medium engine load condition and increases the BTE at higher engine load condition. The reduction of BTE which was found to be significant in most of the cases at lower and medium engine load condition, can be explained by attributing the following points:

(a) At low engine loads, low equivalence ratio due to excessively lean mixture causes the deterioration of combustion efficiency and thus reducing BTE.

(b) The large heat of vaporization of alcohol resulting in the cooling of the combustible mixture and thus drop in BTE.

The increase of BTE at higher engine loads can be explained by attributing the following reasons:

(a) The enhanced rates of combustion for homogeneous air/alcohol mixture at high loads facilitates more premixed combustion that tends to increase the BTE.

(b) Excessively lower cetane number of alcohol increases the ignition delay. Hence the energy is released within a very short time resulting in reduction of the heat loss from the engine as there is no sufficient time for transferring heat through the cylinder wall to the coolant.

Alcohol has high laminar flame propagation speed that results into increased premixed combustion which was evident by higher rate of pressure rise and increased in-cylinder pressure values for increasing rate of ethanol substitution during 320 °CA to about 350 °CA.

The increased premixed combustion due to enhanced combustion of homogeneous air-ethanol mixture at higher engine loads increases BTE. Further, the lower cetane number of ethanol and consequently increased ignition delay causes greater heat release rate (HRR) and reduced heat losses from the cylinder wall to the coolant, resulting in increased BTE. Also, the higher oxygen content present in ethanol enhances the combustion with the higher flow rates of ethanol.

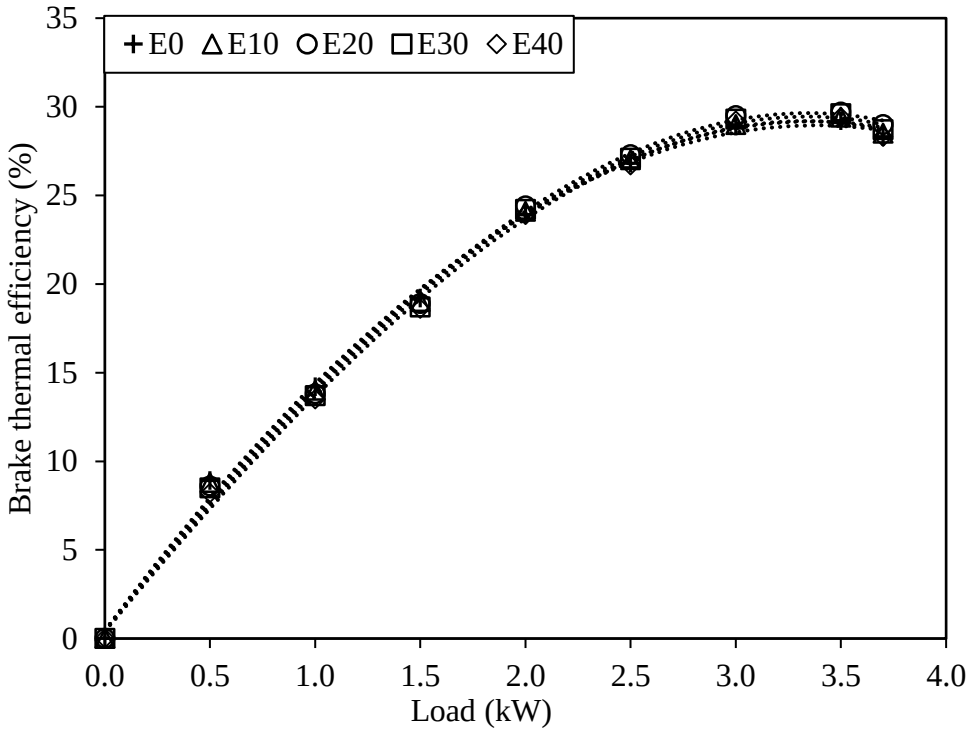

Fig. 4.3 Variation of brake thermal efficiency with load for different percentage of ethanol fumigation

4.1.3 Exergy efficiency

A simple combustion process is an exothermic chemical reaction. The reactants are usually air and fuel and the products that are mainly mixture of common environmental substances. Exergy efficiency of combustible substance may be calculated by the following expression [70,76] given by equation 4.3.

$$\psi = \frac{\dot{Ex}_w}{\dot{Ex}_{in}} = \frac{P_b}{\dot{Ex}_{in}} \qquad (4.3)$$

where, net exergy work rate is equal to the brake power and input exergy rate represents only chemical exergy of fuel (neglecting the exergy rate of air and water). Therefore, input exergy rate [77] is defined by

$$\dot{E}x_{in} = q_{m,d}\varepsilon_d + q_{m,e}\varepsilon_e \tag{4.4}$$

where, $\varepsilon_d = LHV_d\phi_d$ and $\varepsilon_e = LHV_e\phi_e$

The chemical exergy factor [70,77], φ which is equal to the ratio of chemical exergy to the net calorific value for solid and liquid fuels is same as for pure chemical substance having the same ratios of constituent chemicals. φ is defined by the following expression (equation 4.5).

$$\varphi = 1.0401 + 0.1728\frac{h}{c} + 0.0432\frac{o}{c} + 0.2169\times\frac{\alpha}{c}\left(1 - 2.0268\frac{h}{c}\right) \tag{4.5}$$

where h, c, o and α are the mass fraction of hydrogen carbon oxygen and sulphur in the fuel respectively.

The values are presented in Table 3.1 for diesel and ethanol fuels. The mass-fraction of sulphur α, is generally assumed to be zero.

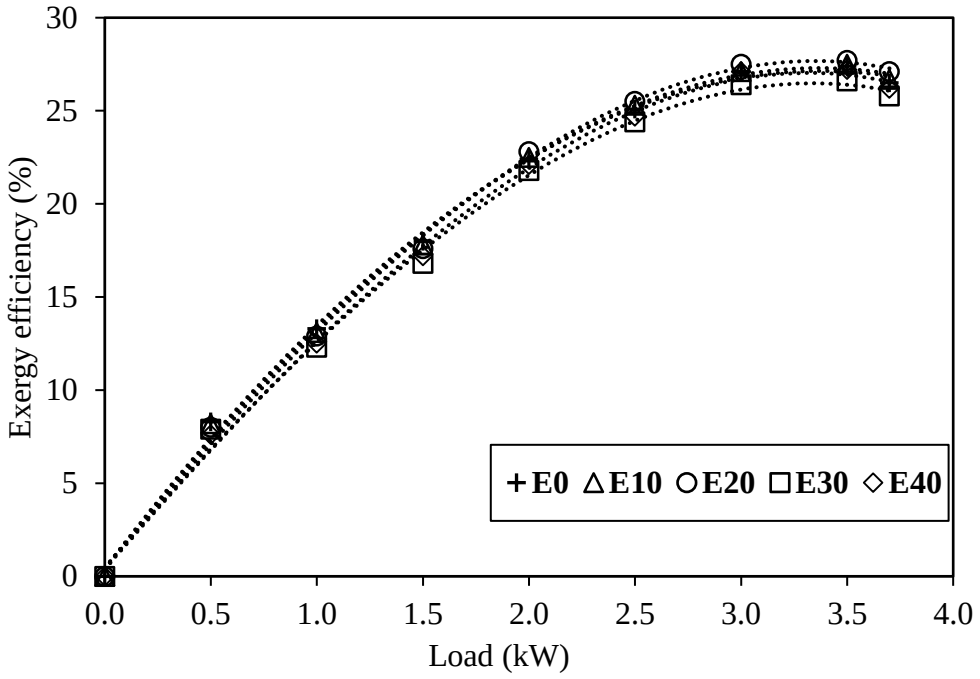

Fig. 4.4 Variation of Exergy efficiency with load for different percentage of ethanol fumigation

Fig. 4.4 shows the variation of exergy efficiency at various loads for different levels of fumigation. The exergy efficiencies of the engine under investigation exhibit similar behaviour to the thermal efficiencies given in Fig.4.3. The exergy efficiencies are slightly lower than the corresponding thermal efficiencies because higher amount of fuel exergy compared to the fuel energy is supplied to the engine. Since the exergy efficiency takes into account not only the first but also the second law of thermodynamics, it provides a better measure of the performance for a thermal system.

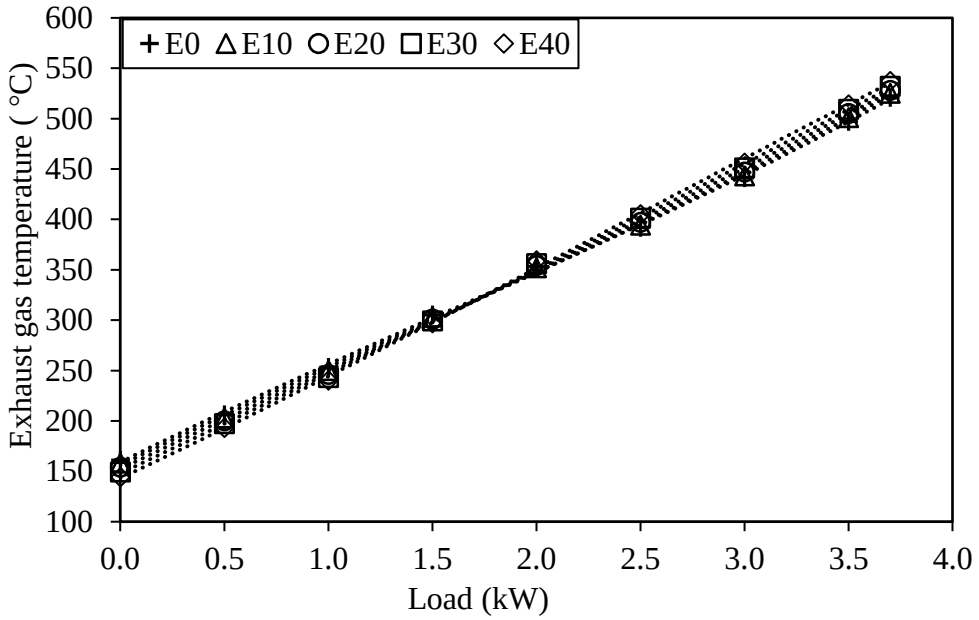

Fig. 4.5 Variation of exhaust temperature at various loads for different percentage of ethanol fumigation

4.1.4 Exhaust gas temperature

Fig. 4.5 shows the variation of exhaust temperature of diesel fuel along with different levels of ethanol fumigation for various engine loads. It is obvious that exhaust temperature increases with the load for diesel as well as for all levels of ethanol fumigation as the heat release rate is increased. The results show that the exhaust gas temperature decreased with increase in ethanol substitution from no load to 1.5 kW which can be attributed to quenching of cylinder charge due to higher latent heat of evaporation of ethanol. But at loads higher than 1.5 kW, the exhaust gas temperature rises with increasing ethanol fumigation. At full load, exhaust temperature of 521ºC was observed for E0 which increased up to 537ºC for E40. The increase in exhaust temperature is caused due to higher release rate caused by greater

availability of oxygen. The increase of exhaust temperature is also attributed to increase in ignition delay that results in delayed combustion.

4.1.5 Volumetric efficiency

The variation of volumetric efficiency with load and level of fumigation is depicted in Fig. 4.6. It is observed from the figure that the volumetric efficiency decreases with load due to increase in displacement of air by vaporised fuel. Moreover, the decrease in volumetric efficiency with increasing level of fumigation is observed due to displacement of more quantity of air due to fumigated ethanol. It is apparent that the factor of increased density of air due to cooling of charge does not have any effect in the increase of volumetric efficiency. With ethanol fumigation, the volumetric efficiency is found to be 1-7.6% lower at all loads as compared to E0.

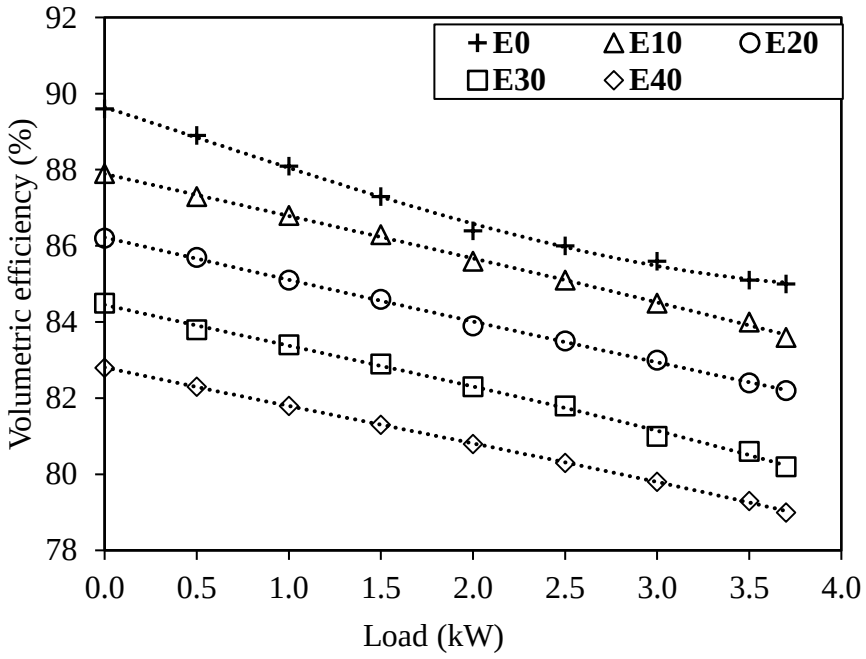

Fig. 4.6 Variation of volumetric efficiency at various loads for different percentage of ethanol fumigation

4.1.6 Oxides of Nitrogen (NOx)

NO_x is common term used for the emissions composed of nitric oxide (NO) and nitrogen dioxide (NO_2). It has been observed that NO_x emission decreases with alcohol fumigation due to quenching of cylinder charge thus, reducing the in-cylinder temperature as compared to diesel fuel. The formation of NO_x in a diesel engine strongly depends not only on the combustion temperature, oxygen-concentration and residence-time of oxygen but also on

engine operating conditions such as, injection timing, load, engine speed and fuel to air-fuel ratio.

The factors that contribute to the decreasing levels of NO_x emissions with alcohol fumigation can be explained as follows. The reduction of NO_x in diesel engine may be attributed to the reduction of combustion temperature due to the high latent heat of vaporization of alcohols especially under very lean conditions. Secondly, reduction in air-fuel ratio though mass of air inducted increases with reduction of engine temperature. At high engine load, the increase in ignition delay and richer mixture tend to reduce the cooling effect. However, at high engine load in the fumigation mode, there is a reduction in relative air/fuel ratio and the diesel fuel is now combusted in a mixture of air and alcohol that adversely affects the availability of oxygen for NO_x formation and ultimately resulting in the reduction in NO_x emission at high loads as compared to pure diesel operation.

However, other determinants may result in the elevated NO_x emissions, which are described in the following text. Increase of NO_x emission increases with increasing level of fumigation may be attributed to oxygenated nature of alcohol and its low cetane number. Oxygen-content in alcohol being higher than that in diesel fuel hence NO_xemission increases. Moreover, the poor auto-ignition properties of fumigated alcohol leads to increase of fuel burned in the premixed mode resulting in increased combustion temperature hence, increased NO_x emissions.

As evident from Fig. 4.7, NO_x reduction of 6 to 16%, 5 to 13% and 2 to 9% at low loads, mid loads and full load respectively, is observed for all levels of fumigation as compared to E0. For E10, E20, E30 and E40, the decrease in NOx of 7.4%, 11.7%, 14.5% and 16% respectively have been recorded as compared to E0 at no load condition; the corresponding decrease at full load are 1.8%, 2.3%, 3.2% and 4.4%. Significant reductions in NOx at no load and low loads is attributed to high latent heat of vaporisation that reduces the combustion temperature. However, at high loads, the increase of heat release rate in the pre-mixed combustion phase opposes the cooling effect and results in marginal decrease in NOx emissions. At given load, with the increase of ethanol substitution, NOx emissions tend to decrease owing to cooling of the charge and increased displacement of air by ethanol vapours.

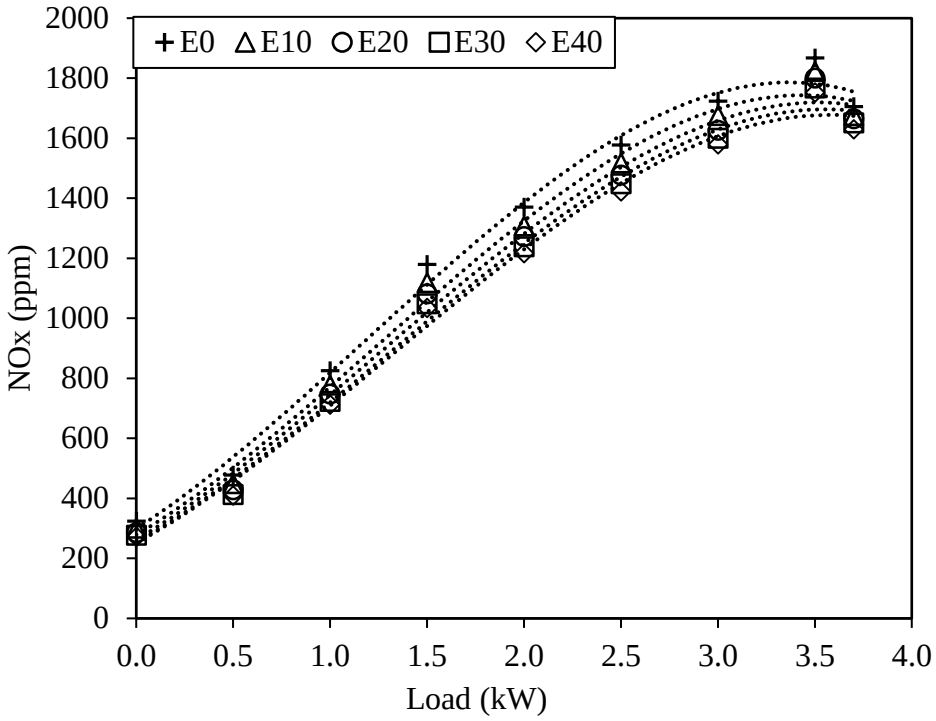

Fig. 4.7 Variation of NOx with load for different percentage of ethanol fumigation

4.1.7 HC and CO emissions

Diesel fuel contains hydrocarbons with high molecular weights and thus high boiling points. The pyrolysis of the fuel compound during combustion process leads to the diesel exhaust composed of unburned and partially oxidized hydrocarbons. In diesel engines, several events like liquid fuel injection, fuel evaporation, fuel-air mixing, combustion and mixing of burned and unburned gases may take place concurrently and combustion is heterogeneous in nature. Overmixing of fuel and air beyond lean flammability limits during delay period, under-mixing of fuel injected towards the end of injection process beyond rich end of flammability, over-penetration of fuel sprays, poor atomized fuel and bulk quenching of combustion due to reduced in-cylinder temperatures during expansion are some of the processes that contribute to the formation of unburned hydrocarbons in diesel engines. The high latent heat of vaporisation of alcohols may slow the vaporisation and also mixing of fuel and air thus, enhancing the levels of HC with increasing level of ethanol substitution. The increase of HC emission may be attributed to the formation of quench layer of unburnt ethanol due to inhibited mixing of ethanol and air particles.

Fig. 4.8 exhibits the increase of HC emissions with engine load for different levels of ethanol fumigation. The HC increase was highest at low loads and lowest at high loads for all the

fumigation percentages of ethanol. In comparison to E0, the increase in HC emission of 42.6%, 63.9%, 86.9% and 149.2% have been observed for E10, E20, E30 and E40 respectively at no load condition. The corresponding increase at full load are 2.5, 7.5%, 17.5% and 27.5%. Over-leaning of the mixture caused due to rapid mixing of fuel with air is an important source of HC emissions at no load and at low loads. Quenching at cylinder walls due to addition of ethanol may result in low wall temperatures and high HC emissions. Unburnt hydrocarbon emission is a useful measure of combustion inefficiency. At high loads, improved mixing and high heat release rate enhances the combustion efficiency, thus reducing HC emissions. HC emissions increases considerably, with increasing rate of ethanol fumigation due to poor combustion attributed to higher latent heat of vaporisation and consequently lower combustion temperature. High ethanol content causes the occurrence of partial burning and misfiring cycles which is indicated by high cyclic variability in the combustion process and same is reflected by moderately high value of CoV of IMEP.

CO, an intermediate product in the combustion of a hydrocarbon fuel, results either due to the deficiency of oxygen or decreased in-cylinder temperature during combustion process, inadequate to support the combustion. The increase in CO emission with the increasing ethanol substitution is the result of incomplete combustion of ethanol-air mixture due to high latent heat of vaporisation. As shown in Fig. 4.9, CO emissions decreased up to certain load and then again increased with the increasing loads. It is explained by the fact that improved combustion with increasing load results into decreased values of CO up to a particular load. But at certain higher load conditions, CO exhibit increasing trend due to rich mixture leading to poor mixing. For E10, E20, E30 and E40, the increase in CO emission of 4.3%, 17%, 36.2% and 53.2% respectively, have been recorded as compared to E0 at no load condition; the corresponding increase at full load are 23.1%, 53.8%, 84.6% and 111.5%. Increase of CO emission with ethanol fumigation was attributed to combustion quenching due to high latent heat of vaporisation thus leading to incomplete combustion. Moreover, the low cetane number renders the fraction of ethanol trapped in crevices, non-ignitable during the expansion stroke thus increasing CO emissions.

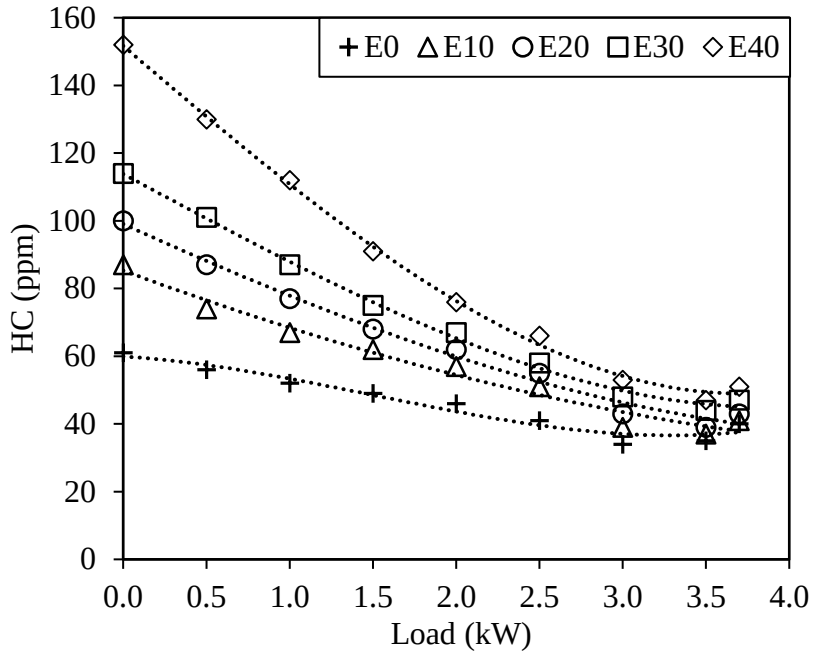

Fig. 4.8Variation of HC with load for different percentage of ethanol fumigation

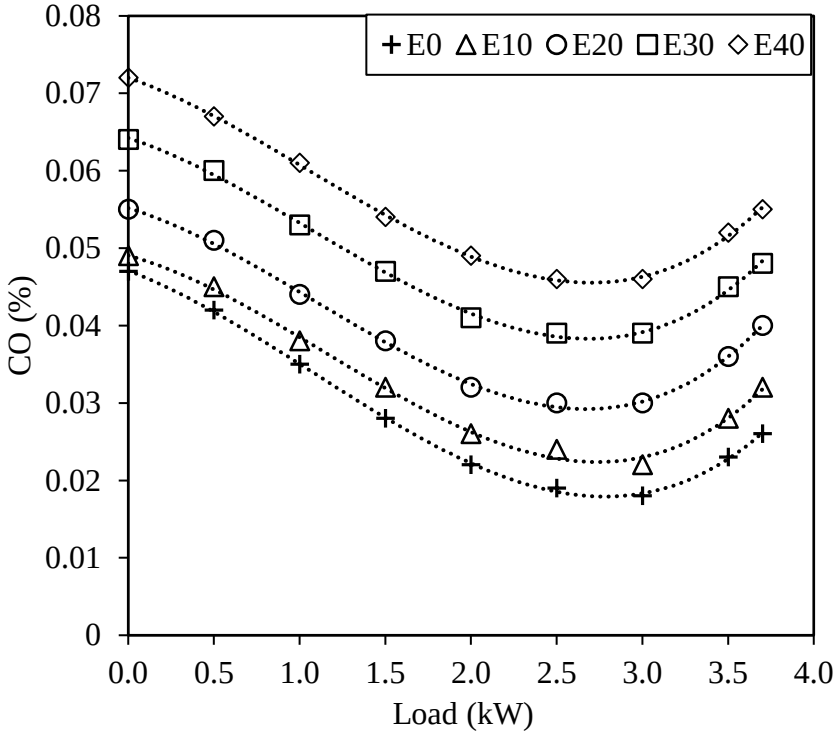

Fig. 4.9Variation of CO with load for different percentage of ethanol fumigation

4.1.8 CO_2 emissions

CO_2, a major greenhouse gas and at higher concentrations is a major contributor to global warming. In comparison to E0, the decrease in CO_2 emission of 5.5%, 10.6%, 14.9% and 18.2%, as shown in Fig 4.10, have been observed for E10, E20, E30 and E40 respectively, at

no load condition; the corresponding decrease at full load are 4.4, 8.4%, 11.9% and 14.5%.As evident, CO_2 concentration is lower at low loads due to poor combustion. The CO_2 concentration increases with the engine load for pure diesel as well as for different levels of fumigation due to enhanced combustion. However, there is reduction of CO_2 concentration when the engine is operated with ethanol fumigation. At low loads, poor combustion decreases CO_2 concentration which increases with increasing load due to improved combustion. With increase in ethanol fumigation, CO_2 concentration decreases due to formation of quenched layer and thus deteriorated combustion. Moreover, at each loading condition, greater the ethanol substitution is applied, the larger the reduction of CO_2 has been observed.

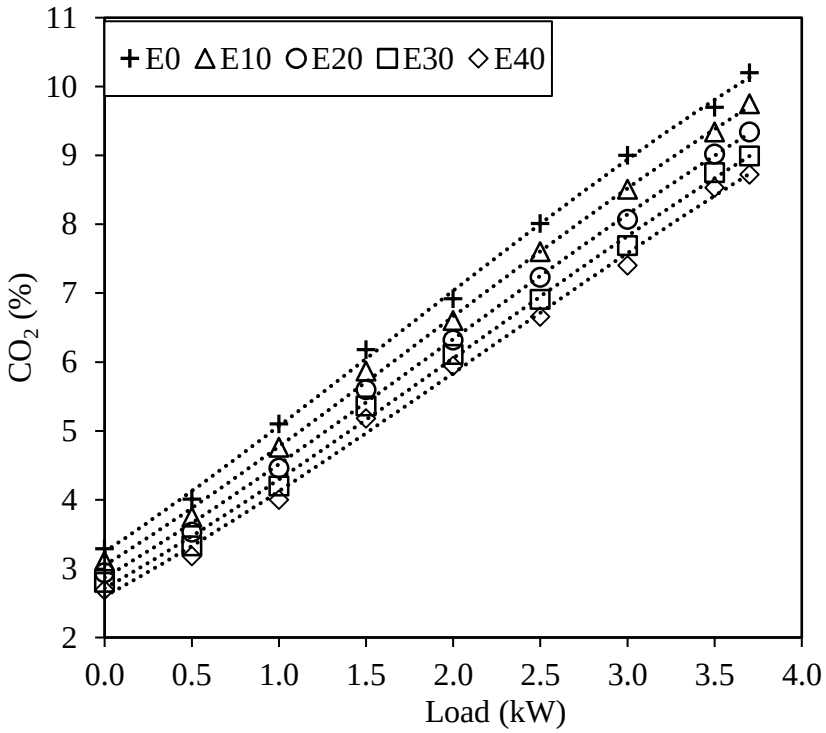

Fig. 4.10 Variation of CO_2 with load for different percentage of ethanol fumigation

4.1.9 Smoke opacity

The smoke is defined as visible product of combustion formed due to lower air fuel ratio and improper mixing thus leading to poor combustion. Smoke might result due to engine design factors such as fuel used, engine rating, injection system characteristics, induction system and governor control. Smoke opacity is an indirect indicator of soot content in the exhaust gases. Smoke-meter quantifies the visible black smoke emission utilizing the physical phenomenon as extinction of a light beam by scattering and absorption.

Fumigation starts pre-combustion reactions before and during the compression stroke resulting in reduced chemical delay because the intermediate products such as peroxides and aldehydes react more rapidly with oxygen than original hydrocarbons. This shortening of delay period inhibits thermal cracking, a factor responsible for soot formation.

Fig.4.11 shows the effect of load and fumigation percentage on smoke opacity. Generally smoke opacity increases with the increase in engine load for pure diesel as well as for various ethanol fumigation modes. Normally, the delay period decreases with increasing load on CI engine. At the engine start conditions, however the delay increases due to the large drop in mixture temperature associated with evaporating and heating the fuel. As load is increased the charge temperature at injection increases thus shortening the ignition delay.

For E10 E20 E30 and E40 the decrease in smoke opacity of 3.7%, 4.7%, 6.8% and 8.2% respectively have been recorded as compared to E0 at no load condition. The corresponding decrease at full load are 5.1%, 10.4%, 16% and 20.8%. With an increase of ethanol fumigation the increase of diesel fuel burned in the premixed mode results in less amount of diesel being burned in the diffusion mode leading to reduction in the smoke emission.

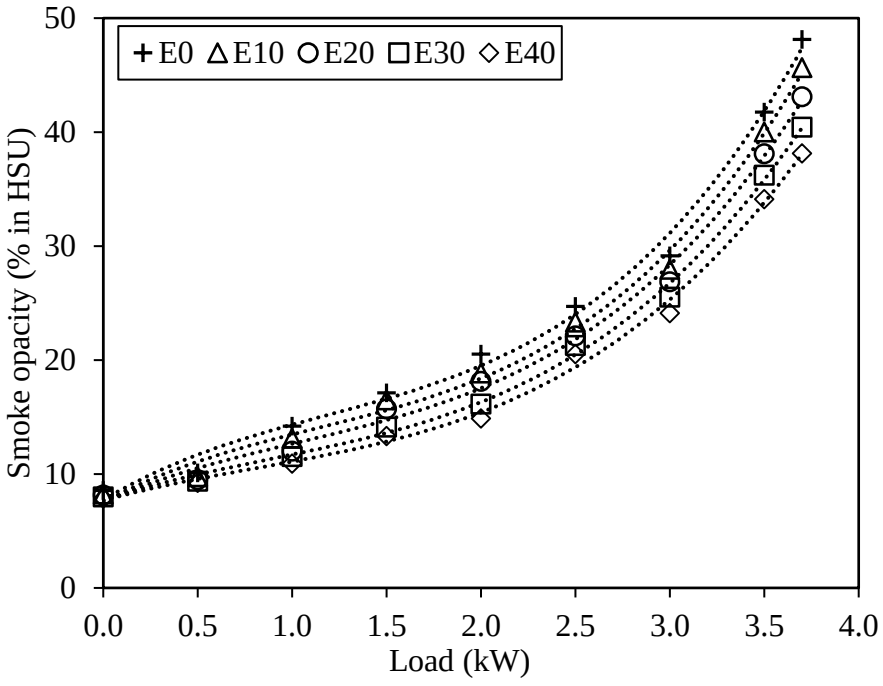

Fig 4.11 Variation of smoke opacity with load for different percentage of ethanol fumigation

4.1.10 Cylinder pressure and rate of pressure rise

The changes in the combustion process is evident with the use of different fuels owing to the physical and chemical differences in their fuel structure. Pressure histories are indicative of

combustion characteristics and engine performance, viz., rate of pressure rise, IMEP (Indicated mean effective pressure), heat release rate, ignition delay and combustion duration. The higher rate of pressure rise may reduce the life of certain engine components and may generate noise.

In-cylinder pressure is one of the important quantity recorded the analysis of which and the derived parameters thereof, furnishes information about the complex process of combustion. Piezo-electric pressure transducer are most commonly used for the purpose of acquiring in-cylinder pressure histories. The transducer is flush mounted to the combustion chamber so that it is directly in communication with combustion gases. The measured cylinder pressure can be displayed by data acquisition system.

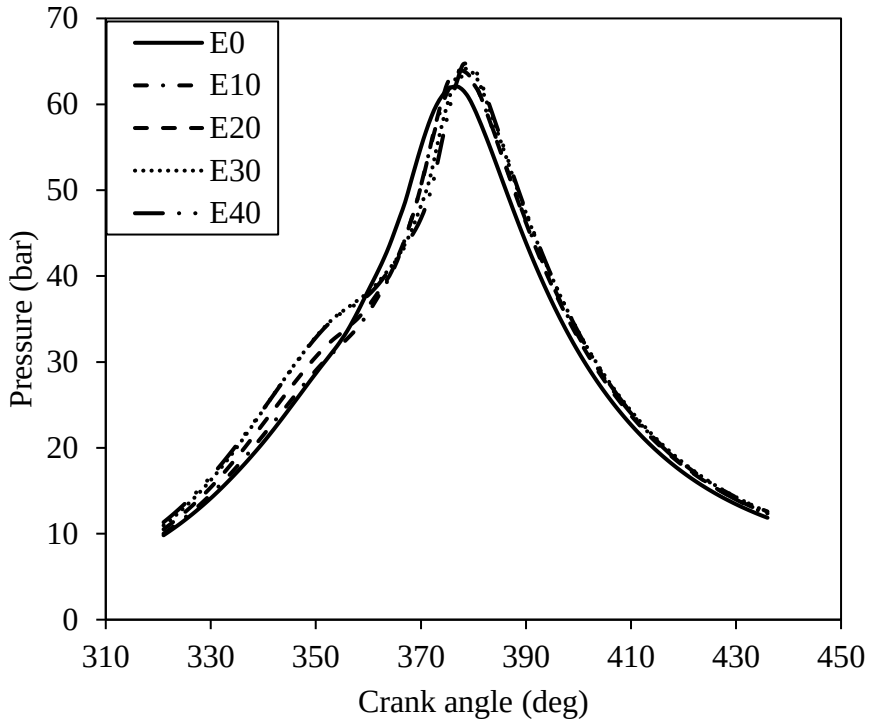

Fig. 4.12 Variation in cylinder pressure with crank angle at full load

As shown in Fig. 4.12, that at any load, the pressure in the cylinder first increases, reaches a maximum value, called peak pressure, and then decreases with crank travel, during a definite period of working cycle. The values of peak pressure (in bars) at full load observed are 62.1, 63.2, 63.9, 64.1 and 64.6 respectively for E0, E10, E20, E30 and E40. The position of occurrence of peak pressure is shifted by 1-2°CA as compared to that in pure diesel case. The peak-pressure for diesel as well as for different modes of fumigation increases consistently

with increasing engine loads and also with increasing ethanol substitution, as evident from Fig. 4.13.

Moreover, as shown in the Fig. 4.12, the marginally higher values for in-cylinder pressures are observed for ethanol fumigation, before the combustion starts. It can explained as follows. The working substance or charge comprises of air and residual gases in case of pure diesel operation whereas in the case of ethanol fumigation mode, it comprises of air, ethanol vapour and residual gases. The compression process in the internal combustion engines is considered as a polytropic process. The value of pressure obtained by the compression of working substance or charge is higher in case of ethanol fumigation (due to higher value of polytropic exponent, n)as compared to that in diesel only operation. As the combustion initiates, the increased rate of pressure rise due to enhanced heat release rate for different modes of ethanol fumigation are noticed, subsequently.

Fig. 4.14 illustrates the trends for the rate of pressure-rise with the crank angle, for pure diesel as well as for different ethanol-fumigation modes. At full load, the maximum rate of pressure rise for E0 was observed to be 2.14 bar/ ºCA at 8° aTDC and the increase in maximum rate of pressure rise of about 0.3-0.5 bar/°CA for E10, E20, E30 and E40 were observed, occurring 3-6 °CA later as compared to E0. It may be due to the longer ignition delay and shorter combustion duration of ethanol fumigation.

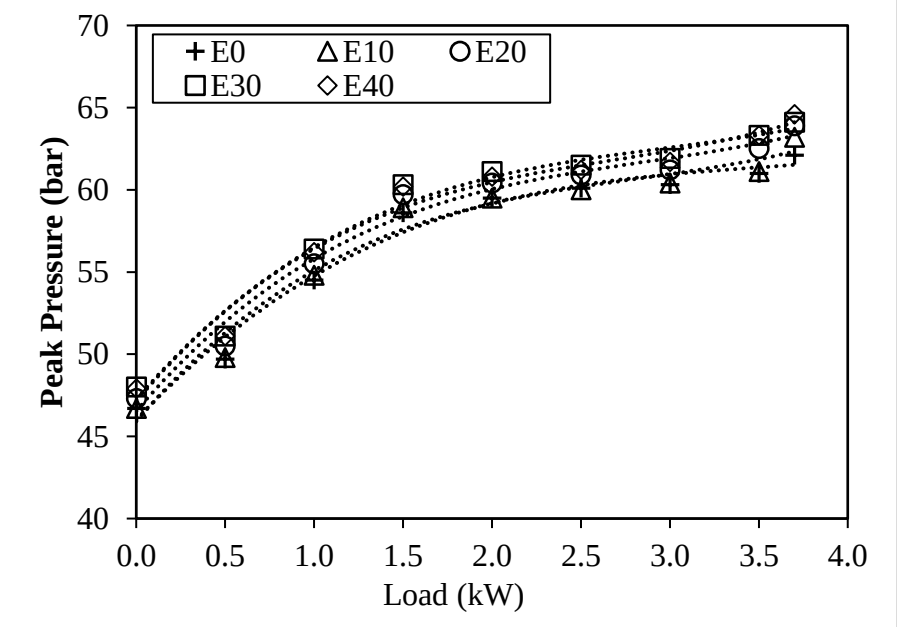

Fig. 4.13 Variation in peak cylinder pressure with load and fumigation

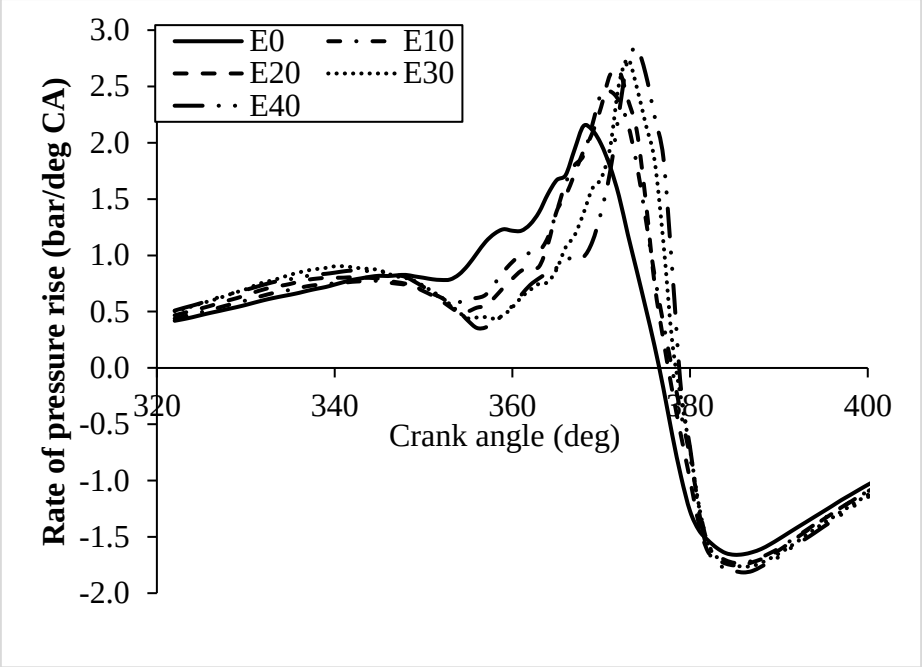

Fig 4.14 Variation in rate of pressure rise with crank angle at full load

4.1.11 Indicated mean effective pressure (IMEP)

Cycle by cycle variability is an important parameter to investigate the combustion characteristics of engine. It is known that the cycle-by-cycle variability in cylinder peak pressures and indicated mean effective pressure (IMEP) is the result of variations in combustion process itself. It has been found that CoV(Coefficient of Variance) of IMEP should not exceed 10% in order to avoid vehicle drivability problems.

In the present investigation, CoV of IMEP for all levels of ethanol fumigation was recorded to be lower than 5%. As the combustion variations are within limits, in-cylinder pressure data from 50 cycles' injection (firing) are sufficient to be recorded for computation of average IMEP. The values of IMEP (in kPa) 756.8, 771.4, 776.3, 790.8 and 810.2 respectively, are obtained at full load for E0, E10, E20, E30 and E40 as shown in Fig 4.15

4.1.12 Heat release rate (HRR)

HRR is one of the most important parameters to characterise the combustion process in compression ignition engine. It is a measure of how fast chemical energy of fuel is converted to the thermal energy by process of combustion and calculated from the acquired pressure histories using the zero dimensional heat release model [78]. HRR can be calculated by equation 4.6.

$$\frac{\delta Q_{net}}{d\theta} = \frac{\gamma}{\gamma-1} p \frac{dV}{d\theta} + \frac{1}{\gamma-1} V \frac{dp}{d\theta} \quad (4.6)$$

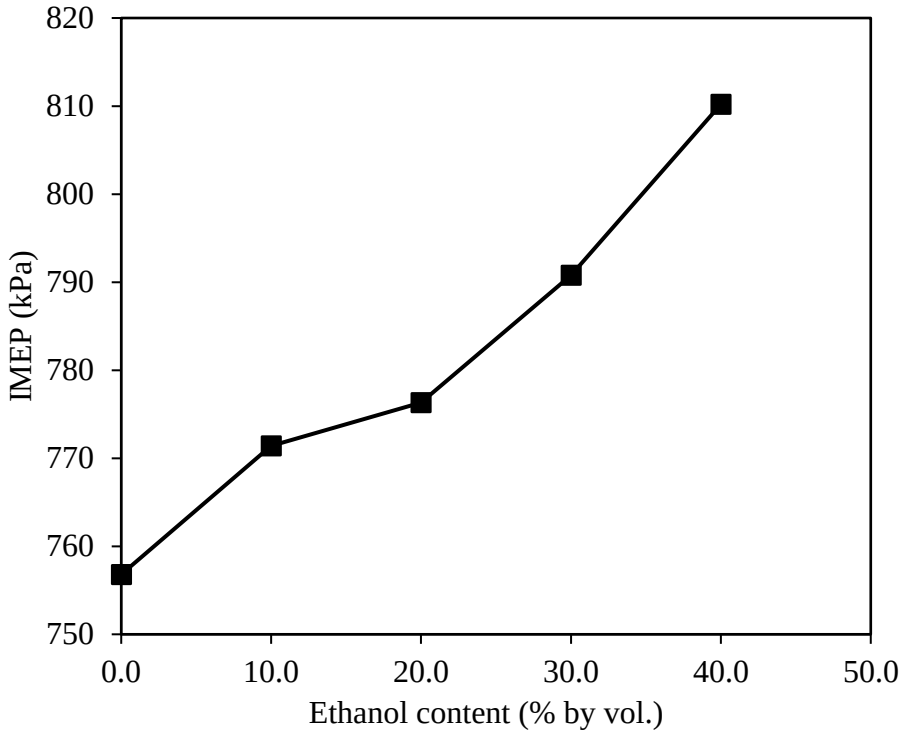

Fig. 4.15 Variation in IMEP with different percentage of ethanol fumigation

The cylinder volume[78] may be determined by using the equation 4.7 which expresses the relation between crank angle and cylinder volume according to engine geometry.

$$V = V_c + \frac{\pi B^2}{4}\left(l + r - r.cos(\theta) - \sqrt{l^2 - r^2 sin^2\theta}\right) \quad (4.7)$$

Fig. 4.16 shows the variation in HRR with the crank angle at full load with pure diesel and all modes of fumigation. For pure diesel, maximum heat release of 52 J/° CA at about 12°CA aTDC is observed and the increase of 3-10 J/°CA is recorded with all modes of ethanol fumigation as compared to baseline diesel case. The occurrence of maximum HRR for any level of fumigation is retarded by 1-5 °CA, in comparison with that of E0. Since ethanol is an oxygenated fuel, HRR increases due to availability of more oxygen and thus improves combustion. Due to increase in HRR, the peak cylinder pressure as well as rate of pressure rise also increases.

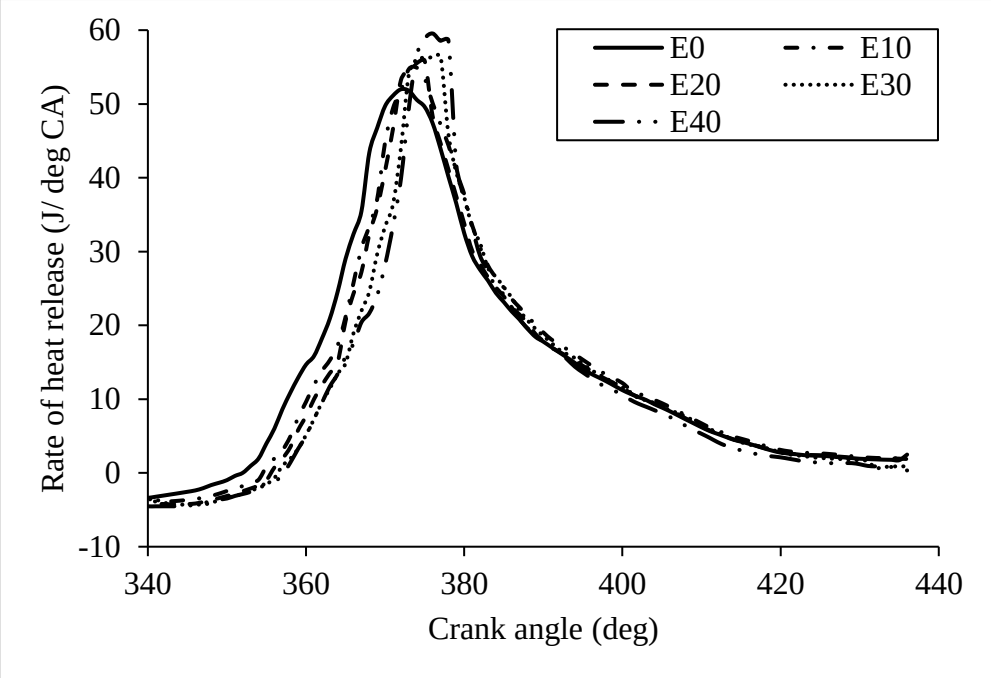

Fig. 4.16 Variation in heat release rate with crank angle at full load

4.1.13 Ignition delay, combustion duration and mass fraction burned

The changes in the combustion process may be observed with the use of different fuels owing to the physical and chemical differences in their fuel structure. Ignition delay, defined as the number of crank angle degrees between the start of injection and the ensuing combustion-induced inflection point on the p-θ curve, is a function of mixture temperature, pressure, equivalence ratio and fuel properties. The fuels with fairly low cetane value and too long an ignition delay, most of the fuel is injected before ignition occurs thus resulting in very rapid burning rates, with high rate of pressure rise and high peak pressures. The duration of ignition delay reflects the ignition characteristics of the fuel. Hence, it is an important property that determines the various engine operating characteristics of CI engine such as thermal efficiency, smoothness of operation, misfire and smoke emissions. For fuels having low cetane numbers with excessively long delay, ignition occurs sufficiently late in the expansion process and quench the burning process, thus leading to incomplete combustion, reduced power-output and lower thermal efficiency. With the increase in loads, decrease in ignition delay is observed, due to richer fuel supply. As shown in Fig. 4.17, the ignition delay of pure diesel at full load is 15 °CA and increases by about 2-5 ºCA at full load for all levels of ethanol substitution. The increased ignition delay is caused due to low cetane number and large latent heat of vaporisation of ethanol.

Start of combustion is more difficult to determine precisely. It is best identified from the change in slope of HRR, determined from cylinder pressure data. The combustion duration is the time interval elapsed or crank angle traversed between 10% mass burned and 90% mass burned. With the increase in load, the combustion duration increases due to better mixing of fuel and air. The combustion duration decreases with increasing rate of fumigation due to increase in ignition delay. The combustion duration of 37.1, 35.6, 35.4, 34.3 and 33.9 (°CA), respectively, were observed for E0, E10, E20, E30 and E40 at full load, as shown in Fig. 4.17. The decreasing values of combustion duration with increasing ethanol content may be attributed to enhanced mixing of fuel and air and increased availability of oxygen.

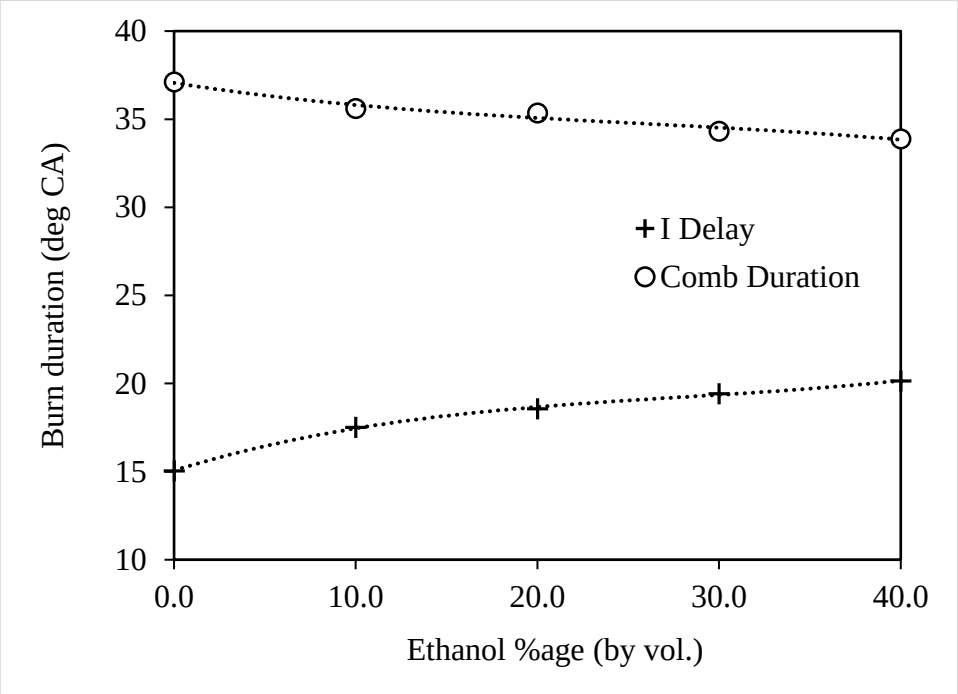

Fig. 4.17 Variation of burn duration with ethanol content at full load

Mass Fraction Burned (Mfb), an indicator of the energy conversion during a combustion cycle at a specific crank angle degree (CAD) and expressed as normalized quantity with a scale of 0 to 1, depends on engine geometry, engine speed, A/F, ignition angle, residual mass etc. Mass fraction burned (Mfb) in each individual engine represents the chemical energy conversion as a function of crank angle. For the estimation of Mfb, a procedure developed by Rassweiler and Withrow, also known as a single-zone heat release method is still widely used owing to its simplicity and computational efficiency. The mass fraction burned at the end of interval may be expressed by equation 4.9, assuming that mass of the charge burned in the interval is proportional to pressure rise due to combustion [78].

$$Mfb = \frac{\sum_{0}^{i} \Delta p_c^*}{\sum_{0}^{N} \Delta p_c^*} \tag{4.9}$$

Fig. 4.18 shows the variation in the Mfb with the crank angle at full load. The mass fraction burnt increases with the level of fumigation due to increase in oxygen content and enhanced HRR. For E0, the combustion was faster up to 18-20° aTDC, after which the combustion rate enhanced for different modes of ethanol fumigation, greater rate for higher ethanol content.

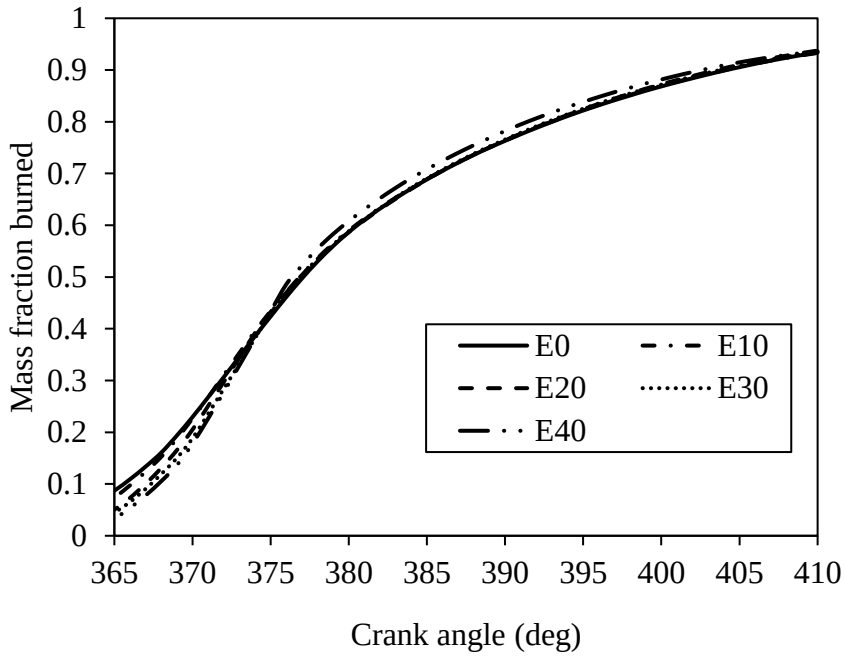

Fig. 4.18 Variation in mass fraction burned with crank angle at full load

4.2 Effect of ethanol on engine performance exhaust emission and combustion parameters for constant flow-rate of ethanol

In the second test-mode, the engine has been operated with pure diesel and different ethanol fumigation rates (0.1, 0.2, 0.3, 0.4 and 0.5 kg/hr) that are designated as e0, e1, e2, e3, e4 and e5.

4.2.1 Relative air-fuel ratio and ethanol energy ratio

Relative air fuel ratio (λ) is an informative parameter for defining mixture composition, as the composition of combustion products vary significantly with the strength of the mixture. It is calculated by equation 4.10.

$$\lambda = \frac{q_{m,air}}{(q_{m,d} \times AFR_{st,d}) + (q_{m,e} \times AFR_{st,e})} \tag{4.10}$$

Fig, 4.19 depicts the variation of relative air fuel ratio λ, at various loads for the different fumigation rates. The stoichiometric air fuel ratio is 14.5 for diesel and 9 for ethanol. In the present study, for the different fumigation rates used, λ varies from 1.5 to 5.1 at various loads. For a given ethanol flow rate, the increased flow rate of diesel with increasing load results in lower values of relative air fuel ratio.

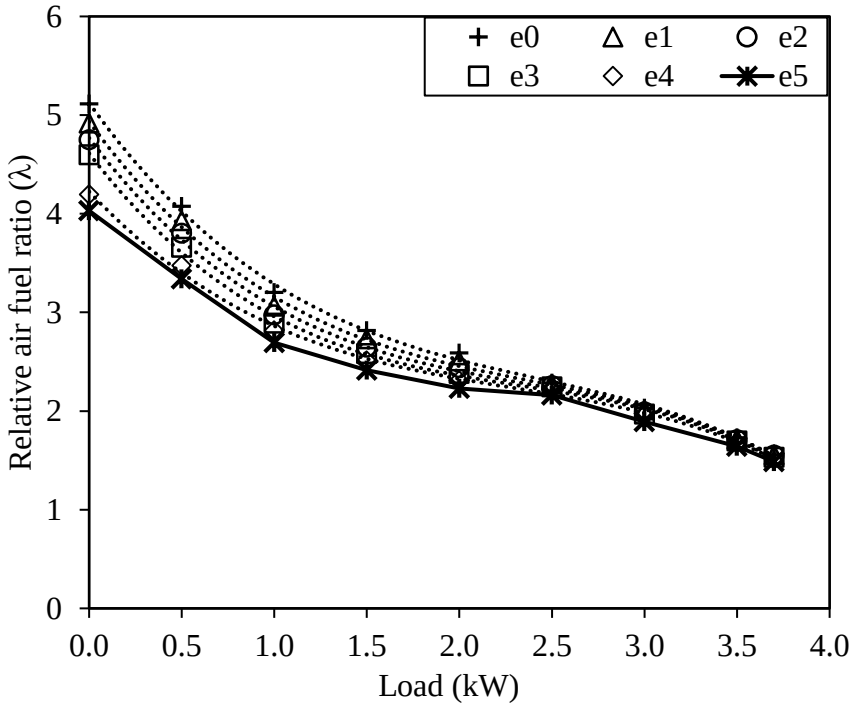

Fig. 4.19 Variation of relative air fuel ratio λ with load

The variation of ethanol energy fraction for different values of λ at different loads is shown in Fig 4.20.Ethanol exhibits an increasing trend with the relative air fuel ratio. As the engine load increases, the amount of energy supplied by ethanol reduces as compared to total energy of fuel. Moreover the amount of fuel increases with load thus decreasing λ. Since, ethanol has lower calorific value as compared to diesel, the energy share of ethanol in required quantity of fuel for a particular load decreases significantly with increasing load whereas increases slightly with increasing ethanol fraction as evident from Fig 4.20.

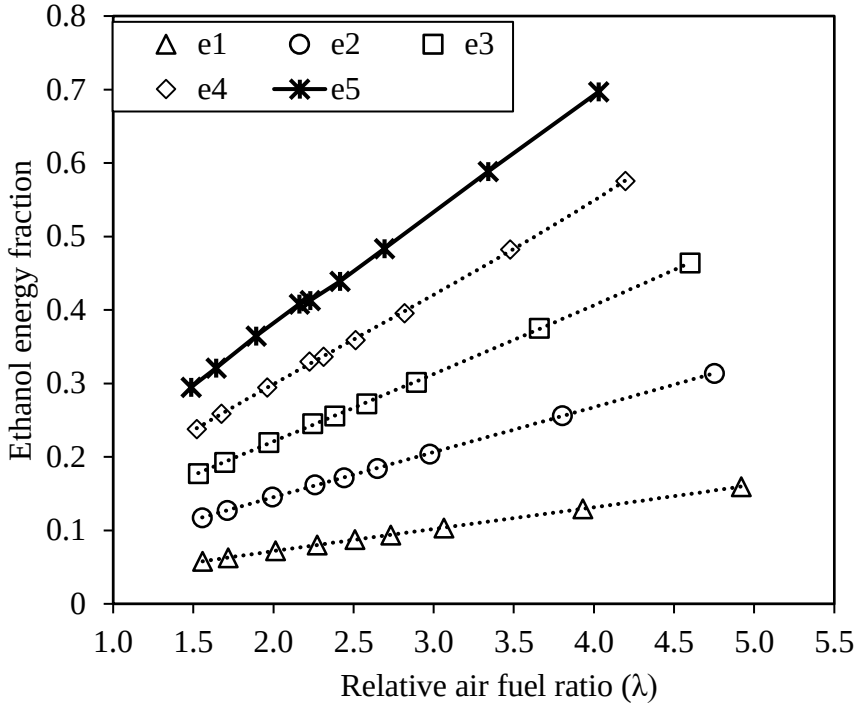

Fig. 4.20 Variation of ethanol energy fraction for different values of λ

4.2.2 Brake thermal efficiency (BTE)

Fig. 4.21 shows the variation of BTE with different rates of ethanol flow rates under various engine loads. At low loads, decrease in BTE up to 11.2% has been observed, whereas BTE increased up to 6% at high loads as compared to e0. At full load, while BTE have been found to be 28.3% for e0, the BTE increase (as compared to e0) of 3.2%, 4.3%, 5.3%, 6% and 5% respectively has been recorded for e1, e2, e3, e4 and e5. The reduction of BTE, which has been found to be significant in most of the cases at lower load conditions can be explained by following facts. At low loads, lean mixture of air and ethanol is formed due to excess amount of air which deteriorates the combustion. Moreover, the higher heat of vaporization of ethanol might cool down the combustible mixture thus decreasing BTE.

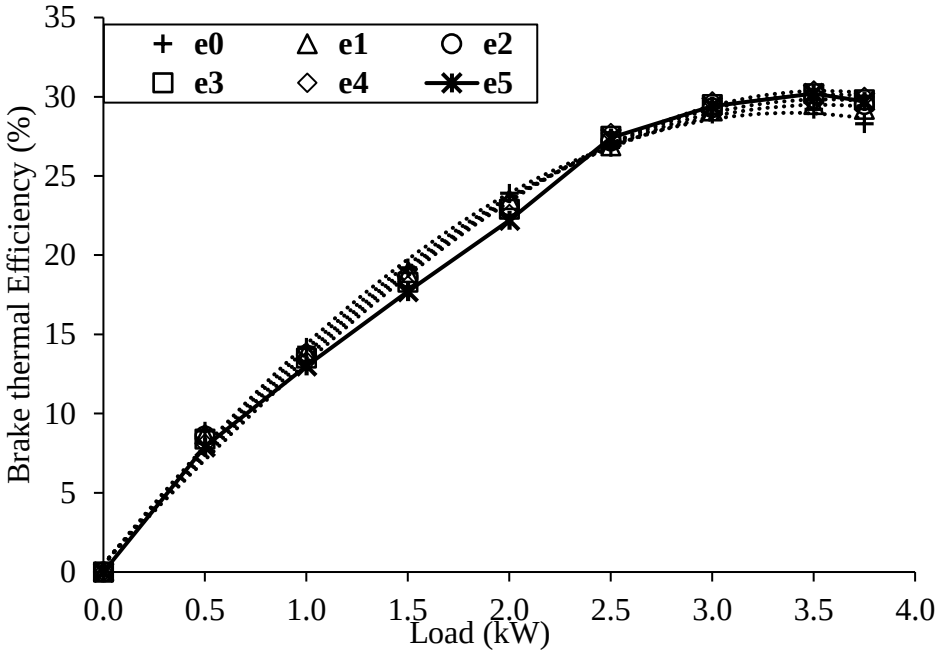

Fig. 4.21 Variation of brake thermal efficiency with load for different ethanol fumigation rates

4.2.3 Exergy Efficiency

The exergy efficiencies (shown in Fig 4.22) of the engine under investigation exhibit similar behaviour to the thermal efficiencies given in Fig. 4.21. The exergy efficiencies are slightly lower than the corresponding thermal efficiencies.

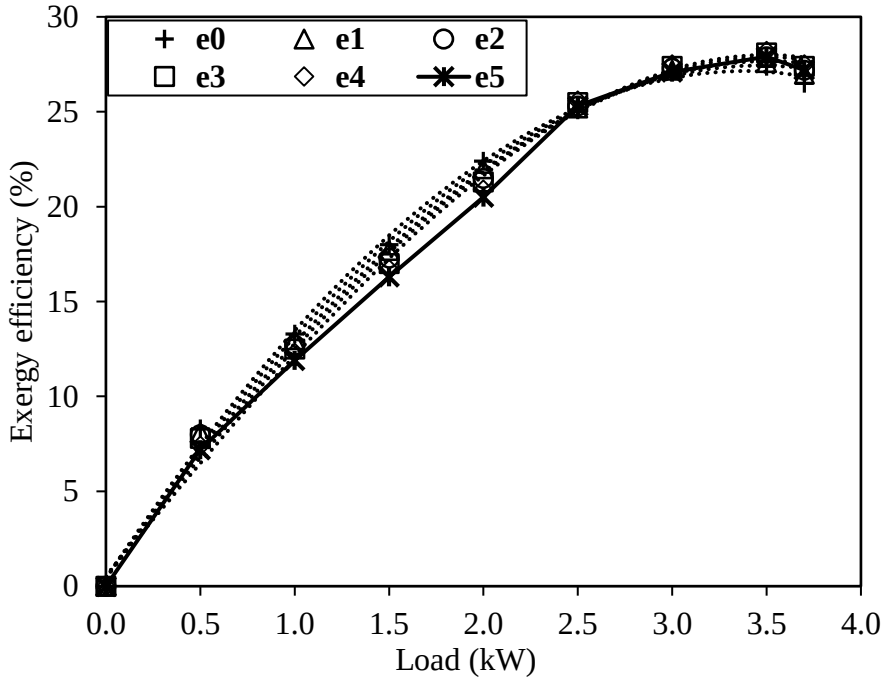

Fig. 4.22 Variation of exergy efficiency with load for different ethanol fumigation rates

4.2.4 Exhaust gas Temperature

Fig. 4.23 shows the variation of exhaust temperature of diesel fuel with different rates of ethanol fumigation for various engine loads. It is obvious that exhaust temperature increases with the load for diesel as well as for all rates of ethanol fumigation, as the heat release rate is increased. The exhaust temperatures (ºC) of 161, 155, 151, 144, 135 and 131 at no-load whereas 521, 524, 528, 533, 538 and 544 at full load were observed at e0, e1, e2, e3, e4 and e5 respectively. The results show that the exhaust gas temperature decreased with increase in ethanol substitution at low and medium loads which is attributed to the quenching of cylinder charge due to higher latent heat of vaporisation of ethanol. The increase of exhaust temperature with increase in ethanol substitution at higher loads is caused due to the increase in heat release rates which predominates the quenching factor.

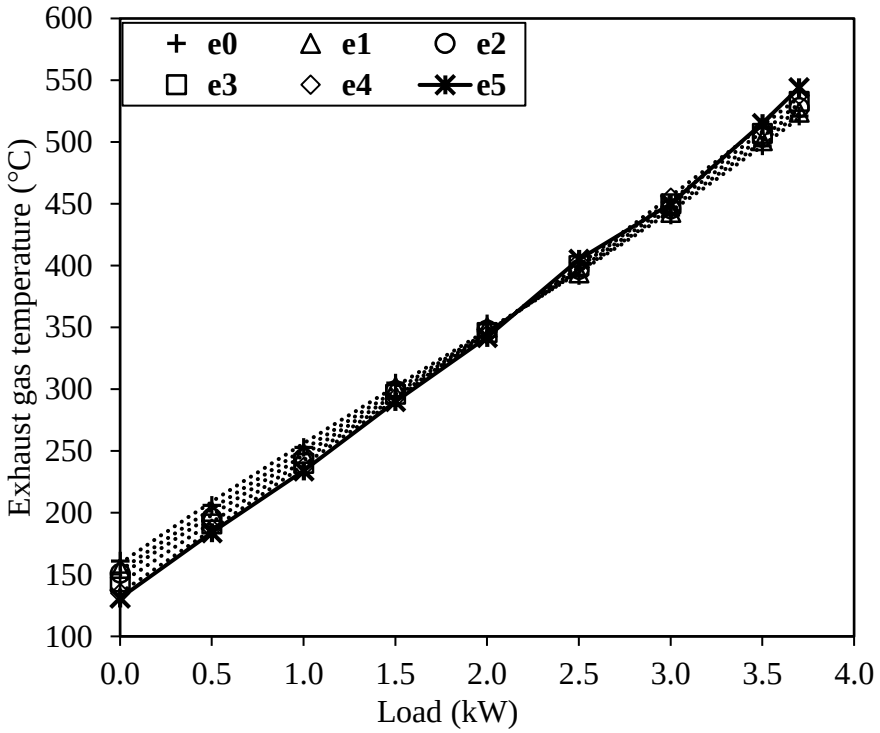

Fig.4.23 Variation of exhaust gas temperature at various loads for different ethanol fumigation rates

4.2.5 NOx emissions

As shown in Fig. 4.24, maximum reduction in NOx emission of 22%, 16%, and 9% respectively, have been observed at low, medium and high loads conditions for all rates of ethanol flow rates as compared to e0. For e1, e2, e3, e4 and e5, the decrease in NOx of about

9%, 14%, 17%, 19% and 22% respectively have been observed as compared to e0 at no load condition.

At low loads, reduction in NOx observed is attributed mainly to higher latent heat of evaporation of ethanol leading to low combustion temperature for all flow rates of ethanol whereas the increase of heat release in the premixed mode at high loads results the insignificant changes in NOx, especially for low flow rates of ethanol, viz., e1 and e2 as compared to pure diesel case.

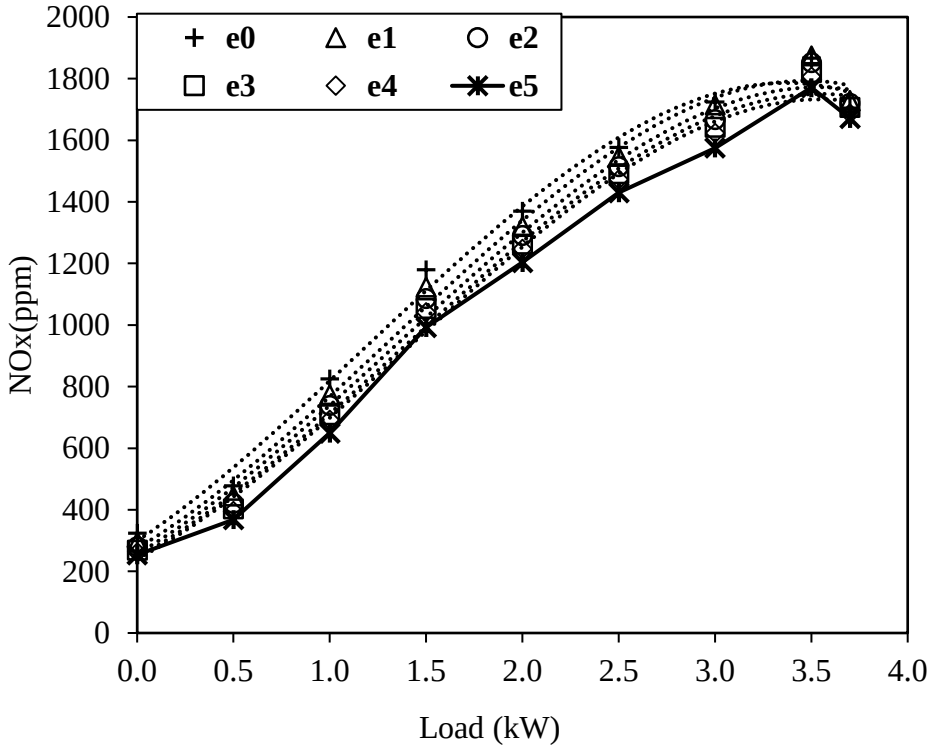

Fig.4.24 Variation of NOx with load for different ethanol fumigation rates

4.2.6 Hydrocarbons and carbon monoxide (HC and CO)

Fig. 4.25 exhibits the increase of HC emission with different rates of ethanol-fumigation. Maximum increase of 144%, 76% and 44% in HC emissions were observed at low, medium and high loads respectively for different ethanol flow rates in comparison with pure diesel. For e1, e2, e3, e4 and e5, there is an increase of about 41%, 61%, 84%, 113% and 144% respectively in HC emissions as compared to e0 at no-load condition. No change in HC emission for e1 and e2 was observed whereas marginal change of about 7%, 12% and 17% respectively have been found at high load conditions. With increasing loads at different

ethanol fumigation modes, HC emissions decreases due to improved mixing of fuel and air and thus, the enhanced combustion.

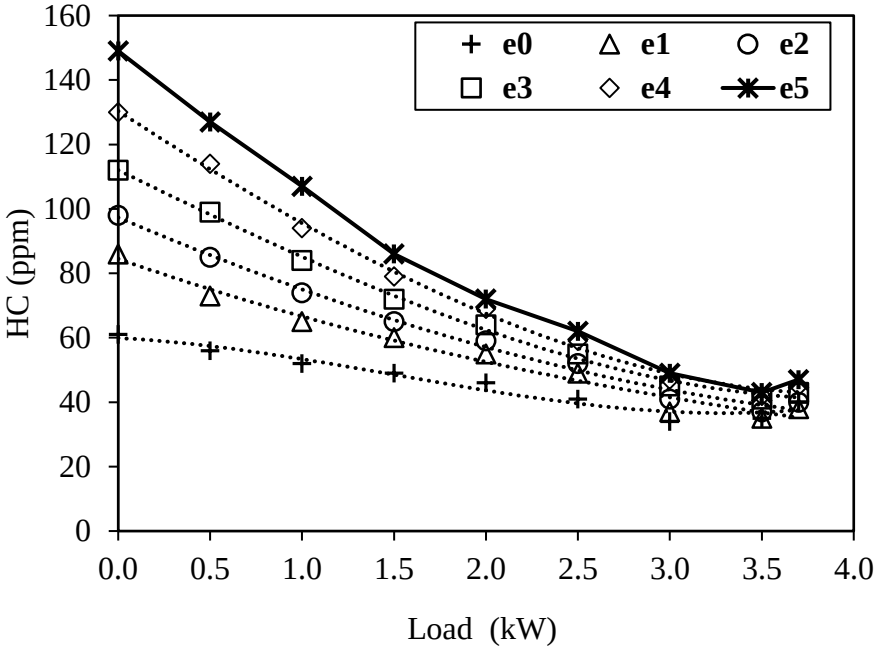

Fig. 4.25 Variation of HC with load for different ethanol fumigation rates

Maximum increase of 21%, 56%, 83%, 106% and 139% in CO emissions respectively for e1, e2, e3, e4 and e5 have been observed as compared to e0. CO emission for different ethanol flow rates, as portrayed in Fig. 4.26 is found to increase up to 66%, 126% and 139% respectively at low, medium and high loads in comparison with baseline diesel case. Increase of CO emission with increasing ethanol substitution is attributed to the combustion quenching due to high latent heat of vaporisation and subsequent charge cooling leading to incomplete combustion. Moreover, the low cetane number renders the fraction of ethanol trapped in crevices, non-ignitable during the expansion stroke thus increasing CO emissions, especially at low loads. At high engine load, the reduced air/fuel ratio associated with poor mixing, leading to higher CO emission.

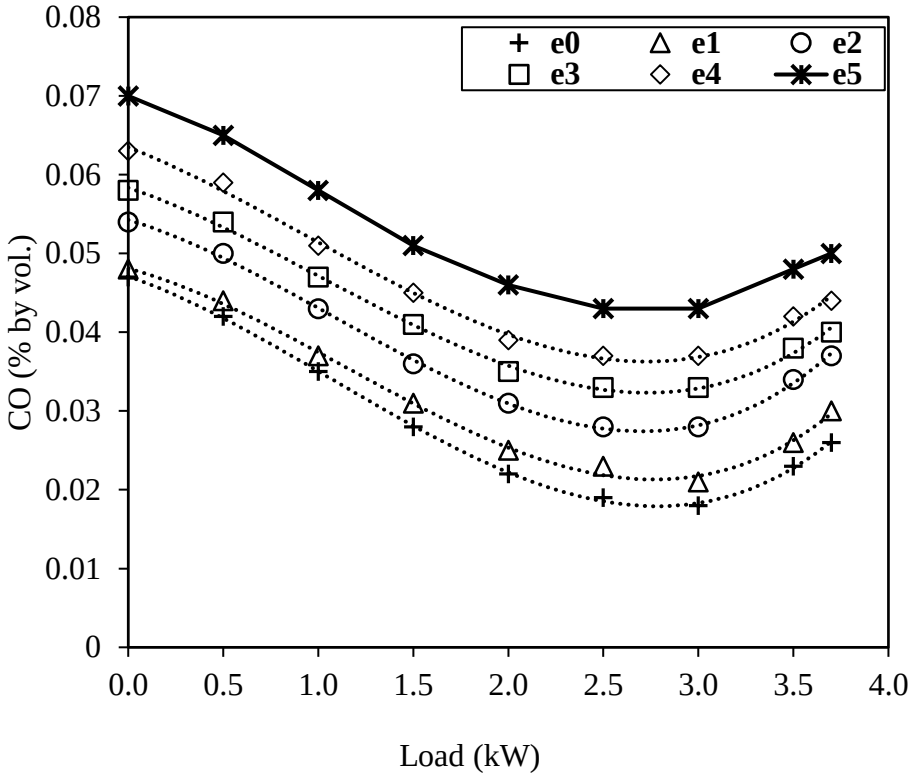

Fig. 4.26 Variation of CO with load for different ethanol fumigation rates

4.2.7 Carbon di-oxide (CO_2)

As shown in Fig. 4.27, the CO_2 concentration increases with the engine load for pure diesel as well as for different ethanol fumigation modes because of enhanced combustion due to availability of more oxygen and higher in-cylinder temperature. As evident, CO_2 concentration decreases with increase in ethanol substitution. It happens due to the fact that the large latent heat of vaporisation of ethanol reduces in-cylinder temperature thus leading to incomplete oxidation of hydrocarbons into CO, during expansion stroke thus decreasing CO_2. In comparison to e0, CO_2 emissions decreased by 7%, 12%, 16%, 19% and 24% respectively, for e1, e2, e3, e4 and e5 at no-load condition. At low engine load, the cooling effect together with the leaner air-alcohol mixture, results in poorer combustion and hence decrease of CO_2emissions, as reflected in the poorer BTE. At high engine load, decrease of 13%, 16%, 19%, 21% and 25% respectively has been observed in CO_2 for e1, e2, e3, e4 and e5 as compared to e0, which can be attributed to the reduced air/fuel ratio and poor mixing leading to decreased CO_2 emissions.

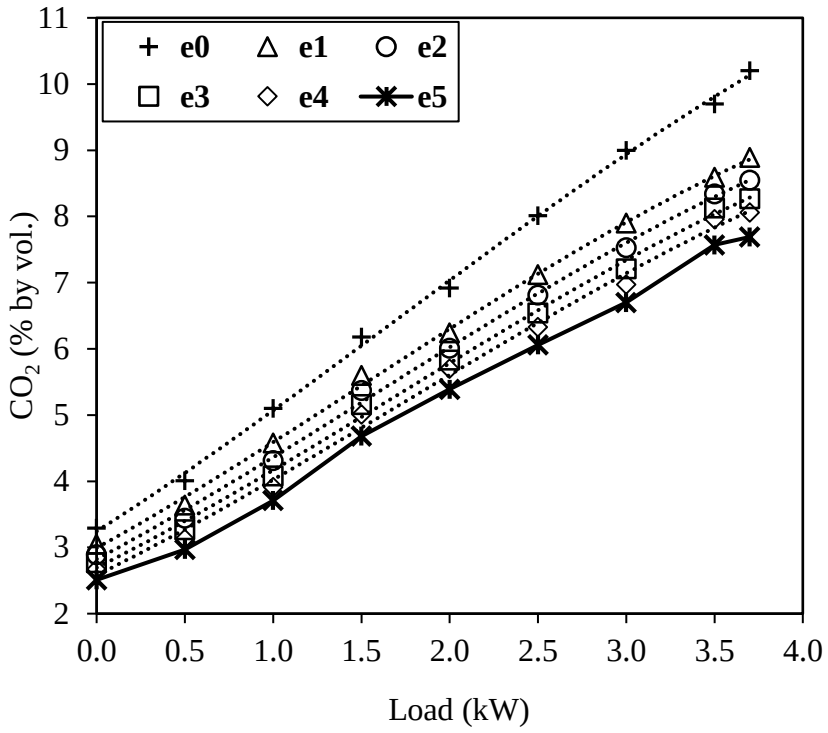

Fig 4.27 Variation of CO_2 with load for different ethanol fumigation rates

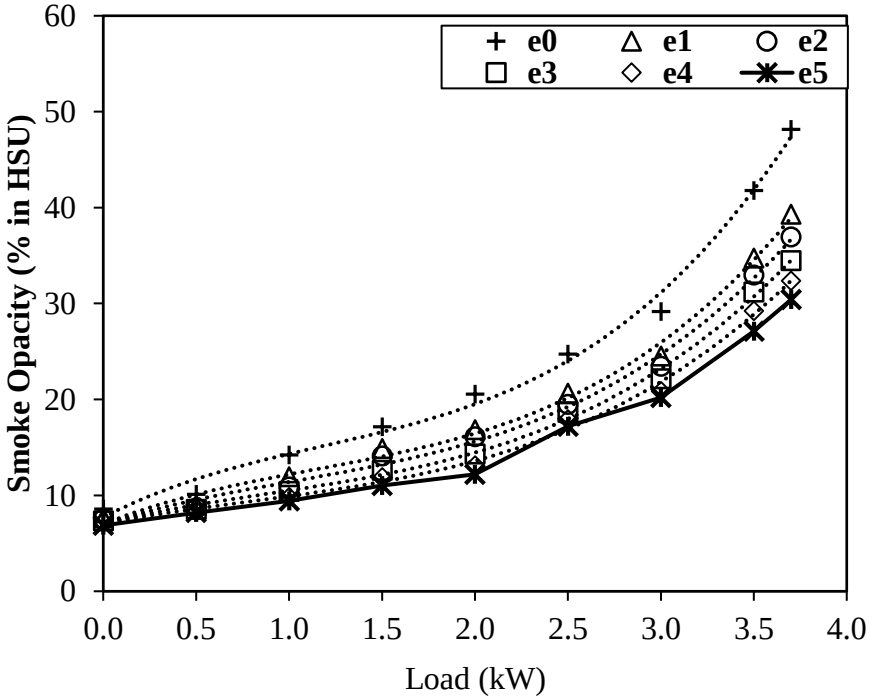

Fig 4.28 Variation of smoke opacity with load for different ethanol fumigation rates

4.2.8 Smoke opacity

With fumigated ethanol, smoke opacity has been found to decrease for the entire load range as shown in Fig. 4.28. However, the reduction in smoke was more obvious at high loads. For e1, e2, e3, e4 and e5 respectively, decrease in smoke opacity of about 11%, 12%, 15%, 16% and 20% has been observed as compared to e0 at no-load condition, whereas corresponding reduction at full load are 18%, 23%, 28%, 33% and 37%. The reduction of smoke emission with ethanol fumigation modes is explained by several reasons. Firstly, the increase in ignition delay increases the amount of diesel fuel burned in the premixed mode, which reduces the amount of diesel fuel burned in the diffusion mode. Secondly, increasing the flow rate of ethanol not only reduces amount of diesel fuel for a given engine load when compared with pure diesel operation but also leads to reduction of aromatics so as to reduce smoke.

4.2.9 In-cylinder pressure and rate of pressure rise

As portrayed in Fig. 4.29, the values of peak pressure (in bars) at full load observed are 62.1, 62.9, 63.3, 63.7, 64.1 and 65.3 respectively for e0, e1, e2, e3, e4 and e5. As evident, the position of occurrence of peak pressure is shifted by 1-2°CA as compared to e0. The rate of pressure rise, once ignition has occurred is also affected by the amount of fuel mixed with air within combustion limits during the delay. Rate of pressure rise influences knock intensity and combustion noise in the engine, while in operation. With the increase of ethanol fumigation rate, combustion rate augments and intensifies and eventually causes objectionable noise and the substantial engine damage resulting in high levels of NOx emissions.

Fig. 4.30 illustrates the trends for the rate of pressure-rise with the crank angle for pure diesel as well as for different ethanol-fumigation rates. At full load, the maximum rate of pressure rise (bar/°CA) has been found to be 2.15, 2.29, 2.43, 2.53, 2.75 and 2.83 for e0, e1, e2, e3, e4 and e5 occurring 1-4 °CA later as compared to e0. The peak-pressure for diesel as well as for different rates of fumigation increases consistently with increasing engine loads and also with increasing ethanol substitution as evident from Fig. 4.31. In general, peak pressure varies from about 46.7 bar to 65.3 bar throughout the entire load range considered for different ethanol flow rates.

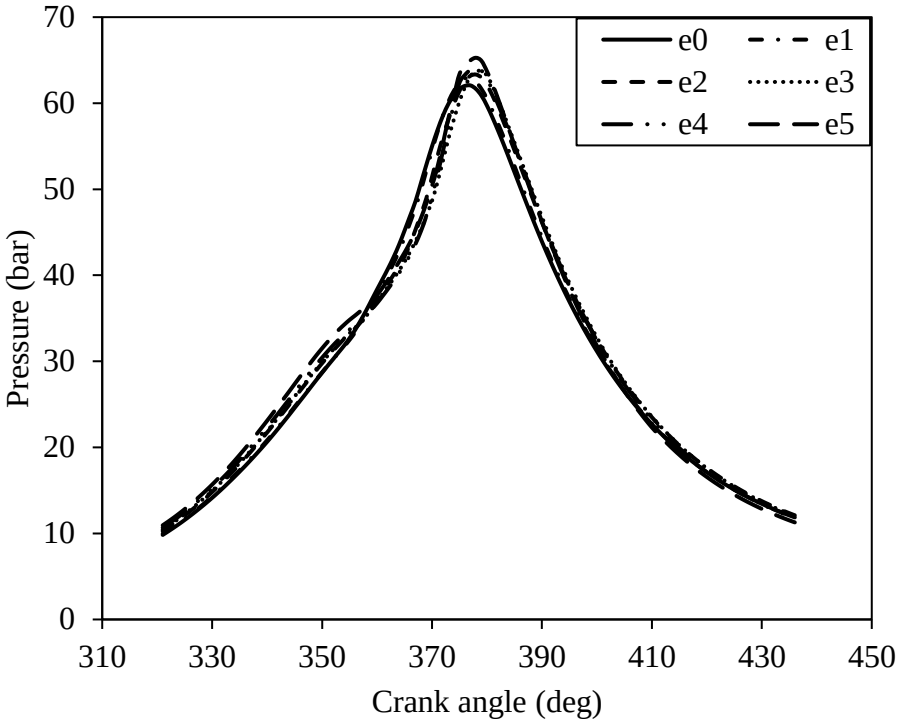

Fig 4.29 Variation in cylinder pressure with crank angle at full load

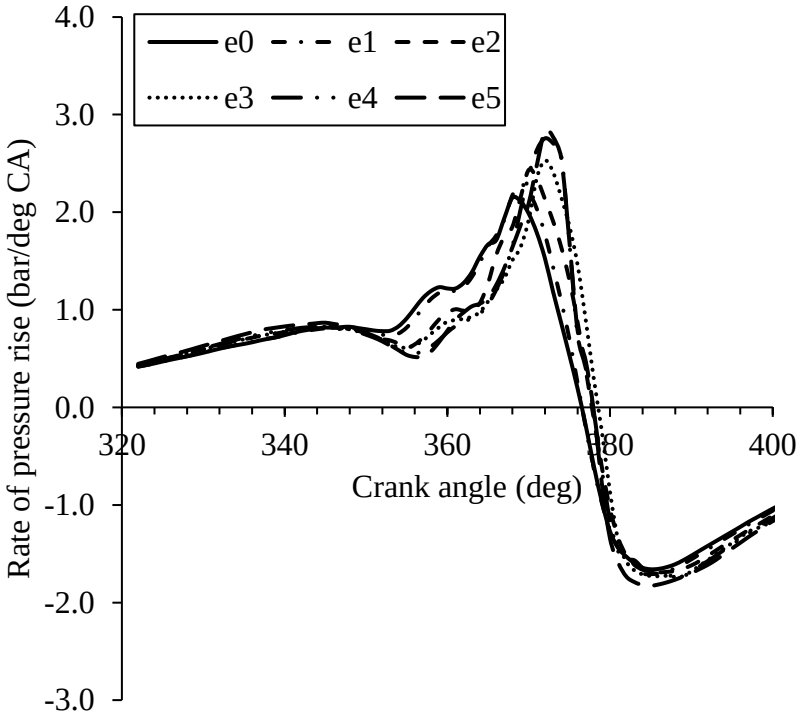

Fig 4.30Variation in rate of pressure rise with crank angle at full load

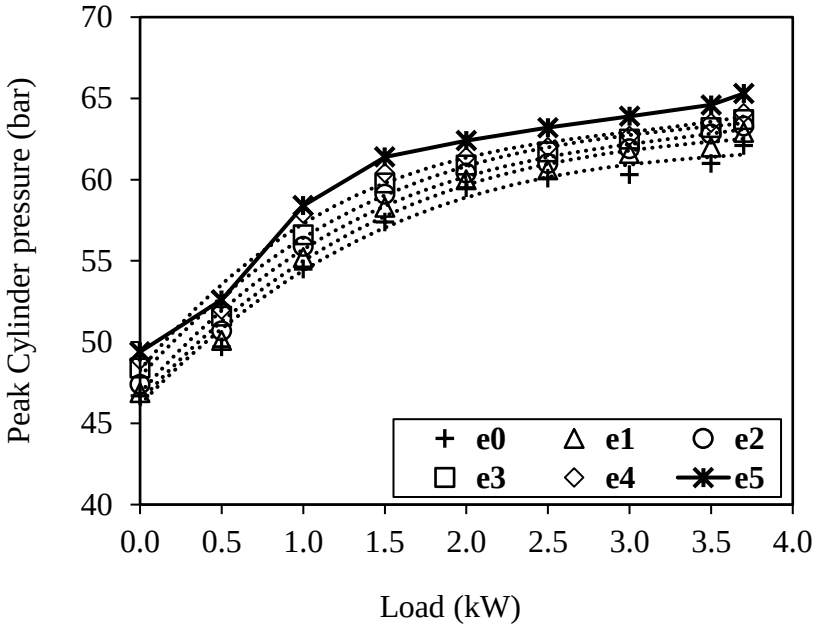

Fig 4.31 Variation in peak cylinder pressure with load and fumigation rates

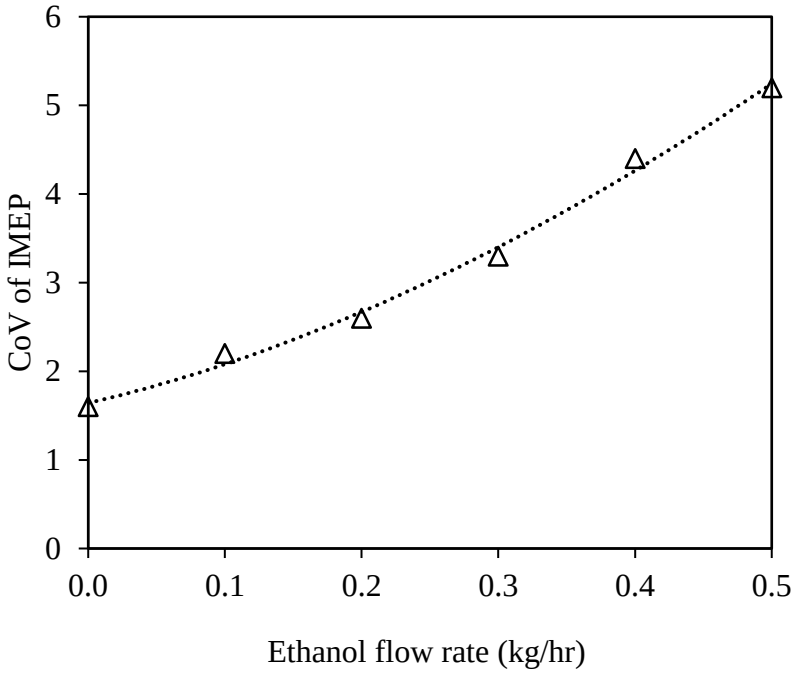

Fig 4.32 Variation in CoV of IMEP with ethanol fumigation rates

In Fig. 4.32, statistical values of cycle to cycle variations are shown as CoV of IMEP. The values of CoV of IMEP(%) were calculated as 1.6, 2.2, 2.6, 3.3, 4.4 and 5.2 respectively for e0, e1, e2, e3, e4 and e5. The cyclic dispersion in IMEP is attributed to the variation in

amount of fuel supplied to the cylinder as well as the variability of mixture composition and gas motion during the combustion within the cylinder. Low value of COV for e0 indicates small cycle to cycle variations in cylinder-pressure and IMEP and great repeatability in combustion process. Higher values of CoV implies the greater combustion variability thus causing rough and unstable operation of the engine and increased hydrocarbon emissions.

4.2.10 Cylinder gas temperature

Fig. 4.33 portrays the variations of cylinder gas temperatures at full load for various ethanol fumigation rates. The cylinder gas temperature is calculated by assuming uniform temperature within the engine cylinder using ideal gas law [8,49]. The results are valid between closing of intake valve and opening of exhaust valve. Peak cylinder gas temperatures are obviously higher at higher loads. At full load condition, the higher cylinder gas temperature were observed for different ethanol fumigation rates as compared to diesel. This is probably due to the augmented heat release rate and increased ignition delay for various ethanol flow rates that outperforms the effect of quenching factor.

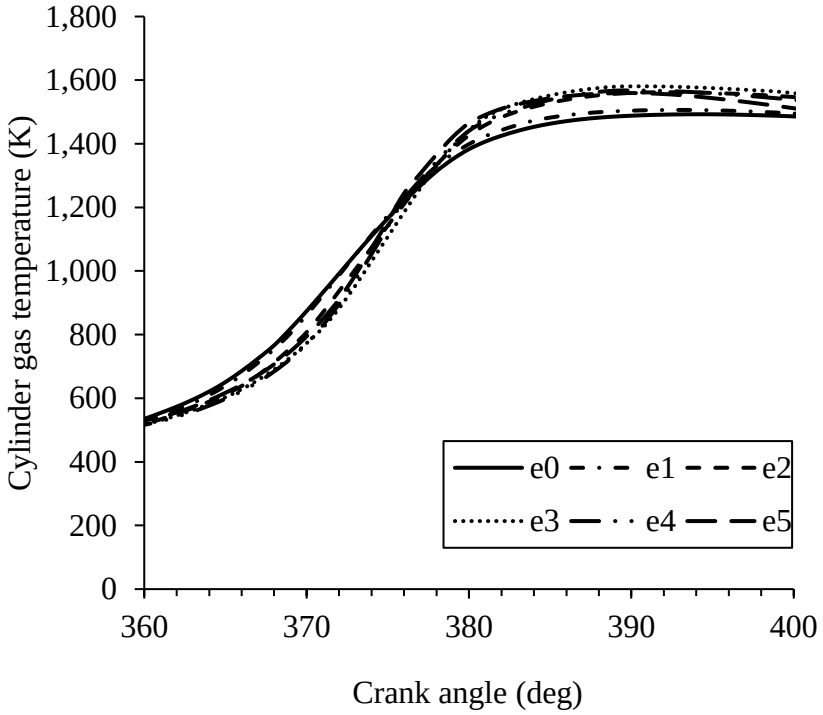

Fig 4.33 Variation in cylinder gas temperature with crank angle at full load

4.2.11 Heat Release rate (HRR)

Fig. 4.34 shows the variation in HRR with the crank angle at full load with pure diesel and all rates of fumigation. The values of HRR have been found to be 52, 54.1, 56, 58.5, 59.6 and

60.8 (J/deg °CA) for e0, e1, e2, e3, e4 and e5. The occurrence of maximum HRR for different rates of fumigation is retarded by 1-4 °CA in comparison to that of e0. Ethanol being oxygenated fuel, HRR increases due to availability of more oxygen and thus improved combustion. Due to increase in HRR, the peak cylinder pressure as well as rate of pressure rise also increases.

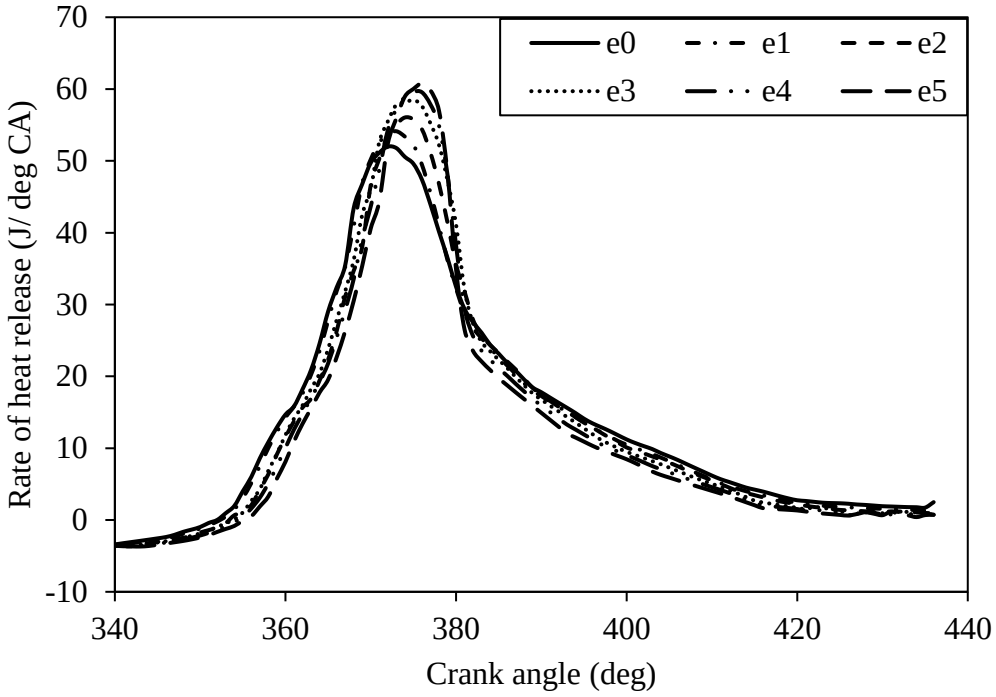

Fig 4.34 Variation in heat release rate with crank angle at full load

4.2.12 Ignition delay, combustion duration and mass fraction burned

As shown in Fig. 4.35, the ignition delay of e0 at full load is 15 °CA and increases by about 1-3 ºCA at full load for all rates of ethanol substitution. The increased ignition delay is caused due to low cetane number and large latent heat of vaporisation of ethanol. The ignition delay (°CA) of 15, 15.3, 16.4, 16.8, 17.4 and 18.2 and the combustion duration (°CA) of 37.3, 36.9, 35.3, 34.9, 34.4 and 32.9 respectively were observed for e0, e1, e2, e3, e4 and e5 at full load as shown in Fig. 4.34. The decreasing values of combustion duration with increasing ethanol content is attributed to enhanced mixing of fuel and air and increased availability of oxygen.

The initial (or premixed) burn duration is characterised by the difference between CA10 (crank angle at which 10% of mass fraction burned) and CA50 (crank angle corresponding to 50% mass fraction burned). CA50-CA10 is the duration where the heat release is driven mostly by the combustion of both diesel and ethanol in a pre-mixed mode. It can be observed

from Fig. 4.35 that the premixed burn duration decreases with increasing ethanol fraction, thus indicating the fast burning of the premixed charge and consequently increasing IMEP and BTE.

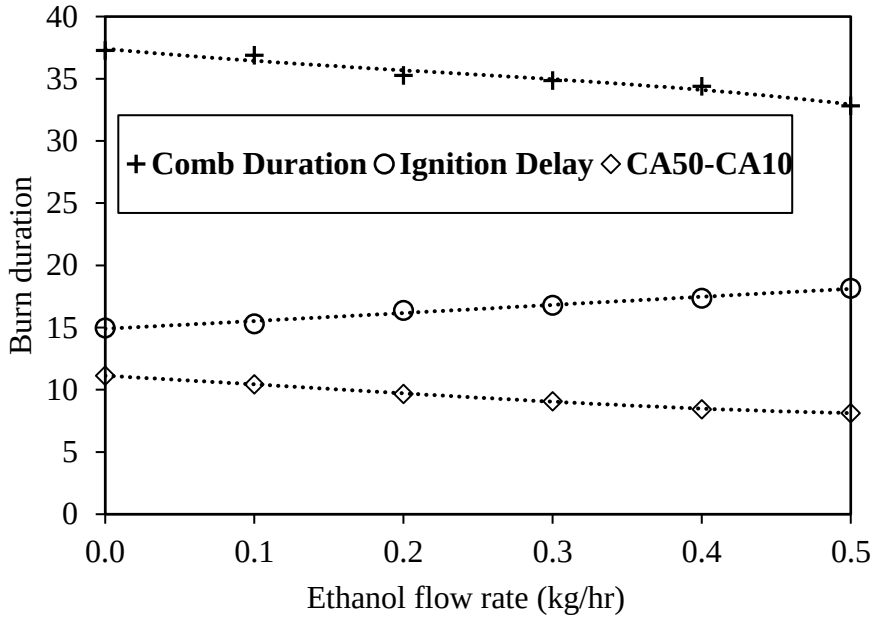

Fig 4.35 Variation of burn duration with ethanol content at full load

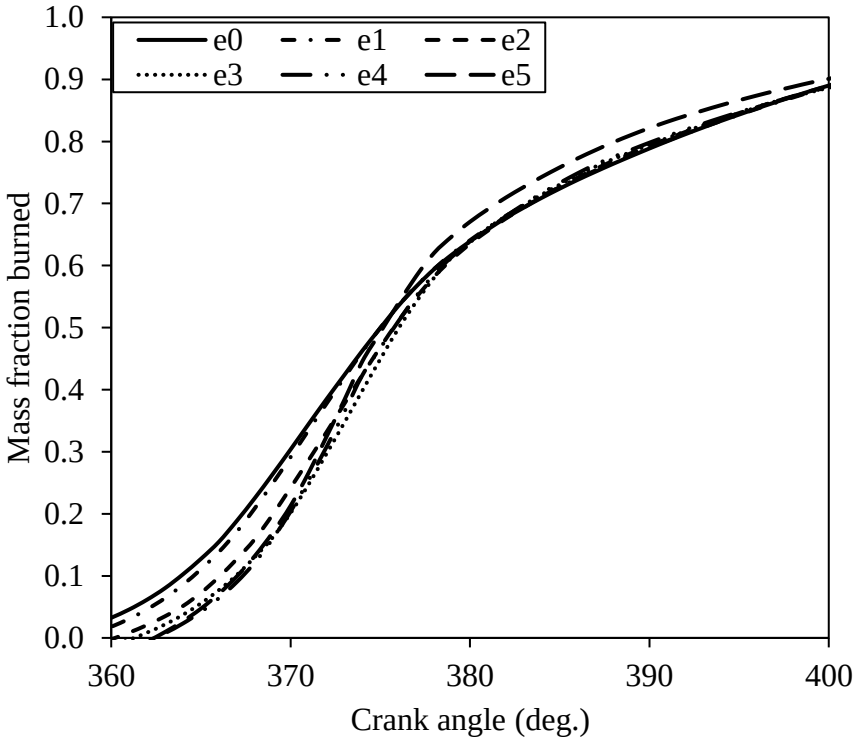

Fig 4.36 Variation in mass fraction burned with crank angle at full load

Fig. 4.36 shows the variation in the Mfb with the crank angle at full load. The mass fraction burned increases with the rate of fumigation due to increase in oxygen content and enhanced HRR. For e0, the combustion has been found to be faster up to 17-18° aTDC, after which, the combustion rate enhanced for different rates of ethanol fumigation, the rate increasing with increasing ethanol content.

4.3 Effect of ethanol on engine performance exhaust emission and combustion parameters with varying ethanol energy fractions

In third mode, the diesel engine was operated using various ethanol energy fraction, designated as eef0, eef1, eef2, eef3, eef4 and eef5.

4.3.1 Fuel consumption and effective equivalence ratio

The variation of mass consumption rate of diesel fuel in kg/hr with varying ethanol energy fraction at different loads is shown in Fig.4.37. Since ethanol has lower calorific value as compared to that of diesel, mass flow rate of ethanol increases thus decreasing the mass flow rate of diesel with increasing ethanol energy fraction at a particular load. The decrease of mass flow rate in diesel is pronounced at high loads due to the reason that, with increasing load, the total fuel-energy requirement of the engine increases which decrease the diesel consumption for a given ethanol fraction. For a higher value of ethanol fraction greater quantity of ethanol is required that keeps on increasing with the load.

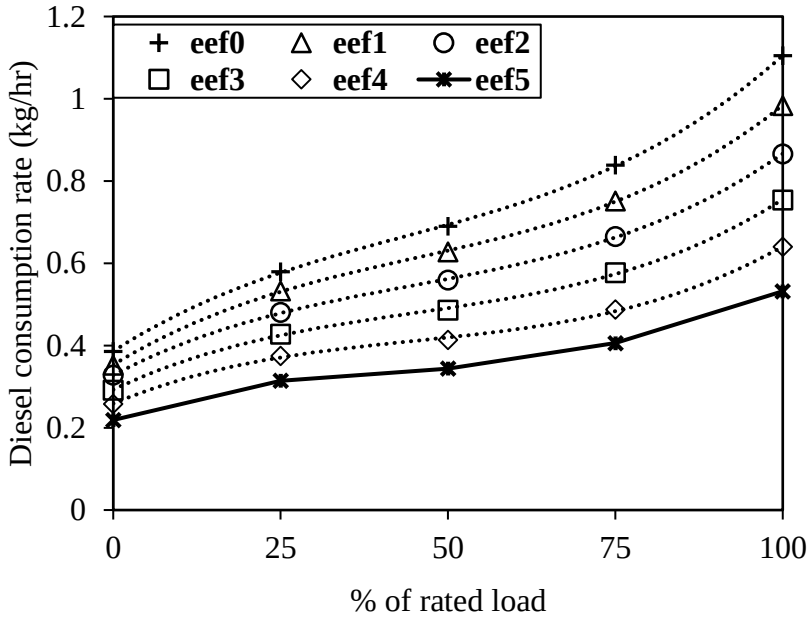

Fig 4.37 Comparison of mass consumption rate of diesel at various loads for different ethanol energy fraction

Fig.4.38 depicts the variation of effective equivalence ratio at various loads for different percentage of ethanol fumigation where the stoichiometric air fuel ratio is 14.5 for diesel and 9 for ethanol. In the present study, for the different fumigation levels used the effective equivalence varies from 0.2 to 0.7 at various loads.

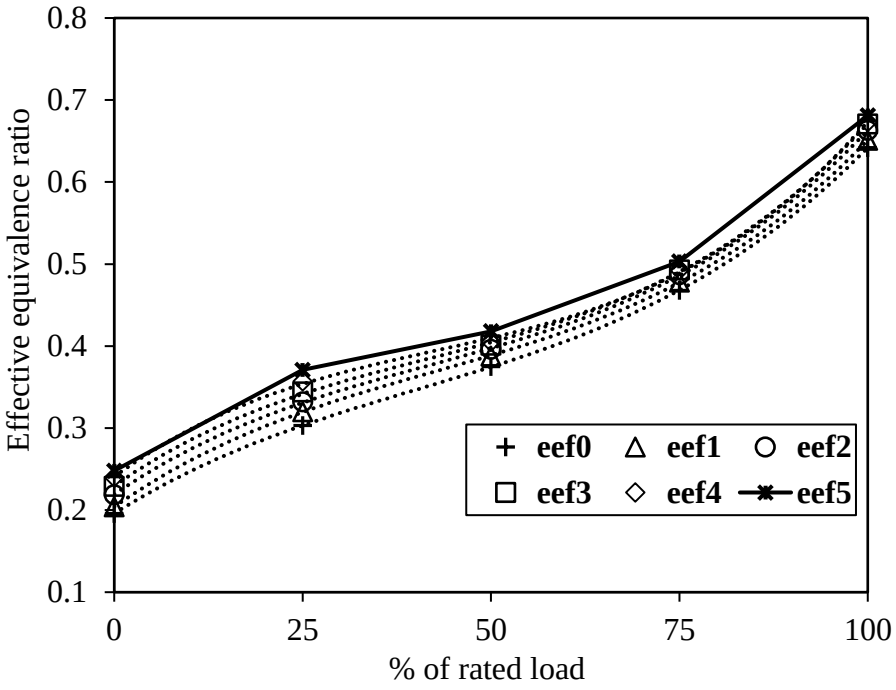

Fig 4.38 Comparison of effective equivalence ratio at various loads for different ethanol energy fraction

4.3.2 Brake thermal efficiency (BTE)

Fig. 4.39 shows the variation of BTE with different rates of ethanol energy fractions under various engine loads. Ethanol substitution reduces BTE at low engine load and increases it at high engine load compared to diesel fuel. For different ethanol energy fractions, decrease in BTE up to 11.7% has been observed for no load and 25% of rated load conditions. The decrease in BTE at low loads is attributed to the ethanol-air mixture which is too lean to support combustion owing to high excess air ratio. Moreover, the high latent of vaporisation has led to the cooling of combustible mixture thus contributing to decrease in BTE. At high loads, viz., 75% and 100% of rated load, BTE increased up to 4.6% and 4.3 % respectively as compared to baseline diesel case. The increase of BTE with increase in load is caused by homogeneous air-ethanol mixture thus resulting into enhanced combustion. Apart from this,

the increased ignition delay augments the energy release rate and reduces heat losses due to non-availability of sufficient time to transfer heat from cylinder walls to the coolant.

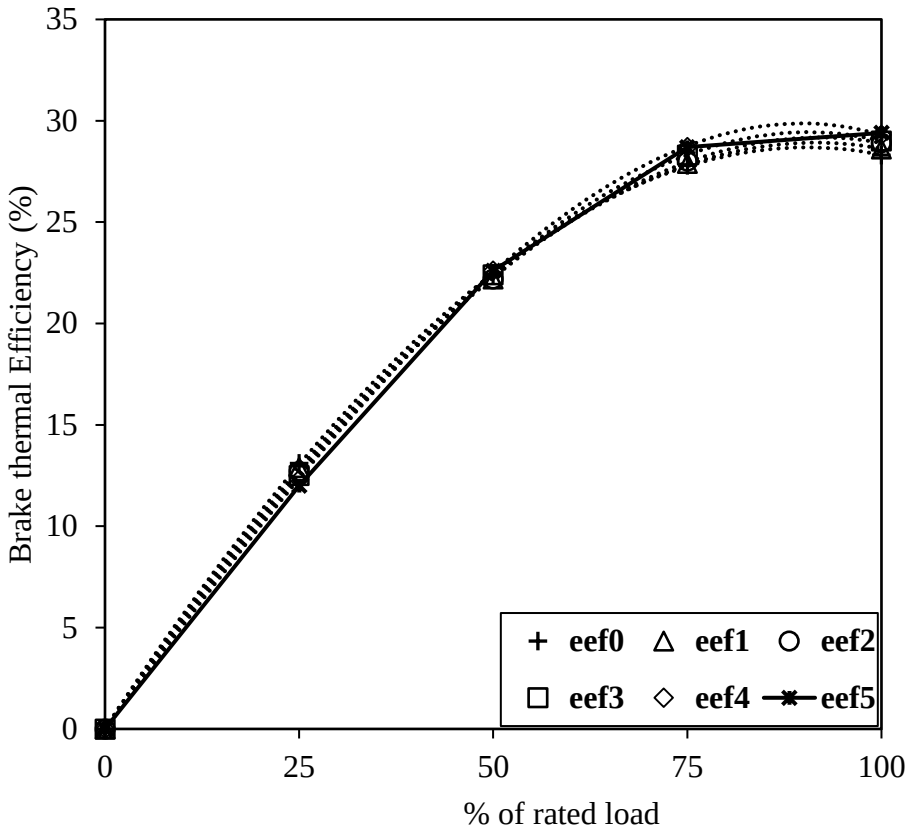

Fig 4.39 Variation of Brake thermal efficiency with load for different ethanol energy fraction

4.3.3 Exergy efficiency

The exergy efficiencies (as shown in Fig. 4.40) of the engine under investigation exhibit similar behaviour to the thermal efficiencies as given in Fig. 4.39. The exergy efficiencies are slightly lower than the corresponding thermal efficiencies. The exergy losses due to the exhaust gas and heat flow from the engine are other contributors to system inefficiency, apart from the irreversibilities of the combustion process. The destruction of exergy (or exergy loss) due to the heat carried away by the exhaust gas can be decreased by reducing the exhaust gas temperature.

4.3.4 Exhaust gas temperature

Fig. 4.41 shows the variation of exhaust temperature of diesel fuel with different rates of ethanol fumigation for various engine loads. It is obvious that exhaust temperature increases with the load for diesel as well as for all rates of ethanol fumigation as the heat release rate is increased. The exhaust temperatures (ºC) of 161, 156, 149, 143, 135 and 125 at no-load

whereas 521, 527, 532, 538, 543 and 550 were observed at full load for eef0, eef1, eef2, eef3, eef4 and eef5 respectively. The results show that the exhaust gas temperature decreased with increase in ethanol energy fraction for conditions of no load and 25% of rated load, that can be attributed to quenching of cylinder charge due to higher latent heat of evaporation of ethanol. However, the increase of exhaust temperature at higher loads is due to increase in heat release rates which outweighs the quenching factor.

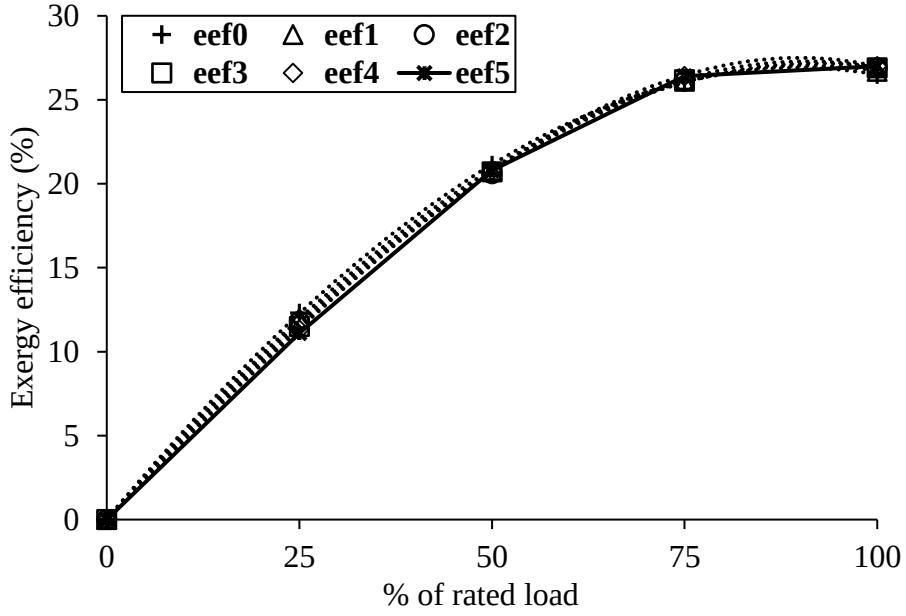

Fig 4.40 Variation of Exergy efficiency with load for different ethanol energy fraction

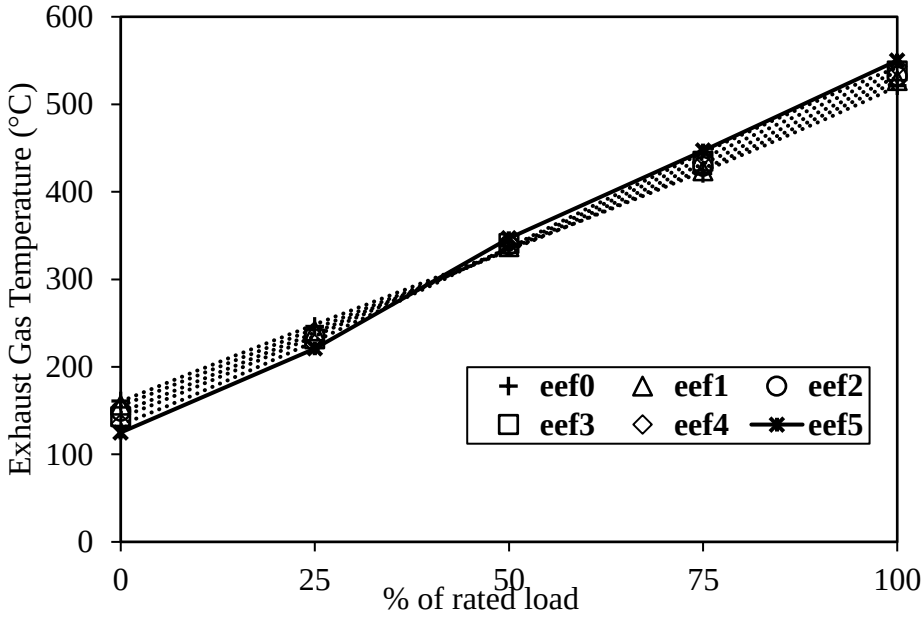

Fig 4.41 Variation of exhaust temperature at various loads for different ethanol energy fraction

4.3.5 Oxides of Nitrogen (NOx)

As evident from Fig. 4.42 maximum reduction in NOx emission of 35%, 30%, 24%, 19% and 9% at no load, 25%, 50%, 75% and 100% of rated load is observed for all rates of ethanol energy fraction as compared to eef0. The decrease in NOx emission with increase in ethanol energy fraction is attributed to high latent heat of vaporisation which reduces the combustion temperature. In general, the drop in NOx emission was observed to increase with higher ethanol energy fraction modes.

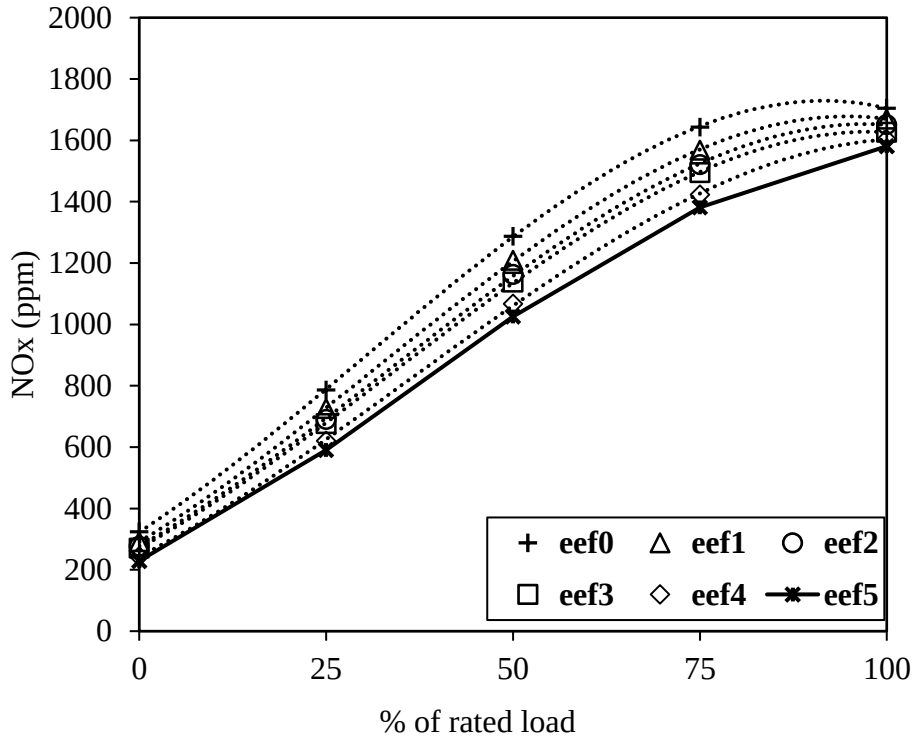

Fig 4.42 Variation of NOx with load for different ethanol energy fraction

4.3.6 Hydrocarbons and carbon monoxide (HC and CO)

Fig. 4.43 exhibits the increase of HC emission with engine load for different rates of ethanol-fumigation. Comparing with eef0, HC increase of 54%-281% at no load, 41%-214% at 25% of rated load, 31%-158% at 50% of rated load, 24%-115% at 75% of rated load and 5%-73% at full load were observed for different ethanol energy fractions.

As shown in Fig. 4.44, CO emissions decreased up to certain load value and then again increased with the increasing loads. It can be explained by the fact that improved combustion with increasing load results in decreasing values of CO up to a particular load. But at a

certain higher load condition CO exhibit increasing trend due to rich mixture leading to poor mixing. As compared to eef0, maximum increase in CO emissions of 93%, 1.24 times, 1.9 times, 2.4 times and 1.83 times respectively have been recoded for various ethanol energy fractions at 0, 25%, 50%, 75% and 100% of rated load.

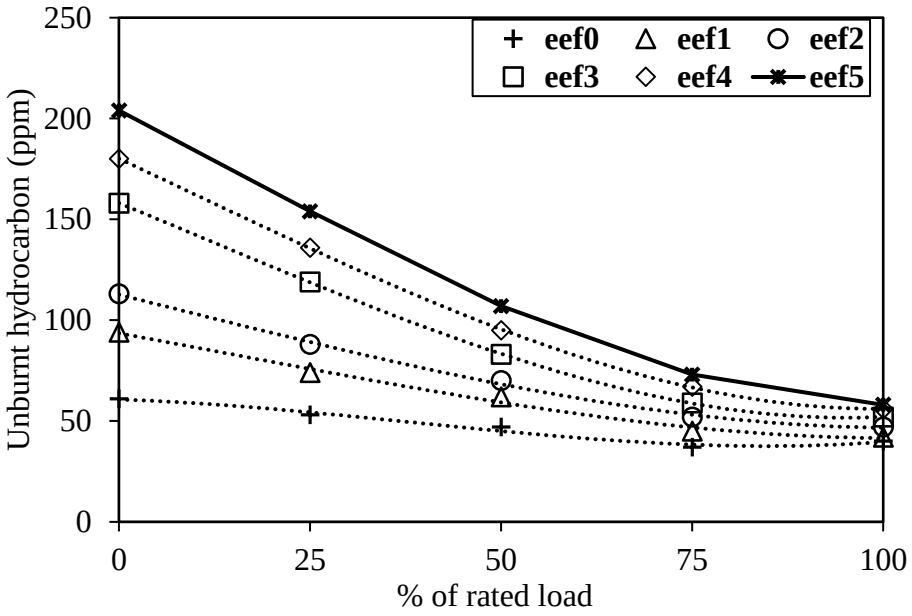

Fig 4.43 Variation of HC with load for different ethanol energy fraction

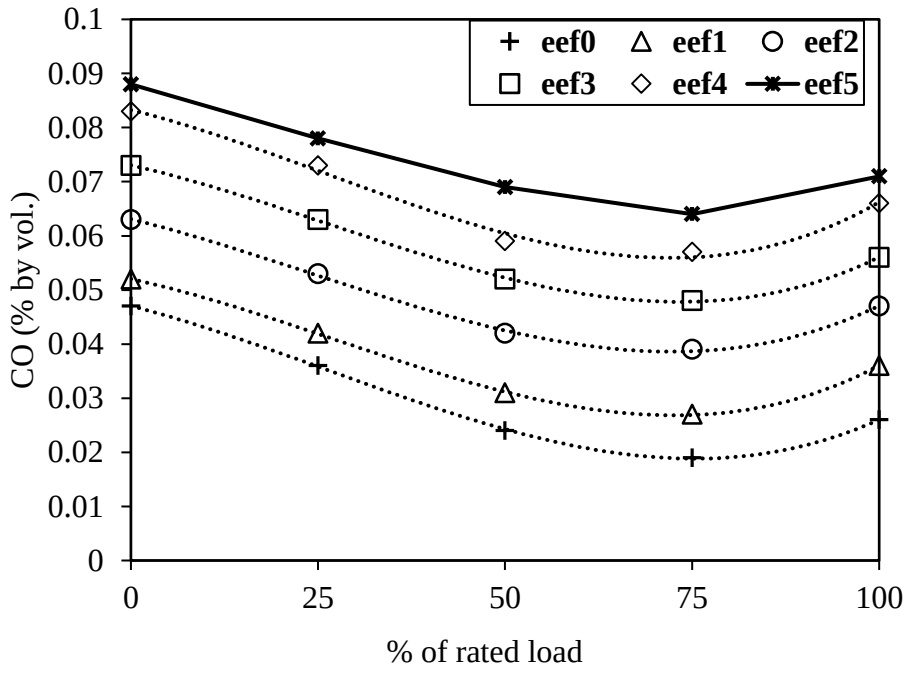

Fig 4.44 Variation of CO with load for different ethanol energy fraction

4.3.7 Carbon di-oxide (CO_2)

As shown in Fig 4.45, CO_2 concentration increases with the engine load for pure diesel as well as for different ethanol energy fractions because of enhanced combustion due to availability of more oxygen and higher in-cylinder temperature. Maximum decrease of 8%, 17%, 22%, 28% and 38% respectively have been observed in CO_2 for eef1, eef2, eef3, eef4 and eef5 as compared to eef0.

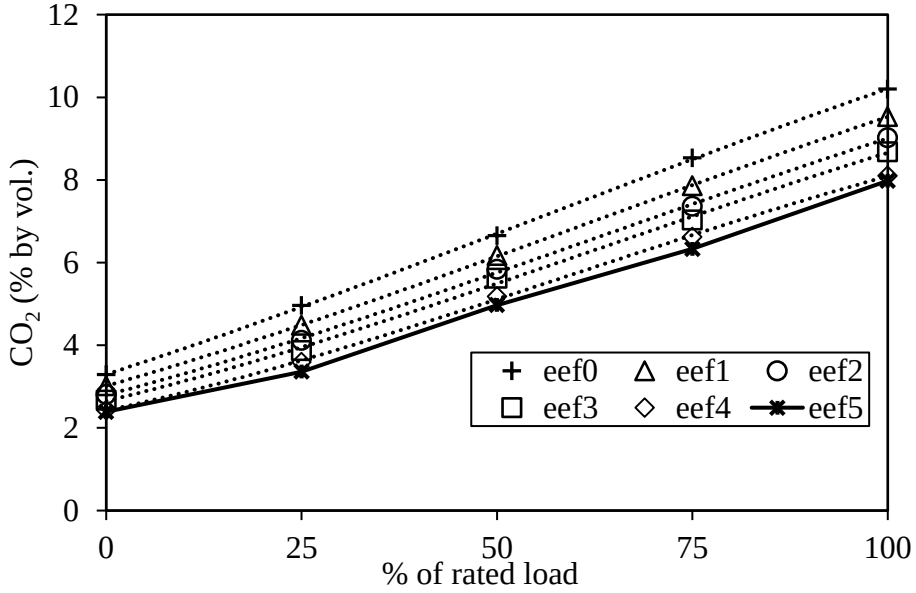

Fig 4.45 Variation of CO_2 with load for different ethanol energy fraction

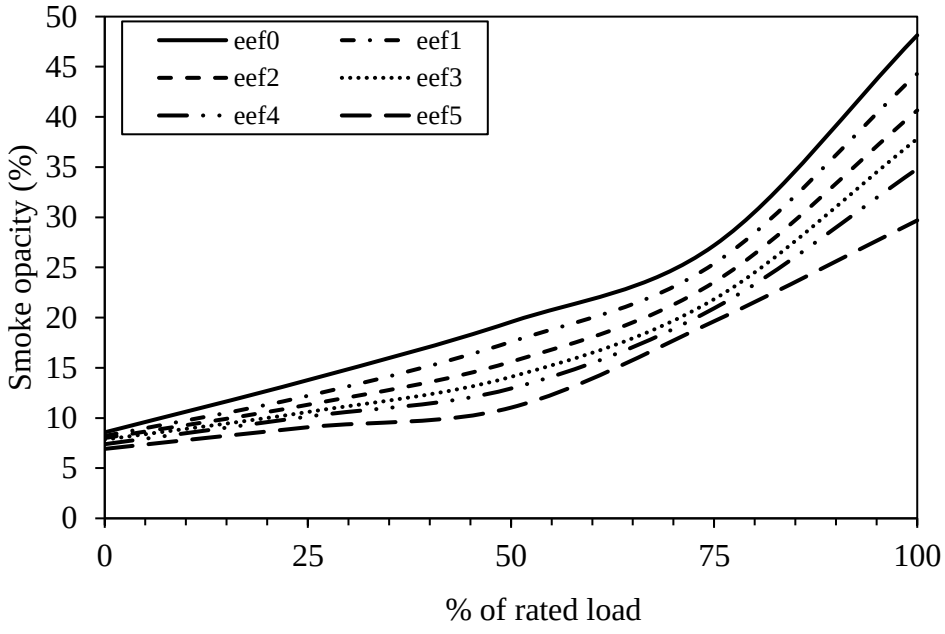

Fig 4.46 Variation of smoke opacity with load for different ethanol energy fraction

4.3.8 Smoke opacity

As shown in Fig. 4.46 maximum decrease of 20%, 28%, 34%, 44% and 47% respectively has been recorded in smoke opacity for eef1, eef2, eef3, eef4 and eef5, as compared to eef0. Due to large latent heat of vaporisation the increase of ethanol energy fraction will increase the ignition delay, leading to decrease in the smoke opacity.

4.3.9 In-cylinder pressure and rate of pressure rise

As shown in Fig. 5.47, the values of peak pressure (in bars) at full load observed are 62.1, 63.1, 63.7, 64.9, 63.2 and 58.2 respectively for eef0, eef1, eef2, eef3, eef4 and eef5. The position of occurrence of peak pressure is shifted by 1-4°CA as compared to eef0.

Fig. 5.48 illustrates the trends for the rate of pressure-rise with the crank angle for pure diesel as well as for different ethanol-fumigation rates. At full load, the maximum rate of pressure rise (bar/°CA) has been found to be 2.15, 2.37, 2.53, 2.49, 2.44 and 2.17 for eef0, eef1, eef2, eef3, eef4 and eef5 occurring 2-8 °CA later as compared to eef0. It is due to the longer ignition delay and shorter combustion duration of ethanol fumigation.

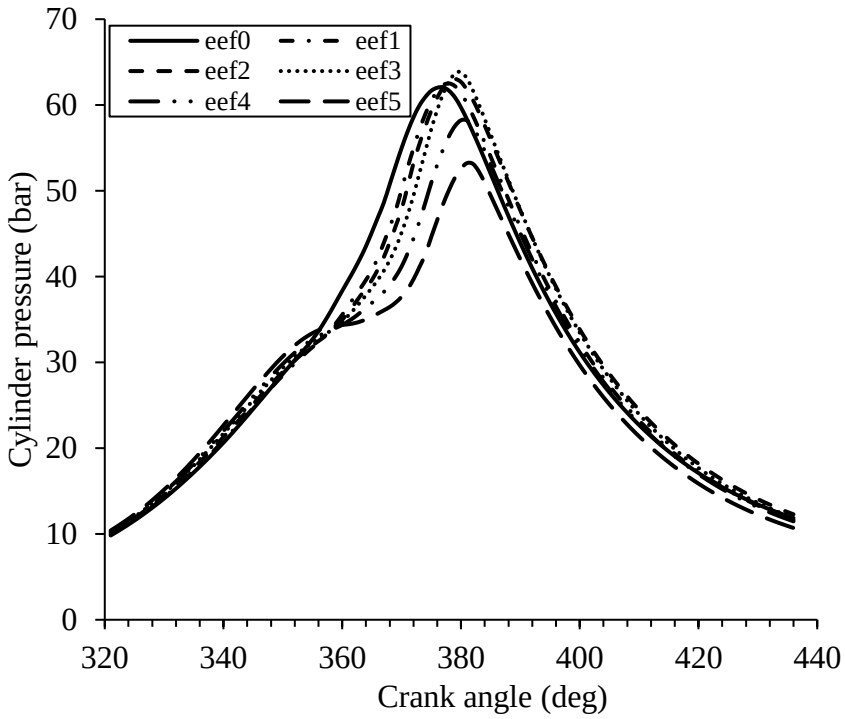

Fig 4.47 Variation in cylinder pressure with crank angle at full load

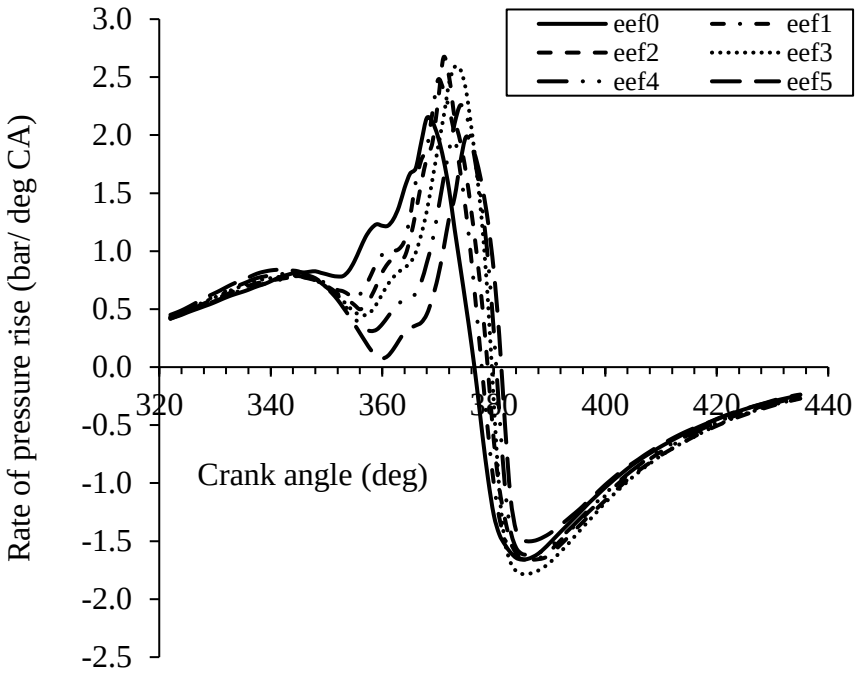

Fig 4.48 Variation in rate of pressure rise with crank angle at full load

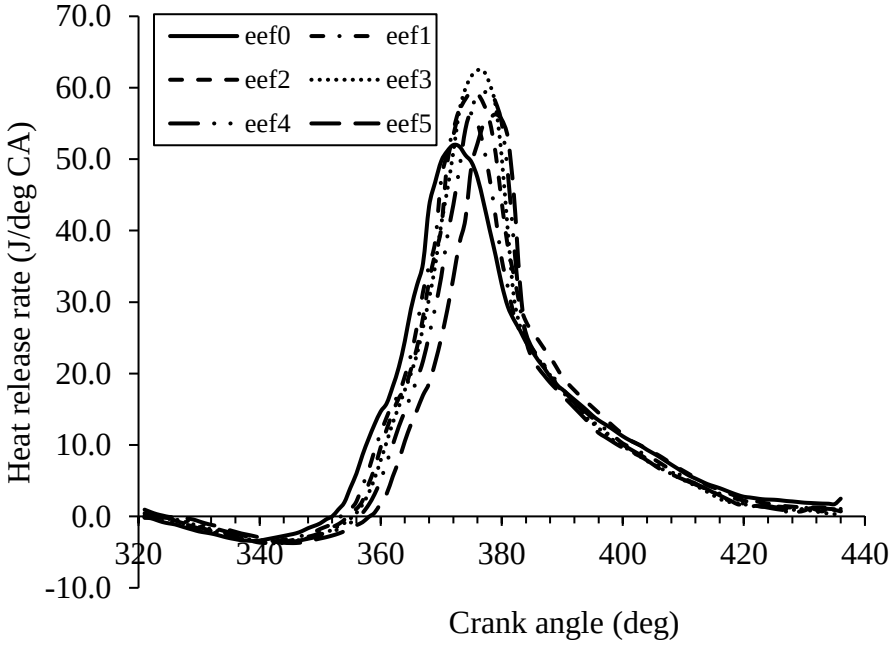

Fig 4.49 Variation in heat release rate with crank angle at full load

4.3.10 Heat release rate (HRR)

Fig. 4.49 shows the variation in HRR with the crank angle at full load with pure diesel and all ethanol energy fractions. The values of HRR has been found to be 52, 56.8, 59.5, 62.5 and 62

(J/deg °CA) for eef0, eef1, eef2, eef3, eef4 and eef5. The occurrence of maximum HRR for any rate of fumigation is retarded by 1-8 °CA, in comparison with that of eef0. Ethanol being oxygenated fuel, HRR increases due to availability of more oxygen and thus improved combustion. Due to increase in HRR, the peak cylinder pressure as well as rate of pressure rise also increases.

4.3.11 Ignition delay, combustion duration and mass fraction burned

As shown in Fig. 4.50, the ignition delay of eef0 at full load is 15 °CA and increases by about 2-5 ºCA at full load for all rates of ethanol energy fractions. The increased ignition delay is caused due to low cetane number and large latent heat of vaporisation of ethanol. The ignition delay (°CA) of 15, 16.4, 17.4, 18.4, 19.4 and 21.1 and the combustion duration (°CA) of 37.3, 36.4, 34.9, 33.6, 33.1 and 32.0 respectively were observed for eef0, eef1, eef2, eef3, eef4 and eef5 at full load as shown in Fig 4.50. The decreasing values of combustion duration with increasing ethanol content is attributed to enhanced mixing of fuel and air and increased availability of oxygen.

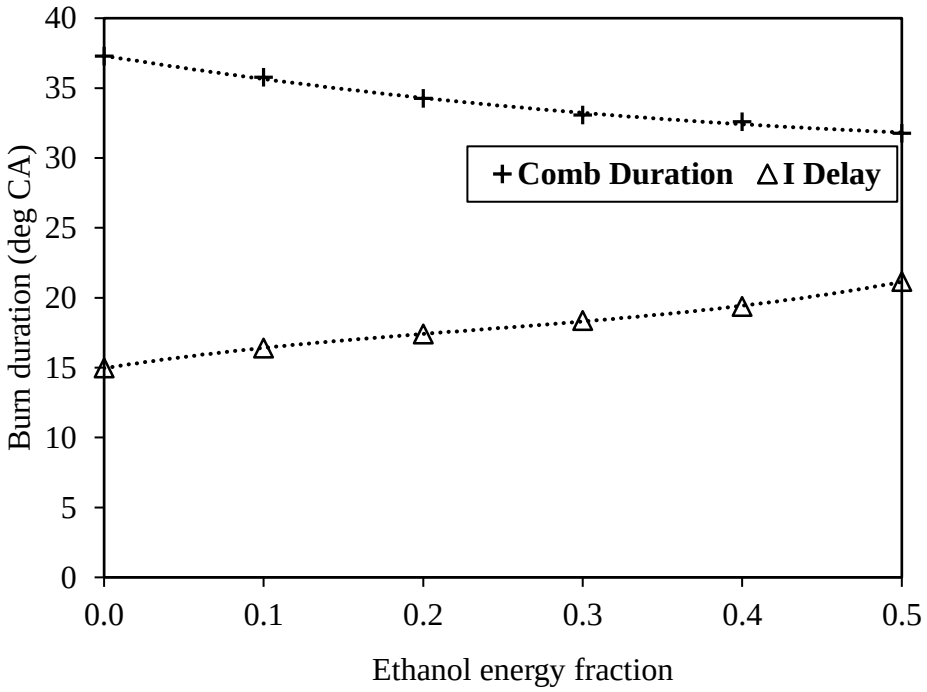

Fig 4.50 Variation of burn duration with different ethanol energy fraction at full load

Fig. 4.51 shows the variation in the Mfb with the crank angle at full load. The mass fraction burnt increases with the rate of fumigation due to increase in oxygen content and enhanced HRR. For eef0, the combustion has been found to be faster up to 15-16° aTDC, after which

the combustion rate enhanced for different rates of ethanol fumigation the rate increasing with increasing ethanol content.

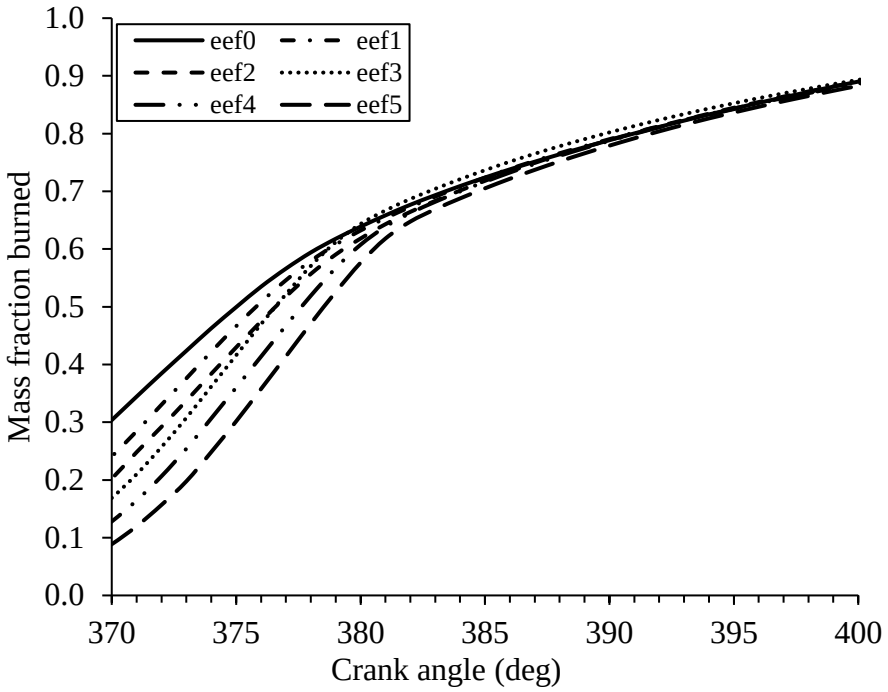

Fig 4.51 Variation in mass fraction burned with crank angle at full load

4.4 Effect of ethanol on engine performance exhaust emission and combustion parameters with various diesel-injection advance angles at constant ethanol flow rate

In fourth mode**,** test-runs were conducted on the engine using various ethanol fumigation rates at different diesel injection timings, viz., 29°, 26°, 23°, 20° and 17° CA bTDC.

4.4.1 Brake thermal efficiency (BTE)

Fig. 4.52 illustrates the variation of BTE with load for diesel and different rates of fumigation at varying injection timing. At fixed ethanol flow rate and given load, the efficiency increased up to maximum of 11.7% by advancing diesel injection timing (as shown in Fig 4.52) due to proper positioning of combustion with respect to crank position. Over-retarded combustion is likely to cause misfiring and consequent decrease in BTE up to 8.6%. The advanced diesel injection prolongs the misfiring limit and allows increased ethanol substitution up to 0.8 kg/hr.

4.4.2 Oxides of nitrogen (NOx)

As shown in Fig. 4.53, NOx increases considerably (up to 36.3%) with increase in diesel injection timing as indicated by the increase in cylinder-pressure implying the rise of the combustion temperature. NOx emission decreased up to 15.7% with delayed diesel injection when compared with original injection timing.

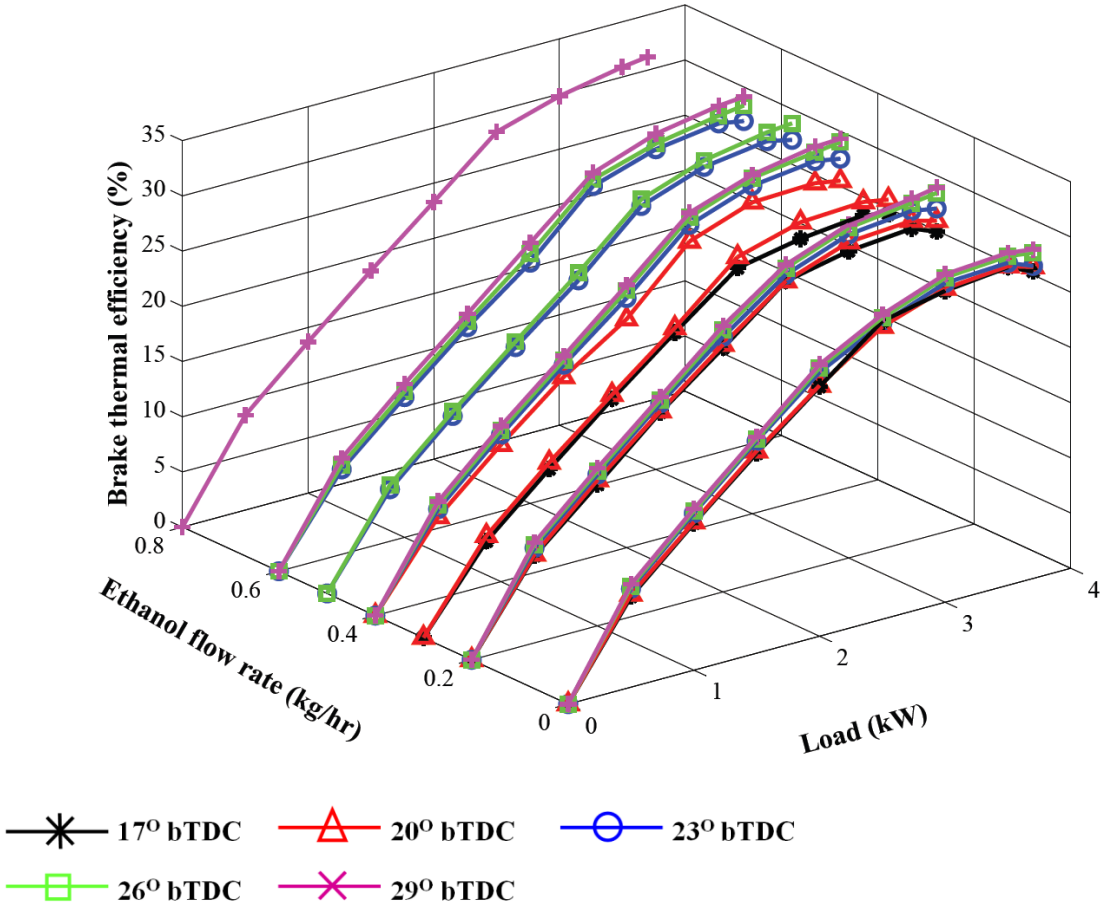

Fig 4.52 Variation of Brake Thermal efficiency with ethanol flow rate and diesel injection timing

4.4.3 HC emissions

As evident from Fig 4.54, the decreased HC emission up to 28.6% with increase in advance of diesel injection timing may be explained by the enhanced combustion caused due to the increased combustion temperatures, which in turn occurs due to the increased in-cylinder pressure and heat release rate. Similarly, the increased HC emission up to 37.7% with retardation of diesel injection timing can be attributed to the bulk gas quenching due to low combustion temperature.

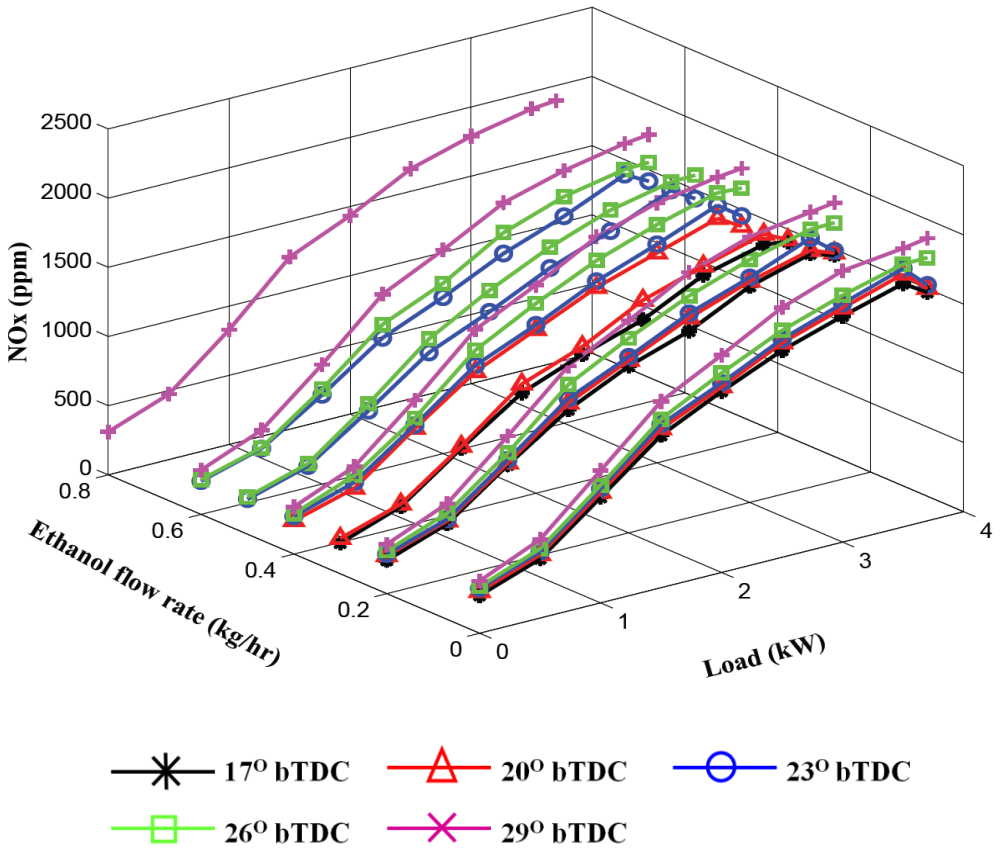

Fig 4.53 Variation of NOx emission with ethanol flow rate and diesel injection timing

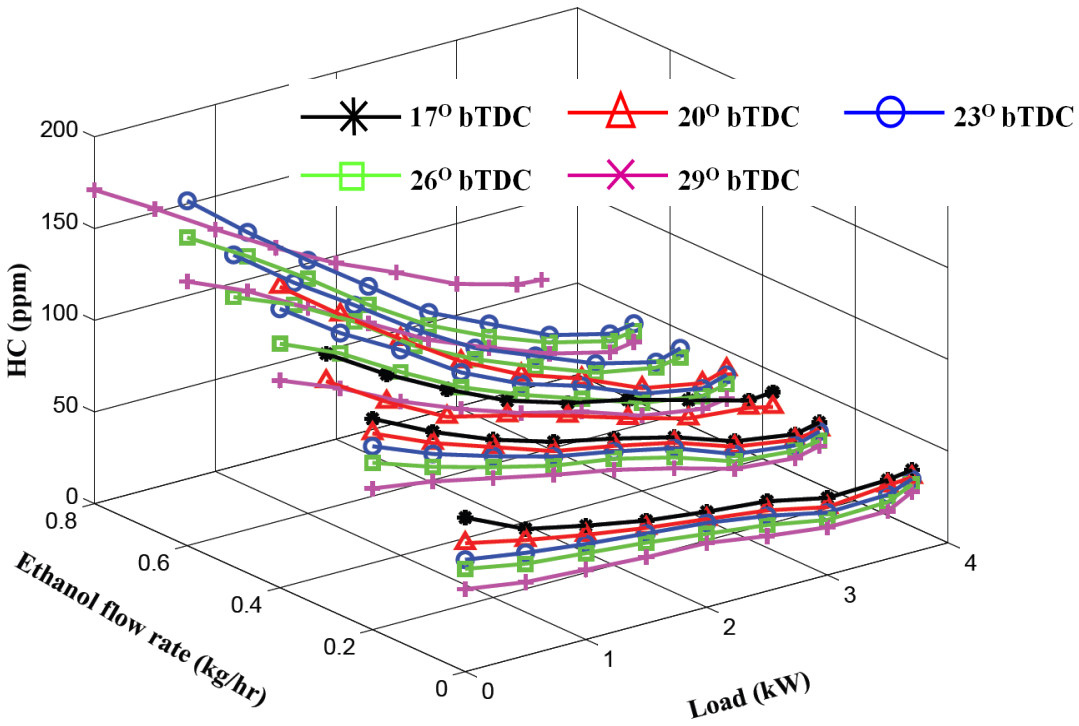

Fig 4.54 Variation of HC emission with ethanol flow rate and diesel injection timing

4.4.4 CO emissions

CO emission decreases with advance in injection timings due to increased combustion temperature and enhanced combustion as shown in Fig 4.55. The decrease of CO emission up to 31.8% at low loads was observed with advance of injection timing for different ethanol flow rates. The occurrence of misfiring at retarded injection timings renders the self-sustenance of combustion difficult due to its occurrence in later part of the expansion stroke. Thus, the retardation of injection timing contributes to increase CO emission as evident from Fig 4.55.

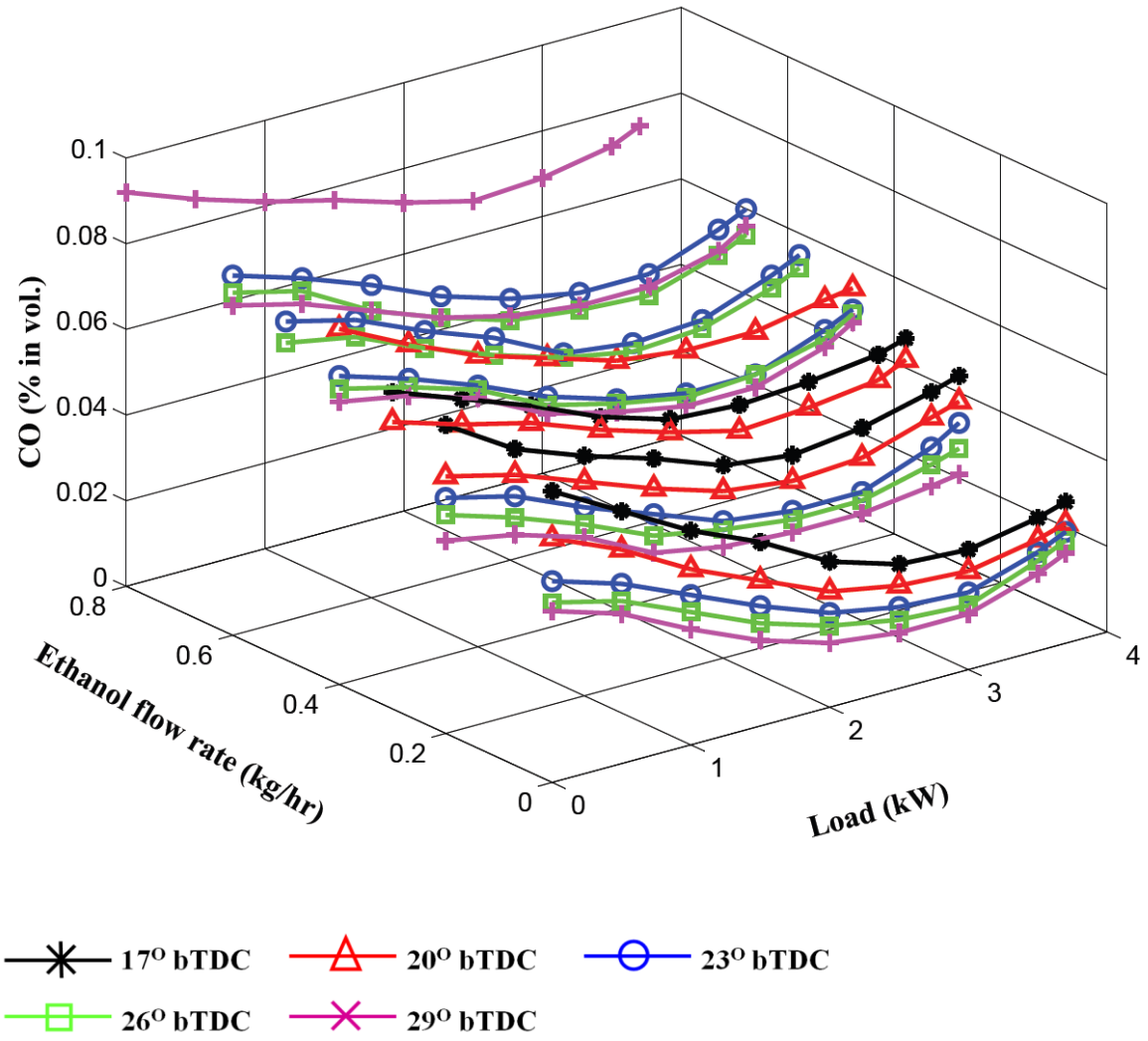

Fig 4.55. Variation of CO emission with ethanol flow rate and diesel injection timing

4.4.5 CO_2 emissions

As shown in Fig. 4.56, CO_2 concentration increases with the advance of diesel injection timing due to higher combustion temperature.

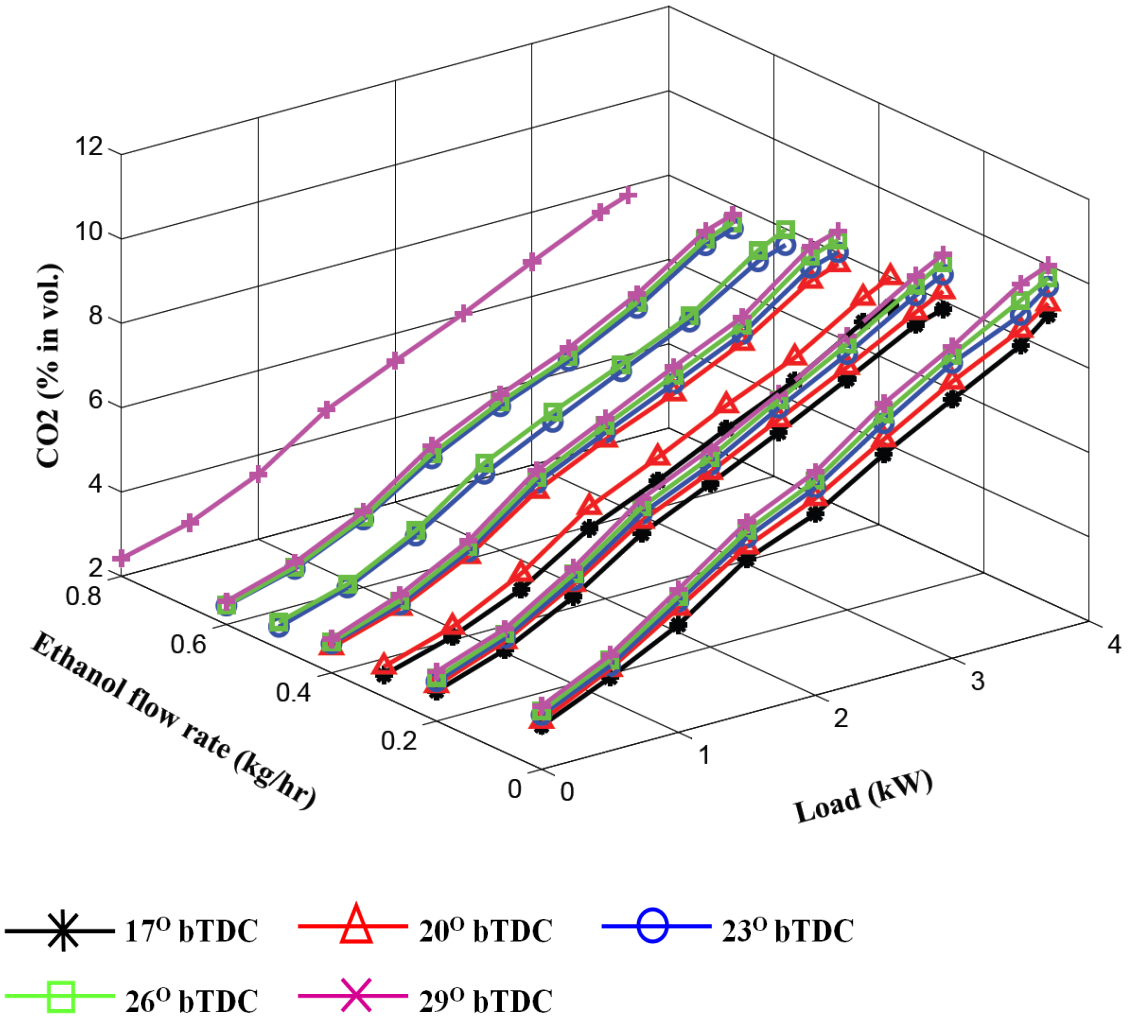

Fig 4.56. Variation of CO_2 emission with ethanol flow rate and diesel injection timing

4.4.6 Smoke Opacity

Advancing the injection timing also reduced the smoke emissions as shown in Fig 4.57. The earlier injection led to higher temperatures during the expansion stroke and more time in which oxidation of the soot particles occurred. Quite high opacity, as much as 13.4% higher as compared to original injection timing was evident at retarded diesel injection timings due to presence of unburnt hydrocarbons.

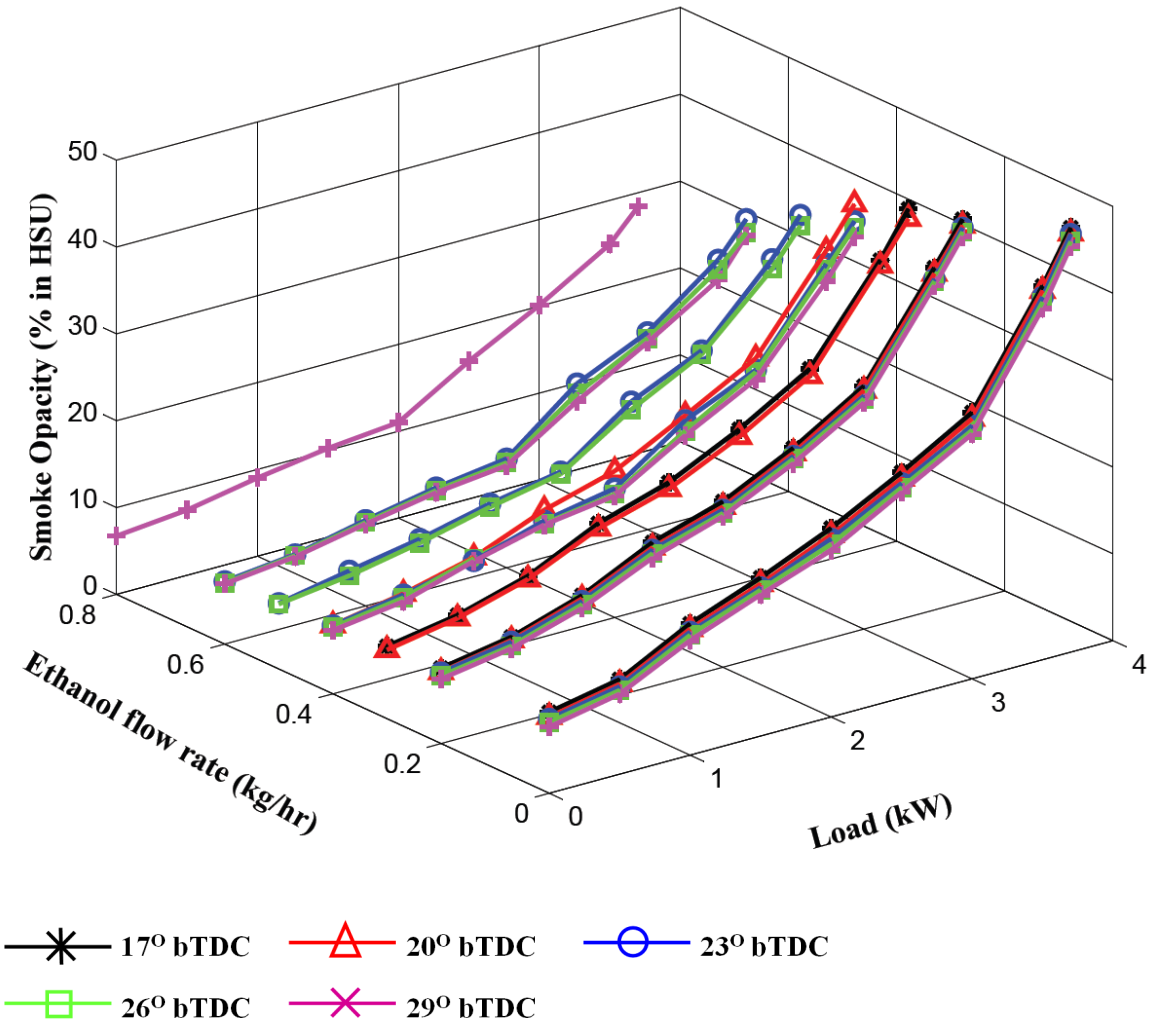

Fig 4.57 Variation of smoke opacity with ethanol flow rate and diesel injection timing

4.4.7 In-cylinder pressure

Advanced diesel injection extends the limit of utilisation of higher ethanol flow rate. With increase in injection advance, considerably higher peak pressure and high rate of pressure rise may be observed as shown in Figs. 4.58 and 4.59. The extent of injection advance is limited by occurrence of knock. Moreover, injection advance beyond a certain limit decreases the maximum attainable pressure owing to the fact that when injection takes place too early, the fuel is not properly prepared for combustion. This may be attributed to the lower air temperature in the combustion chamber at the time of fuel injection and also due to lack of intermixing of fuel and air during the early part of the injection period. The retardation of diesel injection timing beyond a certain limit enhances the likelihood of misfiring. The condition of misfiring limits the maximum ethanol substitution for a given operating condition. When late injection occurs maximum pressure decreases appreciably (as shown in

Fig. 4.58) because by the time combustion takes place, the piston is on its way down on the power stroke. Consequently, part of pressure rise due to combustion is utilised in overcoming the expanding volume of the cylinder thus, decreasing the maximum pressure within the cylinder.

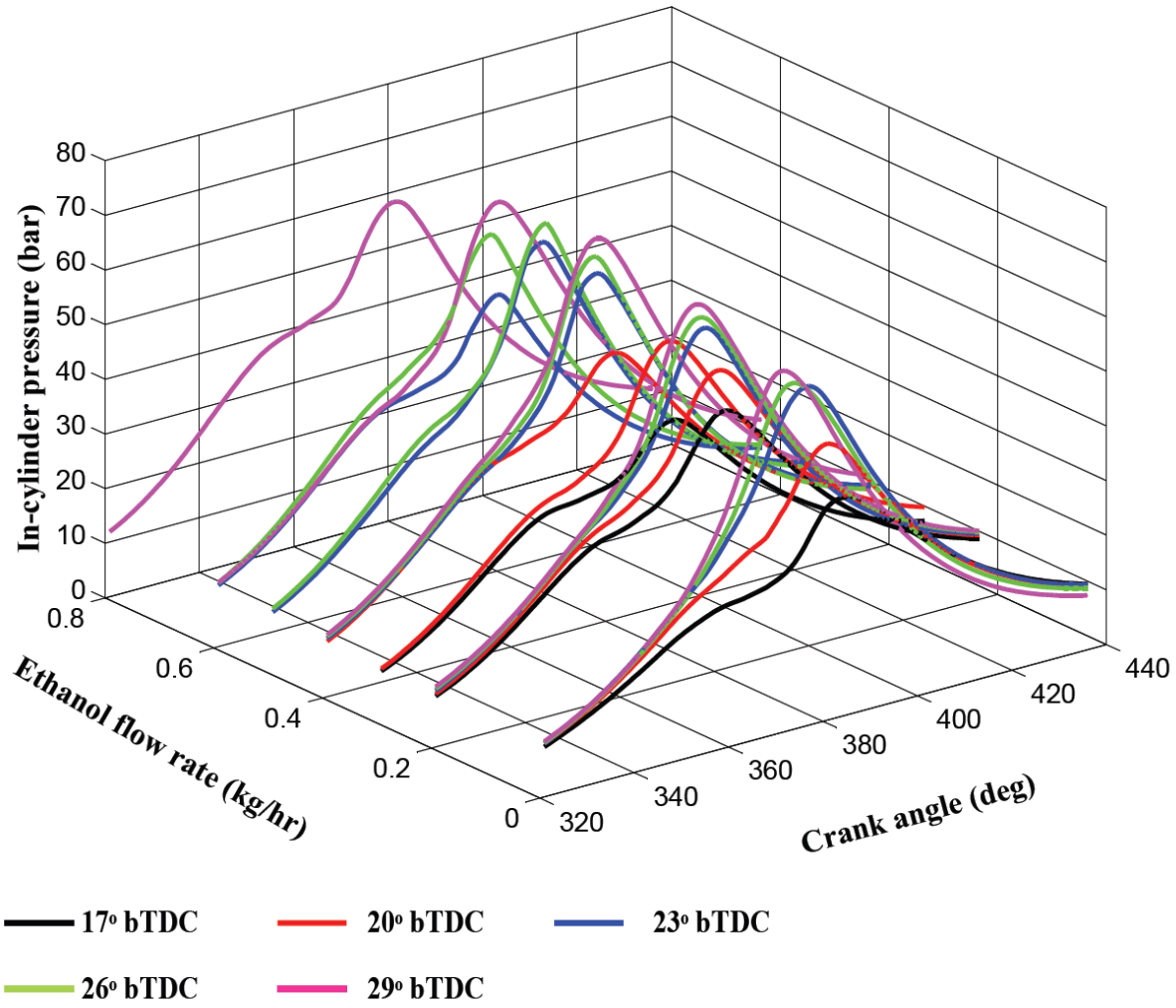

Fig 4.58. Variation of cylinder pressure with ethanol flow rate and diesel injection timing

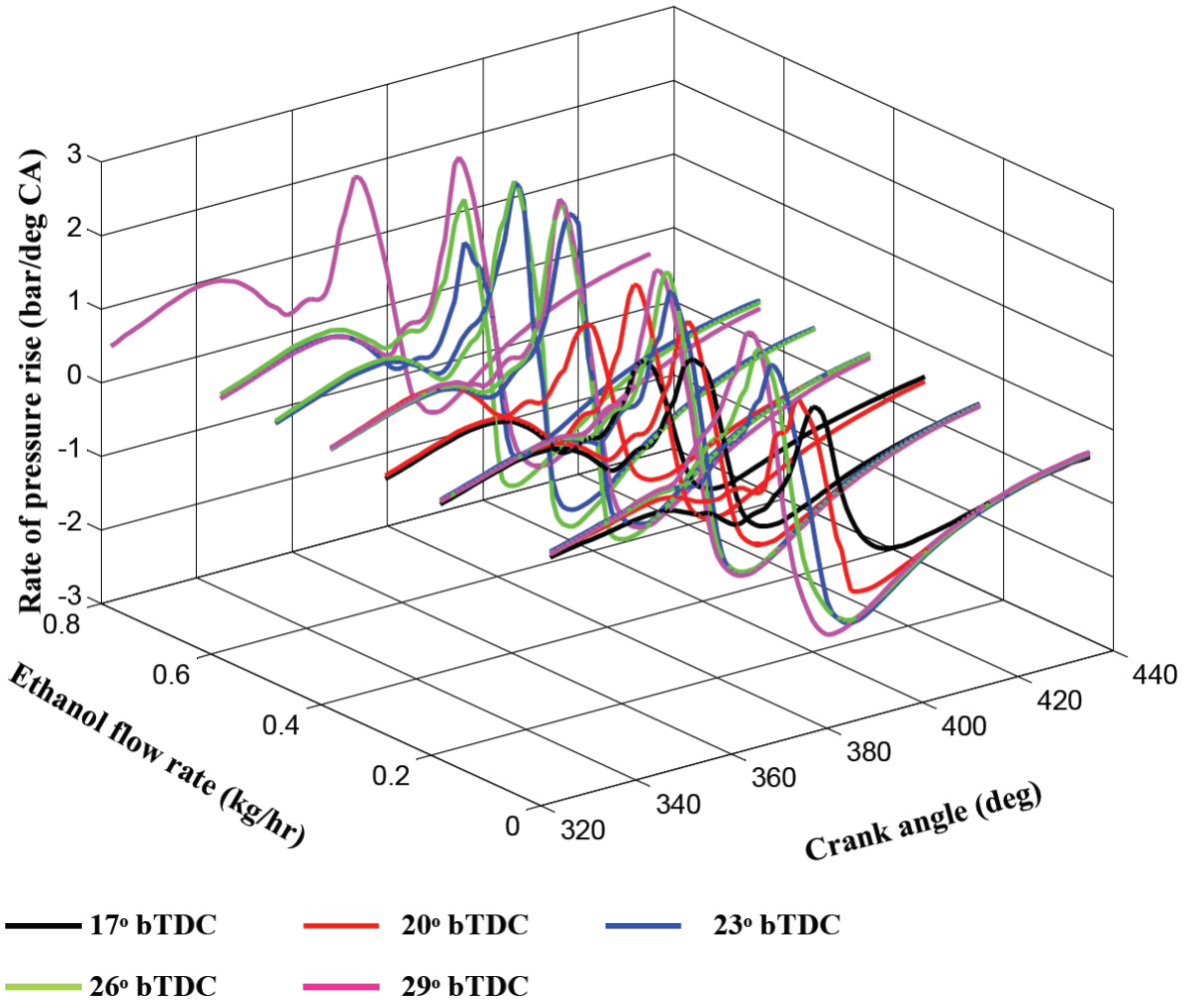

Fig 4.59 Variation of rate of pressure rise with ethanol flow rate and diesel injection timing

4.4.8 Heat Release rate (HRR)

The advance of injection timing yields increased HRR, as shown in Fig. 4.60, due to two factors: (a) increased fraction of burning occurring in uncontrolled combustion stage and (b) increased ignition delay allowing better mixing of ethanol in air. For a given diesel injection timing with the increase of ethanol flow rates the point of occurrence of peak pressure and peak HRR shifted 1-4ºCA later in a cycle which is attributed to increased ignition delay.

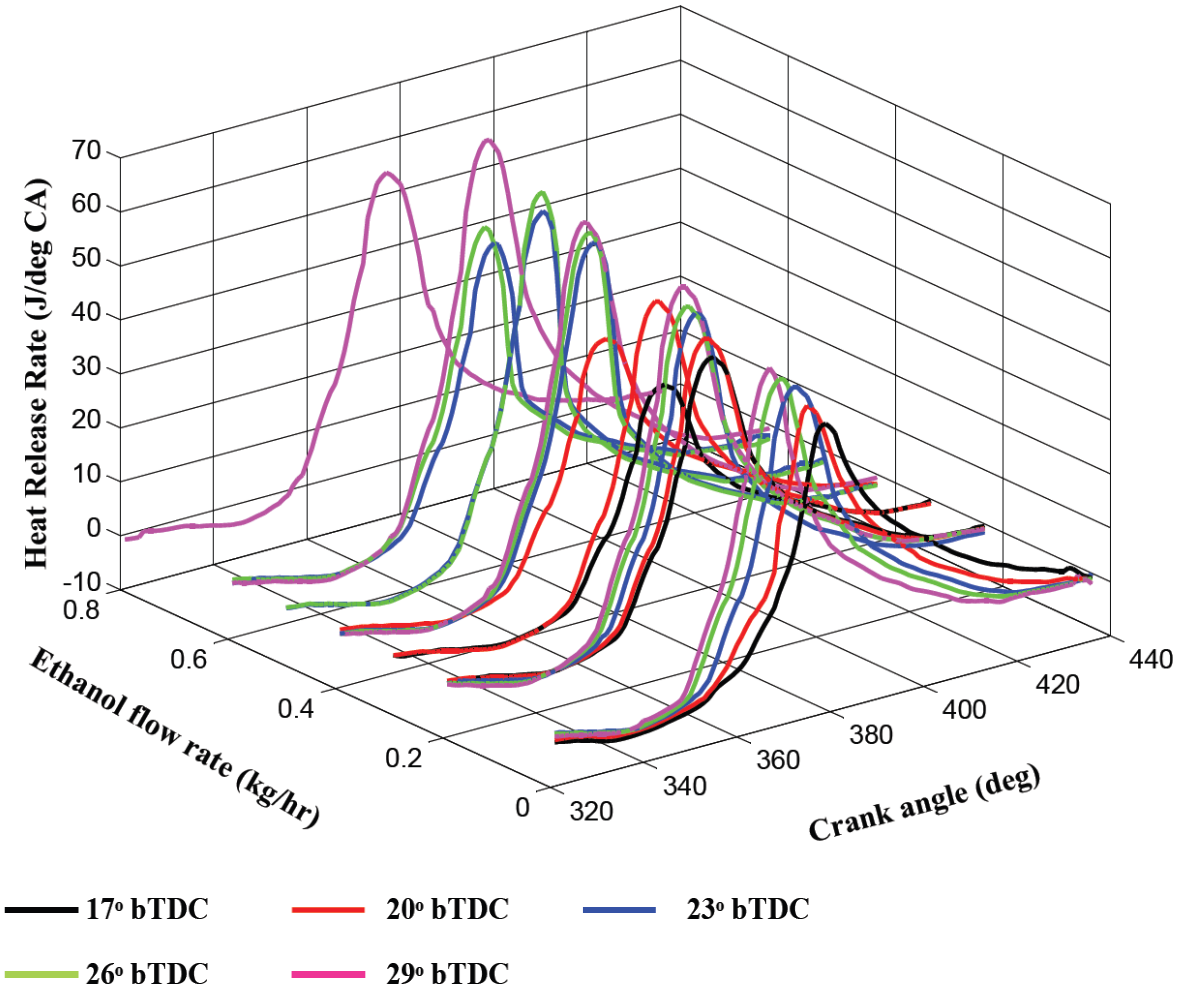

Fig 4.60 Variation of heat release rate with ethanol flow rate and diesel injection timing

4.4.9 Burn duration

At advanced diesel injection timing, in-cylinder pressure and temperature are not sufficient to ignite the fuel and consequently, increased amount of evaporated fuels (ethanol and diesel) get accumulated during the ignition delay period. This longer ignition delay may lead to rapid burning rate in premixed mode causing shorter combustion duration resulting in drastic rise of pressure and temperature. But, in the case of retarded injection timing, in-cylinder pressure and temperature are sufficient to ignite the fuel and relatively small amount of fuel(s) gets accumulated during the ignition delay period. This shorter ignition delay leads to slow burning rate in premixed mode rather than diffusion mode resulting in slow rise in pressure and temperature and longer combustion duration. Reductions in pre-mixed burn duration with increase in advance angle were observed for various ethanol fumigation rates. The variations of ignition delay, combustion duration and pre-mixed burn duration with different ethanol flow rates and various diesel injection angles has been depicted in Fig 4.61.

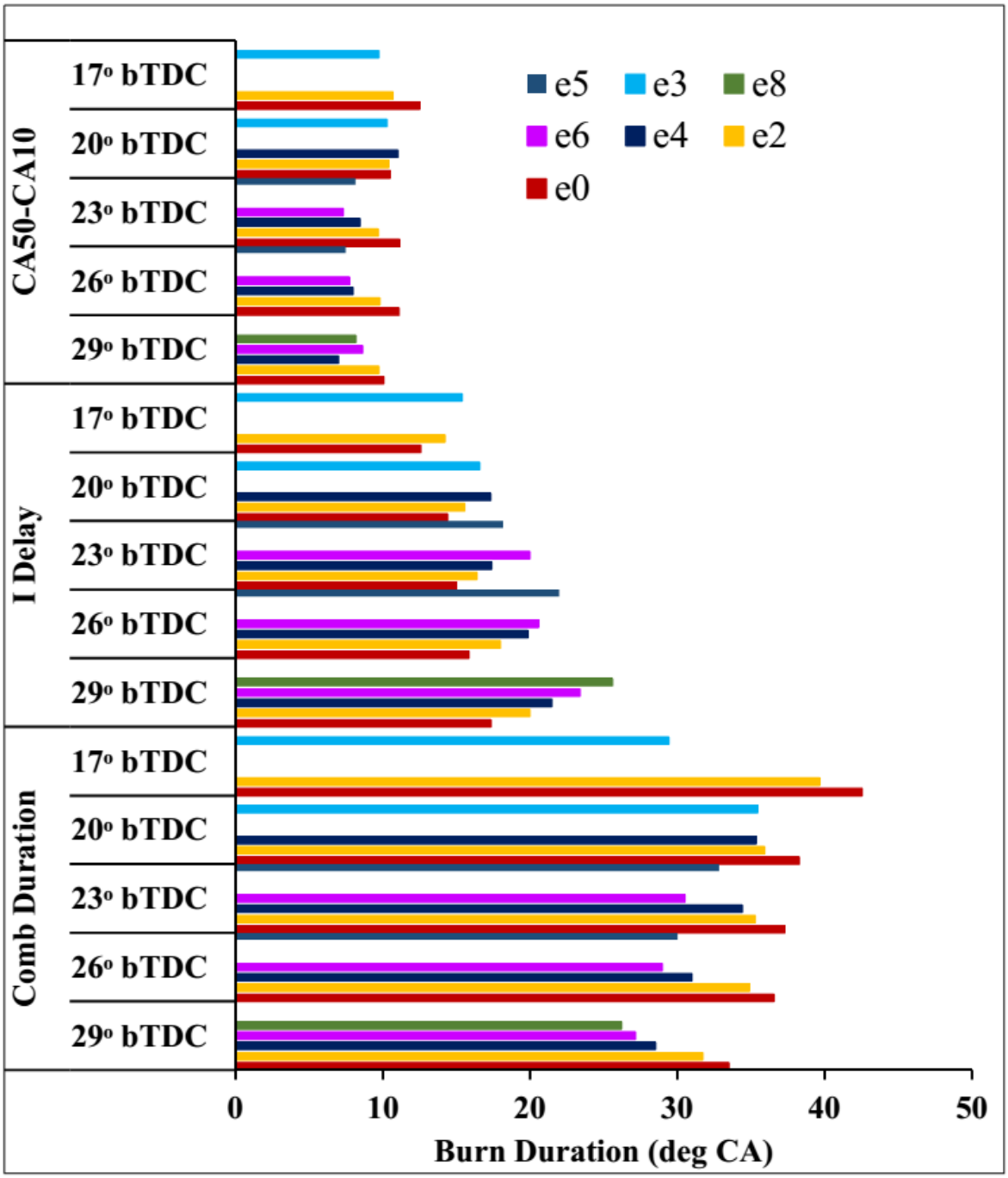

Fig 4.61 Variation of burn duration with ethanol flow rate and diesel injection timing

4.5 Effect of ethanol on engine performance exhaust emission and combustion parameters with pre-heating of ethanol at constant ethanol flow rate

In fifth mode**,** test-runs were conducted on theengine using various ethanol fumigation rates at different ethanol preheating temperatures, 40° and 60° C and the results obtained are compared with those of unheated mode. The ethanol has been heated utilising the heat of the exhaust gases. With the help of heat exchanger, the heat from the exhaust of the engine was recovered to preheat the ethanol upto desired temperature within permissible tolerance of ±2 °C, before it is inducted into the engine. The by-pass valve operated manually is fitted to by-pass the exhaust gases to atmosphere (without tapping its heat energy). Thus, the mass flow rate of exhaust gases is regulated manually to the heat the ethanol to desired temperature. Changes have been incorporated in the figure showing experimental set up and methodology adopted has been included in the manuscript.

4.5.1 Brake thermal efficiency (BTE)

It can be seen that the brake thermal efficiency (shown in Fig. 4.62) increases slightly with preheated ethanol at all the preheating temperatures. The maximum increase of 2.7% in BTE at PHT60 was noticed for e5. The increase in BTE with pre-heating temperatures is probably due to its reduced likelihood of charge-cooling thus resulting the enhanced combustion.

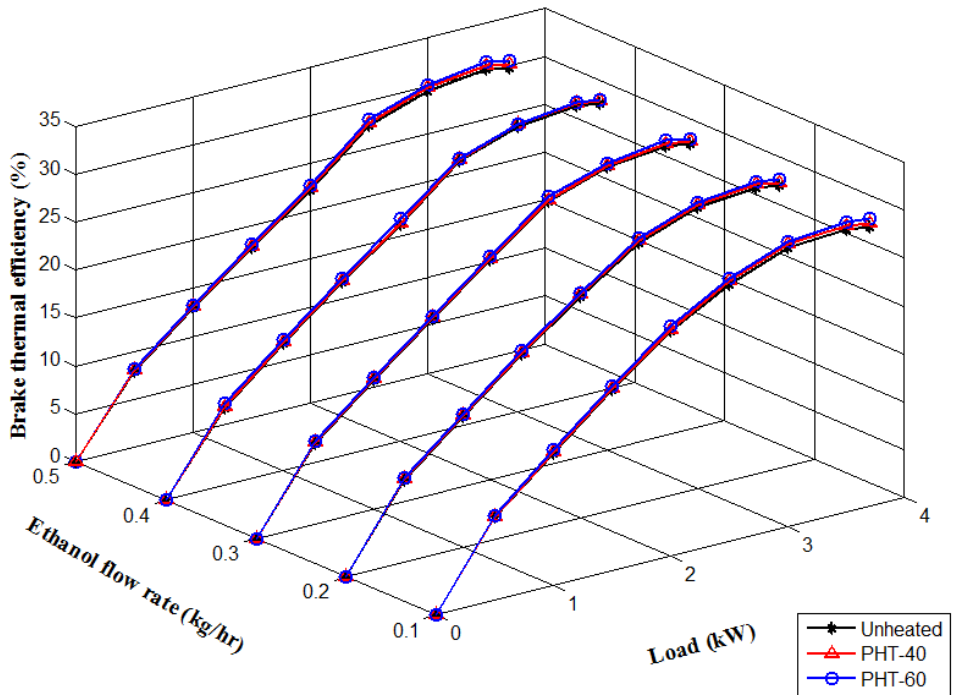

Fig 4.62 Variation of Brake thermal efficiency with ethanol flow rate and ethanol pre-heating temperatures

4.5.2 NOx emissions

The variation of NOx emission with engine-load is shown inFig.5.63. NOx formation in diesel engine is particularly due to high combustion temperature and availability of oxygen. Fuel preheating shows rising trend of NOx emissions due to rapid burning and increased fuel inlet temperatures. This is one of the draw back associated with fuel preheating.

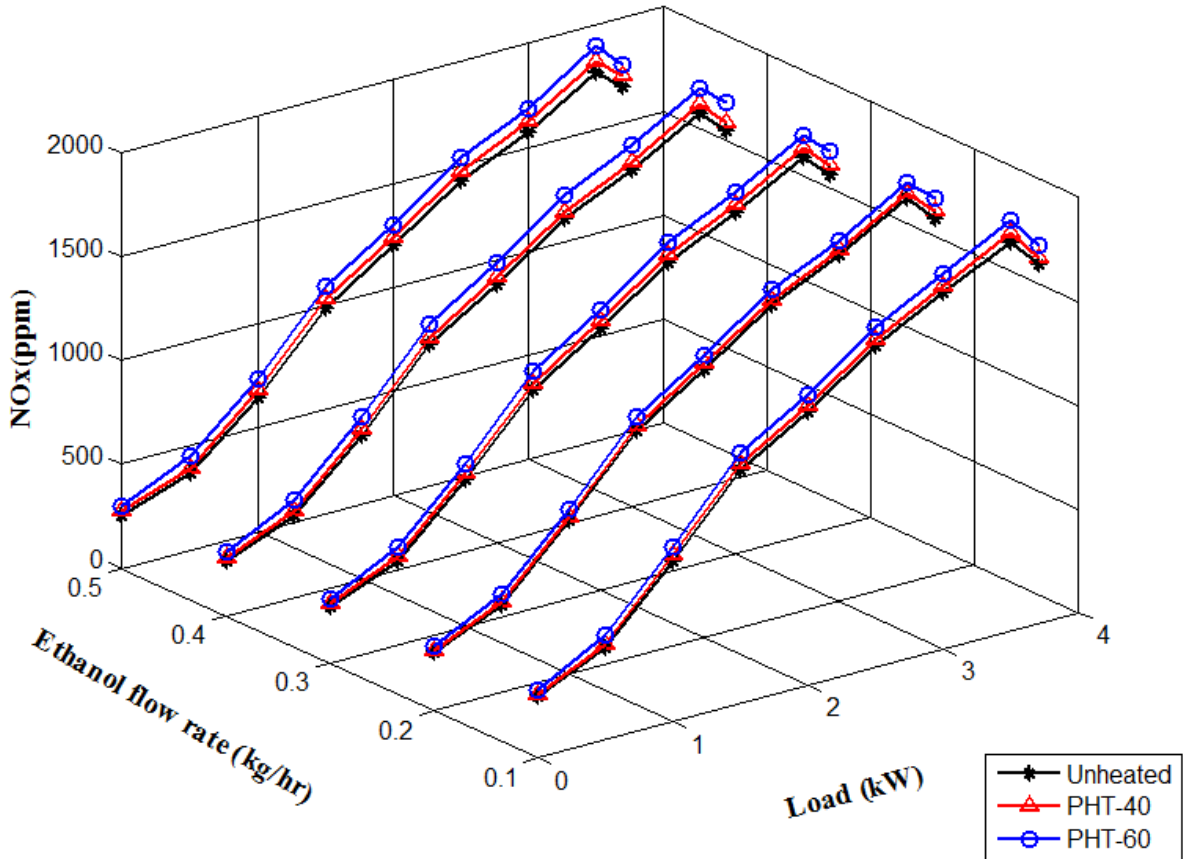

Fig 4.63 Variation of NOx emissions with ethanol flow rate and ethanol pre-heating temperatures

4.5.3 HC emissions

The variation of hydrocarbon emissions with ethanol at different temperatures is shown in Fig. 4.64.As discussed earlier, ethanol-substitution leads to higher HC emissions than pure-diesel operation. Unburnt hydrocarbons are the results of incomplete combustion. Poor volatility of ethanol results in poor mixing of the fuel with air and leading to more hydrocarbon emission at normal temperature. However with the preheated ethanol, there is a reduction in HC emission. Due to the improved vaporization and fuel air mixing rates,

combustion enhances and results in low hydrocarbon emissions with the preheated ethanol. Maximum decrease of 43% in HC emissions was evident at low load condition at PHT-60.

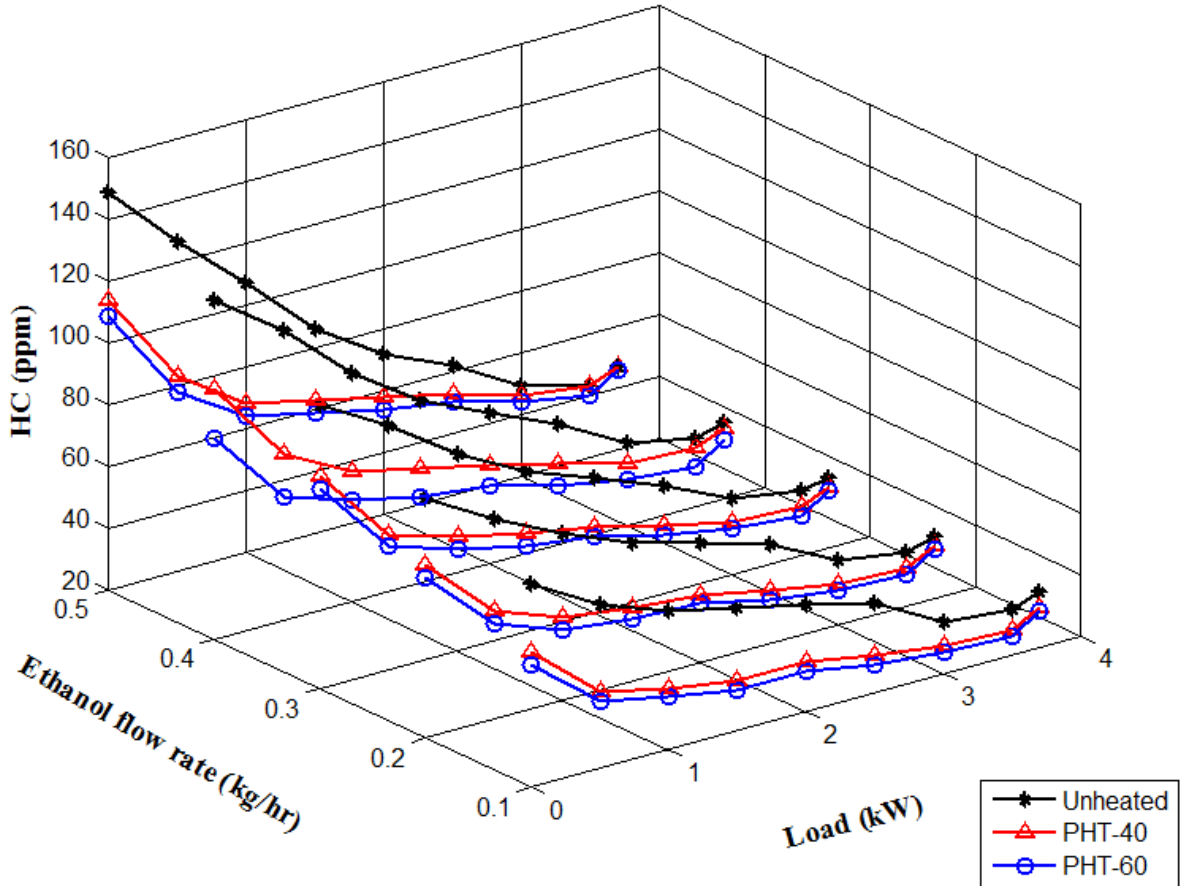

Fig 4.64 Variation of HC emissions with ethanol flow rate and ethanol pre-heating temperatures

4.5.4 CO emissions

Ethanol leads to higher CO emissions than diesel at normal temperature as seen in Fig. 4.65. In addition to the other factors mentioned earlier, fuel richness due to non-availability of sufficient oxygen for complete combustion are also responsible for this behaviour. Rich pockets formed in the cylinder cause more CO emissions with ethanol at normal temperature. However, fuel preheating leads to complete combustion and reduced CO emission. It is apparent that significant increase in HC and CO emissions decreased thermal efficiency at low loads whereas at high loads, slight influence of high heat release rate outweigh the effect of increase of HC and CO emissions thus increasing efficiency.

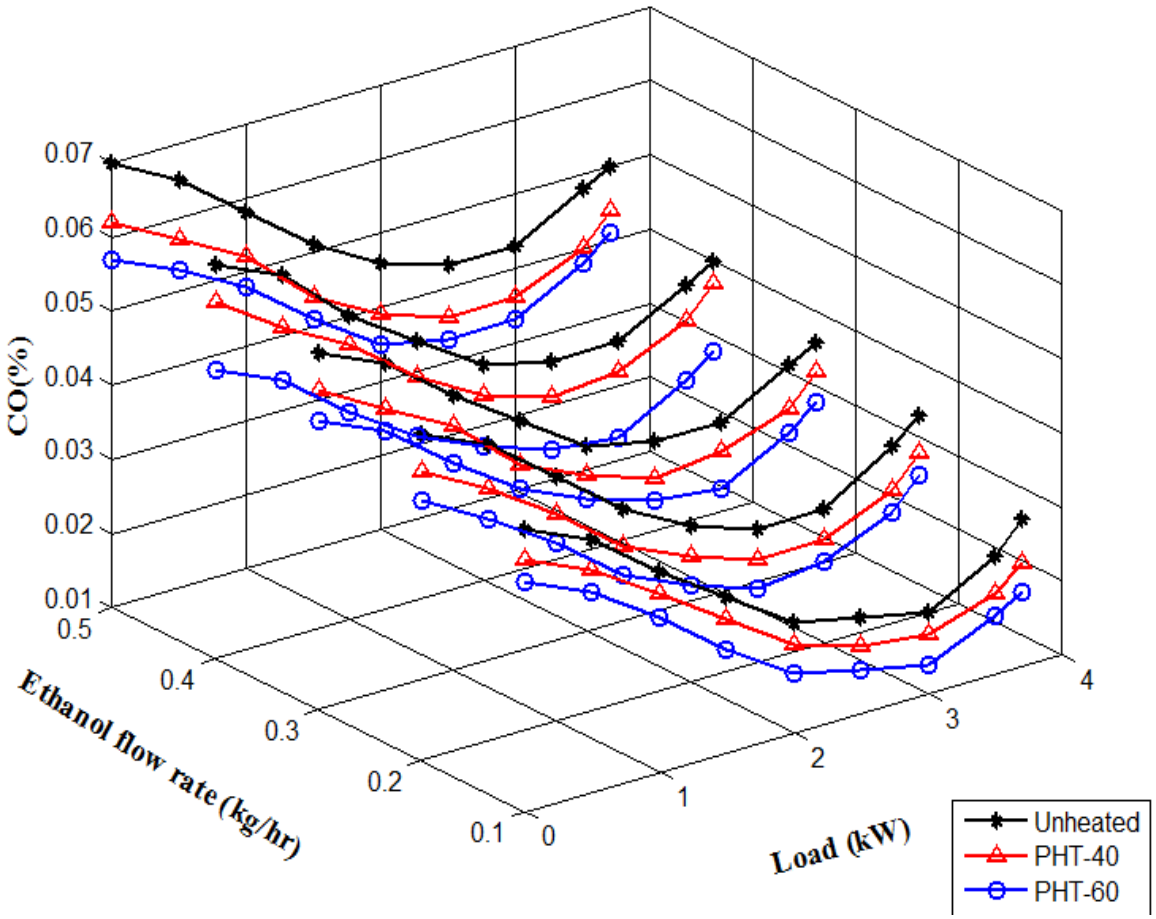

Fig 4.65 Variation of CO emissions with ethanol flow rate and ethanol pre-heating temperatures

4.5.5 Smoke opacity

Smoke opacity (shown in Fig. 4.66) indicate the presence of carbon particles in the exhaust as a result of incomplete combustion. Smoke emission is further reduced with ethanol substitution at increased fuel inlet temperatures. As mentioned earlier induction of pre-heated ethanol results in better vaporization leading to complete combustion of the injected fuel. This results in reduced smoke emissions.

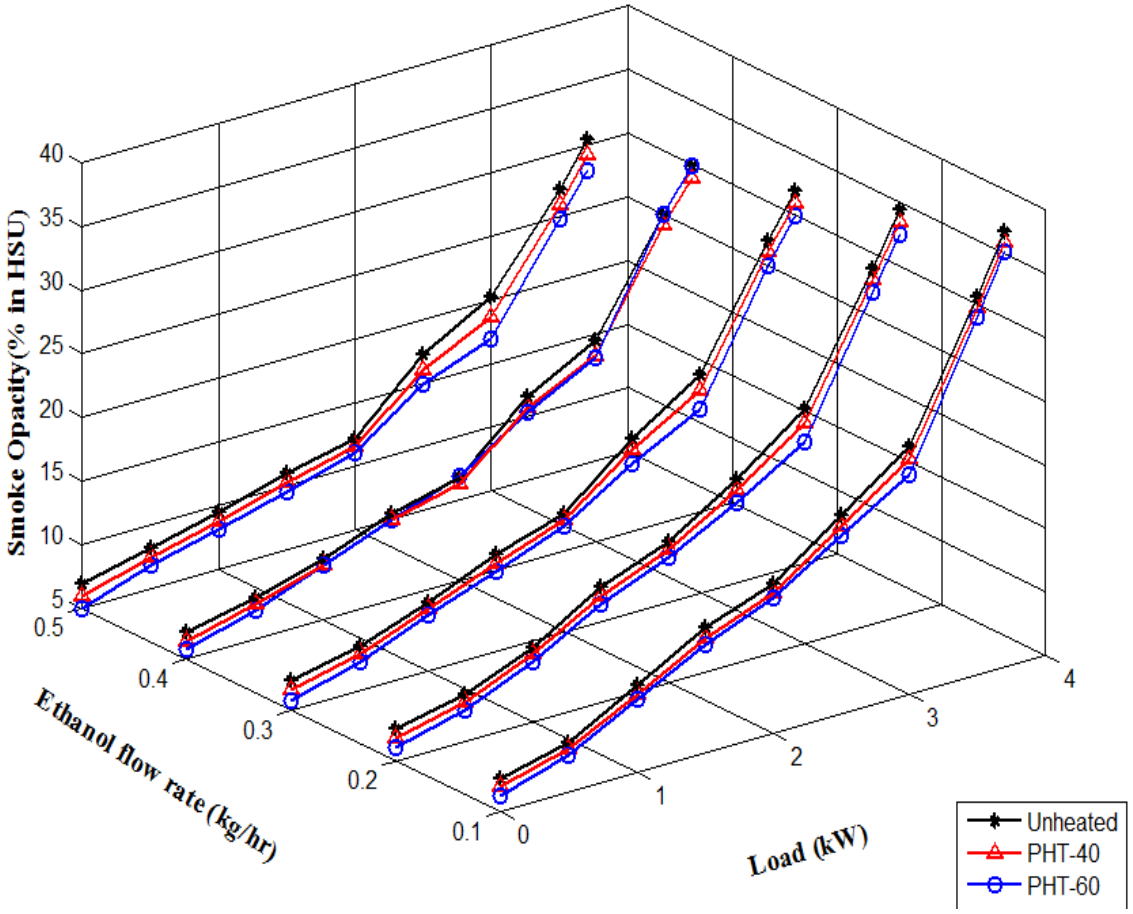

Fig 4.66 Variation of smoke opacity with ethanol flow rate and ethanol pre-heating temperatures

4.5.6 In-cylinder pressure

The increase in peak pressure and maximum rate of pressure rise as portrayed in Figs. 4.67 and 4.68 respectively were observed due to suppression of quenching effect due to preheating and consequent enhanced burning of the ethanol-air-diesel mixture. The values of peak pressure (in bars) at full load respectively for e0, e1, e2, e3, e4 and e5 are 62.1, 62.9, 63.3, 63.7, 64.1 and 65.3 in unheated mode, whereas 63.9,64.6,65.7,66.2, 66.5 at PHT-40 and 65.8, 66.8,67, 67.7, 68.6 at PHT-60 were observed for e1,e2,e3,e4 and e5.

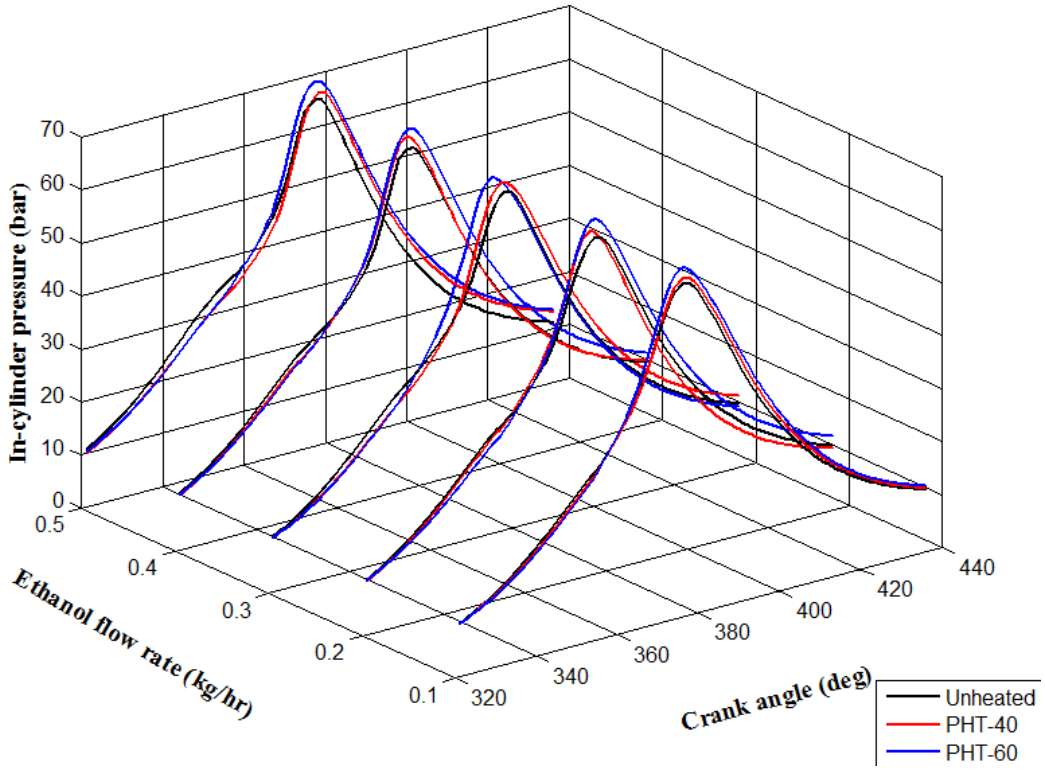

Fig 4.67. Variation of in-cylinder pressure with ethanol flow rate and ethanol pre-heating temperatures

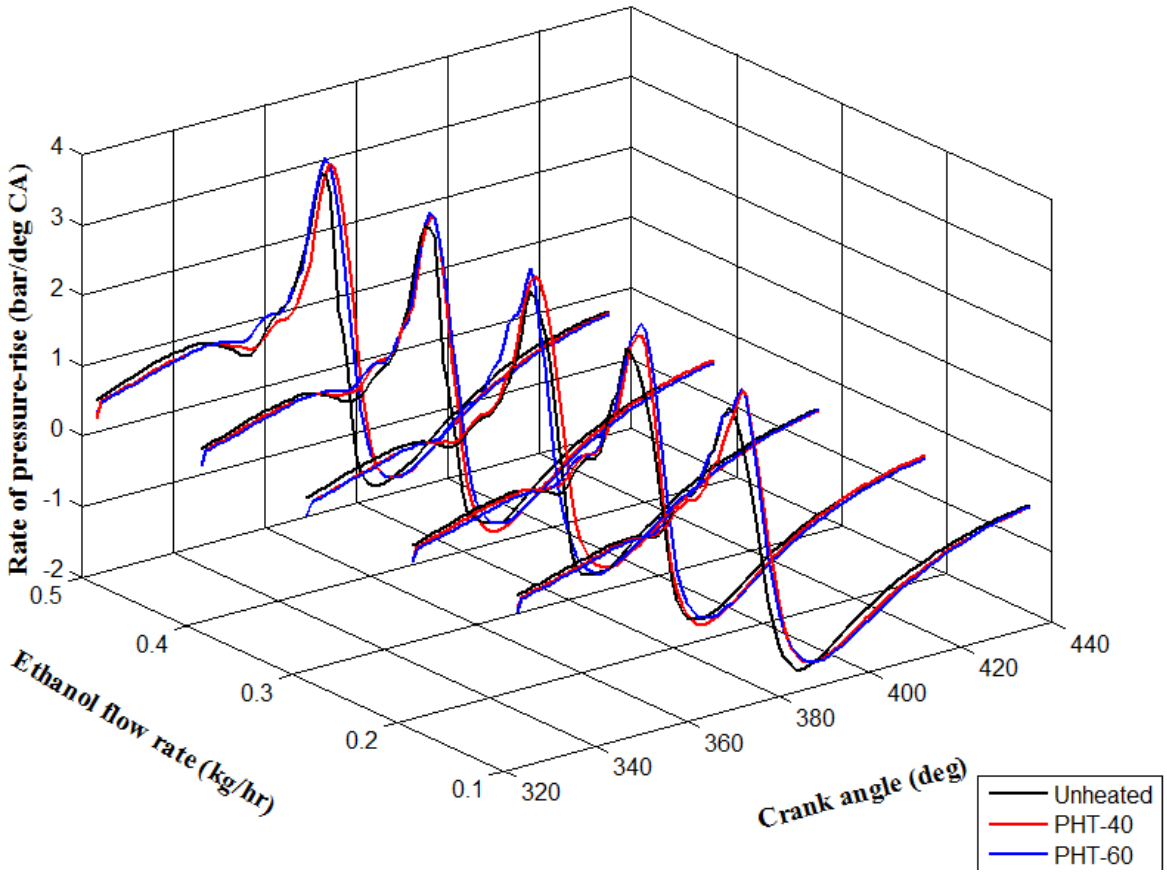

Fig 4.68. Variation of rate of pressure rise with ethanol flow rate and ethanol pre-heating temperatures

4.5.7 Heat release rate

The variation of heat release rate with ethanol at different fuel inlet temperatures are shown in Fig. 4.69. At high fuel inlet temperatures, there is an improvement in heat release rate with ethanol. Preheating improves atomisation and vaporisation of ethanol. The reduced ignition delay of the preheated ethanol enhances the combustion. This results in high heat release rates. The location of peak pressure and peak HRR are advanced with decrease in ignition delay, which are evident from Figs. 4.67 and 4.69.For a given ethanol flow rate, with increase of ethanol pre-heating temperature, the point of occurrence of peak pressure and peak HRR get shifted 1-4ºCA earlier in a cycle, which can be ascribed to the reduced ignition delay.

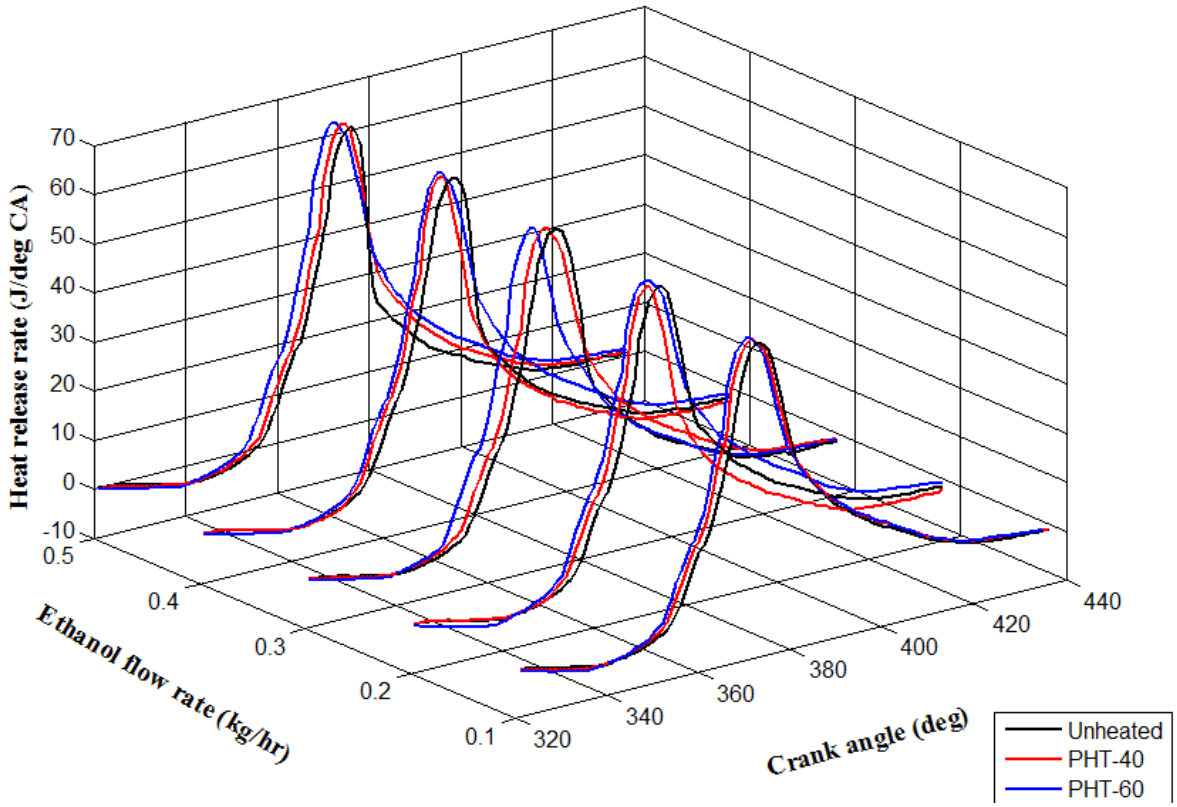

Fig 4.69 Variation of heat release rate with ethanol flow rate and its pre-heating temperatures

4.5.8 Ignition delay and combustion duration

The increase in ignition delay with ethanol is due to low cetane number and poor volatility which slow vaporisation and fuel air mixing rates and extend the physical delay. However, preheated ethanol exhibits reduced ignition delay probably due to improved vaporisation and thus, better mixing of fuel and air. However, preheated ethanol shows slight increase in combustion duration at high temperatures, as shown in Fig 5.70.

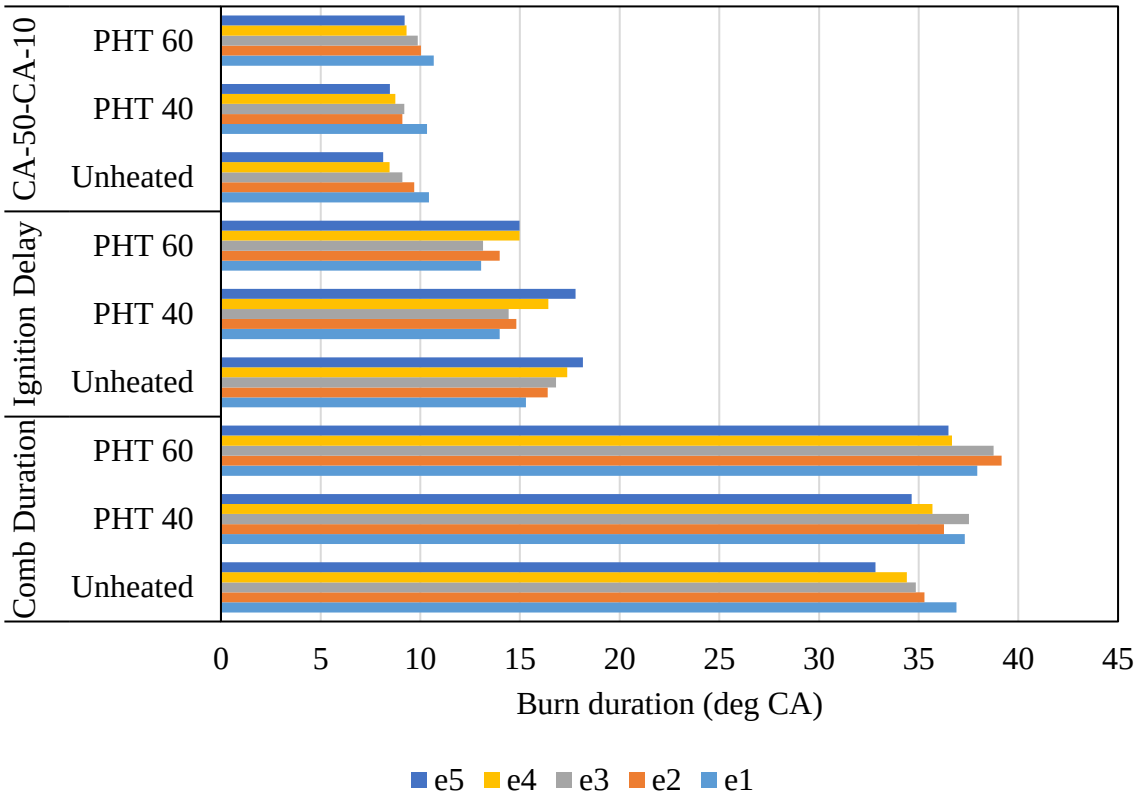

Fig 4.70 Variation of burn duration with ethanol flow rate and ethanol preheating temperature

The various ethanol fumigation modes results in improved thermal efficiency with simultaneous reduction of NOx, smoke and CO_2 along with the increase in HC and CO. Moreover, the values of various combustion characteristics, viz., peak pressure, peak HRR, ignition delay and combustion duration vary for different ethanol modes as compared to baseline diesel case. At fixed ethanol flow rate, thermal efficiency, peak pressure, peak HRR and NOx increases whereas HC and CO emission decreases, with the advance of injection timing. Preheating the ethanol enhances brake thermal efficiency, peak pressure, peak HRR and NOx with simultaneous decrease in smoke, HC and CO. The increase in rate of pressure rise evident along with decrease in ignition delay. The combustion duration is increased with ethanol as compared to diesel. This is due to injection of high quantities of ethanol.

The conversion efficiency of micro-CHP system utilizing heat of exhaust gases has been observed to be 61.8%, when the engine is operated on pure diesel.

CHAPTER 5

CFD MODELLING OF CI ENGINE

Computational Fluid Dynamics or CFD is computational tool used for the solution and analysis of the systems involving fluid flow, heat transfer and chemical reactions with the aid of numerical methods and algorithms. In CFD, the entire system is resolved into small cells or grids and governing equations (mass, momentum, and energy conservation equations) are applied on these discrete elements to find its numerical solution. High speed computational facilities are used to perform the millions of calculations required to simulate the interaction of fluids and gases with the complex surfaces used in engineering. In order to investigate the complex physics and fluid interactions that occur in a compression ignition engine, a model was created that would computationally simulate the combustion process of direct injection compression ignition engine for the given engine conditions with the help of Ansys Fluent.

Computational Fluid Dynamics (CFD) technique facilitates the solution in a shorter time at a lower cost thus dispensing the experimental work. The solution includes detailed information of the flow variables at each grid. In CFD analysis, the flow phenomena that can be visualized on 3D geometry and analyzed numerically with the help of fundamental mathematical equations provide deep insight into the complex fluid dynamic interactions between air flow, fuel injection, moving geometries, and combustion. Fluid dynamics phenomena like jet formation, wall impingement with swirl and tumble and turbulence generation are important for higher engine performance and lower emission levels. As the capability of computers to solve complex equations continues to increase, the use of CFD in the design and analysis of engineering and industrial processes is becoming more popular.

5.1 CFD Methodology

Mass, momentum, and energy conservation equations are the laws that govern the fluid flow and expressed in the form of PDE. These PDEs are replaced by a set of algebraic equations and solved with respect to the specified boundary conditions using the finite volume method as implemented in the commercial CFD code ANSYS WORKBENCH TOOL FLUENT. There are three components in CFD analysis; the *pre-processor*, the *solver*, and the *post-processor*. Pre-processor processes input data to produce output that is used as an input to the processor. The pre-processor also defines general surface types (for example - inlet/outlet areas) to regions of the domain. Design Modeler (DM) is used to create and modify the geometry of the system under consideration and decompose it into predefined nomenclature

and name selection for meshing. Mesh Modeler is a general-purpose meshing tool that automatically creates meshes for decomposed geometry according to the name selection specified in DM. The mesh influences the accuracy, convergence and speed of the solution. Specifications of all the geometric and material properties as well as generation of solid and finite element models are conducted at the pre-processor level.

The solver represent or approximate the differential equations using discrete quantities by algebraic equations that can be solved numerically using the finite volume method. The principal basis of almost all CFD problems are the Navier-Stokes equations which define many single-phase (gas or liquid, but not both) fluid flows. These equations can be simplified by eliminating terms describing viscous actions to yield the Euler equations.

CFD tools provide a deeper insight of the pattern of fluid flow and the distribution of fluid velocity and temperature within an enclosed space, such that these tools not only furnish detailed, informative and analytical results but reduce the efforts required and capital involved in the research.

5.2Advantages of CFD

Although there are few shortcomings associated with use of CFD, but these are outweighed by associated benefits. There are instances where comprehensive fundamental knowledge of all the underlying physics may not exist thus leading to inherent assumptions in the mathematical model adopted resulting in erroneous outcomes. Nonetheless, CFD offers many advantages contributing to the growing applications of general-purpose CFD codes. Few of the advantages are as follows:

(a) Ability to study systems where controlled experiments are not feasible.

(b) CFD provide wide range of comprehensive data, in case where equipment or technique restrictions may limit the experimental data range.(c) CFD facilitates the simultaneous modelling of the inherent complex physical interactions which occur in a flow situationthus, dispensing limiting assumptions.

(d) CFD is preferably referred as flow visualization technique rather than a source of quantitative data in most of the engineering applications.

5.3 Overview of CFD Simulation

CFD codes are constituted by the numerical algorithms that can solve a variety of fluid flow problems. CFD packages incorporate advanced user-friendly interfaces to feed in problem parameters and to examine the results. Hence the codes contain three main elements: (a) a

pre-processor, (b) a solver and (c) a post-processor. These interfaces enable the user an easy access to CFD codes.

5.3.1 Pre-Processor

Pre-processing is a program that processes fluid flow parameters to a CFD program by means of an operator-friendly interface and the successive transformation of this input into a user-friendly form with the help of the solver. Once the mesh is created or imported into the CFD code, the next step is to set up the physics of the flow through defining physical models, material properties, domain properties and boundary conditions.

The sequence of the user activities carried out at the pre-processing stage are outlined in the following paragraph.The region of interests, i.e., the computational domainis defined and then divided into a number of smaller and non-overlapping sub-domains. Subsequently, the selection and the definition of flow behaviour is followed by the specification of the necessary boundary conditions on the cell zones.

The solution to a flow problem (velocity, pressure, temperature etc.) is defined at nodes inside each cell. The accuracy of a CFD solution is governed by the number of cells in the grid. In general, the larger the number of cells the better is the accuracy of solution. Both, the accuracy of a solution and its cost in terms of necessary computer hardware and calculation time are dependent on the fineness of the grid. Optimal meshes are often non-uniform: finer in areas where large variations occur from point to point and coarser in regions with relatively little change.

5.3.2 Solver

At this stage, numerical algorithms are used for solving different equation of fluid flow and heat transfer. Finite volume method (FVM) is most popular technique in CFD analysis. The numerical methods that form the basis of the solver perform the following major steps:

- *Approximation* of the unknown flow variables by means of simple functions.
- *Discretization* by transformation of the differential equations of the mathematical model into algebraic relations between discrete values of velocity, pressure, temperature, etc., located on the computing mesh which conforms to the geometry of the combustion chamber with its moving valves and piston.
- *Solution* of the algebraic equations.
- *Translation* of the numerical algorithm into computer language by computer codes and facilitating easy interfaces for the input and output of information.

The numerical algorithm consists of the following steps:

- Formal integration of the governing equations of fluid flow over all the finite control volumes(CVs) of the solution domain. At the centroid of each CV, lies a computational node at which variable values are to be calculated. Interpolation is used to express variable values at the CV surface in terms of the nodal values. As a result, algebraic equation for each CV is obtained in which a number of nodal values appear.
- Discretization is performed using an integral form of the governing equations and is directly related to the physics of the problem. Apart from the ease of formulation of a flow problem, the added advantage of the geometric flexibility in the choice of grids and definition of discrete flow variables the makes the finite volume method most suitable for problems involving fluid flow heat and mass transfer.

5.3.3 Post-Processor

The CFD package provides data visualization tools to conceptualize the results of the flow problem. This includes vectors plots, domain geometry and grid display line and shaded counter plots particle tracking etc. Recent facilities are aided with animation for dynamic result display and they also have data export facilities for further manipulation external to the code.

5.4 CFD Analysis Procedure

A successful CFD analysis requires the following information:

(a) A grid of points to store the variables calculated by CFD.

(b) *Boundary conditions* for defining the conditions at the boundaries of the flow domain that enables the boundary values of all variables to be calculated.

(c) *Fluid properties* such as viscosity and thermal conductivity.

(d) *Flow models* that define the various aspects of the flow, such as turbulence, mass and heat transfer, species transport and multiphase models.

(e) *Initial conditions* used to provide an initial guess of the solution variables in a steady state simulation or the initial state of the flow for a transient simulation.

(f) Solver control parameters required to control the behavior of the numerical solution process.

The complete CFD analysis procedure can be divided into the following six stages.

Solution of the equations governing scalars (e.g. temperature, pressure, species concentrations) requires a discretization scheme [79]. The simplest way to determine the

values at the faces is by using first order upwind differencing. In this case, it is assumed that the value at the face is equal to the value in the center of the cell upstream of the face. This is the simplest numerical scheme. Though, it offers the benefit of the easy implementation and stable calculations, but it has disadvantage of being diffusive. Second Order Upwind scheme is more accurate than the first order upwind scheme, but in regions with strong gradients it can result in face values that are outside the range of cell values. It is then necessary to apply limiters to the predicted face values. There are many different ways to implement this, but second-order upwind with limiters is one of the popular numerical schemes because of its combination of accuracy and stability.

5.5 Governing Equations

The basic equations for all the existing in-cylinder flow calculation methods are the differential equation expressing the conservation laws of mass, momentum(the Navier-Stokes equation), energy and species concentrations. Additional equations for modeling the spray, chemistry and turbulence are given in the following sections. These equations describe the balance of mass (total and individual species), momentum and energy in an unsteady, compressible turbulent flow. The compressibility effects are due to the density changes occurring as a result of change in pressure as well as due to chemical reactions.

For compactness, these equations are written in vector notation. The unit vectors in the x-, y- and z-directions are represented by

$$\vec{x} = x\hat{i} + y\hat{j} + z\hat{k}$$

The vector ∇ is given by

$$\nabla = \vec{i}\frac{\partial}{\partial x} + \vec{j}\frac{\partial}{\partial y} + \vec{k}\frac{\partial}{\partial z}$$

A general balance equation for a variable φ over an element contains terms due to

• Changes caused by flux through the surface due to diffusion, heat conduction, momentum transport, convection etc.

• Changes caused by addition/removal of heat or species due to chemical reaction within the volume of the element.

• Changes caused by long range processes like radiation and/or gravity, from surrounding elements.

It can be given by equation 5.1.

$$\frac{\partial(\rho\phi)}{\partial t} + \nabla.(\rho\vec{u}\phi) = \nabla.(\tau_\phi \nabla\phi) + S_\phi \qquad (5.1)$$

5.5.1 Species Mass Balance

If there are n numbers of species, then the partial mass densities of each species add up to form the total density ρ. Similarly, local flow velocity $\vec{u}_i$ of species i is composed of total velocity $\vec{u}$ and the diffusion velocity $\vec{V}$. Since species are formed and consumed, a production term is present in the equation 5.2 which is a product of the molar mass M_i and molar rate of formation ω_i.

$$\frac{\partial\rho_i}{\partial t} + \nabla.(\rho_i\vec{u}_i) + \nabla.\vec{J}_i = \dot{\rho}_i^{\,c} + \dot{\rho}_i^{\,s} \qquad (5.2)$$

where, the superscript c and s stand for chemistry and spray source terms respectively. The spray term is applicable only to the fuel species in a diesel engine. The chemistry source term is given by Eq 5.3

$$\rho_i^{\,C} = M_i\omega_i \qquad (5.3)$$

and the diffusion vector is given by equation 5.4.

$$J_i = \rho_i\vec{V}_i = -\rho D_i \nabla Y_i \qquad (5.4)$$

The mean diffusion coefficient D_i of species i into the rest of the mixture can be calculated from the Stefan's law of diffusion using the binary diffusion coefficients, D_{ij}

$$D_i = \frac{1-w_i}{\Sigma i \neq j \dfrac{x_i}{D_{ij}}}$$

Assuming equal diffusivities for all species, the diffusion coefficient is given by equation 5.5.

$$D = \frac{\mu_{eff}}{\rho Sc} \qquad (5.5)$$

μ_{eff} is the dynamic viscosity and S_c is Schmidt Number.

5.5.2 Momentum Equation

The velocity field is governed by momentum equations represented by 5.6

$$\frac{\partial(\rho u_i)}{\partial t} + \frac{\partial(\rho u_i u_j)}{\partial x_i} = -\frac{\partial p}{\partial x_i} + \frac{\partial \tau_{ij}}{\partial x_i} + F_i \qquad (5.6)$$

Where $\partial \tau_{ij}$ is viscous stress tensor and F_i is the body force (which includes gravity).

5.5.3 Energy Equation

In combusting flows, the temperature depends on the thermodynamic state and the composition of the mixture. Most of combustion models (other than laminar flamelet model) require transport equation for enthalpy. Chemical energy is released as heat during combustion and the resulting enthalpy is obtained by solving its transport equation, given by equation 5.7.

$$\frac{\partial(\rho h)}{\partial t} + \frac{\partial(\rho u_i h)}{\partial x} = \frac{\partial y}{\partial x_i}\left[\frac{\mu}{\sigma_h}\frac{\partial h}{\partial x_i} + \mu\left(\frac{1}{Sc_k} - \frac{1}{\sigma_h}\right)\sum_{k=1}^{N} h_k \frac{\partial Y_k}{\partial x_i}\right] + \frac{\partial P}{\partial t} + S_{rad} \qquad (5.7)$$

5.6 Averaging of Equations

Averaging the instantaneous variable provides a way of describing the mean flow field where the local fluctuating quantities and turbulent structures are integrated into the mean quantities and circumvents the need to describe them in the simulation.

Each quantity ϕ can be split into a mean quantity $\bar{\phi}$ and a fluctuating quantity ϕ'. Thus, a statistical method is used to describe the randomness in the flow. The mean of the fluctuations is equal to zero while the mean of the square of the fluctuations is called the variance and is given by set of equations 5.8.

$$\phi = \bar{\phi} + \phi'$$

$$\bar{\phi}' = 0$$

$$\phi'^2 = \overline{\phi^2} + \bar{\phi}^2 \qquad (5.8)$$

Averaging over a very small time interval is called ensemble averaging or Reynolds Averaging technique, we get equation 5.9

$$\overline{\phi(t)} = \frac{1}{t - t_0} \int_{-}^{t} \phi(t') dt' \tag{5.9}$$

5.7 Modelling and Meshing

In order to investigate the complex physics and fluid interactions that occur in a compression ignition engine, a model was created that would computationally simulate the compression ignition engine, the specification of which are outlined in Table 3.2. The software package used to carry out the computational simulations, Ansys Fluent, requires a starting volume mesh and description of the motion of moving zones within the model, thus necessitating extra steps to prepare the model before simulation could begin. The process of creating the Fluent model began by creating a Geometry of combustion chamber of the diesel engine. From this geometry, a mesh is generated in Ansys Meshing to be used for modeling. This allowed for an accurate recreation of the physical engine in the computational domain.

Following are the requirements of computing mesh. First, it should adequately fit the topography of the combustion chamber and/or inlet port including the moving components. This requirement pertains to the need of simulating the effects of change in engine geometry. Secondly, it should allow control of local resolution to obtain the maximum accuracy with a given number of grid points. It arises due to the fact that computing time increases with the number of mesh points. Thirdly, each interior grid point should be connected to the same number of neighboring points. It stems from the fact that mesh needs to be topologically rectangular in some transformed space so that highly efficient equation solvers for such mesh systems can be utilized.

For generating mesh of Engine geometry, ANSYS Meshing Software package is used. In order to facilitate meshing, the geometry first had to be refined. Several new faces and volumes were created, meshed and finally refined until the max cell skewness was within acceptable limits. While applying the mesh, it is always necessary to check for highly skewed elements. Skewness of zero is highly desirable, but a value of 0.9 or lower also can be considered a good mesh. However, the skew should not exceed 1. Depending on the location, it may be necessary to eliminate highly skewed elements. This is especially critical if the element is in a dynamic mesh zone as this region needs to be meshed with as little skew as possible to ensure a fast and accurate simulation. The dynamic mesh model will move

boundaries or objects and then adjust the mesh accordingly. This is well suited for boundaries that move rigidly with respect to each other, such as the motion of the piston with respect to the engine cylinder.

5.8 Computational Models

The computational models presented in this section are all built into the Ansys Fluent software package. However, it is prudent to expound on their attributes before continuing on to the simulations.

5.8.1 Turbulence Models

Turbulence is an important engine process having significant effect on various engine processes viz., fuel-air mixing, combustion and heat transfer in diesel engine, etc.

CFD method is suitable for investigating the influence of the complex geometry. For applying CFD, the proper selections of grid level and turbulence model are important to describe fluid motions. However, no single turbulence model with fixed grid size is universally accepted as being superior for all classes of problems. Fluent provides many different options for turbulence modeling.

A turbulence model is a computational procedure to close the system of mean flowequations. Turbulence models allow the calculation of the mean flow without first calculating the full time-dependent flow field.

The choice of turbulence model depends upon considerations such as physics encompassed in the flow, the established practice for a specific class of problem, level of accuracy required, available computational resources and the amount of time available for simulation. For a turbulence model to be useful it must not only have wide applicability, but accurate, simple and economical to run.

5.8.1.1 The Spalart- Allmaras model

This model can be used for all the Low-Reynolds-number flows. This is a relatively simple one-equation model that solves a modeled transport equation for the kinematic eddy viscosity. This might be a good choice for relatively crude simulations where accurate turbulent flow computations are not critical. It has proved to be economical and accurate for flows with mild separation and recirculation. There are a few drawbacks such as

- It cannot be relied upon to predict the decay of homogenous, isotropic flows.

- One-equation models are often not capable of capturing rapid changes in the length scale, which might be necessary when flow changes from wall-bounded to free shear flow.
- It is not recommended for :
  - Massively separated flows.
  - Free shear flows.
  - Decaying turbulence.

5.8.1.2 Standard k-ε model

This is one of the simplest two-equation turbulence model in which the solution of two transport equations determines the turbulent velocity and length scales independently. The *k*-ε model focuses on the mechanisms that affect the turbulent kinetic energy (per unit mass) *k*and its dissipation rate (ε). The model equation for k was derived from the exact equation whereas the model equation for ε was obtained using physical reasoning. It is relatively simple to implement and leads to stable calculations that converge relatively easily. This model yields reasonable predictions for wide range of turbulent flows. However, this model has certain setbacks. For instance, it provides poor predictions for swirling and rotating flows, flows with strong separation, fully developed flows in non-circular ducts etc.

The assumptions made in this model are: Flow is fully turbulent and effects of molecular viscosity are negligible. As strengths and weaknesses of the standard k-ε model have become identified, advances have been made to the model in order to improve its performance. Two variants of the standard k-ε model are available in Fluent: the RNG k-ε model [80] and the realizable k-ε model [81].

5.8.1.3 RNG k-ε model

The RNG k-ε model was derived using a statistical technique called renormalization group theory. It is similar in form to the standard model, but includes the following refinements. The RNG model has an additional term in its equation that improves the accuracy for rapidly strained flows. The effect of swirl on turbulence is included in the RNG model enhancing accuracy for swirling flows. The RNG theory provides an analytical formula for turbulent Prandtl numbers, while the standard k-ε model uses user specified constant values. While the standard model is a high-Reynolds number model, the RNG theory provides an analytically-derived differential formula for effective viscosity that accounts for low-Reynolds number effects[80]. However, effective use of this feature depends on an appropriate treatment of the

near-wall region. These features make the RNG k-ε model more accurate and reliable for a wide class of flows than the standard k-ε model. The RNG-based - turbulence model is derived from the instantaneous Navier-Stokes equations using a mathematical technique called “renormalization group” (RNG) method. The analytical derivation results in a model with constants different from those in the standard k-ε model and additional terms and functions in the transport equations.

5.8.1.4 Realizable k- ε model

The realizable k-ε model is a relatively recent development and differs from the standard k- ε model in two important ways. The realizable k-ε model includes new formulation for the turbulent viscosity and the dissipation rate. The term *realizable* means that the model satisfies certain mathematical constraints on the Reynolds stresses consistent with the physics of turbulent flows. Realizable k-ε model gives a more accurate prediction of the spreading rate of both planar and round jets than the standard k-ε model. Also, it is likely to provide superior performance for flows involving rotation, boundary layers under strong adverse pressure gradients, separation and recirculation. This model differs from the standard model in two important ways. The realizable model contains new formulation for the turbulent viscosity. A new transport equation for the dissipation rate, ε has been derived from an exact equation for the transport of the mean-square vorticity fluctuation [81].

Neither the standard k- ε model nor the RNG k- ε model is realizable. An immediate benefit of the realizable k- ε model is that it accurately predicts the spreading rate of both planar and round jets. Both the realizable and RNG k- models have shown substantial improvements over the standard k-model where the flow features include strong streamline curvature, vortices and rotation. Since the model is still relatively new, it is not clear in exactly which instances, the realizable k- model consistently outperforms the RNG model. However initial studies have shown that the realizable model provides the best performance of all the k- ε model versions for several validations of separated flows and flows with complex secondary flow features.

5.9 Combustion Models

Computational fluid dynamics modeling of combustion necessitates the proper selection and implementation of a model suitable to represent the complex physical and chemical phenomenon associated with any combustion process accurately. Fluent utilizes five different methods for modeling species transport and combustion including: species transport; non-

premixed combustion; premixed combustion; partially premixed combustion; and composition PDF transport.

5.9.1 Species Transport

This approach solves the conservation equations for convection, diffusion and reaction sources for multiple component species.Multiple simultaneous chemical reactions can be modeled with reactions occurring in the bulk phase (volumetric reactions) and/or on wall or particle surfaces.

5.9.1.1 The Laminar Finite-Rate Model

The laminar finite-rate model computes the chemical source terms using Arrhenius expressions and ignores the effects of turbulent fluctuations. The model is exact for laminar flames but is generally inaccurate for turbulent flames due to highly non-linear Arrhenius chemical kinetics. The laminar model may however be acceptable for combustion with relatively slow chemistry and small turbulent fluctuations such as supersonic flames.

5.9.1.2 The Eddy-Dissipation Model

Eddy-dissipation model is a turbulence-chemistry interaction model, based on the work of Magnussen and Hjertager[82]. Most fuels are fast burning and the overall rate of reaction is controlled by turbulent mixing. In non-premixed flames, turbulence slowly convects/mixes fuel and oxidizer into the reaction zones where they burn quickly. In premixed flames, the turbulence slowly convects/mixes cold reactants and hot products into the reaction zones, where reaction occurs rapidly. In such cases, the combustion is said to be mixing-limited, and thecomplex and often unknown chemical kinetic rates can be safely neglected. Combustion proceeds whenever turbulence is present ($k = \varepsilon > 0$) and an ignition source is not required to initiate combustion. This is usually acceptable for non-premixed flames, but in premixed flames, the reactants will burn as soon as they enter the computational domain upstream of the flame stabilizer. To solve this, FLUENT provides the finite-rate/eddy-dissipation model where, both the Arrhenius and eddy-dissipation reaction rates are calculated.

5.9.1.3 The Eddy-Dissipation-Concept (EDC) Model

The eddy-dissipation-concept (EDC) model is an extension of the eddy- dissipation model to include detailed chemical mechanisms in turbulent flows [82]. It assumes that reaction occurs in small turbulent structures called the fine scales. The EDC

model can incorporate detailed chemical mechanisms into turbulent reacting flows. However, typical mechanisms are invariably stiff and their numerical integration is computationally costly. Hence, the model should be used only when the assumption of fast chemistry is invalid, such as modeling the slow CO burnout in rapidly quenched flames or the NO conversion in selective non-catalytic reduction (SNCR). The double-precision solver is recommended to avoid round-off errors that may occur as a consequence of the large pre-exponential factors and activation energies inherent in stiff mechanisms.

5.9.2 Non-Premixed Combustion

Non-premixed modeling involves the solution of transport equations for one or two conserved scalars (the mixture fractions). Equations for individual species are not solved. Instead, species concentrations are derived from the predicted mixture fraction fields. The thermochemistry calculations are pre-processed and then tabulated for look-up in ANSYS Fluent. Interaction of turbulence and chemistry is accounted for with an assumed-shape Probability Density Function (PDF). For the case of non-premixed combustion, fuel and oxidizer enter the combustion chamber in distinct streams. Examples of non-premixed combustion include pulverized coal furnaces, diesel internal-combustion engines and pool fires. Under certain assumptions the thermochemistry can be reduced to a single parameter: the mixture fraction. The mixture fraction denoted by f, is the atomic mass fraction that originated from the fuel stream. In other words it is the local mass fraction of burnt and unburnt fuel stream elements (C, H etc.) in all the species (CO_2, H_2O, O_2 etc.). The approach is elegant because atomic elements are conserved in chemical reactions. In turn, the mixture fraction is a conserved scalar quantity and therefore its governing transport equation does not have a source term. Combustion is simplified to a mixing problem and the difficulties associated with closing non-linear mean reaction rates are avoided.

5.9.3 Premixed Combustion

FLUENT has a premixed turbulent combustion model based on the reaction progress variable approach. In principle, the mixing between fuel and the oxidizer in the premixed combustion should be complete to the molecular level prior to ignition, though some degree of mixture inhomogeneity is normal in practical engines. Combustion occurs as a flame front propagating into the unburnt reactants. Examples of premixed combustion include aspirated internal combustion engines, lean-premixed gas turbine combustors and gas-leak explosions.

Premixed combustion is much more difficult to model than non-premixed combustion. The reason for the same is, (subsonic) premixed combustion usually occurs as a thin flame that is stretched and contorted by turbulence. The overall rate of propagation of the flame is determined by both the laminar flame speed and the turbulent eddies. The laminar flame speed is determined by the rate that species and heat diffuse upstream into the reactants and burn. To capture the laminar flame speed the internal flame structure would need to be resolved as well as the detailed chemical kinetics and molecular diffusion processes. Since, practical laminar flame thicknesses are of the order of millimetres or smaller, resolution requirements are usually unaffordable. The effect of turbulence is to wrinkle and stretch the propagating laminar flame sheet increasing the sheet area and, in turn, the effective flame speed. The large turbulent eddies tend to wrinkle and corrugate the flame sheet while the small turbulent eddies if they are smaller than the laminar flame thickness, may penetrate the flame sheet and modify the laminar flame structure.

5.10 Autoignition

Auto ignition phenomena in engines are due to the effects of chemical kinetics of the reacting flow inside the cylinder. Fluent considers the ignition delay model in diesel engines. The autoignition model is compatible with any volumetric combustion model with the exception of the purely premixed models. These models are inherently transient and as such are not available with steady simulations. In general, they require adjustment of parameters to reproduce engine data and require tuning to improve accuracy. Once the model is calibrated to a particular engine configuration, then different engine speeds and loads can be reasonably well represented. Detailed chemical kinetics may be more applicable over a wider range of conditions, though are more expensive to solve.

5.11 Injections

Fluent provides several types of injectors including: single, group, solid-cone surface etc. For these simulations solid-cone was selected as it effectively mimicked that of a typical fuel injector. Based on the injector type, several more parameters must be fully defining in order to proceed with injection. The particle type used in this simulation is droplet particle which is a liquid droplet in a continuous-phase gas flow that obeys the force balance and that experience heating/cooling followed by vaporization and boiling. The droplet type is available when heat transfer is being modeled and at least two chemical species are active or partially premixed

5.12 Solver Settings

If the discretised form of the Navier-Stokes system is considered, the form of the equations shows linear dependence of velocity on pressure and vice-versa. This inter-equation coupling is called velocity pressure coupling. The pressure-based solver allows for the problem to be solved in either a segregated or coupled manner. Out of the five methods facilitated by Fluent for pressure-velocity coupling: SIMPLE, SIMPLEC, PISO and Fractional Step Method (FSM)make use of the segregated algorithm; while the coupled scheme is based on the coupled solver. All of these methods except the coupled scheme are based on the predictor-corrector approach.

The SIMPLE (semi-implicit method for pressure linked equations) algorithm uses a relationship between velocity and pressure corrections to enforce mass conservation and to obtain the pressure field [83]. This algorithm substitutes the flux correction equations into the discrete continuity equation to obtain a discrete equation for the pressure correction in the cell. The pressure-correction equation may be solved using the algebraic multigrid (AMG) method. Once a solution is obtained, the cell pressure and the face flux are corrected. The SIMPLEC(SIMPLE-Consistent) is similar to the SIMPLE method with a different expression used for the face flux correction [83]. However both SIMPLE methods are generally used for steady-state calculations and not applicable in this situation.

In the FSM, the momentum equations are decoupled from the continuity equation using approximate factorization [83, 84]. This allows the user to control the order of splitting error. As a result, the FSM employed by Fluent is a velocity-coupling scheme in a non-iterative time-advancement algorithm. As a result, the Fractional Step Method cannot be utilized in this study.

While SIMPLE and SIMPLEC are generally used for steady-state calculations, PISO (Pressure-Implicit with Splitting of Operators) is commonly employed for calculations that are transient. For this study, PISO unsteady pressure-based solver is used for calculations on highly skewed meshes enabling full pressure-velocity coupling. One of the limitations of the SIMPLE and SIMPLEC algorithms is that new velocities and corresponding fluxes do not satisfy the momentum balance after the pressure-correction equation is solved. As a result, the calculation must be repeated until the balance is satisfied [83]. To improve the efficiency of this calculation, the PISO algorithm performs two additional corrections: neighbor correction and skewness correction.

The main idea of the PISO algorithm is to move the repeated calculations required by SIMPLE and SIMPLEC inside the solution stage of the pressure-correction equation. This process (momentum or “neighbor” correction) allows the corrected velocities to satisfy the continuity and momentum equations more accurately. While the PISO algorithm takes a little more CPU time per solver iteration it sharply decreases the number of iterations required for convergence especially for transient problems.

Additionally, it allows for the use of larger time steps while maintaining stable calculations and under-relaxation factors for both pressure and momentum. Meshes that are highly distorted pose convergence difficulties. Fluent uses the process of skewness correction to solve a highly skewed mesh in roughly the same number of iterations as an orthogonal mesh. For skewed meshes, the relationship between the correction of mass flux at the cell face and the difference of the pressure corrections at the adjacent cells is not ideal. The unknown components of the pressure-correction gradient along the cell faces are solved and used to update the mass flux corrections. It is worth mentioning that for meshes with a high level of skewness, the simultaneous coupling of the neighbor and skewness corrections may lead to divergence. This can be solved by utilizing additional iterations of skewness correction for each neighbor correction. It allows a more accurate adjustment of the face mass flux correction, though with additional computational expense.

Gradients are used throughout the calculations from determining values of scalars at the cell faces to discretizing the convection and diffusion terms to computing velocity derivatives. Fluent offers three methods by which gradients can be calculated: Green-Gauss cell-based, Green-Gauss node-based and least squares cell-based. The Green-Gauss cell-based method uses an arithmetic average of the values at the neighboring cell centers to calculate the value at a given cell center. However, the node-based method uses an arithmetic average of the nodal values on the face of neighboring cells utilizing a weighted average similar to that proposed by Holmes and Connel [85] and Rauch et al. [86]. While the node-based method is more accurate than the cell-based method, it is prohibitively more expensive computationally. The least squares method assumes that the solution varies linearly from cell center to cell center. This method uses the Gram-Schmidt process[85] to solve the minimization problem for a linear system of non-square coefficient matrix in a least squares sense. For skewed or distorted unstructured meshes the least-squares accuracy is comparable to the node-based method. Additionally, it is less expensive to compute then the node based method, however it

is still substantially costlier to compute then the cell-based method. As a result, Green-Gauss cell-based method was used for determining gradients.

Standard scheme is employed for discretization of pressure while first-order upwind scheme is used for all other equations (density, momentum and energy etc.). While a second-order scheme generally yields more accurate results than a first-order scheme, they are costlier computationally and can lead to convergence problems. Convergence problems met by using a second-order scheme are generally solved by instead utilizing a first-order scheme. Implicit relaxation or under-relaxation can help stabilize convergence issues in the pressure-based solver. While this comes at the expense of computational time, it can help to combat oscillatory convergence as a result of overshooting the apparent solution. Tannehill et al. [83] even suggests that in non-linear problems, it is often necessary for convergence.

The engine geometry in the presented work as shown in Fig 5.1is transformed into 120° sector in-order to reduce mesh size and solution time. The piston bowl shape is prepared from ANSYS Design Modeler. The meshing of in-cylinder fluid domain is performed using ANSYS Meshing. While simulating for the combustion parameters of engine from Inlet Valve Closing (IVC) to Exhaust Valve Opening (EVO), a sector of the complete engine domain is considered for analysis. In the simulation valves are assumed to be closed with moving piston considering cylinder as only important domain. The engine geometry being rotationally symmetric, a sector of only one spray is simulated and other regions are considered periodic thus reducing the computational time involved for combustion simulation.

Figs.5.2 and 5.3 respectively show a typical top view and front view of sector mesh which has periodic faces to replicate the closed engine domain. The periodic faces, head, piston bowl and cylinder wall are shown in the figures. The geometry is being divided into two part for obtaining the better quality mesh. The orthogonal Quality of developed Mesh is 0.607 and the the maximum skewness is 0.58. The mesh is generated at the TDC and with the help of dynamic mesh setup, the mesh is moved at the position of inlet valve closed. For dynamic mesh setup, layering method is used which is based on height of the cells and the value of split factor and collapse factor are 0.4 and 0.06 respectively and the ideal cell height is 0.72 mm which is taken as the height of cells in the clearance volume. The mesh at IVC is also shown in the Fig 5.4 with pure hex cells on the periodic faces and cylinder wall.

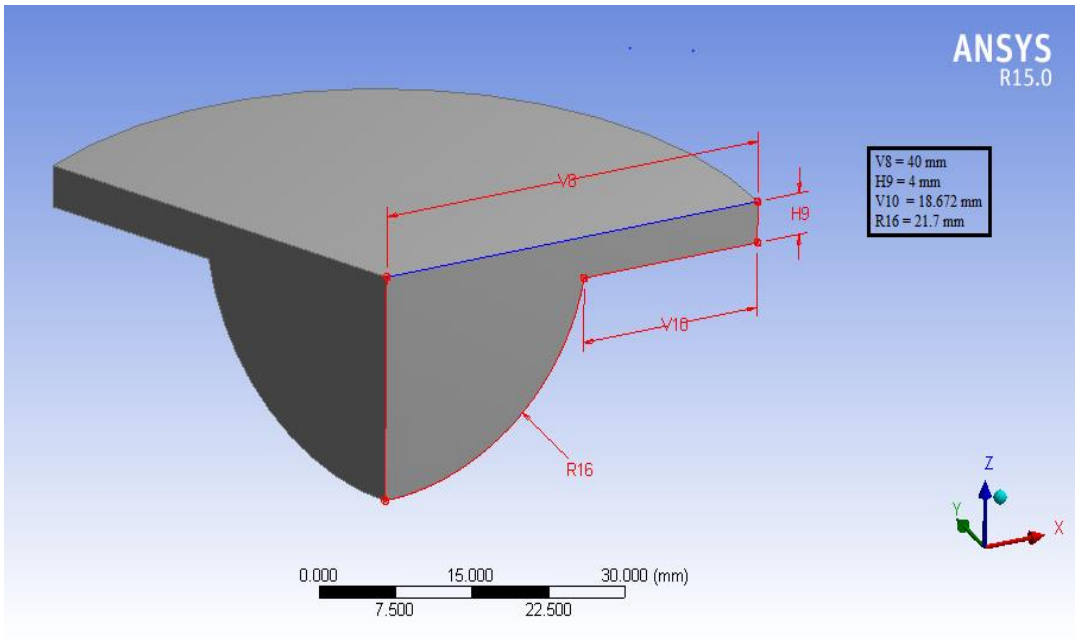

Fig. 5.1 Engine Geometry (Sector of 120°)

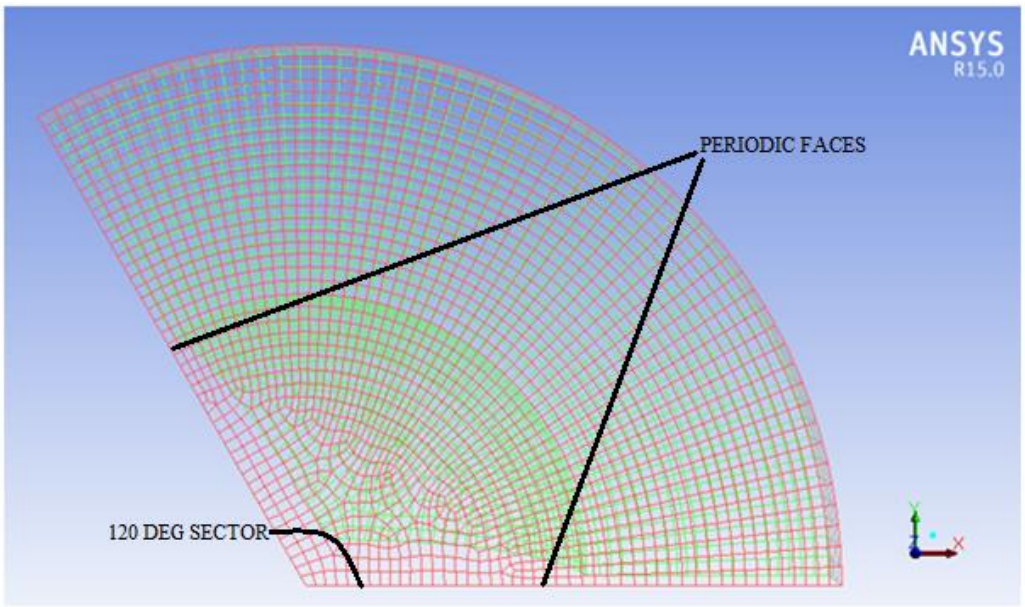

Fig. 5.2 Mesh of Sector (Top view)

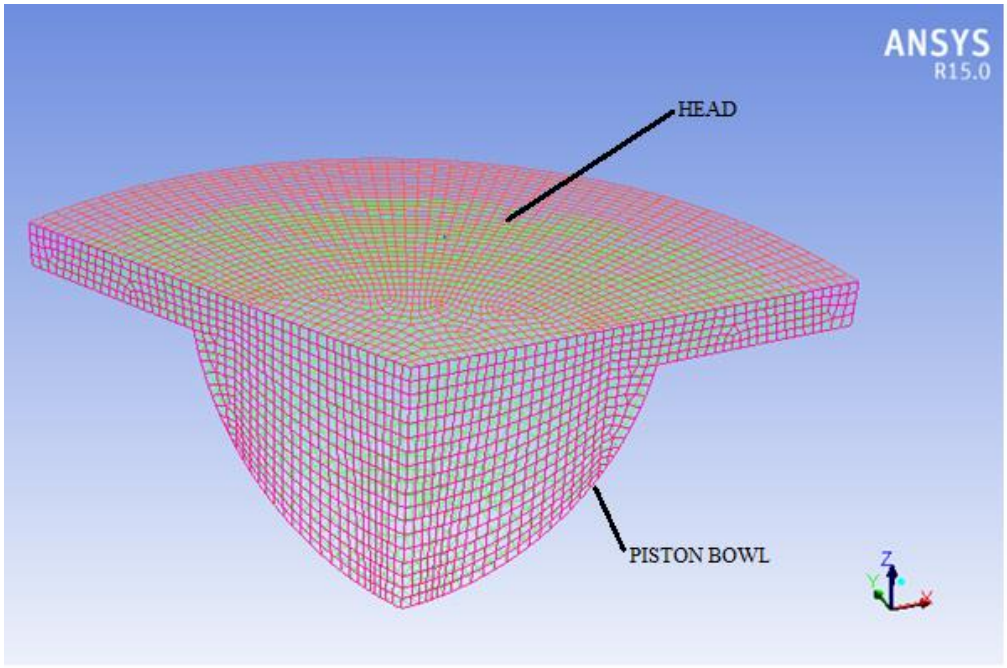

Fig. 5.3 Mesh of Sector (Front view)

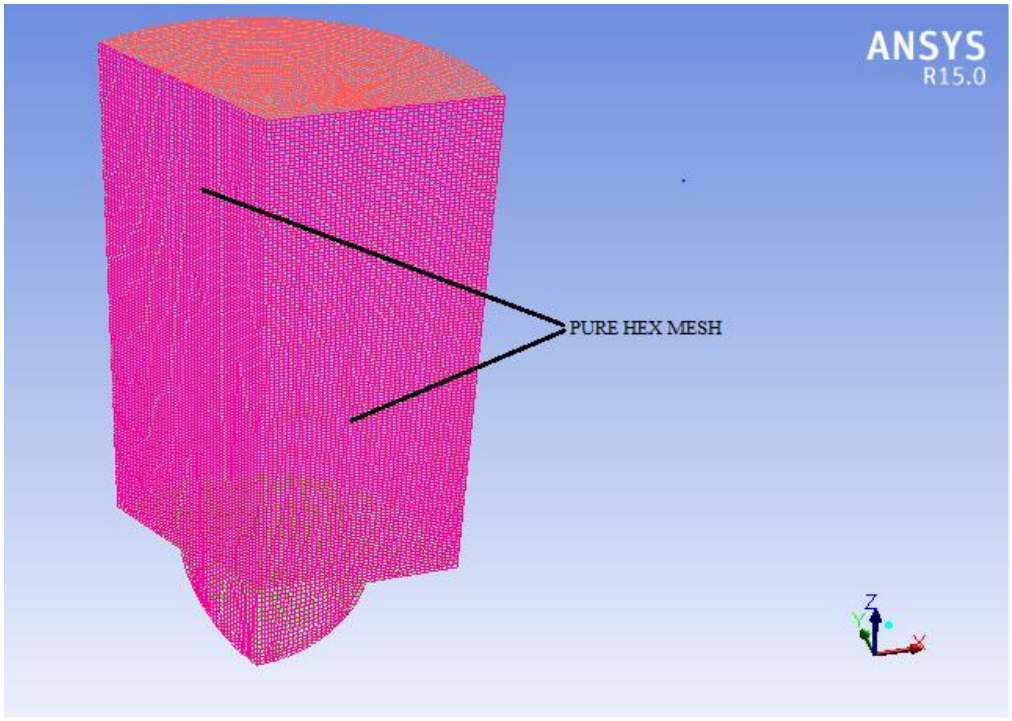

Fig. 5.4 Mesh of Sector at IVC

5.13 Procedure for Solver Setting

The mesh is read and also scaled with suitable unit in ANSYS Fluent. Further,the quality of mesh is checked to assure that there is no negative volume. The dynamic mesh setup is prepared by using layering method and the dynamic zone is created. Following the preview of mesh motion the *libudf* file is loaded for the initial swirl in the cylinder and profile file is read for the injection mass calculation during injection. RNG k-epsilon model is chosen as viscous model whereas the eddy dissipation model along with the options of volumetric reaction and inlet diffusion is selected as the species transport model.

The characteristic properties of material and the mixing rate for diesel-air mixture are specified. For instance, thermal conductivity and viscosity of the fluid are determined by mass weighted mixing law whereas its density is approximated to that of an ideal gas. The isobaric specific heat of every fluid is assumed to be piece-wise polynomial. The boundary condition for the temperature on the wall of sector that contains piston head and cylinder wall is set before solution of the simulation starts. The parameters for the different model, materials, injection, dynamic mesh setup, pressure-velocity coupling and spatial-discretization are presented in Table 5.3.

5.14 Boundary Conditions & Initial Conditions

After verifying that the model and actual engine have the same physical characteristics the next step was to verify that the same conditions were used for each comparison case. The initial conditions represent the initial guess the solver will use for calculations. Boundary conditions are the values defining the limits of the model in the computational domain and were obtained from the experimental data whenever possible such as temperatures for intake and exhaust gas and injected fuel. Tables 5.1 shows some of the boundary and initial conditions and how they relate to the experimental data. Many of these parameters will vary from case to case such as fuel flow rate engine speed pressure etc. The technical specifications of the engine are given in Table 3.2 whereas that of fuel injector are provided in Table 5.2. The Characteristic parameters for computational modelling are outlined in Table 5.3.

Table 5.1: Boundary and Initial Condition

Particular	CFD	Experimental
Fuel used	Decane	
Composition of fuel	100% Decane	
Velocity of injection	94.235 m/s	
Initial Fuel temperature	310 K	308 K
Density of the fuel	820 kg/m^3	840 kg/m^3

Table 5.2: Specifications of the fuel Injector

Particular	Value
Injection Duration	21º
Start of Injection	23º bTDC
End of Injection	2º bTDC
Spray Orientation Angle	70º
Total Fuel Injection Per Cycle	24.5525 mg
Nozzle Hole Diameter	0.25 mm
Number of Injector Holes	3

Table 5.3: Characteristic parameters for computational modelling

Parameters	Conditions
Turbulence	RNG K-∈ Standard Wall Function
Species Transport	Eddy Dissipation Model Volumetric Reaction Inlet Diffusion and Diffusion Energy Source
Materials	Fluent Database
Pressure Velocity Coupling	(PISO); Skewness Correction=0
Spatial Discretization	Second Order Upwind
Initial Swirl ratio	1.2
Primary Breakup	Solid Cone; Droplet (Laws)
Secondary Breakup	Wave Model ; B1=15

5.15 Validation of computational model

Validation of the computational model is carried out to ensure that the model matches the experimental set up in geometry, ambient conditions and output. The direct injection compression ignition engine having available experimental data is used to validate the simulation method that is being used. The results obtained by computational method with the help of commercial software are in good agreement with the experimental results.The

validation is undertaken in two phases: firstly, validation of geometry and boundary conditions and secondly, the validation of the results

5.15.1 Validation of geometry and boundary conditions

The computational engine model used in simulations is prepared using the actual geometric parameters of the engine. These data are not only used for the construction of the model and modeling the computational engine but also aid in the definition of the mesh motion of the model. Table 5.3 shows the comparison of technical and geometric specifications used in computational model with those in actual design. Further, it is ascertained that the parameters for boundary conditions in computational and experimental environments are exactly the same. The magnitude of connecting rod length furnished will constrain the length through which the mesh should generate. The value of compression ratio facilitates the estimation of in-cylinder pressure and power output of the engine. As discussed in earlier sections, modeling is done in Design Modeler (DM) and Mesh Modeler (MM) with double precision, so that model developed is highly accurate and exactly resembles the engine in computational domain. Hence it is geometrically well validated.

5.15.2 Validation of results

After being validated with reference to geometrical specifications and boundary conditions, numerical calculations are done on the computational model, results of which are compared to the experimental results. The pressure history of the single cylinder engine is plotted for experimental and computational setups. It is evident that the pressure produced from the computational model under the same operating conditions follows the exact trend of the original engine. Though the peak pressure vary the computational results are very close to the experimental. The pressure histories and heat release rates, respectively for different fuel configurations viz. e0 (pure diesel), e1, e2, e3, e4 and e5 are compared to that with data obtained from computational modelling in Figs.5.5-5.10 and Fig 5.11-5.16. The computational model does not account for the pressure losses which are inevitable in mechanical systems. Moreover, it does not consider for limitations of pressure sensors that are used to measure the pressure inside the chamber. Considering the mechanical difficulties in measuring the pressure and limitations of numerical calculation to predict the exact behavior of real systems, the results obtained are considered to be very acceptable. The contours of in-cylinder pressure and cylinder temperature for different test fuels are exhibited in Figs.5.17 to 5.22 and Figs.5.23 to 5.28 respectively.

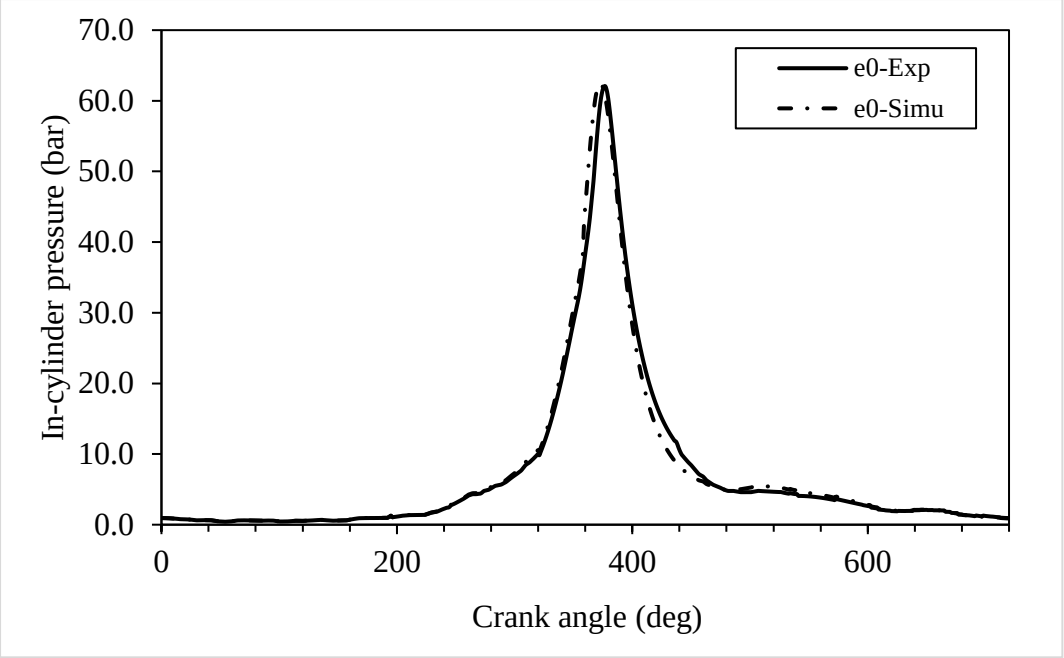

Fig 5.5 Comparison of experimental and simulation pressure histories for pure diesel

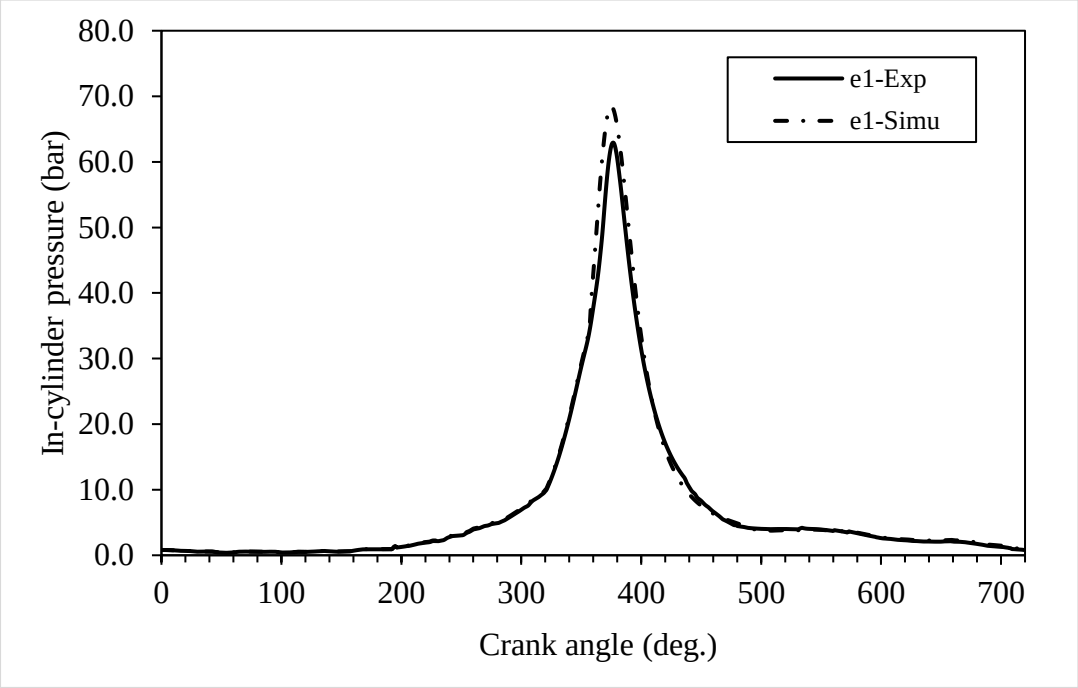

Fig 5.6 Comparison of experimental and simulation pressure histories for e1

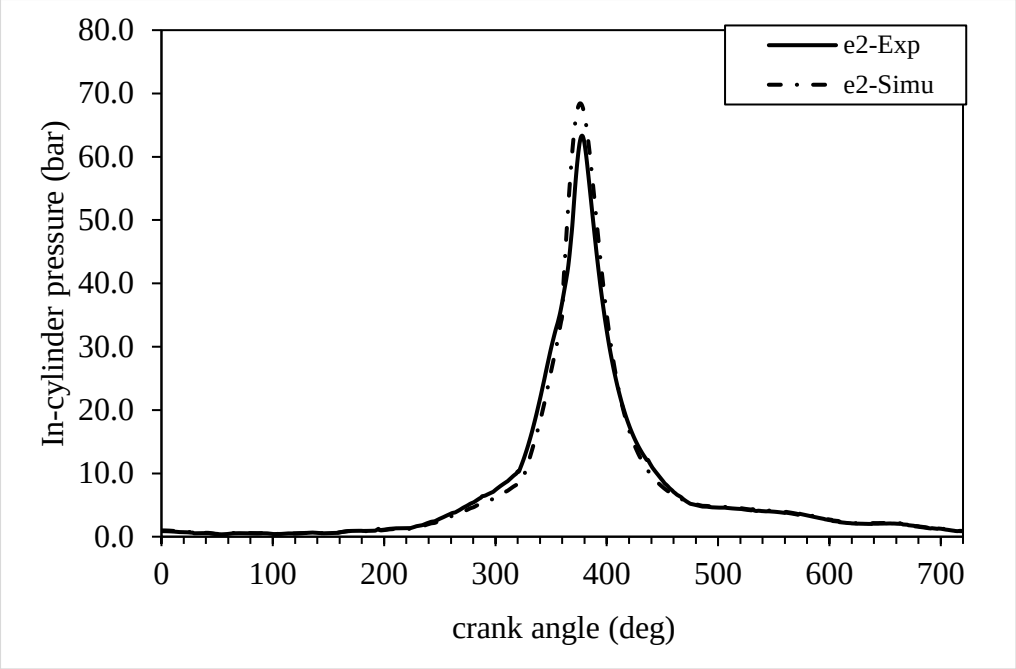

Fig 5.7 Comparison of experimental and simulation pressure histories for e2

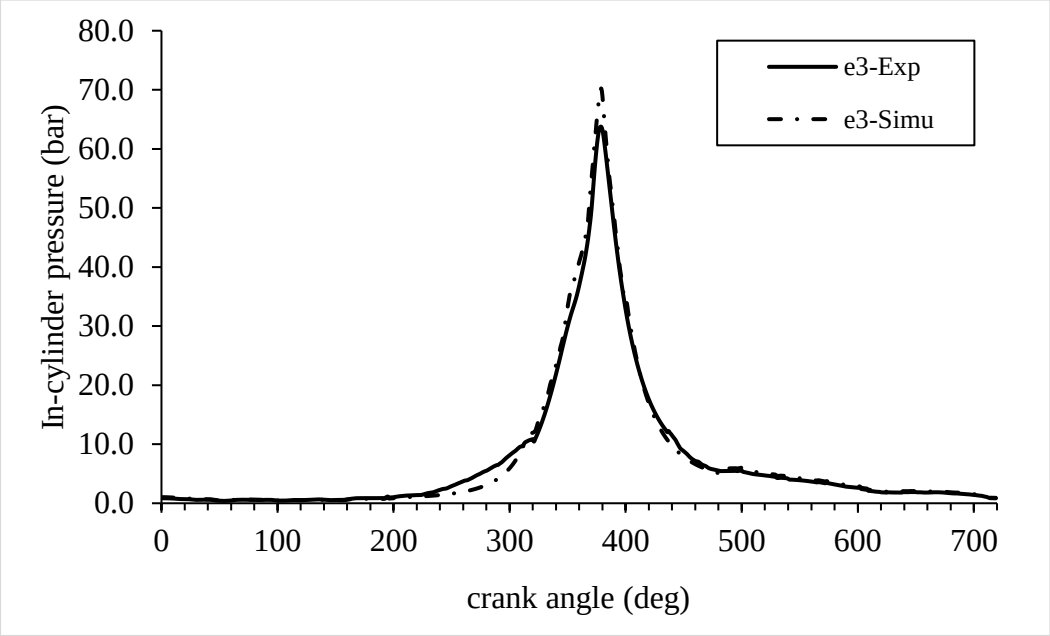

Fig 5.8 Comparison of experimental and simulation pressure histories for e3

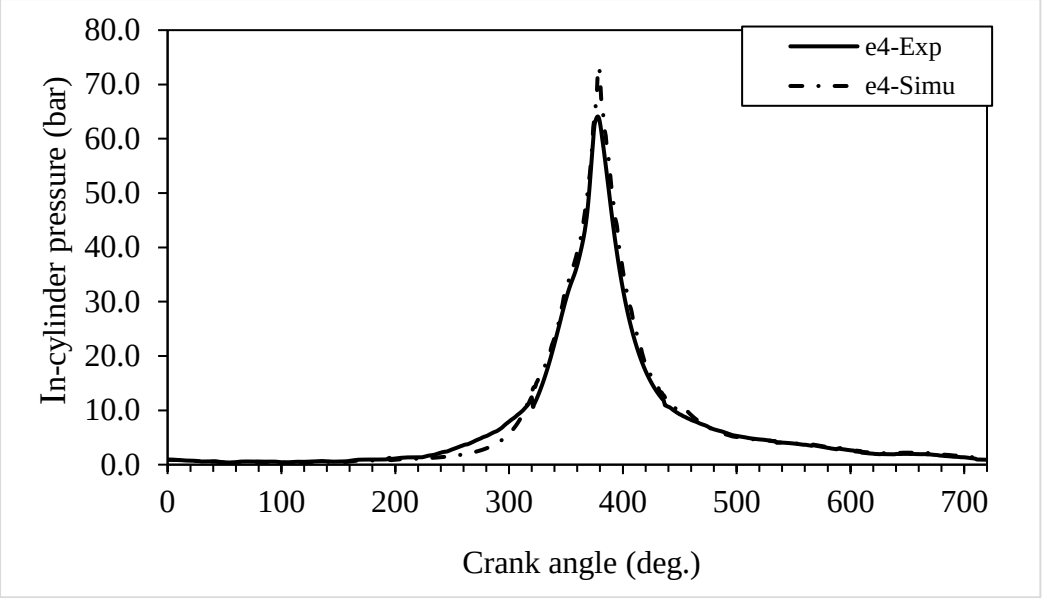

Fig 5.9 Comparison of experimental and simulation pressure histories for e4

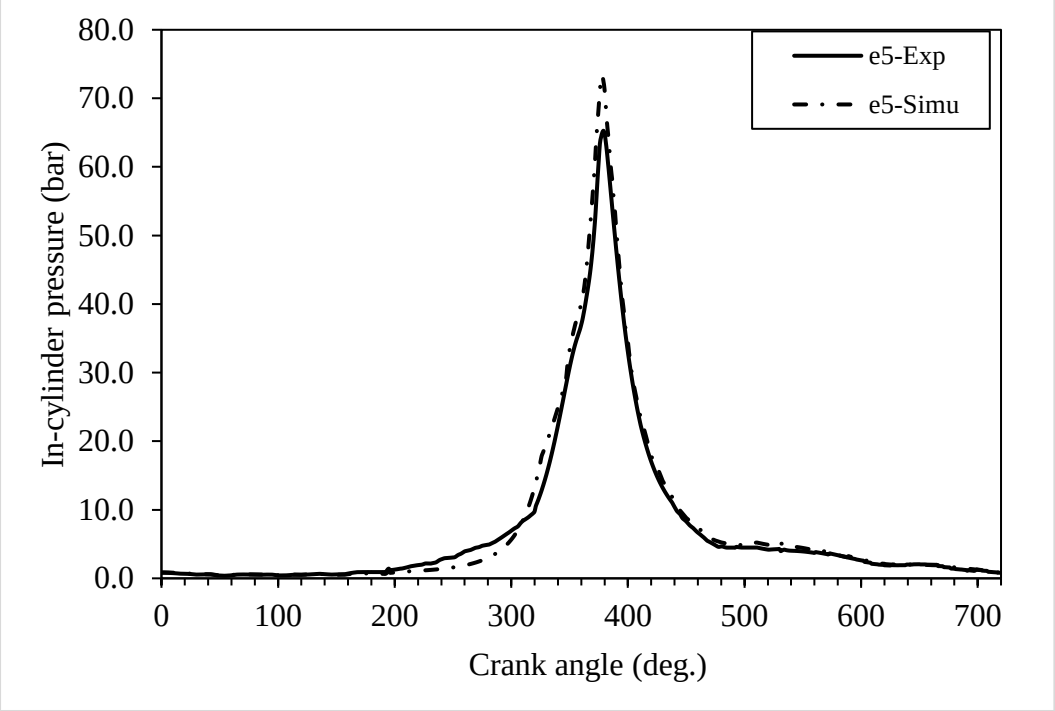

Fig 5.10 Comparison of experimental and simulation pressure histories for e5

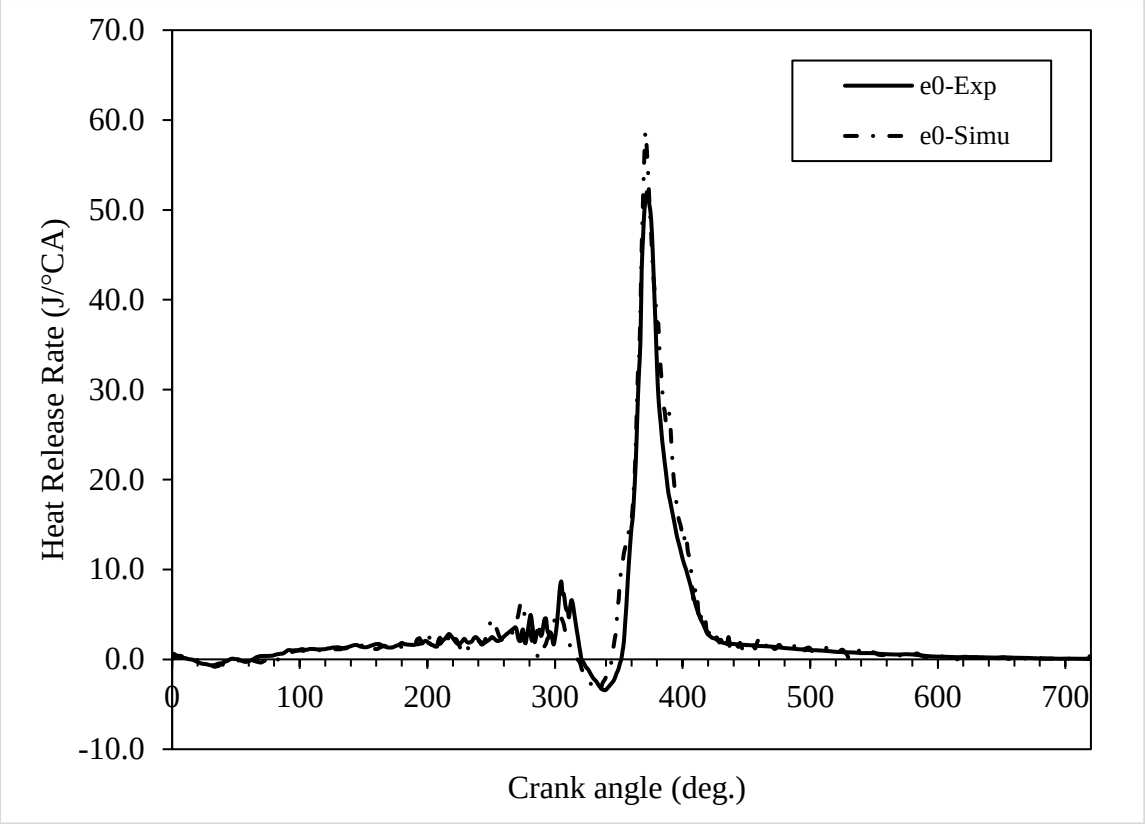

Fig 5.11 Comparison of experimental and simulation heat release rates for pure diesel

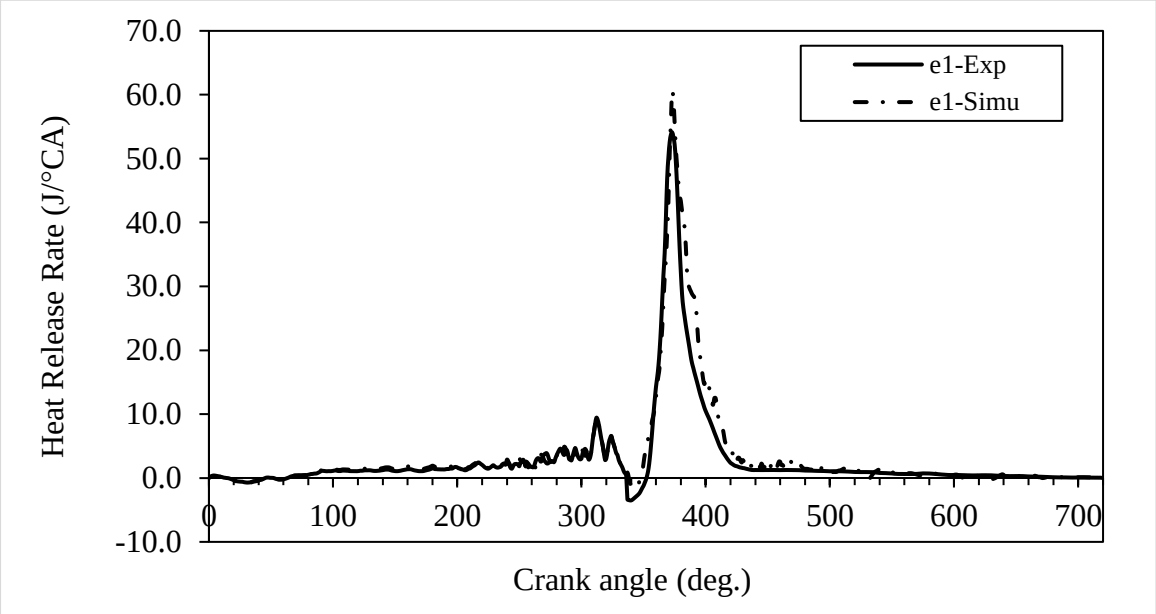

Fig 5.12 Comparison of experimental and simulation heat release rates for e1

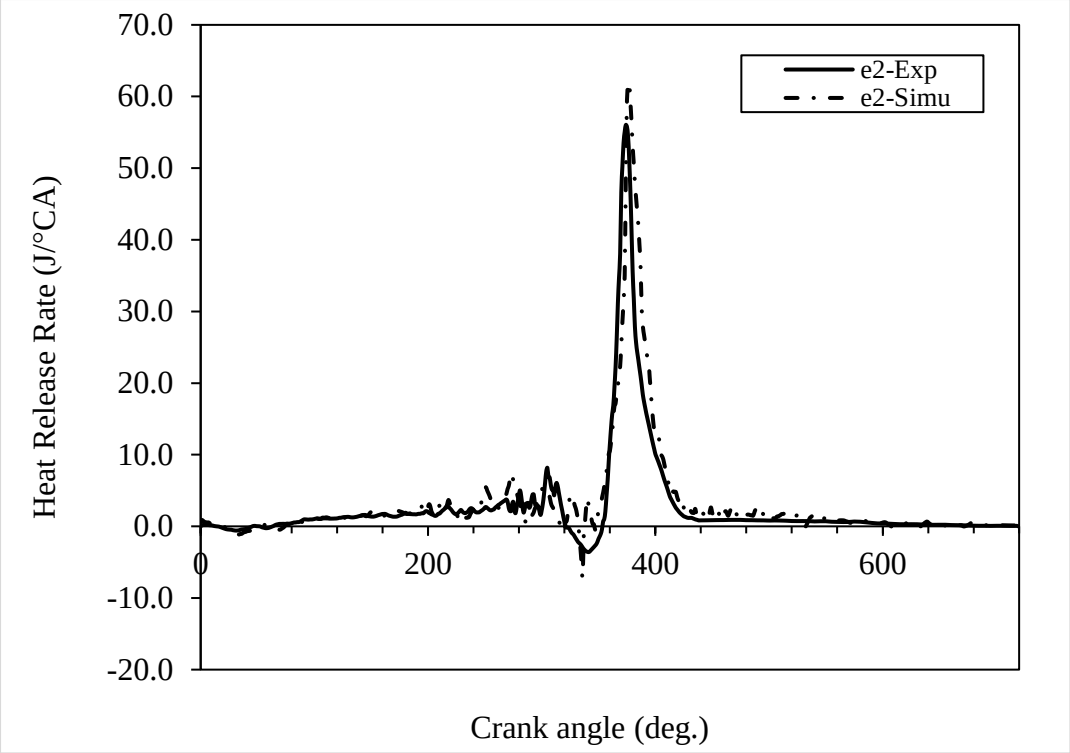

Fig 5.13 Comparison of experimental and simulation heat release rates for e2

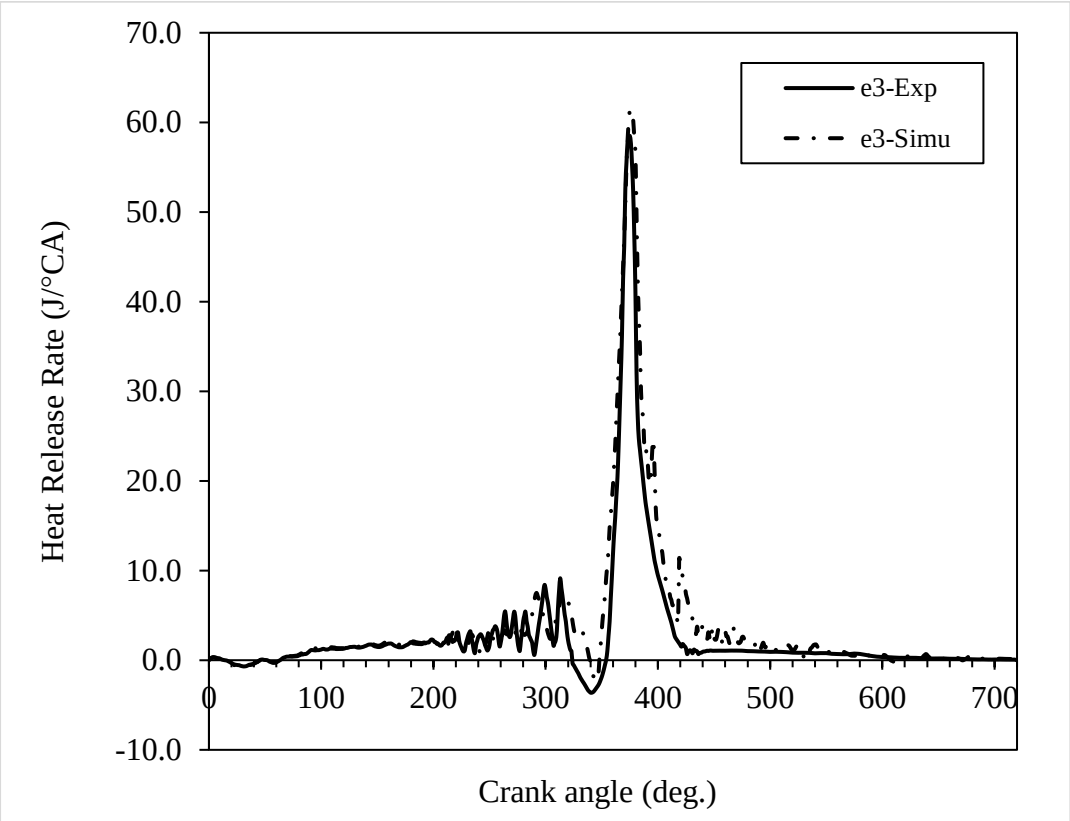

Fig 5.14 Comparison of experimental and simulation heat release rates for e3

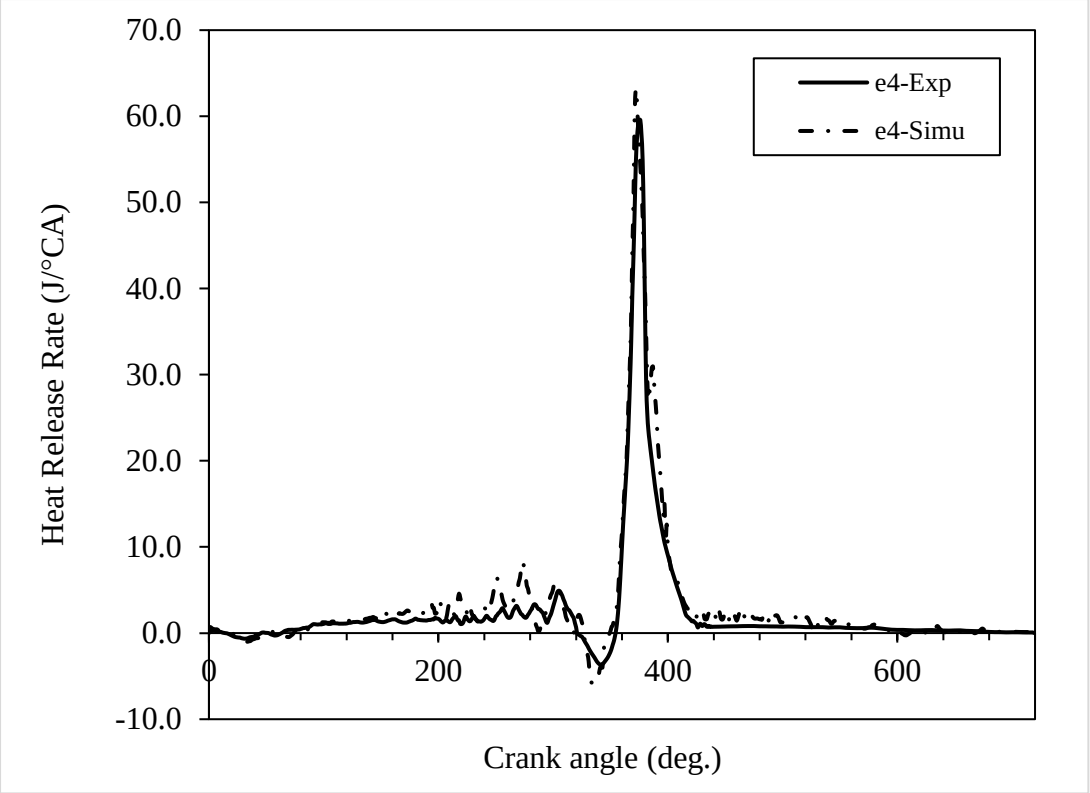

Fig 5.15 Comparison of experimental and simulation heat release rates for e4

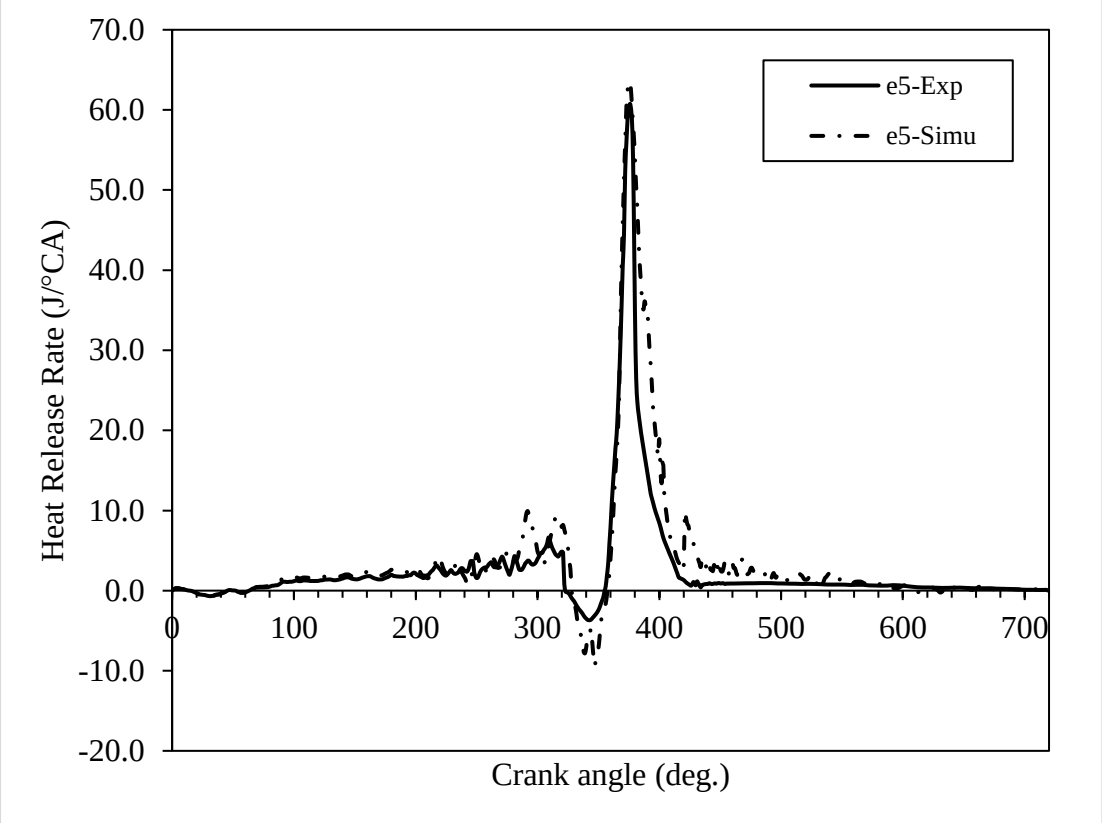

Fig 5.16 Comparison of experimental and simulation heat release rates for e5

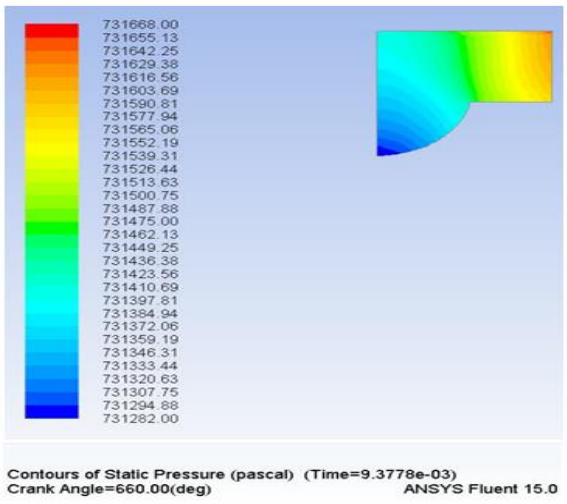

Pure diesel at 60° CA bTDC

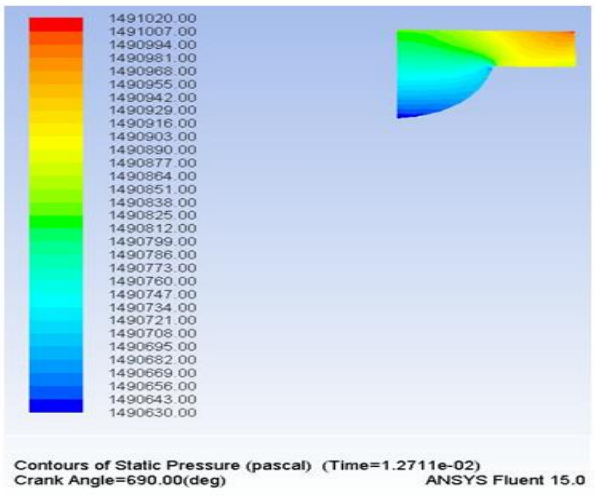

Pure diesel at 30° CA bTDC

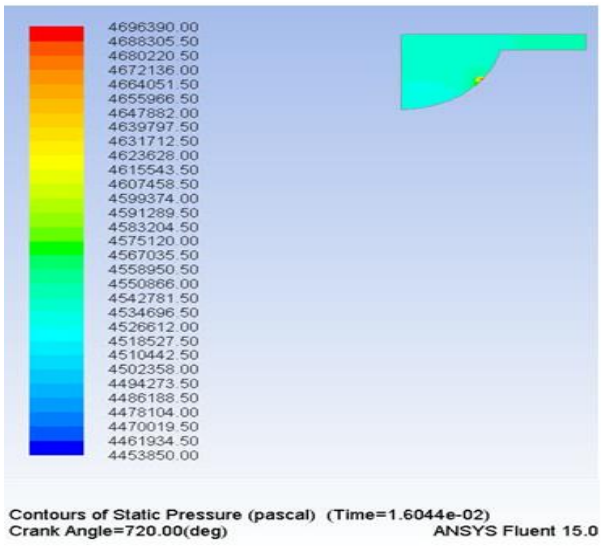

Pure diesel at TDC

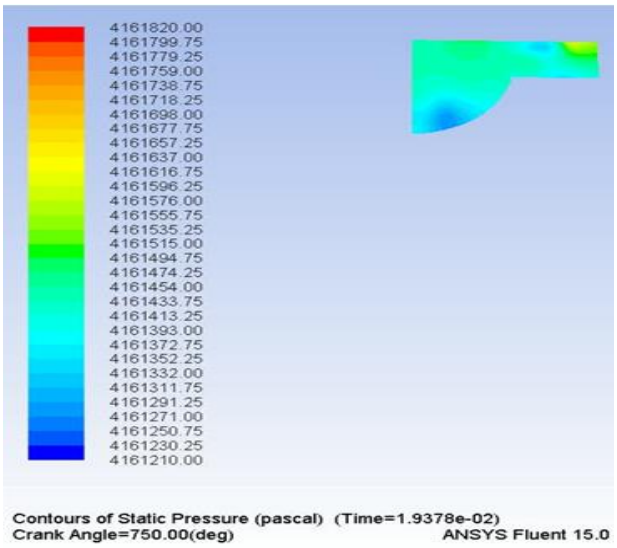

Pure diesel at 30° CA aTDC

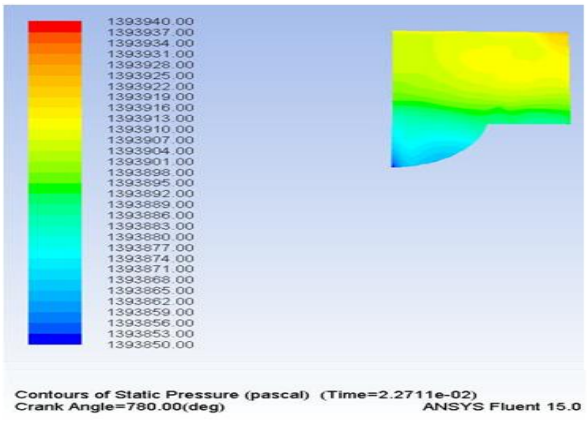

Pure diesel at 60° CA aTDC

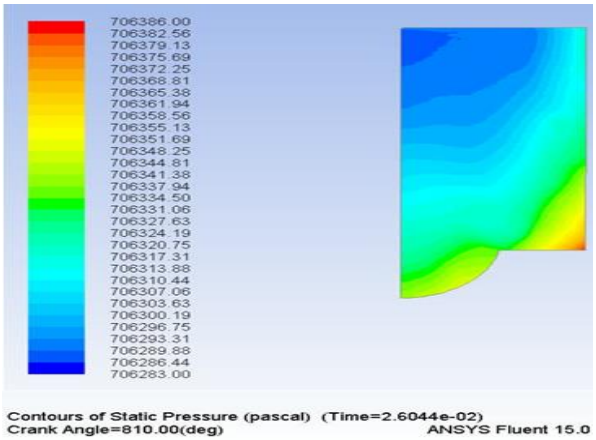

Pure diesel at 90° CA aTDC

Fig 5.17 Pressure Contours for Pure diesel at different crank angles

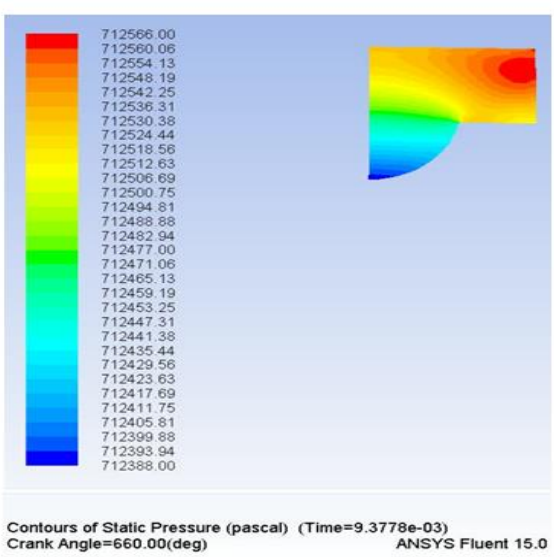

e1 at 60° CA bTDC

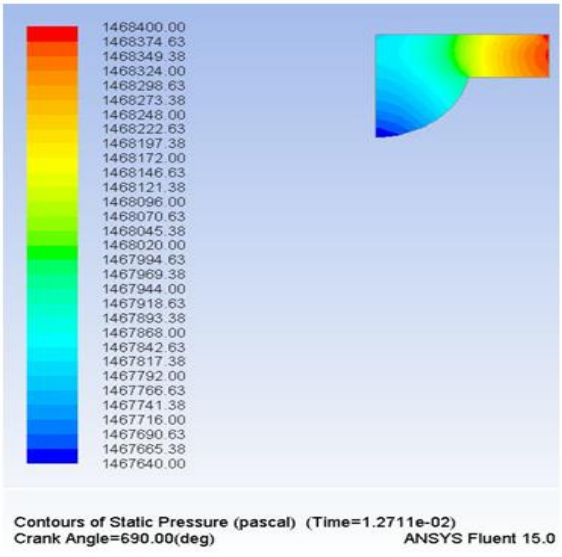

e1 at 30° CA bTDC

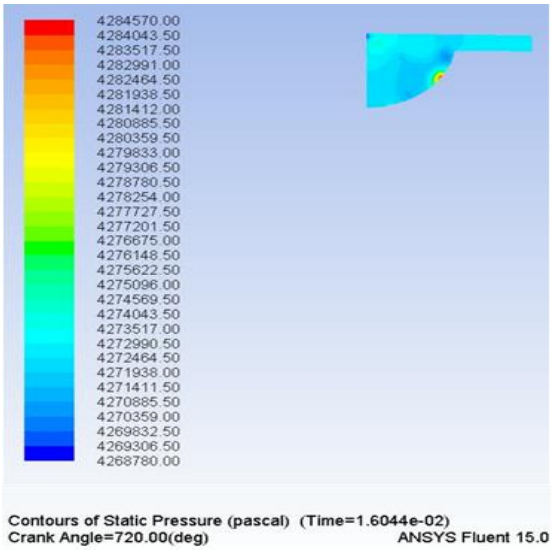

e1 at TDC

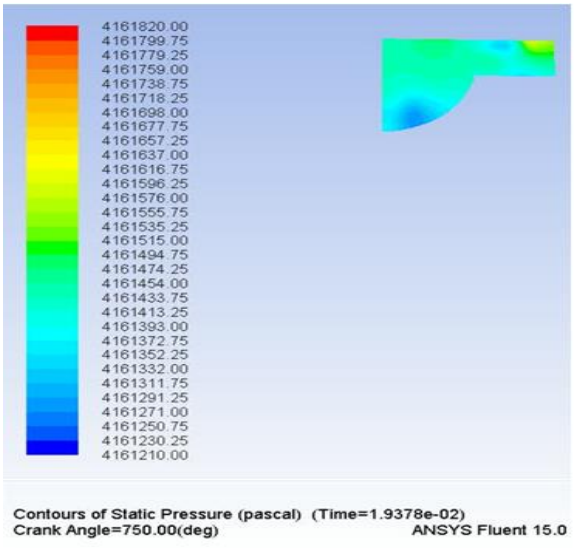

e1 at 30° CA aTDC

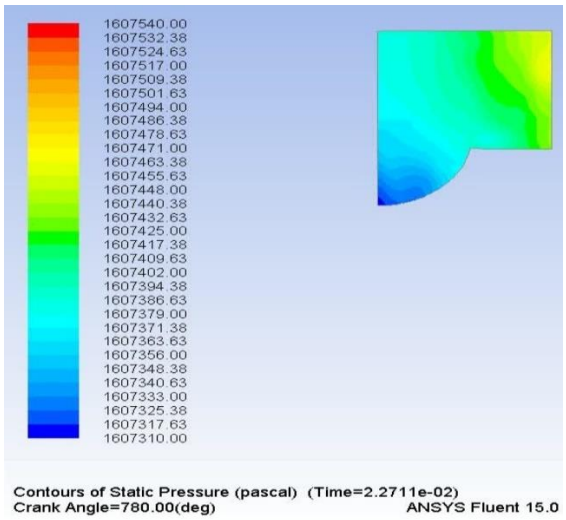

e1 at 60° CA aTDC

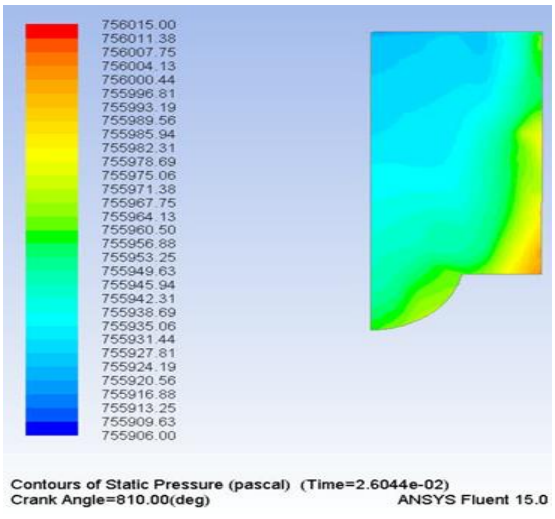

e1 at 90° CA aTDC

Fig 5.18 Pressure Contours for e1 at different crank angles

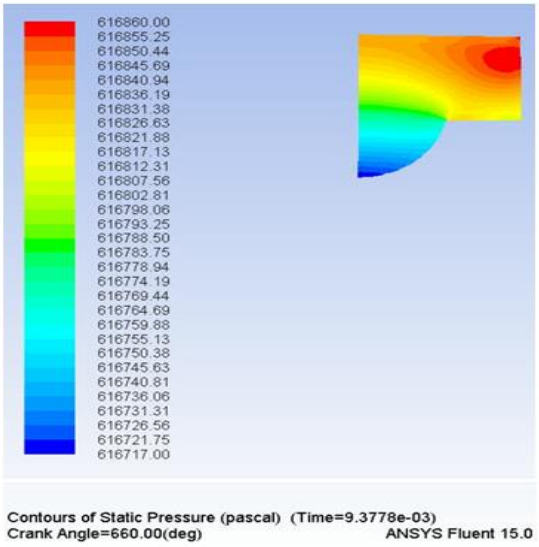

e2 at 60° CA bTDC

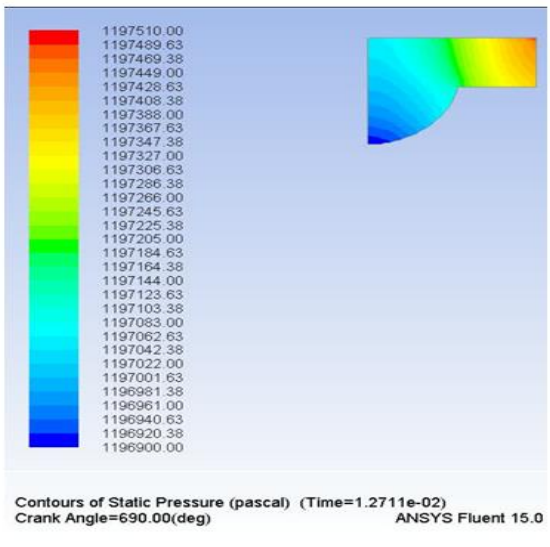

e2 at 30° CA bTDC

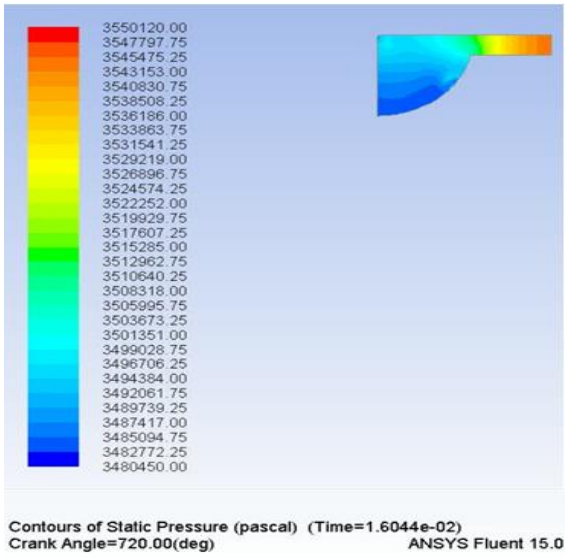

e2 at TDC

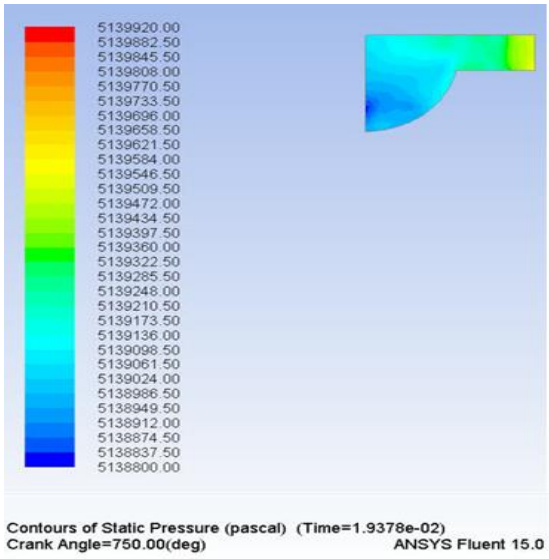

e2 at 30° CA aTDC

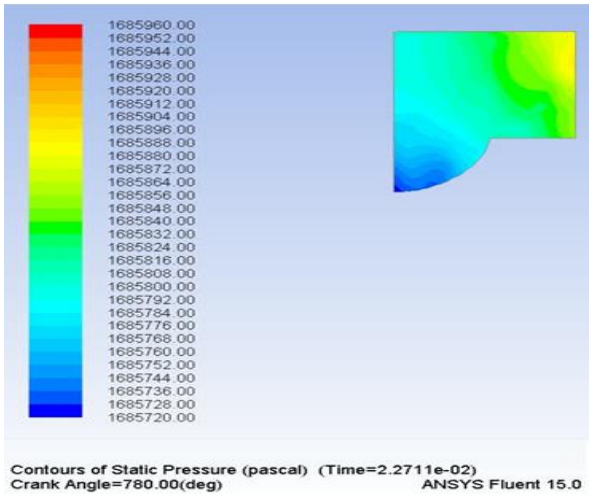

e2 at 60° CA aTDC

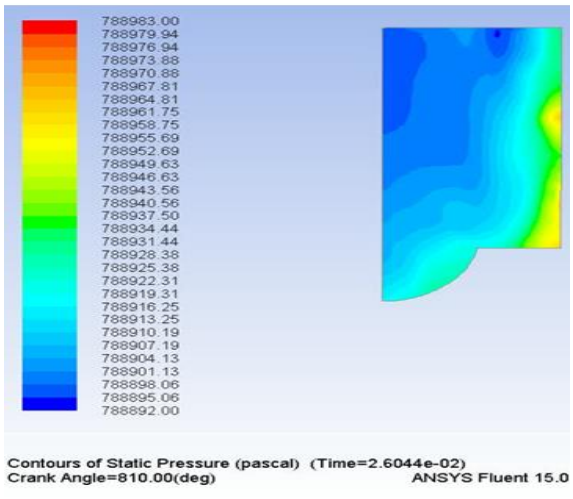

e2 at 90° CA aTDC

Fig 5.19 Pressure Contours for e2 at different crank angles

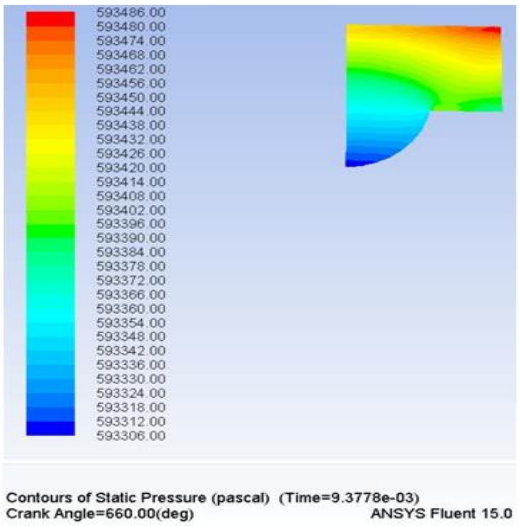

e3 at 60° CA bTDC

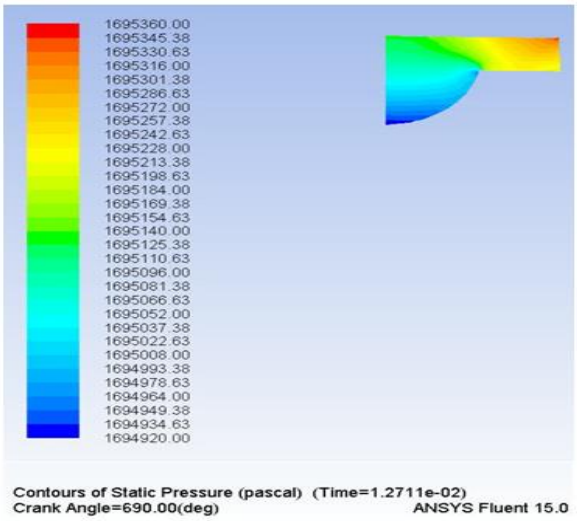

e3 at 30° CA bTDC

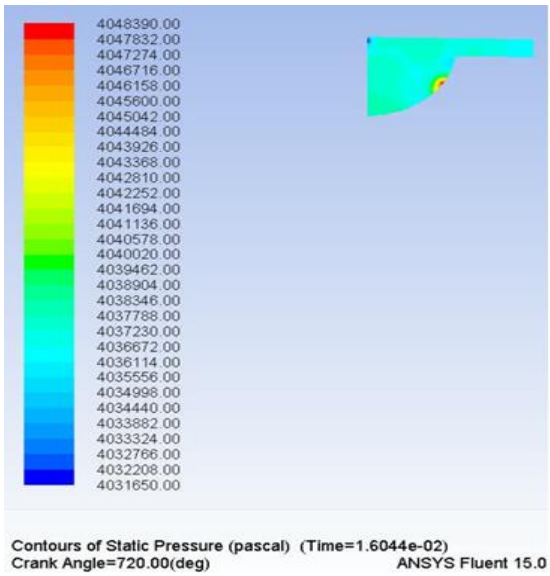

e3 at TDC

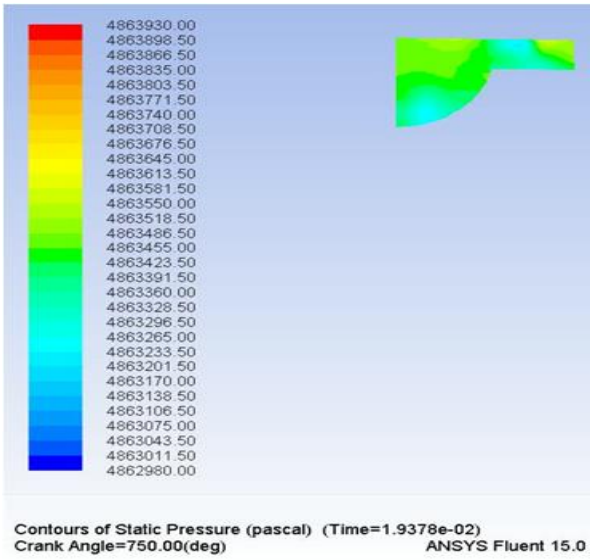

e3 at 30° CA aTDC

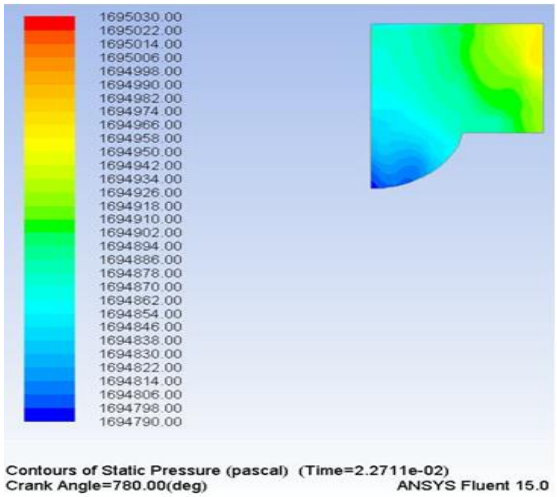

e3 at 60° CA aTDC

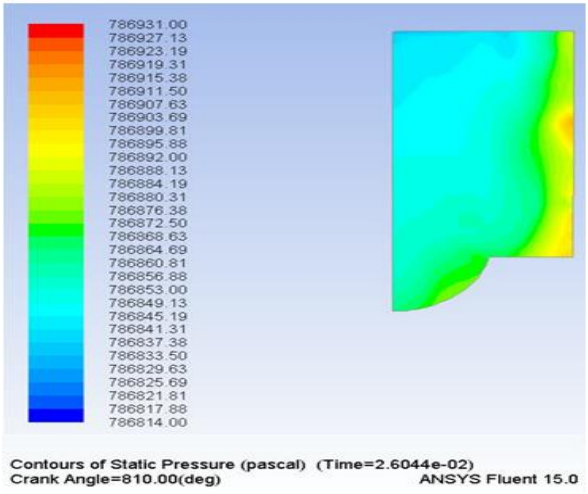

e3 at 90° CA aTDC

Fig 5.20 Pressure Contours for e3 at different crank angles

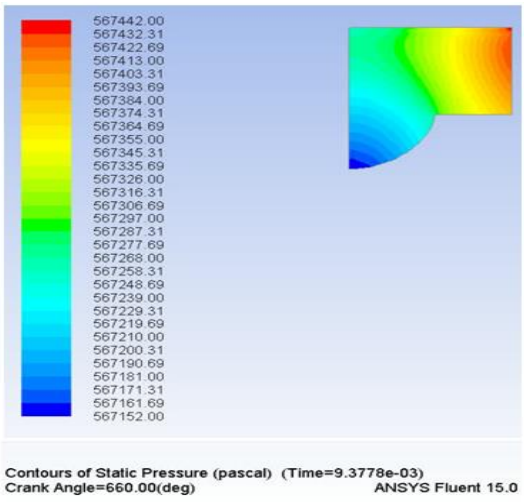

e4 at 60° CA bTDC

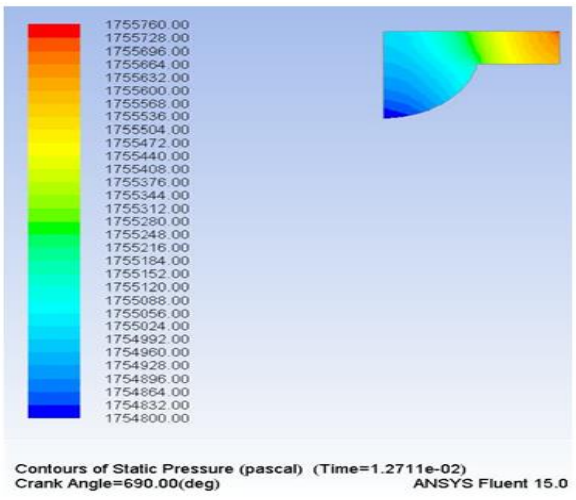

e4 at 30° CA bTDC

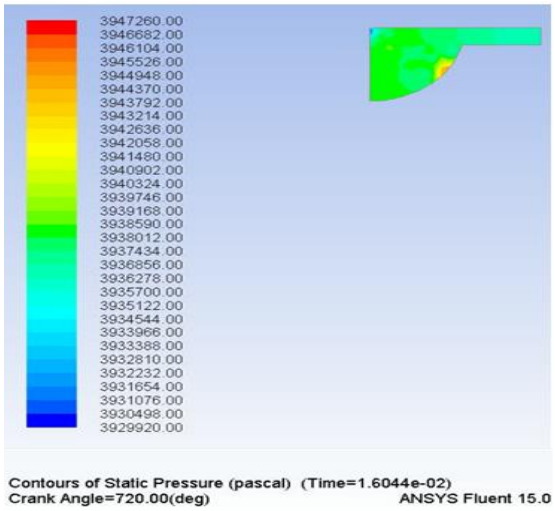

e4 at TDC

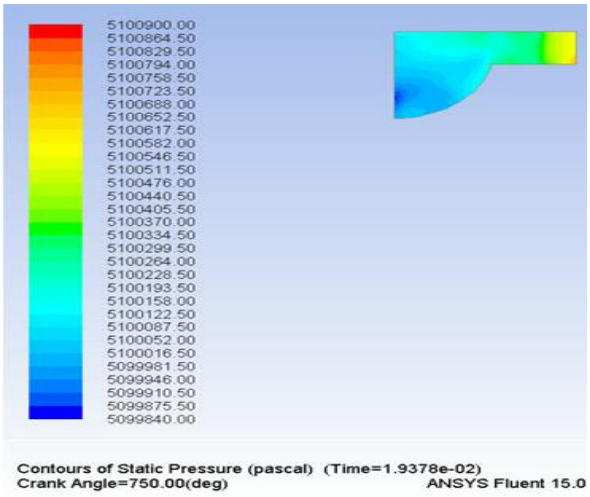

e4 at 30° CA aTDC

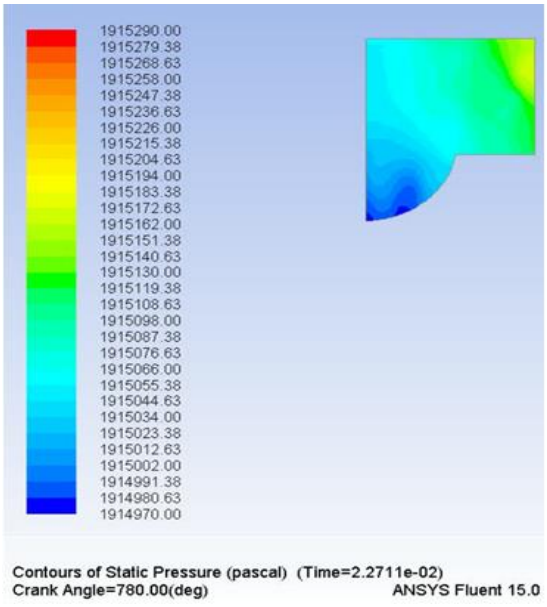

e4 at 60° CA aTDC

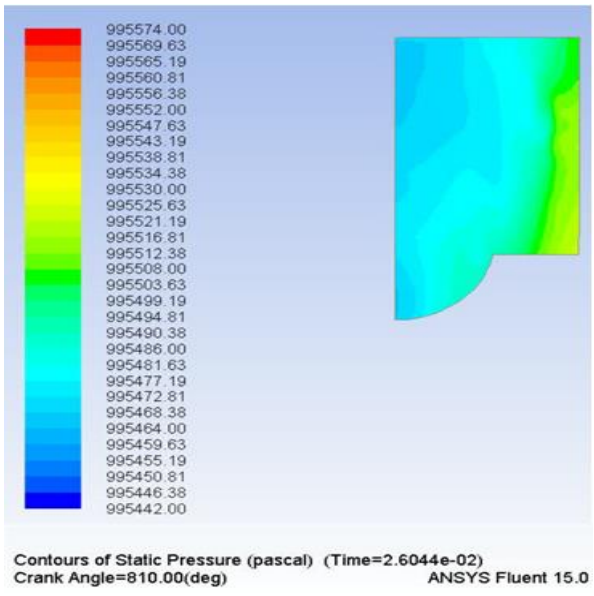

e4 at 90° CA aTDC

Fig 5.21 Pressure Contours for e4 at different crank angles

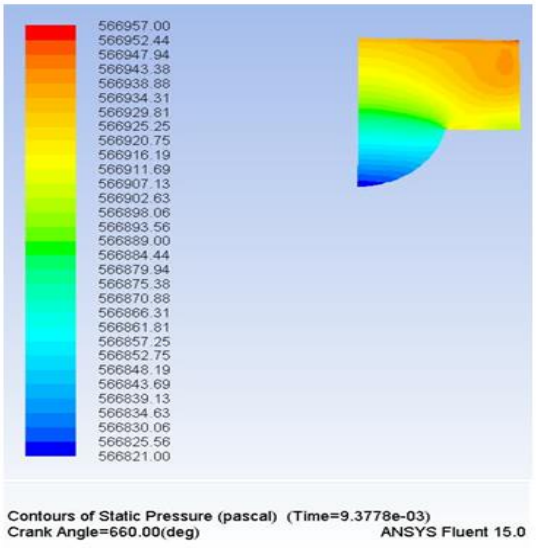

e5 at 60° CA bTDC

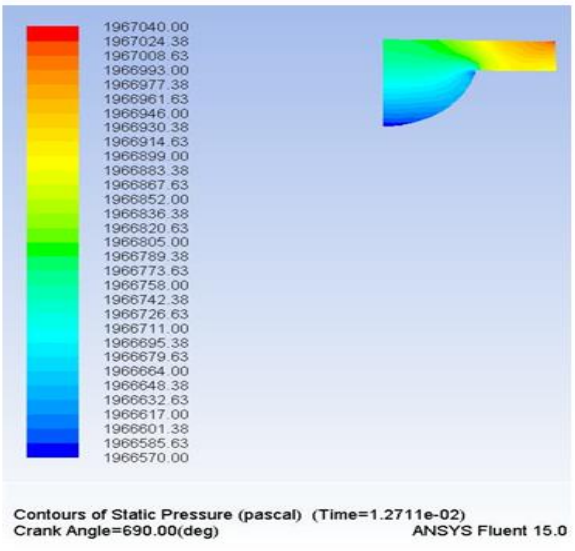

e5 at 30° CA bTDC

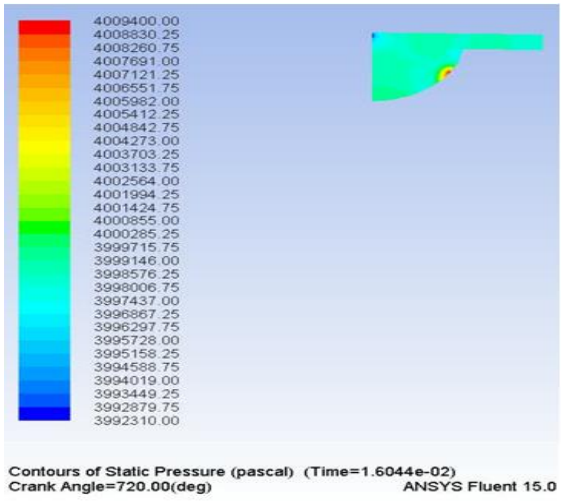

e5 at TDC

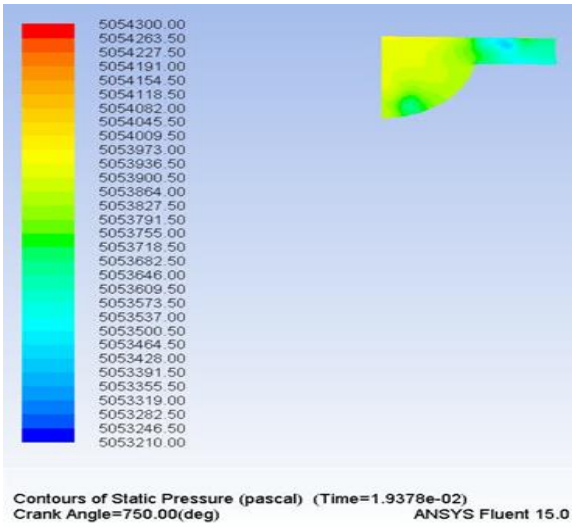

e5 at 30° CA aTDC

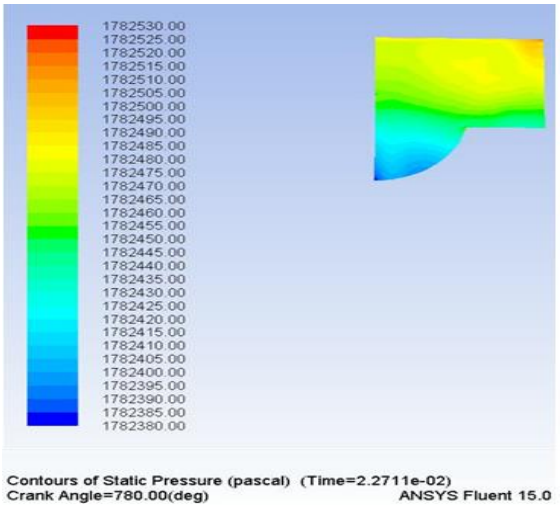

e5 at 60° CA aTDC

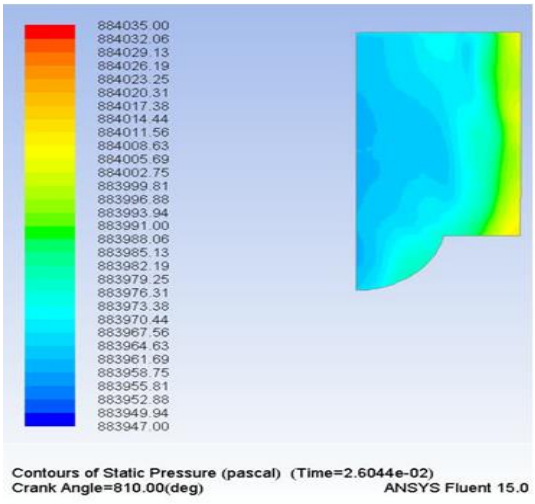

e5 at 90° CA aTDC

Fig 5.22 Pressure Contours for e5 at different crank angles

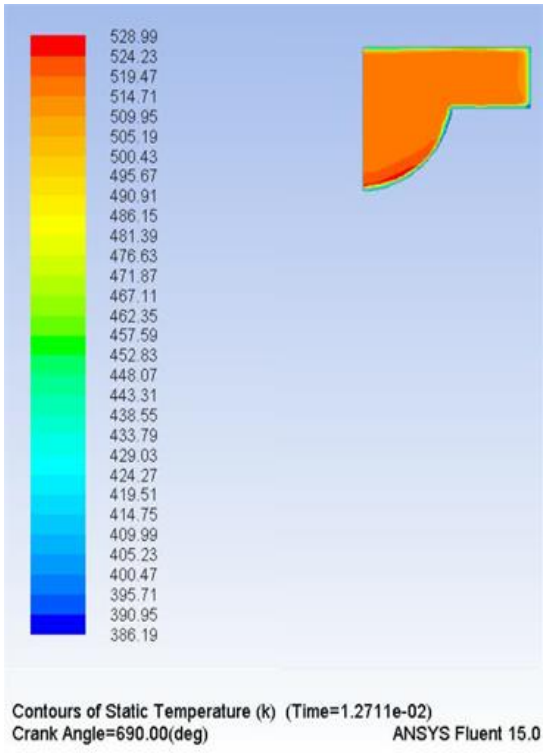

Pure diesel at 30° CA bTDC

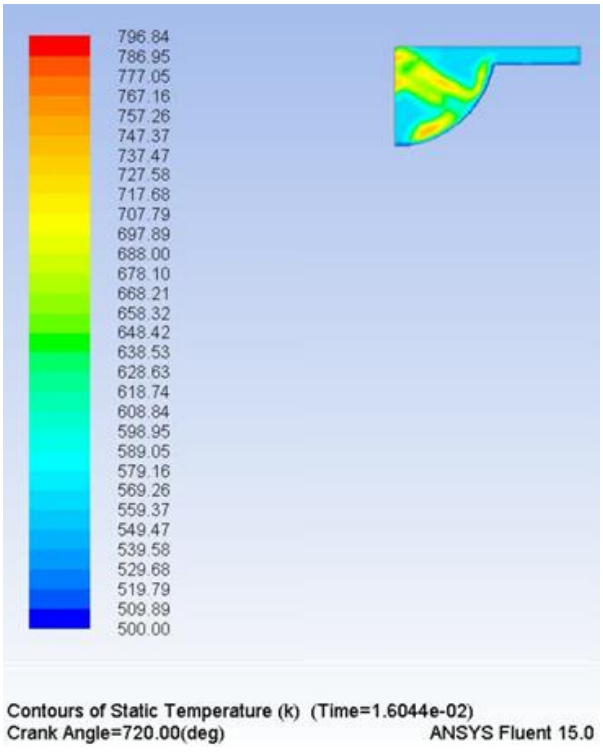

Pure diesel at TDC

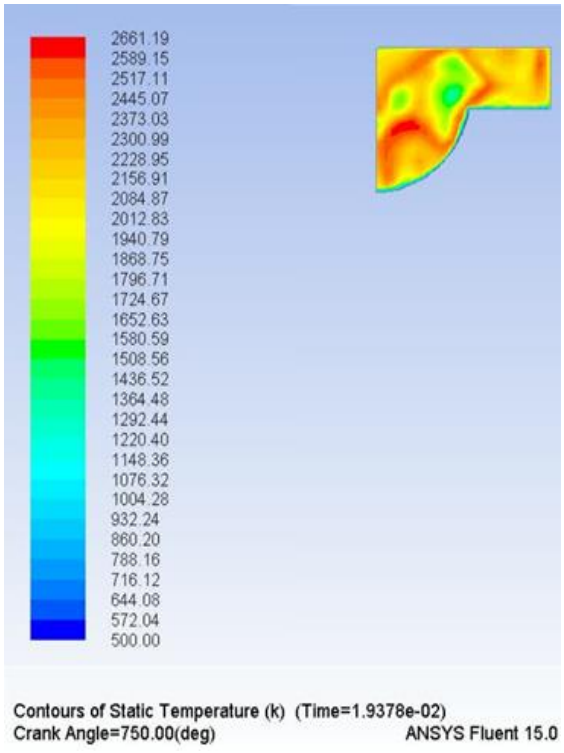

Pure diesel at 30° CA aTDC

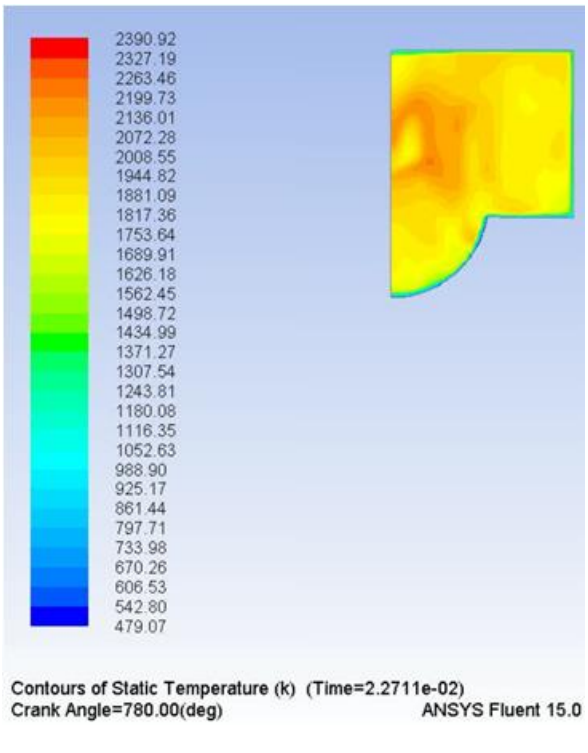

Pure diesel at 60° CA aTDC

Fig 5.23 Temperature Contours for Pure diesel at different crank angles

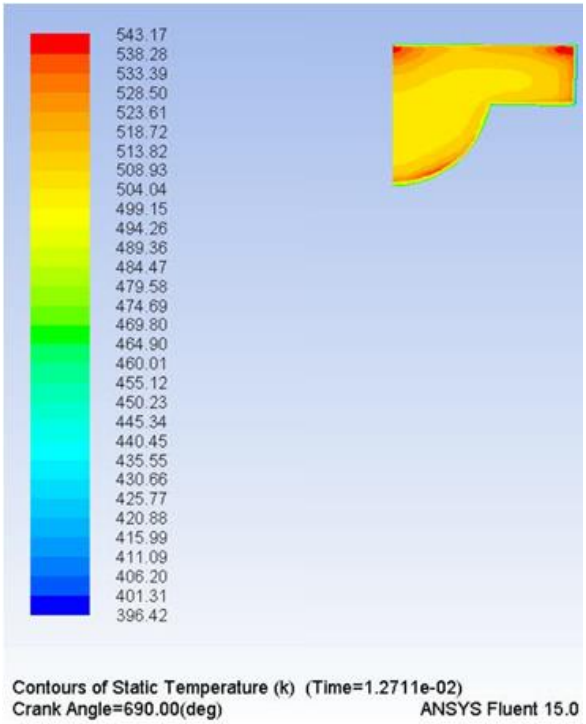

e1 at 30° CA bTDC

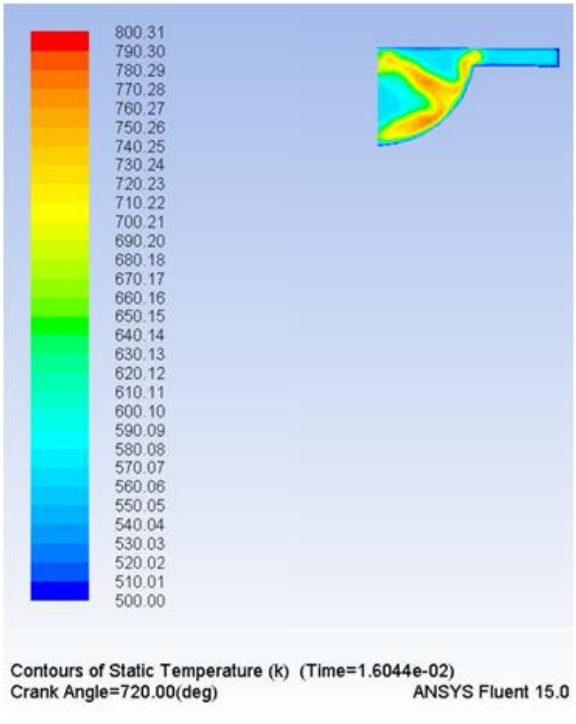

e1 at TDC

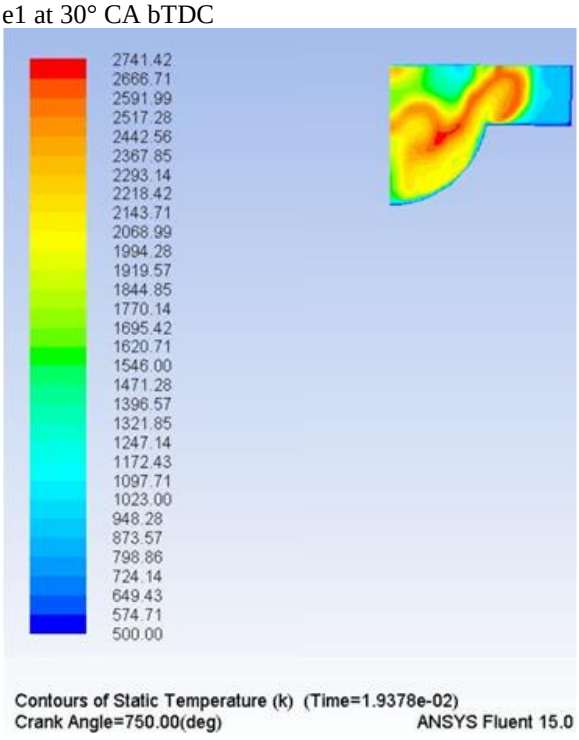

e1 at 30° CA aTDC

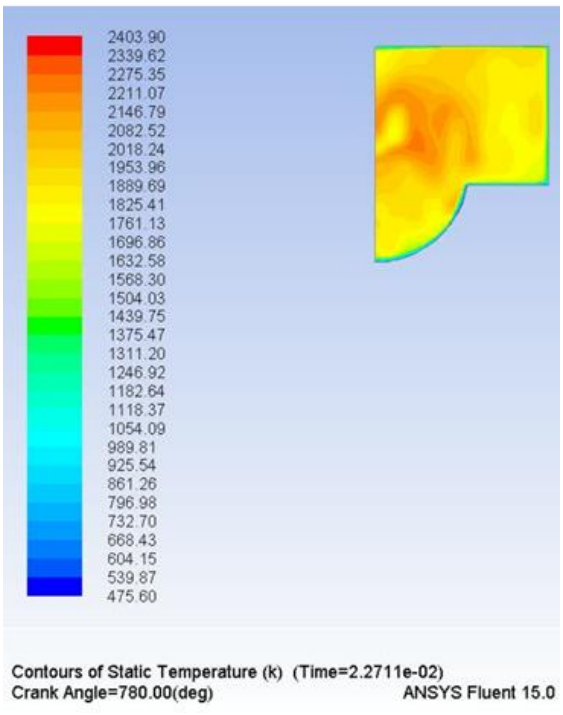

e1 at 60° CA aTDC

Fig 5.24 Temperature Contours for e1 at different crank angles

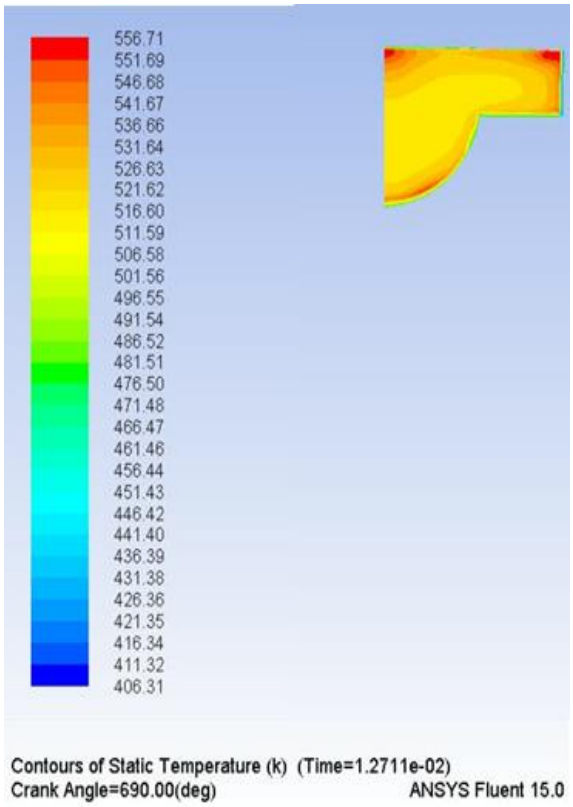

e2 at 30° CA bTDC

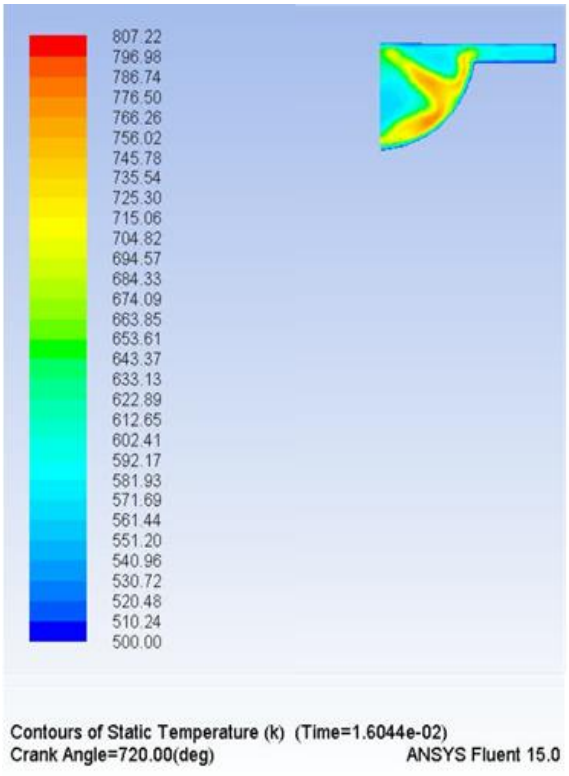

e2 at TDC

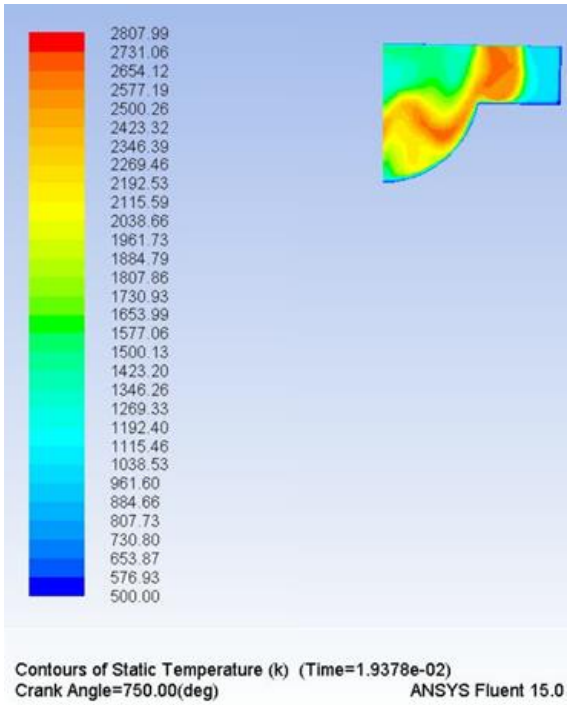

e2 at 30° CA aTDC

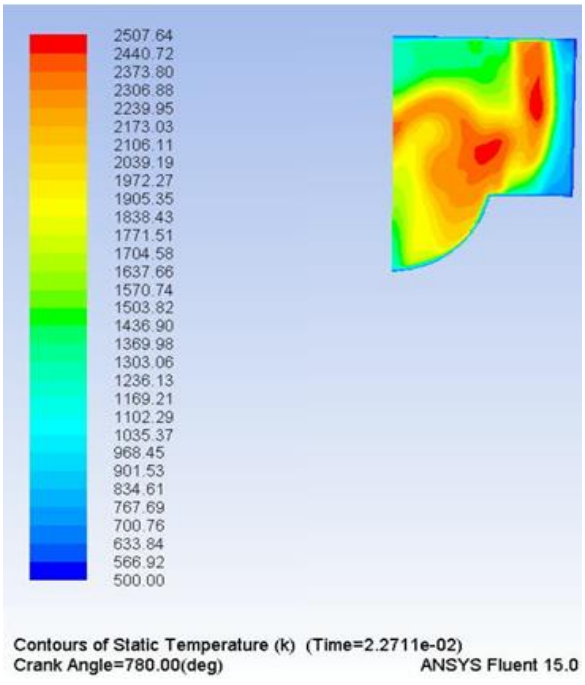

e2 at 60° CA aTDC

Fig 5.25 Temperature Contours for e2 at different crank angles

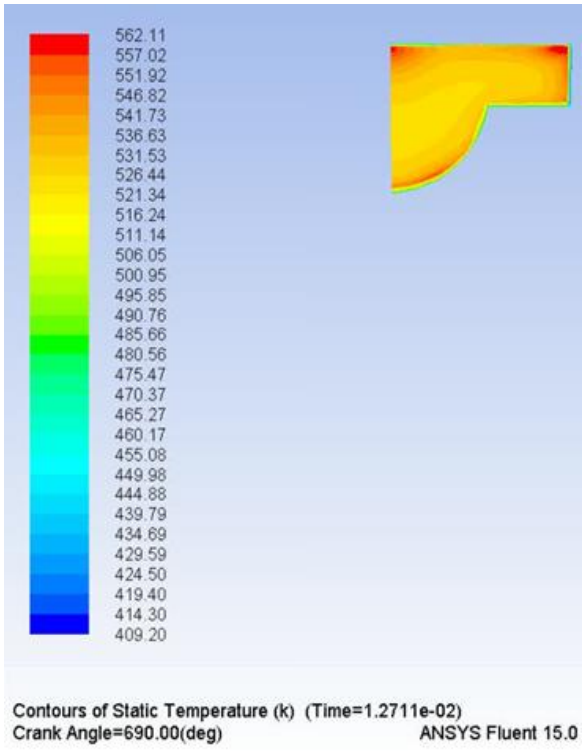

e3 at 30° CA bTDC

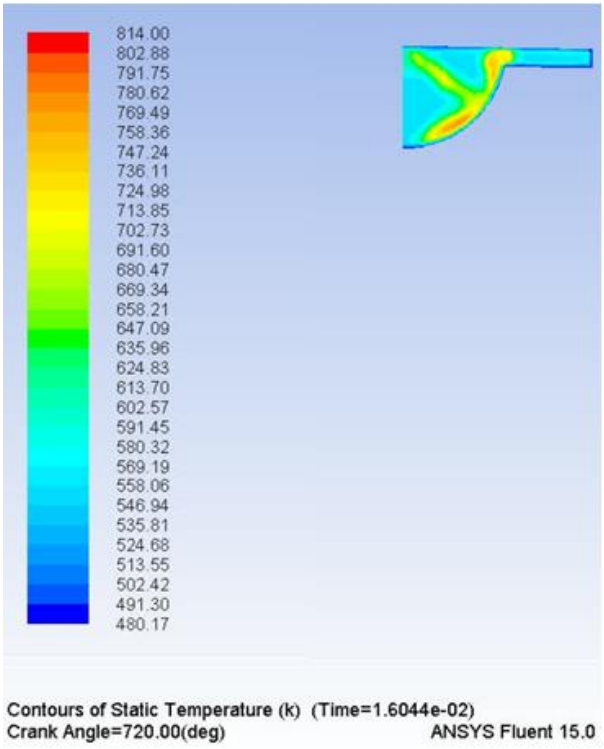

e3 at TDC

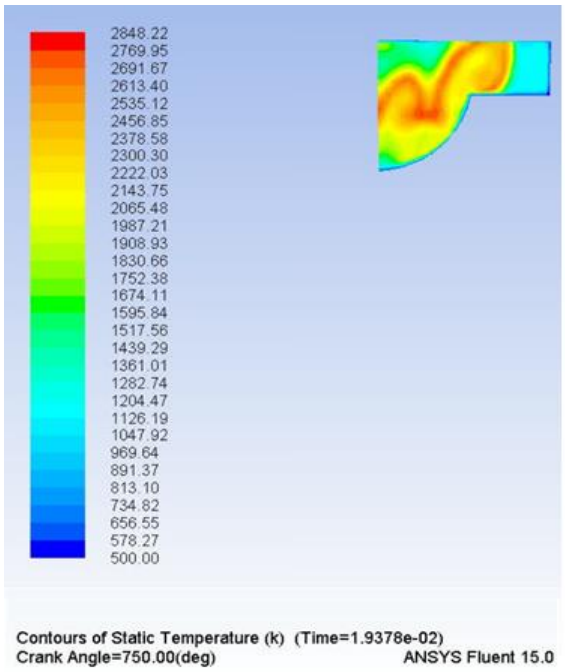

e3 at 30° CA aTDC

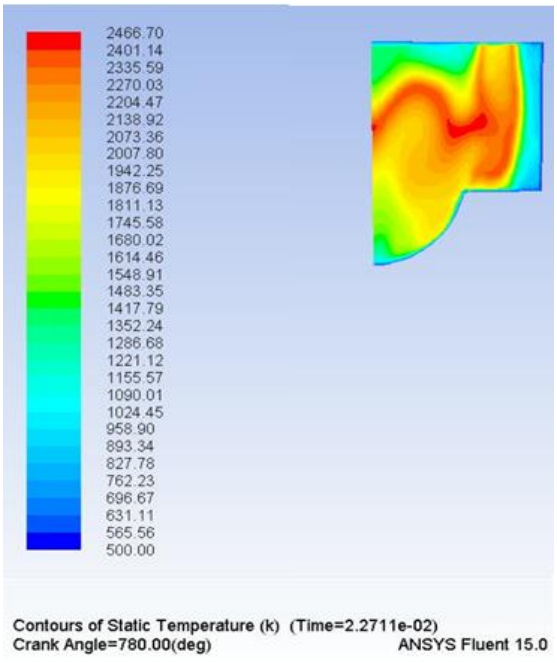

e3 at 60° CA aTDC

Fig 5.26 Temperature Contours for e3 at different crank angles

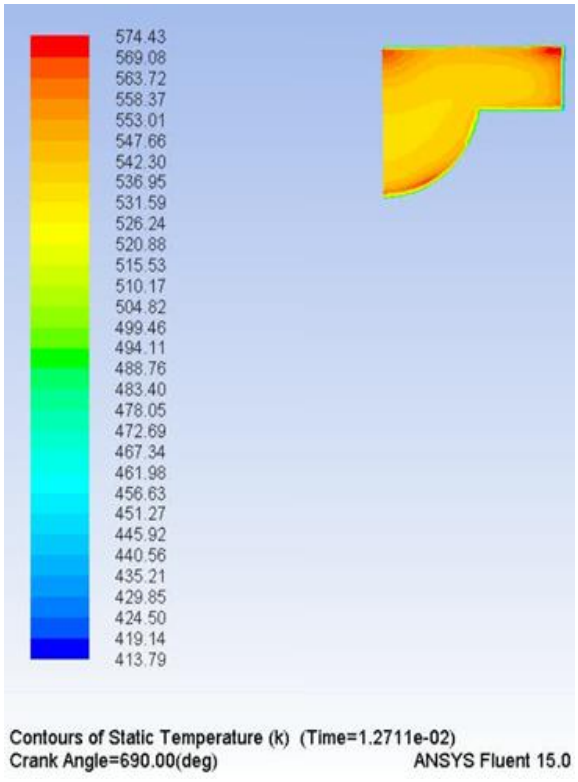

e4 at 30° CA bTDC

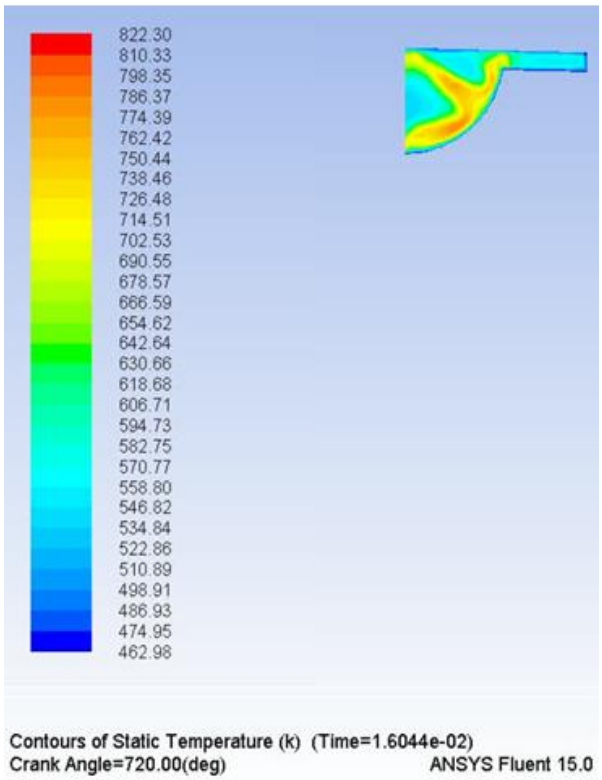

e4 at TDC

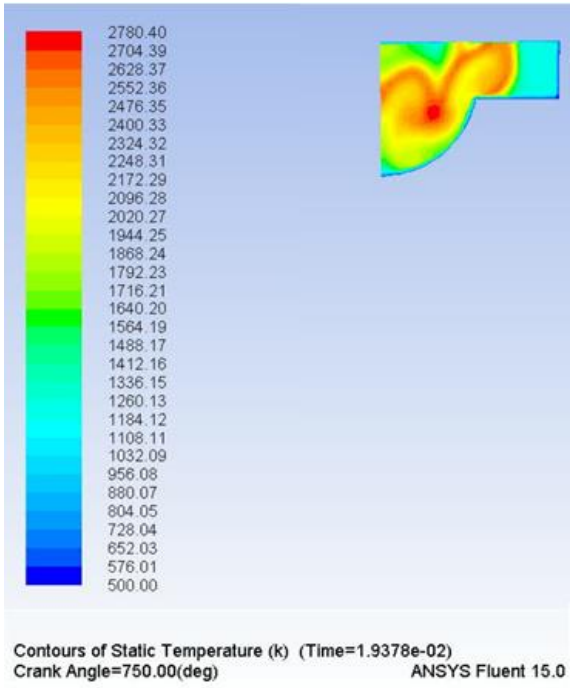

e4 at 30° CA aTDC

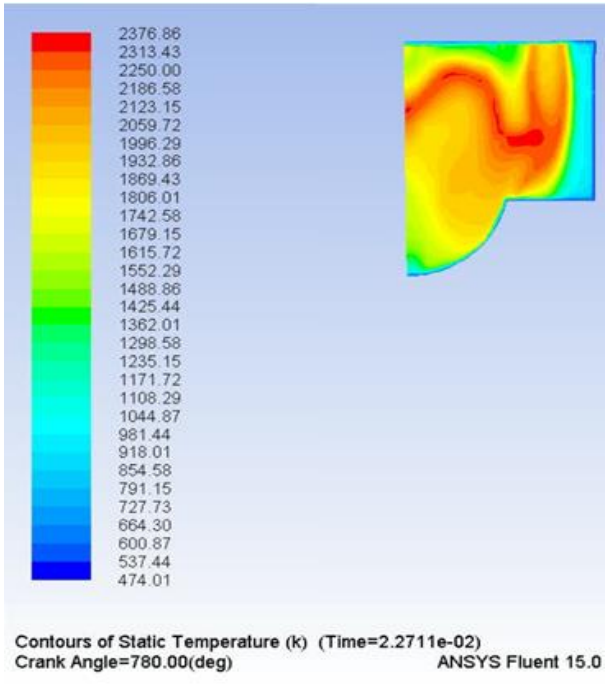

e4 at 60° CA aTDC

Fig 5.27 Temperature Contours for e4 at different crank angles

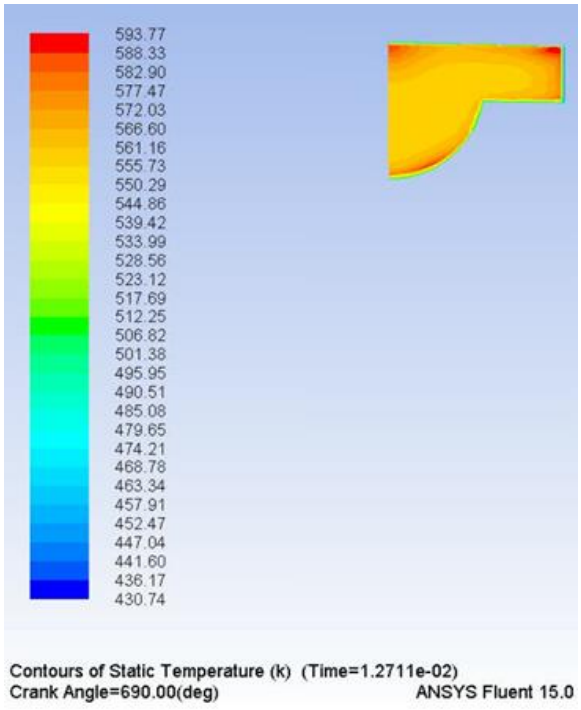

e5 at 30° CA bTDC

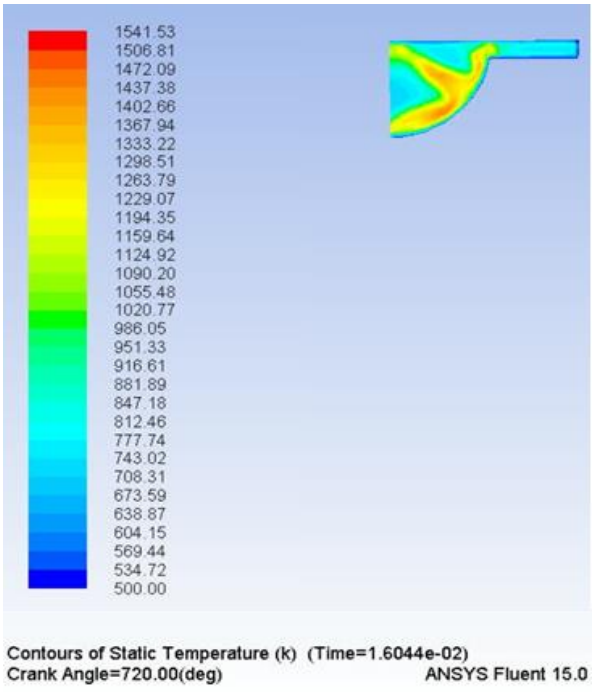

e5 at TDC

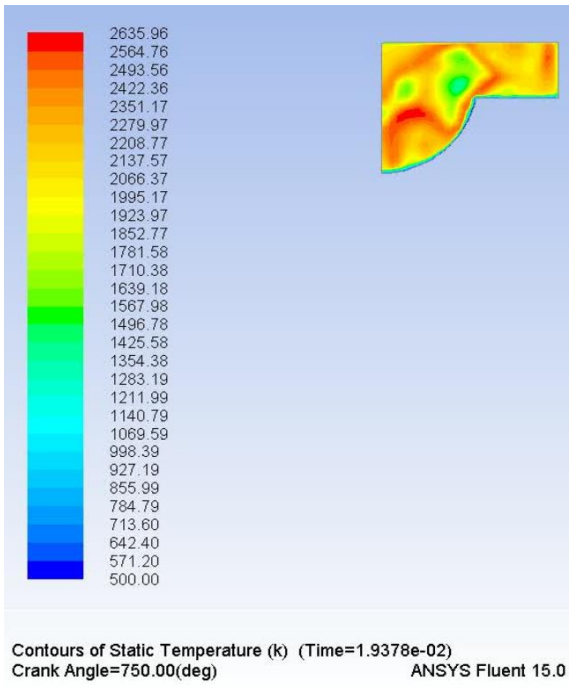

e5 at 30° CA aTDC

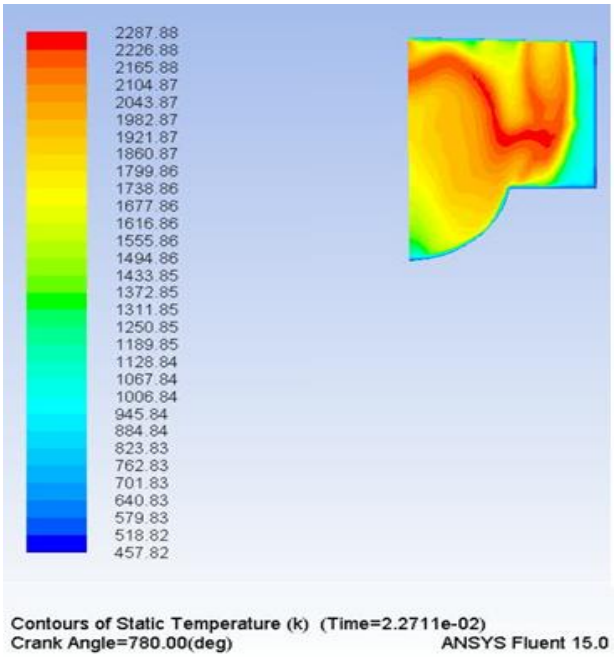

e5 at 60° CA aTDC

Fig 5.28 Temperature Contours for e5 at different crank angles

A diesel engine CFD model was developed to simulate the combustion phenomena of the engine the results of which were in good agreement with the experimental results.

CHAPTER 6

CONCLUSIONS

The research work was undertaken to investigate the variations in the engine performance, exhaust emissions and combustion characteristics of single cylinder four stroke water cooled stationary diesel engine using ethanol in various mode. The significance of evaluating the different modes performance, exhaust emissions and combustion characteristics of engine lies in the fact that the results obtained may facilitate the end-user a great variety of operating conditions for improved performance and/or emissions. The fumigations system was successfully developed to supply metered quantity of ethanol without having any significant effect on the engine performance. The performance characteristics, exhaust emissions and combustion parameters have been recorded and analysed at different engine loads with variation of other engine operating parameters. As shown by the results, fumigation of ethanol is a feasible solution for ethanol substitution in CI engine.

In the first test-mode, the engine has been operated with pure diesel and different ethanol proportions designated as E0, E10, E20, E30 and E40.With ethanol fumigation, decrease in BTE up to 8% have been observed at low loads, whereas BTE increased up to 2.5% at high loads, as compared to E0. For E10, E20, E30 and E40, the maximum decrease in NOx of 7.4%, 11.7%, 14.5% and 16% respectively, have been recorded as compared to E0. In comparison to E0, the increase in HC emission of 42.6%, 63.9%, 86.9% and 149.2% with corresponding increase of 23.1%, 53.8%, 84.6% and 111.5% in CO emissions respectively, have been observed for E10, E20, E30 and E40. CO_2 decreased by 5.5%, 10.6%, 14.9% and 18.2% and smoke opacity decreased by 5.1%, 10.4%, 16% and 20.8% respectively, for E10, E20, E30 and E40. The values of peak pressure and heat release rate increases with ethanol fumigation. The position of occurrence of peak pressure is shifted by 1-2°CA as compared to that in pure diesel case. The maximum rate of pressure rise for ethanol fumigation is found to be higher by about 0.3-0.5 bar/°CA than that of diesel operation. The location of maximum HRR is shifted by 1-4 °CA, than that of E0. The values of IMEP (in kPa) 756.8, 771.4, 776.3, 790.8 and 810.2 respectively are obtained at full load for E0, E10, E20, E30 and E40. The ignition delay increases and combustion duration decreases for all levels of fumigation. High ethanol content causes the occurrence of partial burning and misfiring cycles which is indicated by high cyclic variability in the combustion process and evidenced by moderately

high value of CoV of IMEP. In the second test-mode, the engine has been operated with pure diesel and different ethanol fumigation rates designated as e0, e1, e2, e3, e4 and e5.At a certain high engine load, a maximum of 6% efficiency gain (as compared to baseline diesel case) is achieved with ethanol flow rate of 0.4 kg/hr. The various ethanol energy fumigation modes results into maximum reduction of 22% in NOx emission, 27% in CO_2 emission and 41% in smoke opacity. The different ethanol fumigation modes can yield the increase of 144% and 133% in HC and CO emissions, respectively. Simultaneous reduction of NOx, smoke and CO_2 whereas increase in HC and CO has been observed with increasing rate of fumigation. At full load, the values of peak pressure and peak HRR respectively, increases from 62.1 bar and 52 J/deg °CA (pure diesel) to 65.3 bar and 60.8 J/deg °CA (for ethanol flow rate of 0.5 kg/hr). The maximum increase in ignition delay of about 3 °CA whereas maximum decrease in combustion duration of about 5 °CA were observed for different ethanol modes as compared to baseline diesel case. With the induction of ethanol in CI engine, increased rate of heat release and increased peak pressure increases thus enhancing the thermal efficiency.

In third mode, the diesel engine was operated using various ethanol energy fractiondesignated as eef0, eef1, eef2, eef3, eef4 and eef5. With various ethanol energy fraction modes, BTE increased up to 4.6% at high loads as compared to baseline diesel case. The various ethanol energy fumigation modes results into maximum reduction of 35% in NOx emission, 38% in CO_2 emissions and 47% in smoke opacity. Also, these modes can yield the increase of 2.8 times and 1.9 times respectively, in HC and CO emissions. At full load, the values of peak pressure and HRR respectively, increases from 62.1 bar and 52 J/deg CA (pure diesel) to 64.9 bar and 62.5 J/deg CA (for eef3), and then decreases up to 58.2 bar and 56.2 J/deg CA (for eef5). The position of occurrence of peak pressure and peak HRR respectively are shifted by 1-4°CA and 1-8 °CA as compared to eef0. The maximum increase in ignition delay (°CA) of about 6 °CA whereas maximum decrease in combustion duration of about 5 °CA were observed for different ethanol modes as compared to baseline diesel case.

In fourth mode**,** test-runs were conducted on theengine using various ethanol fumigation rates at different diesel injection timings. At fixed ethanol flow rate and given load, the efficiency increased by advancing diesel injection timing. As compared to original injection timing, NOx and smoke opacity increases with simultaneous decrease of HC and CO emissions by advancing diesel injection timing. Advanced diesel injection extends the limit of utilisation of

higher ethanol flow rate. With increase in injection advance, considerably higher peak pressure and high rate of pressure rise along with extended ignition delay and shorter combustion duration is observed. The extent of injection advance is limited by occurrence of knock. Moreover, injection advance beyond a certain limit decreases the maximum attainable pressure owing to the fact that when injection takes place too early, the fuel is not properly prepared for combustion. The retardation of diesel injection timing beyond a certain limit enhances the likelihood of misfiring. The condition of misfiring limits the maximum ethanol substitution for a given operating condition

In fifth mode**,** test-runs were conducted on theengine using various ethanol fumigation rates at different preheating temperatures. Fuel preheating increases efficiency. NOx emissions due to rapid burning and increased fuel inlet temperatures. Increase in NOx emissions with decrease in smoke opacity, HC and CO with fuel preheating. The increase in peak pressure and maximum rate of pressure rise results along with simultaneous improvement in heat release rate due to improved atomisation and vaporisation of the ethanol. The preheated ethanol exhibits reduced ignition delay. The conversion efficiency of micro-CHP system utilizing heat of exhaust gases has been observed to be 61.8%, when the engine is operated on pure diesel.A simulation strategy for an efficient and significant simulation of a single-cylinder four-stroke engine was developed, which needs only a small number of revolutions. The strategy leads to a faster convergence of the simulation, especially for the simulation of the injection, the mixture formation, and the combustion. Besides, the presented results show that the first fuel injection generates almost the same fuel distribution inside the engine as the following injections of the subsequent revolutions. This means further that for the analysis of different injection strategies in a development process of a new engine already the first injection can be used for a suitable evaluation. After the selection of the best variants further investigations can be realized.

REFERENCES

[1] www.indiaenvironmentportal.org.in/files/file/pngstat%202014-15.pdf Last accessed on 27 June 2016

[2] http://www.iea.org/publications/freepublications/publication/energy-efficiency-indicators-fundamentals-on-statistics---.html. Last accessed on 27 June 2016

[3] A. Demirbas, A Realistic Fuel Alternative for Diesel Engines *Springer*, 2008

[4] C.P. Cigar, S.L Soni, D. Sharma, "Effect of LPG induction on performance and emission characteristics of bio-diesel in a CI engine". *Energy Sources Part A*. 2008;30(16):1451-59

[5] S.L. Soni, "Compressed Natural Gas (CNG) Fuelled Spark Ignition Engine-Gas Injection, Combustion, Performance and Exhaust Emission Studies". Ph.D. Thesis, Mechanical Engineering Department, IIT Delhi 1997.

[6]R. Mythili, P. Venkatachalam, P. Subramanian, D. Uma. Production characterization and efficiency of biodiesel: a review. *International Journal of Energy Research* 2014; 38(10):1233–59.

[7] C.D. Rakopoulos, K.A. Antonopoulos, D.C. Rakopoulos, D.T. Hountalas, E.G. Giakoumis. Comparative performance and emissions study of a direct injection diesel engine using blends of diesel fuel with vegetable oils or bio-diesels of various origins. *Energy Conversion and Management* 2006;47:3272–87.

[8] J. Turner, G. Sverdrup, M.K. Mann, P.C. Maness, B. Kroposki, M. Ghirardi, R.J. Evans, D. Blake, "Renewable hydrogen production". *International Journal of Energy Research* 2008;32(5): 379–407

[9] N. Saravanan, G. Nagarajan, "Experimental investigation on a DI dual fuel engine with hydrogen injection". *International Journal of Energy Research* 2009;33(3):295–308

[10] V.S. Yadav, S.L. Soni, D. Sharma, "Performance and emission studies of direct injection CI in dual fuel mode (hydrogen-diesel) with EGR". *Int J hydrogen energ* 2012;37(4):3807-17.

[11] V.S. Yadav, S.L. Soni, D. Sharma, "Engine performance of optimised hydrogen-fueled direct injection engine". *Energy*. 2014;65:116-22.

[12]V.S. Yadav, S.L Soni, D. Sharma, "An experimental investigation of hydrogen-enriched unmodified DI diesel engine in dual fuel mode". *International Journal of Renewable energy* 2013;4(4):358-69.

[13] A. Imran, N. Varman, H.H. Masjuki, M.A. Kalam, “Review on alcohol fumigation on diesel engine: A viable alternative dual fuel technology for satisfactory engine performance and reduction of environment concerning emission”. *Renewable and Sustainable energy review* 2013; 26:739-51.

[14] W. Tutak, K. Lukàcs, S. Szwaja, À. Bereczky, “Alcohol-diesel fuel combustion in the compression ignition engine”. *Fuel* 2015;154:196-206

[15] B.Q. He, S.J. Shuai, J.X. Wang, H. He. “The effect of ethanol blended diesel fuels on emissions from a diesel engine”. *Atmospheric Environment* 2003;37: 4965–71.

[16] A. Bilgin, O. Durgun, Z. Sahin, “The effects of diesel–ethanol blends on diesel engine performance”. *Energy Source* 2002;24:431–40.

[17] M. Lapuerta, O. Armas, J.M. Herreros, “Emissions from a diesel–bioethanol blend in an automotive diesel engine”. *Fuel* 2008;87:25–31.

[18] H. Kim, B. Choi, “Effect of ethanol–diesel blend fuels on emission and particle size distribution in a common-rail direct injection diesel engine with warmup catalytic converter”. *Renewable Energy* 2008;33:2222–8.

[19] D.C. Rakopoulos, C.D. Rakopoulos, E.C. Kakaras, E.G. Giakoumis. “Effects of ethanol-diesel fuel blends on the performance and exhaust emissions of heavy duty DI diesel engine”. *Energy Conversion and Management* 2008;49:3155–62.

[20] L. Xing-cai, Y. Jian-guang, Z. Wu-gao, H. Zhen, “Effect of cetane number improver on heat release rate and emissions of high speed diesel engine fueled with ethanol–diesel blend fuel”. *Fuel* 2004;83:2013–20

[21] J. Huang, Y. Wang, Li. Shuangding , P.R. Anthony, Yu Hongdong, Li Huifen, “Experimental investigation on the performance and emissions of a diesel engine fuelled with ethanol-diesel blends”. *Applied Thermal Engineering* 2009;29: 2484–2490

[22] T. Murayama, N. Miyamoto, T. Yamada, J. Kawashima, “A study on Diesel-engines with alcohol fuels (Engine performance with ethanol-castor oil fuel blends)”. *Bulletin of JSME* 1983;26(216):1043–9.

[23] K. Weidmann, H. Menrad, “Fleet test, performance and emissions of Diesel engines using different alcohol-Diesel fuel blends”. *SAE*. 1984;841331.

[24] A.C. Hansen, P.W. Taylor, L. Lyne, P. Meiring, " Heat release in the compression-ignition combustion of ethanol". *Transactions of ASAE* 1989; 5:1507–11.

[25] J. Czerwinski, "Performance of HD-DI-Diesel engine with addition of ethanol and rapeseed oil". *SAE* 1994;940545

[26] Y. Ali, M.A. Hanna, J.E. Borg, "Effect of alternative Diesel fuels on heat release curves for Cummins N14-410 Diesel engine". *Transactions of ASAE* 1996; 2:407–14.

[27] E. A. Ajav, B. Singh, T.K Bhattacharya, "Experimental study of some performance parameters of a constant speed stationary Diesel engine using ethanol-Diesel blends as fuel". *Biomass Bioenergy* 1999;17(4):357–65.

[28] M. Abu-Qudais, O. Haddad, M. Qudaisat, "The effect of alcohol fumigation on diesel engine performance and emissions". *Energy Conversion and Management* 2000;41:389–99.

[29] E.A. Ajav, B. Singh, T. K Bhattacharya, "Thermal balance of a single cylinder diesel engine operating on alternative fuels". *Energy Conversion and Management* 2000;41:1533–41.

[30] X.B. Gao, D. Foster, Z. Ye, "Ignition delay and heat release analysis of an ethanol fumigated turbocharged Diesel-engine. In: 6th Annual energy sources technology and exhibit" *ASME*; 1983. 83-DGP-1.

[31] J.T. Walker, "Diesel tractor engine performance as affected by ethanol fumigation". *Transactions of ASAE* 1984;27(1):49.

[32] G.J. Shropshire, L.L Bashford, "Comparison of ethanol fumigation systems for a diesel engine". *Agricultural Engineering (United States)* 1987;65(5):17–24.

[33] J. Chaplin, R.B. Janius. "Ethanol fumigation of a compression-ignition engine using advanced injection of diesel fuel". *Transactions of ASAE* 1987;30(3): 610–4

[34] M.E.A. Fahd, Y. Wenming, P.S. Lee, S.K. Chou, C.R. Yap, Experimental investigation of the performance and emission characteristics of direct injection diesel engine by water emulsion diesel under varying engine load condition. *Applied Energy* 2013;102:1042–9.

[35] G. Nagafi, T.F. Yusaf, "Experimental investigation of using methanol-diesel blended fuels in diesel engine. *In: Proceedings of the fourth international conference on thermal engineering: theory and applications*". Abu Dhabi, UAE; 2009. p. 1–5.

[36] Z.H. Huang, H.B. Lu, D.M. Jiang, J.Q. Zhang, X.B. Wang, “Combustion behaviors of a compression-ignition engine fuelled with diesel/methanol blends under various fuel delivery advance angles”. *Bioresource Technology* 2004;95:331–41.

[37] C. Yao, C.S. Cheung, C. Cheng, Y. Wang, “Reduction of smoke and NOx from diesel engines using a diesel/methanol compound combustion system”. *Energy and Fuel* 2007;21:686–91.

[38] C. Yao, C.S. Cheung, C. Cheng, Y. Wang, T.L. Chan, S.C. Lee, “Effect of diesel/methanol compound combustion on diesel engine combustion and emissions. *Energy Conversion and Management* 2008;49(6):1696–704

[39] Y. Icingur, D. Altiparmak , “Experimental analysis of the effect of fuel injection pressure and fuel cetane number on direct injection diesel engine emissions”. *Turkish Journal of Engineering and Environmental Sciences* 2003;27:291–7.

[40] F. Payri, J. Benajes, J. Arregle, J.M. Riesco, “Combustion and exhaust emissions in a heavy-duty diesel engine with increased premixed combustion phase by means of injection retarding”. Oil and Gas Science and Technology 2006;61:247–58.

[41] M. Canakci, C. Sayin, M. Gumus, “Exhaust emissions and combustion characteristics of a direct injection (DI) diesel engine fueled with methanol- diesel fuel blends at different injection timings*”. Energy and Fuel* 2008;22:3709–23.

[42] Z.H. Huang, H.B. Lu, D.M. Jiang, K. Zeng, B. Liu B, J.Q. Zhang JQ, “Performance and emissions of a compression ignition engine fueled with diesel/oxygenate blends for various fuel delivery advance angles”. *Energy and Fuel* 2005;19:403–10.

[43] C. Sayan, A.N. Ozsezen, M. Canakci, “The influence of operating parameters on the performance and emissions of a DI diesel engine using methanol blended-diesel fuel”. *Fuel* 2010;89:1407–14.

[44] M. Canakci, C. Sayin, A.N. Ozsezen, A. Turkcan. “Effect of injection pressure on the combustion, performance and emission characteristics of a diesel engine fueled with methanol-blended diesel fuel”. *Energy and Fuel* 2009;23:2908–20.

[45] C. Sayin, M. lhan, M. Canakci, M. Gumus, “Effect of injection timing on the exhaust emissions of a diesel engine using diesel-methanol blends”. *Renewable Energy* 2009;34(5):1261–9.

[46] R.B. Koganti, M. Maheshwari, K.K. Swami, R.K. Malhotra, P. Arora, V.P. Singh, "Performance evaluation of ethanol diesel blend in tractors". *SAE* paper no. 2004-28-0085; 2004.

[47] E.A. Ajav, B. Singh, T.K Bhattacharya. Experimental study of some performance parameters of a constant speed stationary diesel engine using ethanol diesel blends as fuel. *Biomass and Bioenergy* 1999;17:357–65.

[48] A. Bilgin, O. Durgun, Z. Sahin. "The effect of diesel-ethanol blends on diesel engine performance". *Energy Sources* 2002;24:431–40.

[49] D. Li, H. Zhen, L. Xingcai, Z. Wu-Gao, Y. Jian-Guang, "Physicochemical properties of ethanol–diesel blend fuel and its effect on performance and emissions of diesel engines". *Renewable Energy* 2005;30(6):967–76.

[50] D.C. Rakopoulos, C.D. Rakopoulos, E.C. Kakaras, E. Giakoumis. "Effect of ethanol-diesel fuel blends on the engine performance and emissions of heavy duty DI diesel engine". *Energy Conversion and Management* 2008;49(11): 3155–62.

[51] Arapatsakos C. Application of diesel–ethanol mixtures in tractor engine. International *Journal of Energy and Environment* 2009;3(2):77–84.

[52] C.D. Rakopoulos , K.A. Antonopoulos, D.C. Rakopoulos. Experimental heat release analysis and emissions of a HSDI diesel engine fueled with ethanol-diesel fuel blends. *Energy* 2007;32(10):1791–808.

[53] J. Huang, Y. Wang, S. Li, A.P. Roskilly, Y. Hongdong, H. Li, "Experimental investigation on the performance and emissions of a diesel engine fuelled with ethanol–diesel blends". *Applied Thermal Engineering* 2009;29(11– 12):2484–90.

[54] Y. Di, C.S. Cheung, Z. Huang, "Comparison of the effect of biodiesel–diesel and ethanol–diesel on the gaseous emission of a direct-injection diesel engine". *Atmospheric Environment* 2009;43(17):2721–30.

[55] V.N. Banugopan, S. Prabhakar, K. Annamalai, S. Jayaraj, P. Sentilkumar, "Experimental investigation on D.I. diesel engine fuelled by ethanol diesel blend with varying inlet air temperature". *Frontiers in Mechanical Engineering* 2010;25–27:128–34.

[56] S. H. Park, J. Cha, C.S. Lee. "Effects of bioethanol-blended diesel fuel on the combustion and emission reduction characteristics in a direct-injection diesel engine with exhaust gas recirculation (EGR)". *Energy and Fuel* 2010;24:3872–83.

[57] S.H. Park, I.M. Youn, C.S. Lee "Influence of ethanol blends on the combustion, performance and exhaust emission characteristics of a four-cylinder diesel engine at various engine loads and injection timing". *Fuel* 2011;90:748–55.

[58] D.C. Rakopoulos, C.D. Rakopolous, E.G. Giakoumis, R.G. Papagiannakis, D.C. Kyritsis "Experimental–stochastic investigation of the combustion cyclic variability in HSDI diesel engine using ethanol–diesel fuel blends". *Fuel* 2008;87:1478–91.

[59] O. Can, I Celikten, N Usta. Effects of addition on performance and emissions of a turbocharged indirect injection diesel engine running at different injection pressures. *Energy Conversion and Management* 2004;45:2429–40.

[60] M. Lapuerta, O. Armas, R.G. Contreras, "Stability of diesel–bioethanol blends for use in diesel engines". *Fuel* 2007;86:1351–7.

[61] X. Lu, H. Zhen, Z. Wugao, L. Degang, "The influence of ethanol additives on the performance and combustion characteristics of diesel engines". *Combustion Science and Technology* 2004;176:1309–29.

[62] H. Kim, B. Choi, "Effect of ethanol–diesel blend fuels on emission and particle size distribution in a common–rail direct injection diesel engine with warm up catalytic converter". *Renewable Energy* 2008;33:2222–8.

[63] W. Li, X.B. Wang, H. Miao, D.M. Jiang, Z.H. Huang. "Combustion characteristics of a compression ignition engine fuelled with diesel–ethanol blends". *Proceeding of Institute of Mechanical Engineers Part D: Journal of Automobile Engineering* 2008;222:265–74.

[64] Z. Sahin, O. Durgun, C. Bayram. "Experimental investigation of gasoline fumigation in a single cylinder direct injection Diesel engine". *Energy* 2008;33:1298-310

[65] C.H. Cheng, C.S. Cheung, T.L Chan, S.C. Lee, C.D. Yao, K.S. Tsang, "Comparison of emissions of a direct injection diesel engine operating on biodiesel with emulsified and fumigated methanol". *Fuel* 2008; 87:1870–9.

[66] Z.H. Zhang, K.S. Tsang, C.S. Cheung, T.L. Chan, C.D. Yao. "Effect of fumigation methanol and ethanol on the gaseous and particulate emissions of a direct injection diesel engine". *Atmospheric Environment* 2011; 45:2001–8.

[67] Z.H. Zhang, C.S. Cheung, T.L Chan, C.D. Yao. "Experimental investigation of regulated and unregulated emissions from a diesel engine fuelled with Euro V diesel fuel and fumigation methanol". *Atmospheric Environment* 2010; 44: 1054–61.

[68] Z.H. Zhang, C.S. Cheung, T.L. Chan, C.D. Yao, " Emission reduction from diesel engine using fumigation methanol and diesel oxidation catalyst". *Science of Total Environment* 2009; 407:4497–505.

[69] B.S. Chauhan, N. Kumar, S.S. Pal, Y.D. Jun, "Experimental studies on fumigation of ethanol in a small capacity Diesel engine". Energy 36(2011) 1030-1038.

[70] D. Hansdah, S. Murugan. "Bioethanol fumigation in a DI diesel engine". *Fuel* 2014;130:324–33

[71] M. H. Morsy, "Assessment of a direct injection diesel engine fumigated with ethanol/water mixtures". *Energy Conversion and Management* 94 (2015) 406–414

[72] K. Sudheesh, J.M. Mallikarjuna, "Diethyl ether as an ignition improver for biogas homogeneous charge compression ignition (HCCI) operation -An experimental investigation" *Energy* 2010;35:3614-22

[73] C. Can, Ö. Can, F. Sahin, H.S. Yucesu, "Effects of premixed diethyl ether (DEE) on combustion and exhaust emissions in a HCCI-DI diesel engine" *Applied Thermal Eng* 2010;30: 360-65 603

[74] J. Hou, Z. Wen, Z. Jiang, Y. Liu, "Effects of premixed ratio on combustion characteristics of a homogeneous charge compression ignition-direct injection engine fuelled with dimethyl ether". *Journal of Renewable and Sustainable Energy* 2014;6(1): 013106.

[75] D.K. Jamuwa, D. Sharma, S.L. Soni, "Performance, emission and combustion analysis of ethanol fuelled stationary CI Engine". *Biofuels*. 2016. DOI:10.1080/17597269.2016.1163213

[77] D.K. Jamuwa, D. Sharma, S.L. Soni. "Experimental investigation of performance, exhaust emission and combustion parameters of stationary compression ignition engine using ethanol fumigation in dual fuel mode". *Energy Conversion and Management* 115 (2016) 221–231

[77] H. Caliskan, A. Hepbasli, "A review on exergetic analysis and assessment of various types of engines". *International Journal of Exergy* 2010; 7(3): 287-310

[78] T.J. Kotas, "*The Exergy method of thermal plant analysis*". Paragon Publishing; 2012

[79] J.B. Heywood. "*Internal combustion engine fundamentals*". 2nd ed. McGraw-Hill; 2003.

[80] H.K. Versteeg, W. Malalasekera. *An Introduction to Computational Fluid Dynamics, the finite volume method,* 2nd ed.

[81] V. Yakhot, S.A. Orszag, "Renormalization Group Analysis of Turbulence: I. Basic Theory". Journal of Scientific Computing 1986; 1(1):1-51.

[82] T.H. Shih, W.W. Liou, A. Shabbir, Z. Yang, J. Zhu. "A New k-ε Eddy-Vorticity Model for High Reynolds Number Turbulent Flows-Model Development and Validation". *Computers Fluids* 1995; 24(3):227-238.

[83] Ansys Workbench Fluent v15 Theory Guide.

[84] J.C. Tannehill, D.A. Anderson, R.H. Pletcher, "*Computational Fluid Mechanics and Heat Transfer*". Second Edition. Taylor & Francis; 1997.

[85] C. Hirsch, "*Numerical Computation of Internal and External Flows*". Second Edition, John Wiley & Sons; 2007.

[86] D.G. Holmes, S.D. Connel, "Solution of the 2D Navier-Stokes Equations on Unstructured Adaptive Grids". *AIAA 9th Computational Fluid Dynamics Conference*, 1989. 89-1392.

[87] R.D. Rauch, J.T. Batira, N.T.Y. Yang, "Spatial Adaption Procedures on Unstructured Meshes for Accurate Unsteady Aerodynamics Flow Computations". *Technical Report AIAA*-91-1106, 1991

[88] W. Anderson, D.L. Bonhus, "*An Implicit Upwind Algorithm for Computing Turbulent Flows on Unstructured Grids*". Computers Fluids, 23(1):1-21;1994.